

Automated seizure detection for remote monitoring

Citation for published version (APA):

Raghu, R. (2020). *Automated seizure detection for remote monitoring*. [Doctoral Thesis, Maastricht University]. Maastricht University. <https://doi.org/10.26481/dis.20201207rr>

Document status and date:

Published: 01/01/2020

DOI:

[10.26481/dis.20201207rr](https://doi.org/10.26481/dis.20201207rr)

Document Version:

Publisher's PDF, also known as Version of record

Please check the document version of this publication:

- A submitted manuscript is the version of the article upon submission and before peer-review. There can be important differences between the submitted version and the official published version of record. People interested in the research are advised to contact the author for the final version of the publication, or visit the DOI to the publisher's website.
- The final author version and the galley proof are versions of the publication after peer review.
- The final published version features the final layout of the paper including the volume, issue and page numbers.

[Link to publication](#)

General rights

Copyright and moral rights for the publications made accessible in the public portal are retained by the authors and/or other copyright owners and it is a condition of accessing publications that users recognise and abide by the legal requirements associated with these rights.

- Users may download and print one copy of any publication from the public portal for the purpose of private study or research.
- You may not further distribute the material or use it for any profit-making activity or commercial gain
- You may freely distribute the URL identifying the publication in the public portal.

If the publication is distributed under the terms of Article 25fa of the Dutch Copyright Act, indicated by the "Taverne" license above, please follow below link for the End User Agreement:

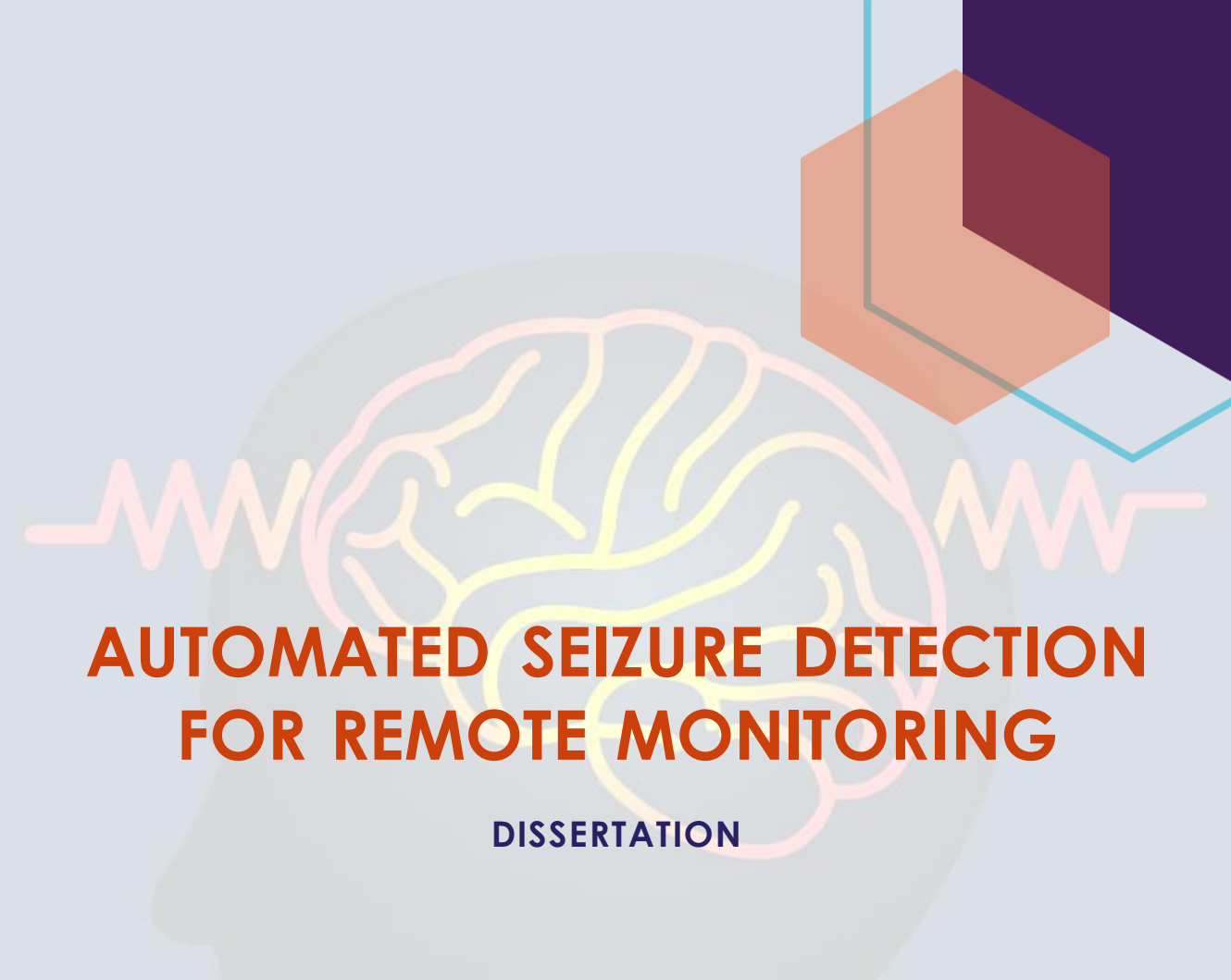
www.umlib.nl/taverne-license

Take down policy

If you believe that this document breaches copyright please contact us at:

repository@maastrichtuniversity.nl

providing details and we will investigate your claim.

A stylized illustration of a human head in profile, facing left. Inside the head, a brain is depicted with yellow and orange outlines. A pink ECG line runs horizontally across the middle of the head, passing behind the brain. In the top right corner, there is a 3D geometric shape composed of orange and red hexagons. In the bottom center, there is another 3D geometric shape, similar to the one in the top right, but with an orange outline and a solid orange fill. A light blue line runs diagonally from the top right towards the bottom left, passing through the 3D shapes.

AUTOMATED SEIZURE DETECTION FOR REMOTE MONITORING

DISSERTATION

Raghu Raghu



Automated Seizure Detection for Remote Monitoring

Copyright© : Raghu Raghu
Email : raghu.sidda@gmail.com
ISBN : 978-94-6423-078-9
Publisher : Maastricht University
Cover & layout : Raghu Raghu

Document Status and Date: Published on December 7th 2020

Citation for Thesis: Raghu, S. (2020). Automated Seizure Detection for Remote Monitoring,

All rights are reserved. For articles published, the copyright has been transferred to the respective publisher. No parts of this thesis may be reproduced, stored in a retrieval system or transmitted in any form or by any means, without prior permission from the author.

**AUTOMATED SEIZURE
DETECTION FOR REMOTE
MONITORING**

DISSERTATION

To obtain the degree of Doctor at Maastricht University,

On the authority of the Rector Magnificus,

Prof.dr. Rianne M. Letschert

In accordance with the decision of the board of deans,

To be defended in public on

Monday 7th December 2020

at 16:00 hours

by

Raghu Raghu

Promotores:

Prof. Dr. Y. Temel

Prof. N. Sriraam (Ramaiah Institute of Technology, Bengaluru, India)

Co-promoters:

Dr. P. L. Kubben

Dr.ir. E. D. Gommer

Assessment Committee:

Prof. Dr. W. Mess (Chairman, Maastricht UMC)

Prof. Dr. N. Ramsey (UMC Utrecht)

Dr. Y. Güçlütürk (Radboud University)

Dr. A. Colon (Kempenhaeghe)

Contents

1	General Introduction	3
2	A novel approach for classification of epileptic seizures using matrix determinant	15
3	Automated detection of epileptic seizures using successive decomposition index and support vector machine classifier in long-term EEG	61
4	Performance evaluation of DWT based sigmoid entropy in time and frequency domains for automated detection of epileptic seizures using SVM classifier	99
5	Complexity analysis and dynamic characteristics of EEG using MODWT based entropies for identification of seizure onset	141
6	Adaptive median feature baseline correction for improving recognition of epileptic seizures in ICU EEG	179
7	Cross-database evaluation of EEG based classification of epileptic seizures driven by adaptive median feature baseline correction	213

8 A convolutional neural network based framework for classification of seizure types	249
9 EEG based multi-class seizure type classification using convolutional neural network and transfer learning	263
10 Application of low-cost mobile health for remote monitoring of epilepsy patients	289
11 General Discussion	303
12 Summary	319
Valorization	325
Acknowledgment	327
Curriculum Vitae	330
Publications	331

List of Abbreviations

AM-FBC	Adaptive median feature baseline correction
ANSFV	Average non-seizure feature values
AUC	Area under the curve
CHB-MIT	Children's Hospital Boston- Massachusetts Institute of Technology
CNN	Convolutional neural network
CS	Classification scenario
CSI	Combined seizure index
DSTFT	Discrete short-time Fourier transforms
DWT	Discrete wavelet transform
EEG	Electroencephalogram
FBC	Feature baseline correction
FDR	False detection rate
GUI	Graphical user interface
ICA	Independent component analysis
ICU	Intensive care unit
IQR	Inter quartile range
K-NN	K-nearest neighbor
LS-SVM	Least square support vector machine
MAF	Moving average filter
MD	Matrix determinant

MDD	Mean detection delay
MDM	Median decaying memory
MLP	Multi-layer perceptron
MODWT	Maximal overlap discrete wavelet transform;
MUMC	Maastricht University Medical Centre
MVMFzEn	Minimum variance modified fuzzy entropy
NPV	Negative predictive value
PPV	Positive predictive value
ReLU	Rectified linear unit
RMCH	Ramaiah Medical College and Hospitals
ROC	Receiver operating characteristic
RP	Relative performance
RVM	Relevance vector machine
SDI	Successive decomposition index
SDK	Software development kit
SDR	Seizure detection rate
STFT	Short-term Fourier transforms
SVM	Support vector machine
TUH	Temple University Hospitals
UBonn	University of Bonn
WPT	Wavelet packet transforms

CHAPTER 1

General Introduction

Telehealthcare service establishes a close connection between the specialist and patients in rural areas and resource-constrained populations, especially in developing countries ensuring an improvement in the quality of living. Among neurological disorders, epilepsy is the third most neurological disorder, affecting 1% of the world population [1]. The connection between rural and sophisticated hospitals needs co-ordination and infrastructure in terms of network connectivity, real-time access to data and necessary clinical diagnosis to treat epilepsy patients. Therefore, remote monitoring of epilepsy patients using continuous electroencephalogram (EEG) recordings and evaluation using state-of-the-art machine learning concepts benefit the epilepsy patients to improve their quality of life. This thesis provides a mobile-based framework for automated detection of epileptic seizures for remote monitoring of epilepsy patients.

An epileptic seizure is a sudden discharge of electrical activity in the brain that causes temporary brain dysfunction and recurrent unprovoked seizures leading to epilepsy [2, 3]. Epilepsy can be treated in various ways, such as medication, vagus nerve stimulation, deep brain stimulation of the anterior nucleus of the thalamus [4], responsive neurostimulation, and dietary therapy [1, 5]. The seizure traces can be identified using EEG, electrocorticography (ECoG), stereo-EEG and non-invasive imaging techniques (e.g., PET, SPECT, and fMRI). EEG is the gold standard for the classification of seizures and the diagnosis of epilepsy. [2, 6, 7, 8, 9, 10]. Evaluation of long-term EEG in remote monitoring provides an insight of epilepsy patients in terms of frequency of seizures, seizure onset, and type of seizure, which helps the neurologist to make further clinical decisions.

Manual intervention of long-term EEG recordings is cumbersome and time consuming for a neurologist to recognize seizures from EEG time series. Therefore, introducing an automated seizure detection system minimizes neurologist involvement and speeds up the treatment procedure. In order to obtain the generalized seizure detection algorithm, the algorithm must be tested on several databases with a good number of epileptic seizure events. Further, the classification of seizure types is a great asset in presurgical evaluation to make the further clinical follow-up. Such attempts have not been made in the existing studies. Hence, the proposed study attempts to overcome the above limitations through the application of novel features and supervised machine learning algorithms using five EEG recordings collected from different centers.

1.1 The 10-20 system

Small metal discs usually made of stainless steel, tin, gold or silver covered with a silver chloride coating are placed on the scalp in special positions to record EEG signals. These positions are specified using the International 10-20 system as shown in Fig. 1.1. The "10" and "20" refer to the actual distances between adjacent electrodes are either 10% or 20% of the total front-back or right-left distance of the skull.

EEG montages: Montage is the placement of the electrodes. The EEG can be monitored with either a bipolar montage or a referential one. Bipolar has two electrodes per one channel and referential montage has a common reference electrode for all the channels. Electrode placements as per International 10-20 system are Fp1, Fp2, F7, F3, Fz, F4, F8, T3, C3, Cz, C4, T4, T5, P3, Pz, P4, T6, O1, and O2.

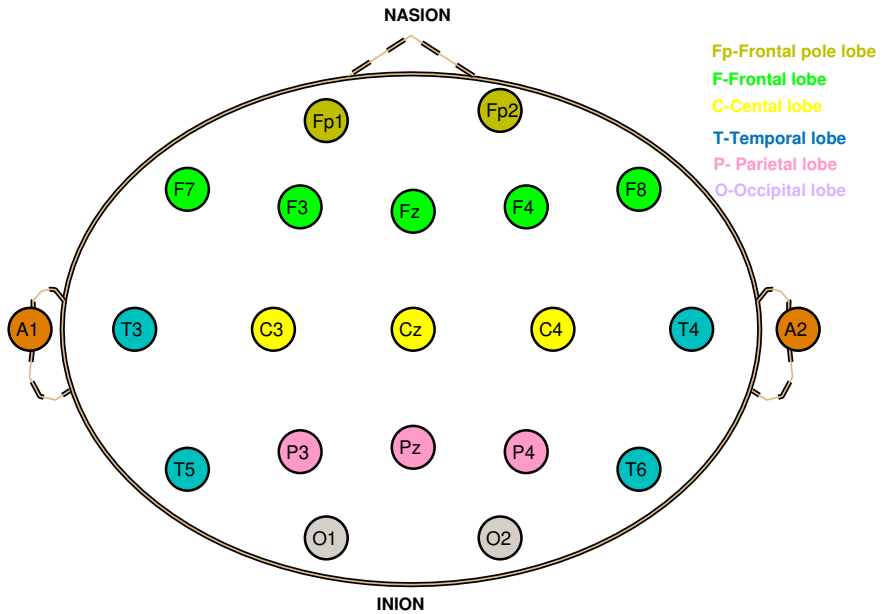


FIGURE 1.1: The International 10-20 system electrodes placement common average montage followed in our study. Even numbers (2,4,6,8) and odd numbers (1,3,5,7) refer to electrode positions on the right and left hemisphere respectively. The letter 'z' refers to an electrode placed on the midline.

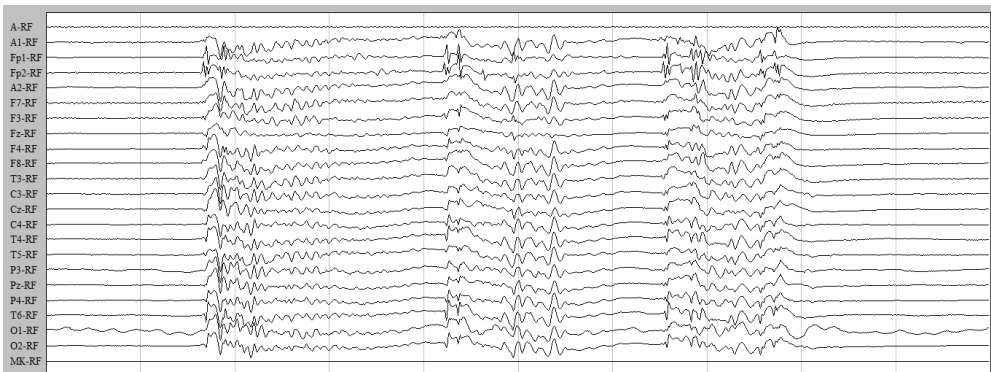


FIGURE 1.2: An example of referential montage scalp EEG recordings collected from Ramaiah Medical College and Hospital.

1.2 EEG

EEG signal contains useful information on physiological states of the brain and has proven to be a potential biomarker to realize the complex dynamic behavior of the brain. EEG waveforms are classified according to their amplitude (μv), frequency (delta ($< 4Hz$), theta ($4 - 8Hz$), alpha ($8 - 12Hz$), beta ($12 - 30Hz$) and, gamma ($> 30Hz$)) and shape [3, 6]. EEG is the gold standard for the classification of seizures and the diagnosis of epilepsy in terms of cost, safety, painless and efficient temporal resolution [2, 6, 7, 8, 9, 10, 11]. The morphological shape of seizure EEG are spikes (20-70 ms), sharp waves (70-200 ms), and spike-and-wave discharges (a spike followed by a slow wave) referred to as epileptic waves [1, 12, 13]. In other words, seizure onset is characterized by a sudden change in frequency and the appearance of a new rhythm. Spikes and sharp wave EEG in a specific area of the brain relates to focal seizure, whereas spike-and-wave discharges, which widely spread over both sides of the brain are referred to as generalized seizures. Therefore, proposing a discriminating feature that is capable of separating normal and epileptic seizures is the most essential and challenging procedure.

1.3 Seizure types

Epileptic seizures are caused by a disturbance in the electrical activity of the brain, which is classified into focal, generalized, and unknown [13, 14]. Focal seizures start on one side of the brain and depending on the patient's level of awareness during a seizure, it is again classified as simple partial and complex

partial seizures [15, 16]. Generalized seizures affect both sides of the brain at the same time and again divided into absence, tonic, atonic, clonic, and tonic-clonic, myoclonic seizures [13]. Generalized seizures are classified based on motor symptoms and non-motor symptoms that involve movement [13, 15, 16]. Motor symptoms include jerking movements (clonic), muscles becoming tense or rigid (tonic), muscles becoming weak or limp (atonic), and brief muscle twitching (myoclonic) [13, 15, 16]. Unknown seizures are the ones when the beginning and where the seizure starts is not known [15, 16]. Accurate classification of epileptic seizure type plays a crucial role in the treatment and disease management of epilepsy patients [17].

1.4 Visual analysis of long-term EEG

In the EEG time series, the appearance of traces of spikes or sharp waves do indicate the reflection of seizure activities. The routine EEG shows the temporal and spatial information regarding brain activity, which is used to diagnose, monitor, and localize the epileptogenic focus. A thorough inspection of the long-term EEG recordings is necessary to recognize the abnormal EEG patterns for presurgical evaluation. However, this procedure is found to be time-consuming, costly and leading to human errors since epileptic activities present in a small percentage of the entire data [9, 18, 19, 20]. Thus, an efficient algorithm that detects brain abnormalities with precise and accurate results would benefit neurologists in saving time and increasing efficiency.

High-frequency oscillations (HFOs) between 80 and 500 Hz have proven particularly important and useful markers for the epileptogenic zone. HFOs show promise for improving surgical outcomes and accelerating intracranial

EEG investigations but not on scalp EEG. Despite promising results, HFOs are not a routine clinical procedure due to the uncertainties about the mechanisms of generation, methods of analysis, and clinical applicability. Therefore, we focus on scalp EEG in our thesis for seizure detection.

1.5 Feature extraction

Feature extraction is one of the major steps in developing a machine learning algorithm for an automated seizure detection model. The features extracted from the EEG signals should be capable of well discriminating seizure and non-seizure activities. Most importantly, the feature should be computationally efficient that leads to low detection delay of seizure recognition. It was reported that features like approximate entropy, sample entropy, Lyapunov exponent, multi-variate features derived from wavelet transforms and empirical mode decomposition are computationally expensive [18, 21, 22]. Therefore, we propose three new feature namely, matrix determinant (MD) (Chapters 2, 6 and 7), successive decomposition index (SDI) (Chapters 3, 6 and 7), and sigmoid entropy (Chapters 4 and 5) that are well discriminate the seizure and non-seizures activities being computationally efficient.

1.6 Classification

The classification is a supervised learning approach in which the algorithm learns from the data input given to it and then uses this learning to classify

new observations. A supervised learning algorithm learns from labeled training data, helps to predict outcomes for unforeseen data. Support vector machine (SVM) is a supervised machine learning algorithm and it classifies the data by finding the best hyperplane that differentiates the two classes very well [23]. The SVM classifier was trained with the predefined class labels of 0 and 1 by experts for normal and epileptic seizures EEG respectively. In Chapter 2, SVM, K-nearest neighbor (K-NN) and multi-layer perceptron (MLP) were used and later SVM only used due to the better results observed. The performance of the epileptic seizure detection algorithm was evaluated in terms of sensitivity, specificity, accuracy, false detection rate, median detection delay, F measure, Cohen's Kappa coefficient, and area under the receiver operating characteristics curve.

1.7 Objectives

Existing studies on seizure detection have validated their algorithms using cross-validation on the same database and no attempts have been made to extend their work on other databases to test the generalization capability. The foremost objective of this thesis is to introduce an optimal database-independent classification model for seizure detection using cross-database evaluation leading to mobile-based analysis for remote monitoring and classification of seizure type. As a state of the art approach, three novel features which are better than existing features and a novel algorithm for feature baseline correction (FBC) have been introduced in this thesis. Further, the classification of seizure types using a convolutional neural network (CNN) based transfer-learning approach has been proposed. The final goal of this thesis is to assess the efficiency of

smartphones for seizure detection, which can be deployed for remote monitoring of epilepsy patients.

1.8 Outline of the thesis

In this section, the relation between the subsequent chapters is described. In the first three chapters, the introduction of novel features namely MD, SDI, and sigmoid entropy were discussed respectively. A novel FBC method was introduced to overcome inter-subject variability in Chapter 6. An Optimized cross-database evaluation was proposed in Chapter 7 using FBC for inter-database variability. Chapters 8 and 9 discusses classification of seizure detection using CNN based transfer learning. The feasibility of smartphones for remote monitoring of epilepsy patients was studied in Chapter 10.

Chapter 1 gives the general introduction about the thesis including problem statement, objective, and outline of the thesis. Chapter 2 introduces a novel feature referred to as MD and evaluated using eleven classification problems on the UBonn database. The classification was performed using SVM, K-NN, and MLP with 10-fold cross-validation. The effect of different square matrix order on classification results was studied. Both equal and unequal numbers of observations were used to perform the classification task. Further, the MD feature was implemented on the RMCH database. The results of this chapter were the basis that MD can be a potential biomarker for seizure detection.

Another novel feature referred to as SDI based on the determinant of the square matrix introduced in Chapter 3. The algorithm was tested on multiple EEG databases proving the robustness. Relative performance in terms of time complexity and classification results were discussed. Comparison of SDI

feature with wavelet energy derived from wavelet decomposition and existing feature extraction methods was performed.

Chapter 4 describes another novel feature referred to as sigmoid entropy derived from discrete wavelet transforms (DWT) coefficients. A thorough investigation was performed to identify the best wavelet and decomposition level (sub-band) using five wavelets. This chapter also describes the results of the segment-based and event-based classification approach. Analysis of Cohen's Kappa coefficient was performed on seizure detection. The performance of sigmoid entropy was compared with other entropy methods like Shannon entropy, Renyi entropy, and Tsallis entropy.

We have investigated six entropies, namely sigmoid, Shannon, wavelet, Renyi, Tsallis, and Steins unbiased risk estimator (SURE) entropies derived from maximal overlap discrete wavelet transform (MODWT) using different wavelets and decomposition levels in Chapter 5. The effect of the decomposition level on energy was studied for all the six entropies.

Chapter 6 introduces a novel approach referred to as adaptive median feature baseline correction (AM-FBC) to overcome inter-subject variability. Various classification scenarios using outliers removal and correction, AM-FBC, and post-processing of classifier output were studied to identify the optimal classification model. We have also investigated the effect of outliers on classification results and loss of diagnostic information.

Chapter 7 introduces an optimal cross-database approach using five EEG databases based on AM-FBC to overcome inter-database variability. Different classification scenarios were considered using AM-FBC, smoothing of the train and test data, and post-processing of the classifier output to improve the

seizure detection results. AM-FBC was applied to the subject's level and then to the database level separately. The SVM classifier was trained and tested with a leave-one-database-out cross-validation approach.

Chapter 8 describes the preliminary work of classification of seizure types using CNN based transfer learning approach which includes simple partial, complex partial, focal non-specific, generalized non-specific, absence, tonic, and tonic-clonic, and non-seizures. In Chapter 9, different pretrained networks such as Alexnet, Vgg16, Vgg19, Squeezenet, Googlenet, Inceptionv3, Densenet201, Resnet18, Resnet50, and Resnet101 were studied for best performance. The two different methods were proposed using CNN: (1) Transfer learning using a pretrained network, (2) Extract image features using a pretrained network and classify using the SVM classifier.

Chapter 10 investigates the feasibility of smartphones for processing larger EEG recordings for the application towards remote monitoring of epilepsy patients.

Finally, general discussion alongside clinical significance, limitations, future directions and concluding remarks were made in Chapter 11.

CHAPTER 2

A novel approach for classification of epileptic seizures using matrix determinant

S Raghu, Natarajan Sriraam, Alangar Sathyaranjan Hegde, Pieter L Kubben

Expert Systems with Applications, 127:323-341

Year: 2019

<https://doi.org/10.1016/j.eswa.2019.03.021>

Abstract

Objective: An epileptic seizure is recognized as a neurological disorder caused by transient and unexpected disturbance resulting from the excessive synchronous activity of the neurons in the brain. Analysis of epileptic seizures derived from long-term recordings of electroencephalogram (EEG) is cumbersome and time consuming for a neurologist. Therefore, introducing an automated detection system surrogate the neurologist involvement all time and speed up the treatment procedure.

Methods: This study introduces a matrix determinant of EEG as a significant feature for recognition of epileptic seizures. Initially, artifact-free filtered EEG time series was arranged sequentially to form a square matrix of order, namely 13, 16, 23, and 32 and determinant was estimated. Assumed that the total elements in the square matrix represent a typical segmentation length. The experiment was conducted using EEG database obtained from the University of Bonn and Ramaiah Medical College and Hospital (RMCH). In total, eleven classification problems among non-epileptic group and epileptic EEG were composed to examine temporal dynamics of brain activity in different states of the epileptic activity. Next, the extracted feature was classified using support vector machine (SVM), K-nearest neighbor (K-NN), multi-layer perceptron (MLP) classifiers with 10-fold cross-validation.

Results: Experimental results revealed the highest classification accuracy of 99.45% (using University of Bonn) and 97.56% (using RMCH). between normal and epileptic EEG. In addition, other classification problems and matrix

orders showed better results using all the classifiers. Further, descriptive analysis, histogram plot in polar coordinates and the bivariate histogram analysis was performed. In conclusion, matrix determinant found to be a potential biomarker for the real-time detection of epileptic seizure with minimal computational complexity.

2.1 Introduction

An epileptic seizure is considered as a neurological disorder caused by transient and unexpected disturbance resulting from the excessive synchronous activity of the neuron in the brain. According to the World Health Organization, 50 million of the world population suffering from epilepsy [1]. Globally, an estimated 2.4 million people are diagnosed with epilepsy each year [1]. The rapid growth in the patient ratio each year indicate the need for robust automatic seizure detection technique from EEG signals. In recent times, automated classification and detection of an epileptic seizure using novel and efficient algorithms have become a challenging task for the biomedical engineering community. It is a well-known fact that long-term EEG for the visual interpretation by neurologists is tedious and cumbersome. Thus, an efficient algorithm which detects the brain abnormalities with precise and impressive results would benefit neurologist in saving their time and handling more patients. In the past, various feature parameters have been proposed for the analysis of EEG signals. It was noticed that the majority of the existing approaches relies on decomposing the EEG signal into several levels to attain better classification results leads to the tedious procedure. Therefore, in this study, for the

first time matrix determinant of EEG was used for classification of epileptic seizure EEG and found to be the most straightforward approach.

The rest of the paper is organized as follows. The related background of the study is reported in Section 2. The proposed methodology is described in Section 3 includes a dataset description, the matrix determinant feature, classifiers and performance measures. Section 4 provides the simulation results obtained. In Section 5, discussion on proposed work and its comparison with state-of-the-art methods was reported. Section 6 concludes with overall remarks [24].

2.2 Related background

Many researchers have proposed several feature extraction methods for the automated detection of epileptic seizure from EEG signals [2, 9, 24, 25, 26, 27, 28, 29]. There is a need to review the state-of-the-art methods, to understand the importance of current state, future trends, and limitations in existing approaches. Gotamn [2] proposed a computerized algorithm for detection of seizures. Later, in [24, 26, 29] different approaches to make the neurologist job easier in analyzing long-term EEG was proposed. Approximate entropy (ApEn) with Elman neural network classifier showed a 100% classification accuracy at the cost of computational expensive [27].

Islam et al. [30] developed threshold-based decision-making algorithm for artifact removal from scalp EEG. Impressive results achieved using sample entropy with support vector machine (SVM) classifier. Samiee et al. [28]

reported an adaptive and localized time-frequency representation of EEG signals using rational functions. They proposed a novel feature extraction approach derived from rational discrete short-time Fourier transform (DSTFT) and showed a classification accuracy of 98.1% using MLP classifier. Zhou et al. [31] proposed an algorithm for intracranial EEG seizure detection using lacunarity and Bayesian linear discriminant analysis (BLDA). In this method, wavelet decomposition of EEG with five scales “Daubechies 4” mother wavelet was used. Results showed a sensitivity of 96.25% and a false detection rate of 0.13/h with a mean delay time of 13.8 s. Another study introduced multi-stage seizure detection system using morphologies of seizures with the average sensitivity of 87.5% for five patients with 24 seizures [32]. One of the recent study [21], proved the presence of line noise in the University of Bonn database [33] with the evidence of spectrogram and power spectral density, the same was eliminated using least mean square adaptive filter technique. The wavelet packet based derived log energy and norm entropies feature using recurrent Elman neural network classifier attained a classification accuracy 99.70%.

Bhattacharyya et al. [34] proposed automatic burst detection in the neonatal EEG using features such as the ratio of mean nonlinear energy, power spectral density, variance, and absolute voltage. These features showed a high degree of separability between burst and normal (non-burst) EEG segments using the SVM classifier. Remarks made in this approach was, the algorithms based on the predefined static voltage or energy thresholds become too specific. Zeng at al. [35] have employed compressive sensing principle for recognizing inter-ictal, pre-ictal, and ictal EEG-based epileptic seizures. Sample and permutation entropies with Hurst index features were applied along with

four variant classifiers, and significant features were selected using an ANOVA test. The performance results obtained were quite promising and confirmed its suitability for telemonitoring of epileptic patients. Best result was achieved using discriminant analysis of compressed sensing structure similarity feature (CS-SSIM). Attempts have been made using wavelet-based entropy [36, 37] and other time-frequency based features [38]. for seizure detection. Recently, 13-layer deep convolutional neural network algorithm was implemented to detect normal, preictal, and seizure classes [39]. This algorithm achieved the accuracy, specificity, and sensitivity of 88.67%, 90.00% and 95.00%, respectively. Multivariate empirical mode decomposition and artificial neural network (ANN) based algorithm was shown better results [40]. In our previous work, threshold-based seizure detection was proposed using a novel approach called minimum variance modified fuzzy entropy [19].

University of Bonn database is one of the widely used standard database for automated detection of epileptic seizures. Refer Section 3.1 for detailed information on the database. Using this database, different classification problems have been formed to classify healthy vs. epileptic EEG.

Bhardwaj et al. [41] extracted features by decomposing EEG signal using empirical mode decomposition (EMD), and constructive genetic programming (CGP) was adopted for classification. Seven different classification problems were classified using discrete wavelet transform (DWT) based features and SVM classifier [42]. Different attempts like, smoothed pseudo-Wigner-Ville distribution (SPWVD) and artificial neural networks [38], tunable-Q factor wavelet transform (TQWT) and bootstrap aggregating [43], analytic time-frequency flexible wavelet transform (ATFFWT) [44] dual-tree complex wavelet

transform (DTCWT) [45], Complex-valued neural networks (CVNN) [46], DWT based ApEn and SVM [47], Teager energy based filter-bank cepstra (TE-FB-CEPs) [48], linear least squares preprocessing and LibSVM [49], multi-wavelet based ApEn and ANN [50], and DWT based ApEn [51] made using the same database with more than five classification tasks. Local mean decomposition (LMD) based hybrid features were classified using genetic algorithm support vector machine (GA-SVM) classifier and achieved the average classification accuracy of 98.10% in all five classification cases. Similarly, methods like temporal and spectral features in the EMD domain with SVM [52], wavelet transform (WT) based linear and nonlinear features with SVM, and complex weighted network combined with the statistical features with least square support vector machine (LS-SVM) [53] was proposed. The different classification problems formed in the existing studies are shown in Table 2.1. In total, eleven classification problems were formed in the present study based on the previous approaches.

In the study [54], matrix determinant was used as a feature for fault detection in power transmission lines using SVM as a classifier. Matrix determinant was used to perform a Hyperspectral image spatial classification [55]. In which, hyperspectral data converted into a gray scaled HSV image and a normalized difference vegetation index representation. Afterwards, Haralick texture features were computed for both pictures, and the resulted features vectors were fused in calculating the determinants of the matrices composed of these characteristics.

From the literature survey it was understood that maximum of seven classification problems were considered on University of Bonn database in previous studies (refer to Table 2.1). In our proposed study, eleven classification problems were considered. In addition, novel feature referred as matrix determinant has been proposed for seizure detection. Most of the studies have applied their algorithm on single database. But, the proposed algorithm was tested on second database collected from Ramaiah Medical College and Hospital (RMCH), Bengaluru, India.

2.3 Material and method

2.3.1 EEG dataset

The proposed approach was evaluated using EEG recordings collected from publicly available database from University Bonn, Germany [33]. This database consists of five subsets namely set A, set B, set C, set D and E (the same database was also labelled as Z, O, N, F, and S respectively) with each containing 100 single channel EEG of 23.6 seconds at 173.61 Hz sampling rate from five different subjects. In our study the EEG datasets namely set A, B, C and D were grouped as non-epileptic and set E as an epileptic condition [47, 48]. In total, EEG dataset contains 39.33 minutes of epileptic seizures data and 157.32 minutes of non-epileptic data. One can refer to [33] for more details on this dataset. Fig. 2.1 shows non-epileptic and epileptic seizure EEG signals used in this study. Table 2.2 shows the further details of the EEG database.

TABLE 2.1: Different classification problems constructed in existing studies using University of Bonn database

Author	Classification problems	Method
[39]	A-E	13-layer deep CNN
[56]	A-E, A-C	CNN
[57]	A-E, B-E, C-E, D-E, ABCD-E AB-CD, AB-CDE, AC-E	CNN
[41]	A-E, ACD-E, ABCD-E, AB-CD-E, A-B-C-D-E	EMD and CGP
[42]	A-E, AB-E, CD-E, A-CDE, ACD-E, AB-CDE, ABCD-E	DWT and SVM
[38]	A-E, AB-CD-E, ABCD-E, A-C-E	SPWVD and ANN
[43]	A-E, C-E, D-E, ABCD-E, A-D-E AB-CD-E, A-B-C-D-E	TQWT and bootstrap aggregating
[45]	A-E, C-E, D-E, ABCD-E, A-D-E AB-CD-E, A-B-C-D-E	DTCWT
[47]	A-E, B-E, C-E, D-E, ACD-E, ABCD-E	DWT based ApEn and SVM
[28]	A-E, B-E, C-E, D-E, AC-E, ABCD-E	DSTFT and MLP
[48]	A-E, ABCD-E, ACD-E, A-C-E, AB-CD-E, CD-E, A-B-C-D-E	TE-FB-CEP feature vectors and RBFNN
[49]	A-E, B-E ABCD-E, ACD-E	Linear least squares preprocessing and LibSVM
[50]	A-E, ABCD-E, ACD-E	Multiwavelet based ApEn and ANN
[58]	A-E, D-E, ABCD-E, A-D-E, A-B-C-D-E	LMD based hybrid features and GA-SVM
[53]	A-E, B-E, C-E, D-E, AB-E, CD-E, ACD-E, ABCD-E	Weighted complex network combined with statistical features and LS-SVM
[52]	A-E, D-E, ABCD-E, A-D-E, AB-CD-E	Temporal and spectral Features in EMD domain and SVM
[59]	A-E, A-D-E, AB-CD-E, ABCD-E, A-B-C-D-E	WT based linear and nonlinear features and SVM

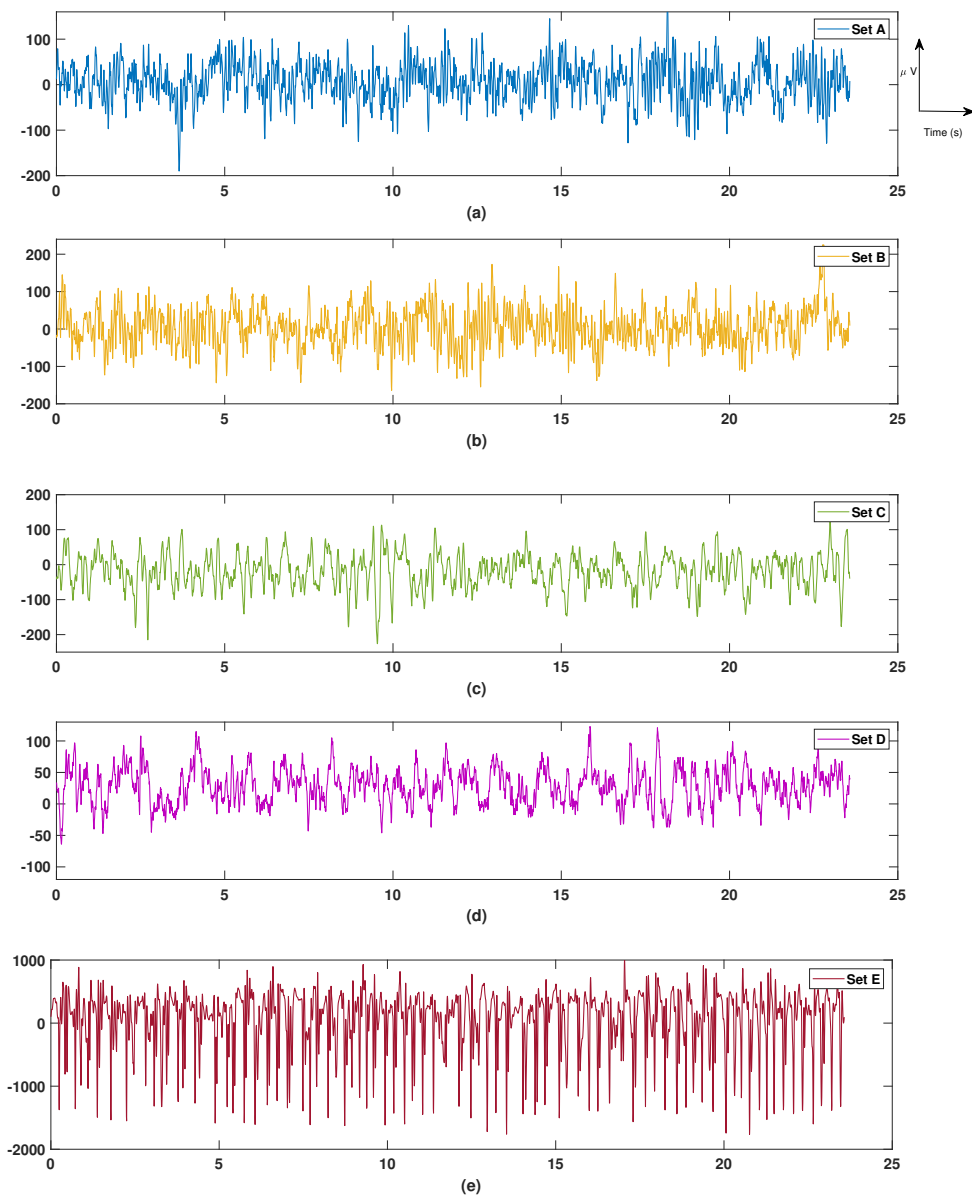


FIGURE 2.1: Plot shows 23.6 seconds single channel EEG signal of (a) Set A (b) Set B (c) Set C (d) Set D (e) Set E. The x-axis indicates times in seconds and y-axis indicates amplitude in μV .

TABLE 2.2: Summary of University of Bonn EEG database used in this study

Subject	Five healthy subjects		Five epileptic subjects		
	Set A	Set B	Set C	Set D	Set E
Other notations used in different studies	Z	O	N	F	S
Patient type	Healthy (eye open)	Healthy (eye closed)	Seizure free (interictal)	Seizure free (interictal)	Seizure activity (ictal)
Patient state	Normal	Normal	Pre-ictal	Post-ictal	Epileptic
Electrodes type	10-20 system	10-20 system	Intracranial	Intracranial	Intracranial
Electrodes placement	Surface	Surface	Within epileptogenic zone	Opposite to epileptogenic zone	Within epileptogenic zone
No. of epochs	100	100	100	100	100
Each file duration (s)	23.6	23.6	23.6	23.6	23.6

2.3.2 Proposed approach

There have been a large number of studies conducted in the past using one of the open source standard database created by University of Bonn, Germany [33], as well as other databases. It was observed that highest of seven classification problems were formed in the studies [42, 43, 45, 48, 53], whereas the proposed study considered eleven classification problems. To the best of the author's knowledge, matrix determinant has not been considered as a feature for recognizing EEG-derived epileptic seizures. Moreover, the time complexity of the matrix determinant is $O(n^3)$, which is better than the features like ApEn, sample entropy, Hurst exponent, and Lyapunov exponent.

Fig. 2.2 shows the schematic of the proposed technique for epileptic seizures detection. In the present study, EEG time series was sequentially arranged to form a square matrix. In order to estimate matrix determinant, the segmentation length was chosen based on the square matrix ($N \times N$, say) order, $N = 13, 16, 23$ and 32 , i.e. $169, 256, 529$ and 1024 samples respectively.

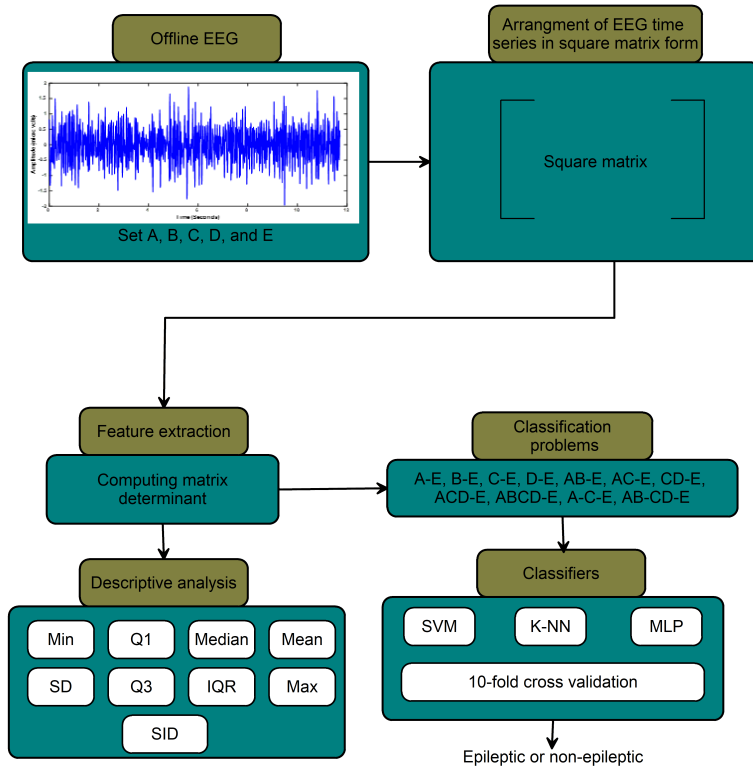


FIGURE 2.2: Matrix determinant based epileptic seizure recognition framework providing a step-by-step overview. Equation (4) in section 3.3 shows the method to obtained square matrix.

Three supervised learning algorithms, namely SVM, K-NN, and MLP with 10-fold cross-validation were used to classify all the eleven classification problems. More importantly, both equal and unequal numbers of observations were used to perform the classification task. A total number of observations used for classification for each matrix order and classification task are shown in Table 2.3. Finally, results of proposed approach were compared with state-of-the-art methods using the same database.

In total eleven classification tasks were performed among epileptic EEG (Set E) and non-epileptic EEG (Sets A, B, C, and D). Clinical significance to

consider the eleven classification problems was to identify the distinct variation between epileptic vs. non-epileptic EEG. Therefore, following eleven classification problems were considered for the study:

1. Classification of EEG sets {A}-{E}
2. Classification of EEG sets {B}-{E}
3. Classification of EEG sets {C}-{E}
4. Classification of EEG sets {D}-{E}
5. Classification of EEG sets {AB}-{E}
6. Classification of EEG sets {AC}-{E}
7. Classification of EEG sets {CD}-{E}
8. Classification of EEG sets {ACD}-{E}
9. Classification of EEG sets {ABCD}-{E}
10. Classification of EEG sets {A}-{C}-{E}
11. Classification of EEG sets {AB}-{CD}-{E}

2.3.3 Feature extraction using matrix determinant

Determinants of matrices are mathematical objects that are very useful in the analysis and solution of systems of linear equations [60]. A determinant is a real number associated with every square matrix [61]. The application of matrix extensively used in the field of signal processing, machine learning and

TABLE 2.3: Total number of observation used for different classification problems

	Matrix order N=13	Matrix order N=16	Matrix order N=23	Matrix order N=32
A-E	2424-2424	1600-1600	774-774	400-400
AB-E	2424-2424	1600-1600	774-774	400-400
	∥∥ 4848-2424	3200-1600	1548-774	800-400
ACD-E	2424-2424	1600-1600	774-774	400-400
	∥∥ 7274-2424	4800-1600	2322-774	1200-400
ABCD-E	2424-2424	1600-1600	774-774	400-400
	∥∥ 9696-2424	6400-1600	3096-774	1600-400
A-C-E	2424-2424-2424	1600-1600-1600	774-774-774	400-400-400
AB-CD-E	2424-2424-2424	1600-1600-1600	774-774-774	400-400-400
	∥∥ 4848-4848-2424	3200-3200-1600	1548-1548-774	800-800-400

Note: Sample size for B-E, C-E, and D-E is same as A-E, and for CD-E, and AC-E is same considered as AB-E. For unbalanced observations class, equal number of observations were from each dataset (e.g. for AB-E, A=2424, B=2424 and E=2424). Symbol || indicates an equal number of observations in both the classes, whereas ∥∥ indicates an unequal number of observations.

much more [62], but determinants are hardly used. The determinant being non-zero is equivalent to the matrix being invertible, whereas zero means the matrix is not invertible. The physical interpretation of matrix determinant represents volume. The enormous amount of information captured by EEG during epileptic activity which influences to rise in the matrix determinant acts as a biomarker to identify those events.

In our research study, the matrix determinant was used as a feature to create the distinction between normal and epileptic activity. The matrix determinant feature captures the variation of the EEG signal amplitude w.r.t time. In the proposed approach the matrix elements are chosen to be EEG time series which are one dimensional. Initially, artifact-free filtered EEG time series were arranged sequentially to form a square matrix, and its determinant was estimated. The total elements in the square matrix represent a segmentation length. Let the EEG time series can be defined as

$$x = \{x_1, x_2, x_3, x_4, \dots, x_n\} \quad (2.1)$$

By taking absolute square i.e.

$$x = |x|^2 \quad (2.2)$$

For better clarity, the procedure with an order $N = 13$, i.e. 13×13 ($r \times c$) square matrix is considered, where the length of the EEG segment is 169 (which is nearly equal to 1 second). The same procedure applies for other orders of the matrices. Defining the matrix A from EEG time series with an order $N = 13$ (i.e. $r=13$ and $c=13$) as,

$$A = \begin{bmatrix} x_1 & x_2 & x_3 & \dots & x_{13} \\ x_{14} & x_{15} & x_{16} & \dots & x_{26} \\ \cdot & \cdot & \cdot & \dots & \cdot \\ \cdot & \cdot & \cdot & \dots & \cdot \\ x_{157} & x_{158} & x_{159} & \dots & x_{169} \end{bmatrix} \quad (2.3)$$

Generally for any matrix order with $N = r = c$, the sequential arrangement of EEG time series into matrix form as follows,

$$A = \begin{bmatrix} x_1 & x_2 & \dots & x_r \\ x_{r+1} & x_{r+2} & \dots & x_{r+r} \\ x_{2r+1} & x_{2r+2} & \dots & x_{2r+r} \\ \cdot & \cdot & \dots & \cdot \\ x_{(r-1)r+1} & x_{(r-1)r+2} & \dots & x_{(r-1)r+r} \end{bmatrix} \quad (2.4)$$

where r is the square matrix order.

According to the property of determinants, it can be both positive and negative [60]. To make features more worthy, absolute followed by the logarithm (base 10) of Det was taken i.e.

$$Determinant = \log_{10} |A| \quad (2.5)$$

Gauss elimination method was used due to its simplicity [63] to calculate the determinant of higher order matrix. The Gauss elimination method uses a sequence of elementary row operations (row reduction) to modify the matrix until matrix elements below the principal diagonal filled with zeros [63]. The following properties of determinant were considered for evaluation [64] for suitability of the proposed feature for the EEG time series.

1. $|A^T| = |A|$

Hence the EEG time series can also be arranged in column wise also.

2. $|B| = -|A|$

If two rows are interchanged to produce a matrix B from matrix A, the determinant remain same.

3. $|A| = 0$

A row where every entry is zero, or a column where every entry is zero.

4. $|A| = 0$

Suppose the square matrix with two equal rows, or two equal columns.

```
1. EEG=data.*data; % Variable data has EEG samples
2. p=1;
3. r=13,c=13; % Assuming order of the matrix is 13x13
4. for i=1:r
5.     for j=1:c
6.         EEG_mat(i,j)=EEG(p);
7.         p=p+1;
8.     end
9. end
10. Determinant=log10(abs(det(EEG_mat)));
```

FIGURE 2.3: MATLAB pseudo code to arrange the EEG time series in square matrix form and to compute its determinant.

5. $|A| = 0$

The matrix is singular if and only if $|A| = 0$

Due to its non-stationarity nature, the EEG time series cannot have zeros sequentially or periodically, hence matrix determinant cannot become zero for EEG time series data. Fig. 2.3 shows the pseudo code to convert EEG time series into matrix form and calculation of determinant value in MATLAB platform. The suggested code is very simple and straightforward, so that, it can be implemented on any software platform with less computational requirements.

2.3.4 Classifiers

To quantify the robustness and efficacy of the matrix determinant feature following three supervised learning algorithms were employed based on the previous best performances [9, 28, 42, 59, 65, 66, 67, 68]. The configuration of the classifiers is briefly described in this section.

2.3.4.1 Support vector machine

SVM is a supervised binary classifier; the kernel function is used to find the best hyperplane, which separates the training samples of binary class [23]. It was reported in the studies [9, 22, 65], that the quadratic kernel function attained better classification results and same was adopted in the present study.

2.3.4.2 K-nearest neighbor

K-NN is a non-parametric lazy learning algorithm for both binary and multi-classification [69]. K-NN algorithm is superior regarding ease to interpret the output, calculation time and predictive power. In this work, 9 nearest neighbors with Euclidean distance was used to compute the distance based on preliminary study results.

2.3.4.3 Multi-layer perceptron

MLP is a feed-forward back propagation network, consist of an input layer, hidden layer, and an output layer [70]. In the present work, optimal configured MLP neural network functions were used from the study [66]. 10 hidden neurons with tan-sigmoid at the hidden layer, pure linear at output layer and

Levenberg-Marquardt as learning function was identified as optimal configurations for the classification of epileptic EEG signals and same was used in our study.

2.3.5 Performance measures

The classification was performed using K-fold (K=10) cross-validation, in which, total observations are split into K folds. For each of K iterations, K-1 folds are used for training and a different fold for testing. The advantage of K-fold cross-validation is that all the observations in the dataset are eventually used for both training and testing. Finally, the performance of the algorithm was evaluated regarding specificity (SP), sensitivity (SE), and classification accuracy (CA), positive predictive value (PPV), and negative predictive value (NPV) [71]. Following terminologies were derived from confusion matrix: true positive (TP), false negative (FN), true negative (TN) and false positive (FP).

$$SE(\%) = \frac{TP}{TP + FN} \quad (2.6)$$

$$SP(\%) = \frac{TN}{TN + FP} \quad (2.7)$$

$$CA(\%) = \frac{TP + TN}{TP + FP + TN + FN} \quad (2.8)$$

$$PPV(\%) = \frac{TP}{TP + FP} \quad (2.9)$$

$$NPV(\%) = \frac{TN}{TN + FN} \quad (2.10)$$

2.4 Results

2.4.1 Descriptive analysis

Different matrix orders were considered for the experimental study. For better brevity, the time series data were appended, and the matrix determinant feature was estimated for the matrix order 13 [51]. Fig. 2.4 demonstrates the feature distribution plot as good discrimination between non-epileptic and epileptic EEG. In Fig. 2.4, the determinant values for epileptic epochs were higher than normal epochs including Set C and Set D. This shows that epileptic EEG using determinant feature is more distinguishable and predictable than normal EEG. Fig. 2.5 shows the Boxplot of five EEG conditions for matrix orders $N = 13, 16, 23,$ and 32 . It is clear that the matrix determinant feature derived from dataset set E is higher as compared to the set A, whereas set C is lower among all five datasets. Further, matrix determinant value is higher for set B as compared to set A, even though both the EEG signals reflect normal condition with differing in eye open and close respectively. Besides, Box plot results show that the increase in the segmentation length or matrix order increase the matrix determinant value.

The descriptive statistics of the matrix determinant feature regarding minimum, median, maximum, mean, standard deviation (SD), lower quartile (Q1), upper quartile (Q3), semi interquartile deviation (SID), and interquartile range

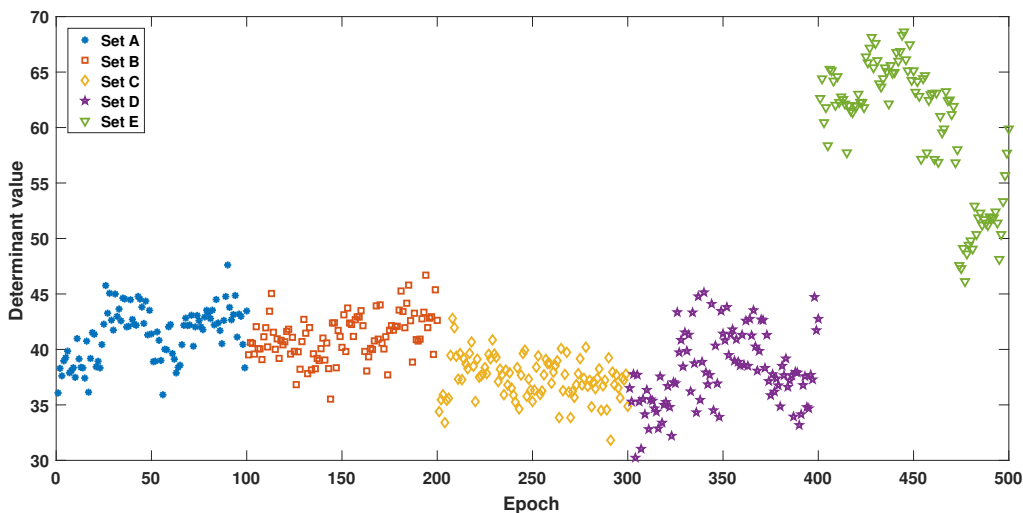
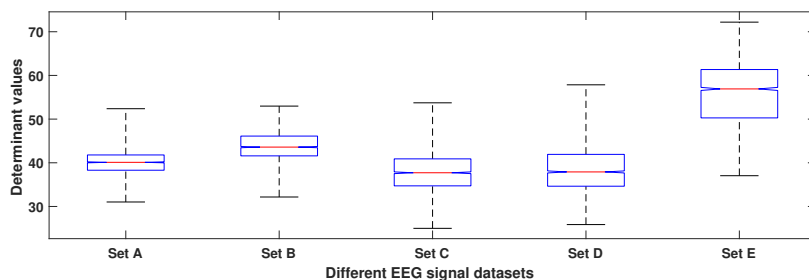
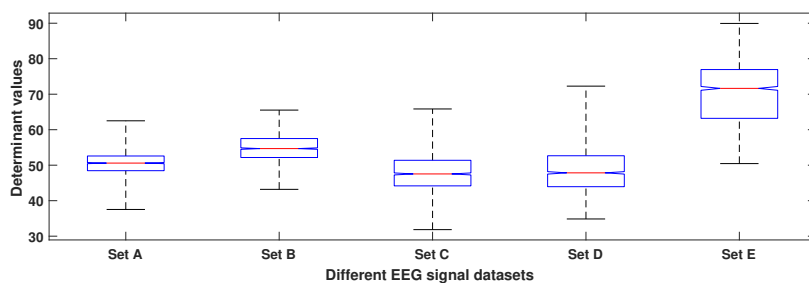


FIGURE 2.4: Matrix determinant feature for each EEG condition for the matrix order 13.

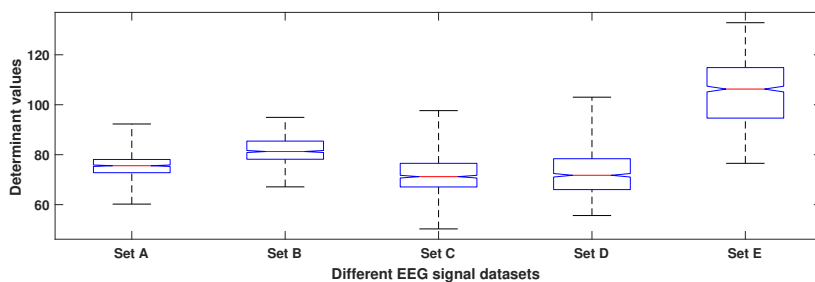
(IQR) was performed. The Q1 is the middle value in the first half of the rank-ordered dataset, and it is also called as $25^{th}\%$ percentile. Similarly, Q3 is the middle value in the second half of the rank-ordered dataset, and it is also called as $75^{th}\%$ percentile. Then, IQR is the difference between Q3 and Q1, and it is a measure of variability, based on dividing a data set into quartiles. Further, SID of a dataset is the half difference between the Q1 and Q3 or half the IQR. Table 2.4 shows the descriptive statistics of matrix determinant for all the five EEG subsets including different matrix orders. As can be seen, descriptive statistics parameters are well distinguishable between non-epileptic and epileptic EEG conditions, and the analysis shows that the matrix determinant values corresponding to epileptic EEG are higher as compared to non-epileptic EEG. It is clear that descriptive parameters increase as the matrix order increase for all the subsets of EEG. During the experimental study, Wilcoxon



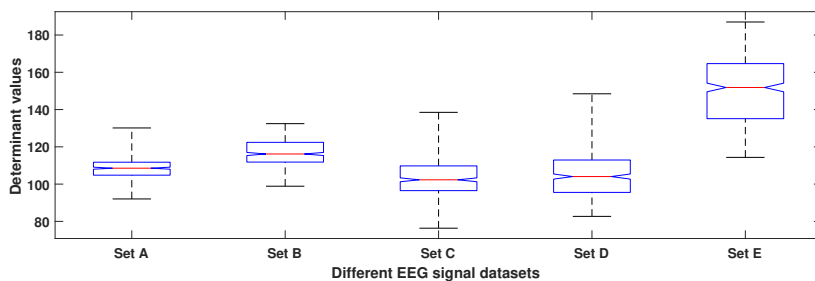
(a)



(b)



(c)



(d)

FIGURE 2.5: Box plot showing for set A, set B, set C, set D and set E EEG signals determinant values for the matrix orders (a) $N = 13$, (b) 16, (c) 23, (d) 32.

TABLE 2.4: Descriptive analysis of the matrix determinant feature.

Matrix order	EEG dataset	Min	Q1	Median	Mean	SD	Q3	IQR	Max	SID
13	Set A	31.02	38.29	40.10	39.95	2.85	41.79	3.49	52.38	1.74
	Set B	32.16	41.58	43.59	43.64	3.26	46.11	4.52	52.97	2.26
	Set C	24.90	34.71	37.71	38.04	4.86	40.89	6.17	53.72	3.08
	Set D	25.85	34.63	37.90	38.43	4.94	41.92	7.28	57.85	3.60
	Set E	37.04	50.27	56.91	56.03	6.73	61.34	72.19	72.198	5.53
16	Set A	37.52	48.43	50.59	50.37	3.34	52.59	4.13	62.50	2.06
	Set B	43.19	52.16	54.67	54.67	3.75	57.50	5.33	65.52	2.66
	Set C	31.84	44.17	47.53	47.97	5.85	51.38	7.20	65.84	3.60
	Set D	34.85	43.94	47.84	48.84	5.90	52.66	8.71	72.27	4.35
	Set E	50.45	63.20	71.64	70.49	8.23	76.94	13.74	89.94	6.87
23	Set A	60.21	72.78	75.58	75.23	4.56	78.08	5.29	92.29	2.64
	Set B	67.12	78.17	81.26	81.41	5.10	85.43	7.26	94.94	3.63
	Set C	50.28	67.08	71.20	71.86	8.12	76.53	9.45	97.64	4.72
	Set D	55.63	66.02	71.75	72.56	8.29	78.38	12.35	103.02	6.17
	Set E	76.54	94.64	106.27	105.02	11.84	114.87	20.22	132.84	10.11
32	Set A	92.03	104.79	108.54	108.06	6.17	111.74	6.95	130.13	3.47
	Set B	98.86	111.81	116.16	116.43	6.99	122.41	10.59	132.44	5.29
	Set C	76.34	96.49	102.30	103.49	11.31	109.76	13.26	138.50	6.63
	Set D	82.68	95.55	104.05	104.74	11.76	112.92	17.37	148.46	8.68
	Set E	114.33	135.11	151.84	150.49	16.82	164.65	29.54	186.98	14.77

rank sum test showed the $p < 0.05$ for all the classification problems indicating very high discrimination ability.

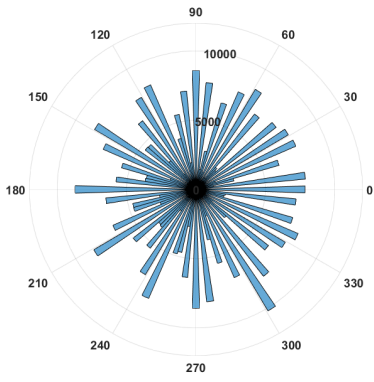
Histogram plot in polar coordinates shows the direction of each value and number of values that occur in each subinterval . Fig. 2.6 shows the histogram plot of five EEG datasets with corresponding matrix determinant values ($N = 13$) in polar coordinates. Fig. 2.6 shows that the set E (epileptic) has spread equally (densely distributed) between 0 to 2π , whereas not in the case of other EEG datasets. Similarly, the extracted determinant features (Matrix order $N = 13$) shows similar distribution. This helps to understand how far EEG values are spread in polar coordinates. Fig. 2.7 shows the bivariate plot for binary classification problems. Only equal numbers of observations in

classification problems were considered for the bivariate plot. Bivariate analysis shows that less overlap (few black boxes) between each class in all the binary classification problems. The lesser the variation implies good discrimination between two classes and produces good classification results. Fig. 2.8 shows mean and SD of extracted matrix determinant feature for all the orders. Above analysis shows that the mean and SD of Set E is high as compared to other subsets. It infers that the mean and SD of epileptic EEG varies significantly as compared to other non-epileptic EEG.

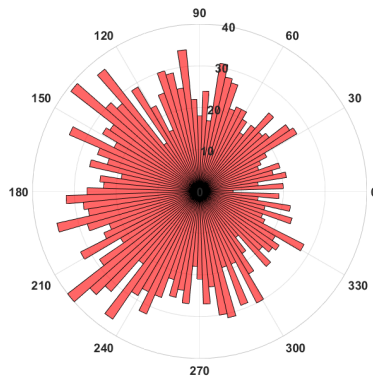
2.4.2 Classification results

The performance of the proposed approach was evaluated in terms of SE, SP, CA, PPV, and NPV. All the classification problems were evaluated using 10-fold cross-validation technique. Tables 2.5-2.13 show the classification results using all three classifiers for all the classification problems. For the most important classification problem {A}-{E}, performance measures were achieved greater than 96.50% using all the three classifiers with the maximum CA of 99.45%. Similarly, the CA of 96.06%, 97.60 %, and 97.60% was attained for the classification problems {B}-{E}, {C}-{E}, and {D}-{E} respectively.

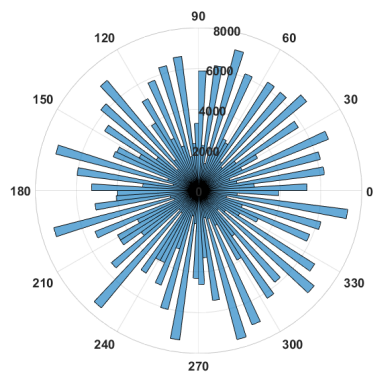
It was inferred from the reported literature that the majority of the studies has conducted the experiments using an equal number of observations in both the classes for classification. Considering only the half or quarter of the dataset makes improper validation of EEG signals for classification problem. In the present study, classification was performed using equal and unequal numbers of observations for the classification problems, namely {AB}-{E}, {AC}-{E}, {CD}-{E}, {ACD}-{E}, {ABCD}-{E}, and {AB}-{CD}-{E} and



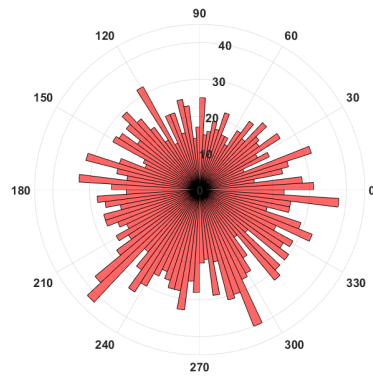
(a)



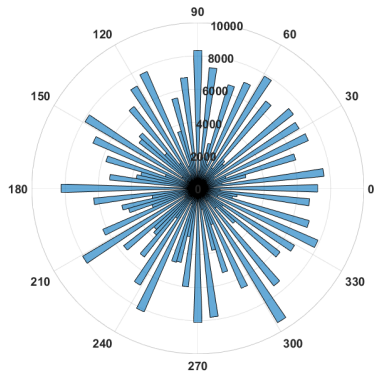
(b)



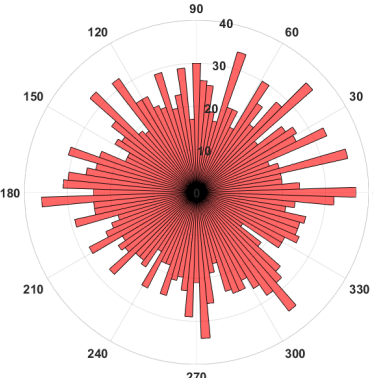
(c)



(d)



(e)



(f)

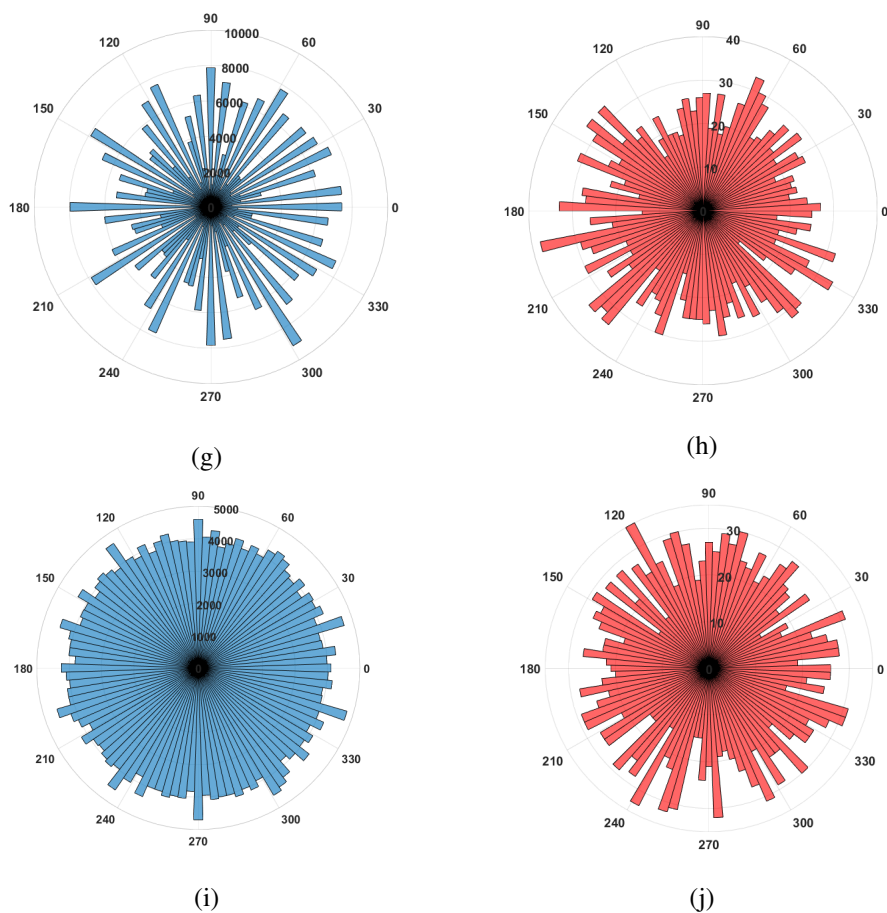


FIGURE 2.6: Histogram plot of EEG and its matrix determinant in polar ordinates. EEG datasets set A, B, C, D, and E is shown in (a), (c), (e), (g), and (i) respectively. Similarly, matrix determinant for EEG datasets set A, B, C, D, and E for matrix order 13 is shown in (b), (d), (f), (h), and (j) respectively.

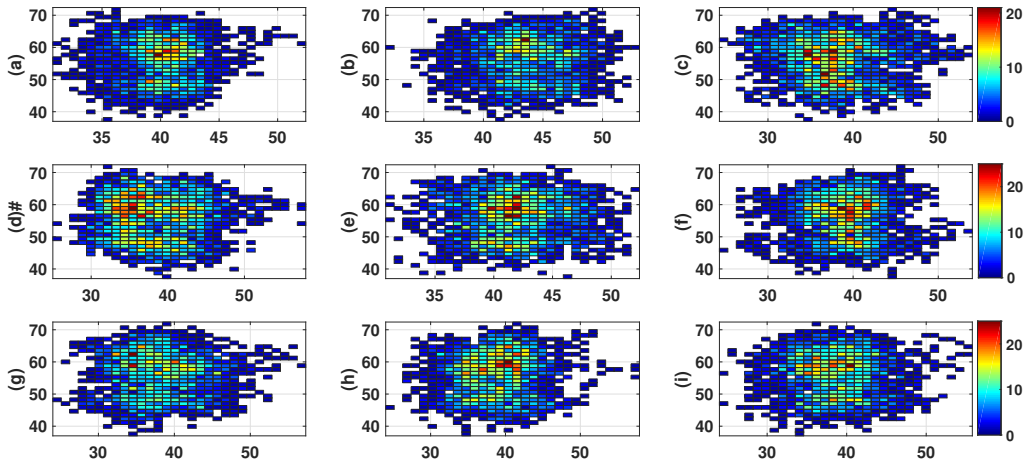


FIGURE 2.7: Bivariate plot for binary classification problems (a) {A}-{E} (b) {B}-{E} (c) {C}-{E} (d) {D}-{E} (e) {AB}-{E} (f) {AC}-{E} (g) {CD}-{E} (h) {ACD}-{E} (i) {ABCD}-{E}.

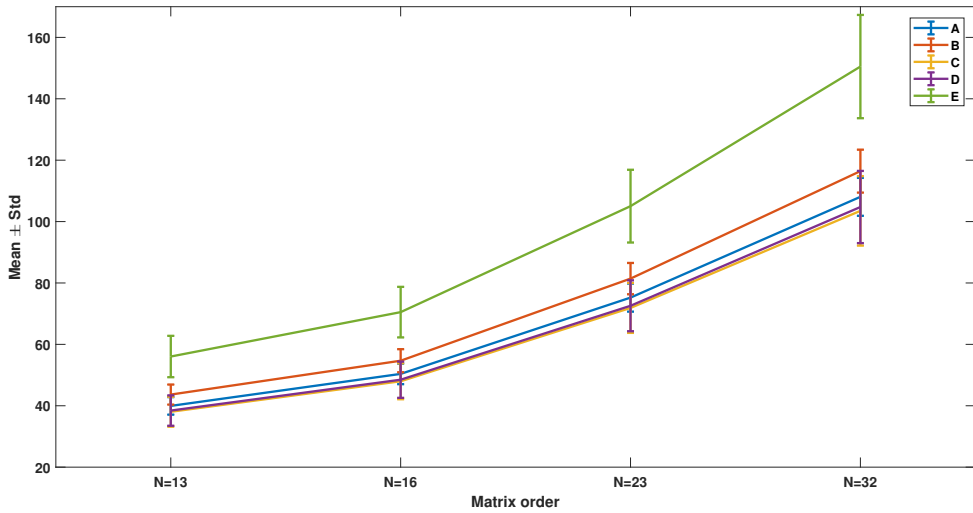


FIGURE 2.8: Mean and SD of the matrix determinant feature for different matrix orders.

its results are shown in Tables 2.7-2.13. Table 2.3 shows the number of observations considered for the classification for each matrix order. Results revealed the average CA of 97.10% and 97.35% for an equal and unequal number of observations for the classification problem {AB}-{E} respectively. Further, other performance measures such as SE, SP, PPV, and NPV showed better results. For the classification problems, {AC}-{E} and {CD}-{E}, average CA of 96.50% and 96.85% were achieved respectively, and it was almost same for both equal and unequal number of observations. Similarly, highest average CA of 96.00% and 97.20% were obtained for the classification problems {ACD}-{E} and {ABCD}-{E} respectively. Interestingly, less NPV was achieved for an unequal number of observations as compared to an equal number of observations for the classification task {CD}-{E}, {ACD}-{E}, {ABCD}-{E} due to less number of observations in set E.

Tables 2.12 and 2.13 shows the results of 3-class classifications problems {A}-{C}-{E} and {AB}-{CD}-{E} respectively. Classification problems {A}-{C}-{E} and {AB}-{CD}-{E} attained the highest CA of 94.75% and 96.52% respectively. The performance measure NPV was found to be less for an unequal number of observations as compared to an equal number of observation for the majority of the classification problems using all three classifiers.

It was further observed that more training time was required for an unequal number of observations for the SVM classifier. More importantly, performance measures were getting better as the segmentation length or matrix order increases for all the classification problems. Overall, all the three classifiers showed consistent results for all the classification problems.

TABLE 2.5: Classification results for classification problem {A}-{E} and {B}-{E}

Classifier	Performance measures	Matrix order							
		N=13	N=16	N=23	N=32	N=13	N=16	N=23	N=32
		Classification problem {A}-{E}				Classification problem {B}-{E}			
SVM	SE (%)	98.05	98.70	99.10	99.10	96.92	96.85	99.50	98.91
	SP (%)	96.50	97.62	98.52	99.25	83.45	86.30	91.24	92.80
	CA (%)	97.27	98.16	98.81	99.23	90.18	91.57	95.37	95.85
	PPV (%)	96.55	97.65	98.63	99.25	85.71	87.82	92.02	93.55
	NPV (%)	98.05	98.62	99.00	99.12	96.14	96.25	99.14	98.50
K-NN	SE (%)	98.08	98.48	98.58	99.13	92.70	96.25	97.46	98.45
	SP (%)	96.72	97.83	99.15	99.27	84.32	86.35	91.74	93.65
	CA (%)	97.40	98.15	98.86	99.20	88.51	91.30	94.60	96.06
	PPV (%)	96.70	97.85	99.15	99.29	85.75	87.82	92.59	94.12
	NPV (%)	97.46	98.16	98.65	99.10	91.89	95.66	97.09	98.16
MLP	SE (%)	97.12	98.05	99.22	99.70	96.23	96.85	95.16	96.10
	SP (%)	97.92	98.45	98.80	99.20	85.64	87.58	94.75	92.95
	CA (%)	97.52	98.25	99.01	99.45	90.93	92.21	94.95	95.52
	PPV (%)	97.90	98.42	98.81	99.25	83.31	85.69	94.68	92.12
	NPV (%)	96.71	98.12	99.24	99.71	97.13	97.54	95.22	96.62

TABLE 2.6: Classification results for classification problem {C}-{E} and {D}-{E}

Classifier	Performance measures	Matrix order							
		N=13	N=16	N=23	N=32	N=13	N=16	N=23	N=32
		Classification problem {C}-{E}				Classification problem {D}-{E}			
SVM	SE (%)	93.80	94.22	95.42	95.75	94.10	95.30	96.02	95.80
	SP (%)	96.10	97.22	98.48	99.45	94.90	96.20	98.08	99.40
	CA (%)	94.95	95.22	96.45	97.60	94.50	95.25	97.05	97.60
	PPV (%)	95.85	96.98	98.46	99.22	94.74	96.20	98.01	99.10
	NPV (%)	94.10	94.43	95.45	95.10	94.60	95.29	96.13	95.85
K-NN	SE (%)	93.26	95.20	95.64	95.20	93.80	95.45	95.38	94.90
	SP (%)	95.50	96.50	97.44	98.70	94.90	96.55	98.60	99.45
	CA (%)	94.38	95.40	96.55	96.95	94.85	95.00	96.39	97.62
	PPV (%)	95.35	96.53	97.72	98.59	94.71	96.42	98.51	99.24
	NPV (%)	93.52	95.14	95.82	95.42	93.82	95.51	95.55	95.32
MLP	SE (%)	96.62	97.82	98.15	98.50	94.82	96.10	99.20	99.20
	SP (%)	93.34	93.92	95.45	95.70	94.80	95.30	95.00	95.50
	CA (%)	94.95	95.86	96.30	97.20	94.81	95.70	97.10	97.35
	PPV (%)	93.08	93.75	98.05	95.20	94.80	96.55	98.90	99.55
	NPV (%)	96.87	95.62	95.54	97.20	94.95	95.25	94.70	95.12

TABLE 2.7: Classification results for classification problem {AB}-{E}

Classifier	Performance measures	Matrix order							
		N=13		N=16		N=23		N=32	
			⌘		⌘		⌘		⌘
SVM	SE (%)	96.30	95.74	96.18	97.40	97.12	97.72	96.40	97.65
	SP (%)	90.75	94.30	93.20	92.00	96.26	95.02	97.20	95.65
	CA (%)	93.65	95.02	94.69	95.70	96.69	96.37	96.80	96.65
	PPV (%)	91.42	93.29	93.50	96.26	96.43	99.20	97.24	99.40
	NPV (%)	95.90	97.89	95.92	97.12	96.87	92.64	96.20	92.11
K-NN	SE (%)	94.30	99.22	96.30	96.38	96.40	95.38	95.55	99.70
	SP (%)	91.25	95.20	92.28	87.90	95.33	90.16	96.70	90.80
	CA (%)	92.77	92.21	94.29	92.14	95.86	92.77	96.12	95.25
	PPV (%)	91.52	94.80	92.71	96.15	91.65	97.05	96.62	97.30
	NPV (%)	93.95	93.85	95.90	96.45	96.27	96.66	95.60	95.79
MLP	SE (%)	92.50	94.80	92.10	95.35	96.40	98.10	95.70	98.20
	SP (%)	94.90	96.90	97.45	98.05	97.45	95.20	98.50	96.50
	CA (%)	93.70	95.85	94.77	96.70	96.92	97.15	97.10	97.35
	PPV (%)	95.15	95.65	97.82	98.62	97.32	99.35	98.75	98.16
	NPV (%)	92.10	85.35	91.42	85.95	96.15	92.42	95.16	93.00

TABLE 2.8: Classification results for classification problem {AC}-{E}

Classifier	Performance measures	Matrix order							
		N=13		N=16		N=23		N=32	
			⌘		⌘		⌘		⌘
SVM	SE (%)	94.14	94.43	94.50	94.66	95.09	95.48	95.00	95.37
	SP (%)	94.39	94.22	95.31	95.37	97.29	96.90	98.00	97.75
	CA (%)	94.27	94.33	94.91	95.02	96.19	96.19	96.50	96.56
	PPV (%)	94.38	97.03	95.27	97.62	97.23	98.40	97.94	98.83
	NPV (%)	94.16	89.43	94.54	89.92	95.2	91.46	95.15	91.36
K-NN	SE (%)	93.07	95.48	94.50	95.87	94.96	96.51	95.25	96.25
	SP (%)	94.06	91.46	96.00	93.44	96.77	93.93	97.75	96.50
	CA (%)	93.56	93.47	95.25	94.66	95.87	95.22	96.50	96.38
	PPV (%)	94.00	95.72	95.94	96.69	96.71	96.95	97.69	98.21
	NPV (%)	93.14	91.01	94.58	91.89	95.05	93.09	95.37	92.79
MLP	SE (%)	95.00	96.40	96.00	97.50	97.00	98.80	97.40	98.80
	SP (%)	93.50	90.90	94.20	90.10	95.20	91.30	95.60	92.40
	CA (%)	94.30	94.50	95.10	94.90	96.10	96.00	96.50	96.60
	PPV (%)	95.10	95.40	96.10	94.80	97.00	95.30	97.50	97.80
	NPV (%)	93.40	92.90	94.10	95.20	95.10	97.20	95.50	96.00

TABLE 2.9: Classification results for classification problem {CD}-{E}

Classifier	Performance measures	Matrix order							
		N=13		N=16		N=23		N=32	
			⊥		⊥		⊥		⊥
SVM	SE (%)	92.25	90.55	93.00	93.28	93.32	93.32	93.75	93.54
	SP (%)	93.50	92.35	94.50	92.52	96.54	95.54	97.85	97.25
	CA (%)	92.85	91.45	93.75	92.90	94.93	94.43	95.80	95.39
	PPV (%)	93.38	92.36	94.50	92.42	96.47	94.55	97.63	98.62
	NPV (%)	92.27	87.45	93.23	88.90	93.55	88.95	93.82	88.95
K-NN	SE (%)	91.40	94.65	93.32	92.50	92.76	91.65	93.80	94.45
	SP (%)	92.65	88.32	94.23	91.56	95.65	95.25	97.75	94.30
	CA (%)	92.02	91.48	93.77	92.03	94.20	93.45	95.77	94.37
	PPV (%)	92.68	94.10	94.13	96.58	95.81	96.93	97.64	97.55
	NPV (%)	91.35	89.12	93.81	87.62	92.92	88.57	93.97	89.02
MLP	SE (%)	93.50	94.30	94.85	95.90	95.20	96.42	97.60	96.28
	SP (%)	92.20	90.40	93.45	92.10	94.60	90.56	94.30	91.36
	CA (%)	92.85	93.35	94.00	94.15	94.40	93.49	96.95	93.82
	PPV (%)	93.75	95.93	95.00	96.38	94.32	92.15	94.25	95.53
	NPV (%)	91.88	88.48	93.00	89.22	95.17	92.22	97.76	93.20

TABLE 2.10: Classification results for classification problem {ACD}-{E}

Classifier	Performance measures	Matrix order							
		N=13		N=16		N=23		N=32	
			⊥		⊥		⊥		⊥
SVM	SE (%)	93.80	92.50	94.46	93.58	94.78	95.65	94.66	95.80
	SP (%)	93.85	93.80	95.03	93.65	97.30	94.45	97.32	96.10
	CA (%)	93.82	93.15	94.74	93.61	96.04	95.05	95.99	95.95
	PPV (%)	93.75	94.58	94.26	94.50	97.12	96.32	97.11	94.44
	NPV (%)	93.91	92.13	94.45	92.60	94.63	92.36	94.82	92.12
K-NN	SE (%)	92.80	96.37	94.32	96.40	94.66	96.41	95.20	95.62
	SP (%)	94.25	87.80	95.32	90.10	96.71	91.21	96.80	92.85
	CA (%)	93.52	92.08	94.82	93.25	95.68	93.81	96.00	94.23
	PPV (%)	94.18	95.87	95.45	96.66	96.57	97.10	96.76	97.59
	NPV (%)	92.74	88.89	94.16	89.50	94.39	89.51	95.15	87.69
MLP	SE (%)	94.45	96.02	96.50	96.05	97.20	97.40	97.80	98.20
	SP (%)	93.05	90.18	93.30	91.35	94.80	90.80	94.05	88.76
	CA (%)	93.75	93.10	94.90	93.70	96.00	94.10	95.92	93.48
	PPV (%)	94.58	96.45	93.25	97.38	97.10	96.65	97.48	94.40
	NPV (%)	93.03	88.36	96.32	87.98	94.30	92.30	94.24	95.40

TABLE 2.11: Classification results for classification problem {ABCD}-{E}

Classifier	Performance measures	Matrix order							
		N=13		N=16		N=23		N=32	
			⊥		⊥		⊥		⊥
SVM	SE (%)	93.72	95.86	94.29	96.52	96.88	96.79	95.79	95.60
	SP (%)	92.45	97.69	94.01	97.72	95.79	96.04	96.72	96.10
	CA (%)	93.08	96.77	94.15	97.12	96.33	96.41	96.25	95.85
	PPV (%)	92.59	97.62	94.30	98.68	95.52	98.11	96.52	98.37
	NPV (%)	93.45	80.28	94.18	81.52	96.93	83.67	95.81	82.59
K-NN	SE (%)	92.35	96.58	94.85	99.55	95.29	98.48	96.35	99.35
	SP (%)	92.42	80.69	93.43	84.47	96.57	87.69	96.35	87.35
	CA (%)	92.38	88.63	94.14	92.01	95.93	93.08	96.35	93.57
	PPV (%)	92.29	96.38	93.62	97.69	96.38	99.02	96.35	98.28
	NPV (%)	92.02	91.21	94.45	92.50	95.29	93.56	96.35	93.05
MLP	SE (%)	92.60	96.40	94.30	97.75	97.20	98.60	96.55	97.90
	SP (%)	93.50	93.60	93.90	94.35	96.30	97.80	96.50	96.50
	CA (%)	93.05	95.00	94.10	96.05	96.80	98.50	96.52	97.20
	PPV (%)	93.50	97.10	94.85	96.20	97.30	96.22	96.35	97.65
	NPV (%)	92.50	80.50	93.36	84.20	96.30	84.50	96.65	85.85

TABLE 2.12: Classification results for classification problem {A}-{C}-{E}

Classifier	Performance measures	Matrix order			
		N=13	N=16	N=23	N=32
SVM	SE (%)	92.85	92.25	94.14	94.10
	SP (%)	89.32	92.35	94.60	94.69
	CA (%)	91.08	92.30	94.37	94.39
	PPV (%)	89.89	92.15	94.27	94.72
	NPV (%)	92.27	92.23	94.21	94.00
K-NN	SE (%)	92.80	92.48	93.15	94.45
	SP (%)	88.69	91.42	94.32	92.08
	CA (%)	90.74	91.94	93.73	92.24
	PPV (%)	89.68	91.50	94.10	93.19
	NPV (%)	92.27	92.36	93.14	92.33
MLP	SE (%)	90.50	92.15	95.40	94.70
	SP (%)	93.70	91.60	93.10	94.80
	CA (%)	92.10	91.87	94.25	94.75
	PPV (%)	94.32	92.63	95.20	94.50
	NPV (%)	92.60	91.27	93.30	94.82

TABLE 2.13: Classification results for classification problem {AB}-{CD}-{E}

Classifier	Performance measures	Matrix order							
		N=13		N=16		N=23		N=32	
			⊥		⊥		⊥		⊥
SVM	SE (%)	94.68	95.66	93.85	96.10	96.84	96.45	96.40	95.36
	SP (%)	91.52	90.38	93.60	97.10	96.23	96.12	96.64	95.70
	CA (%)	93.10	94.02	93.73	96.60	96.53	96.28	96.52	95.53
	PPV (%)	91.80	94.39	93.62	98.50	96.33	95.36	96.57	94.10
	NPV (%)	94.42	95.52	93.83	89.80	96.71	91.30	96.21	91.36
KNN	SE (%)	94.56	94.54	93.84	93.44	95.07	97.40	96.50	95.10
	SP (%)	90.57	92.27	93.63	90.73	96.50	93.57	94.50	97.10
	CA (%)	92.56	93.40	93.73	92.08	95.78	95.38	95.50	96.05
	PPV (%)	91.05	94.60	93.16	97.00	96.31	94.60	95.00	95.86
	NPV (%)	94.48	94.84	93.67	91.50	95.20	92.55	96.50	92.70
MLP	SE (%)	90.05	93.45	94.36	97.45	96.88	98.40	96.40	96.80
	SP (%)	95.46	98.40	93.24	93.20	95.50	92.80	92.30	93.60
	CA (%)	92.75	95.95	93.80	95.32	96.19	94.60	94.35	95.20
	PPV (%)	96.01	94.24	94.10	94.88	90.30	97.36	96.20	95.35
	NPV (%)	94.32	94.40	93.34	91.72	95.10	94.70	96.30	95.56

2.4.3 Classification results using RMCH database

The proposed method validated on another EEG database collected from RMCH, Bengaluru, India after ethical clearance obtained to use the EEG recordings for research purpose. These unipolar recordings were recorded using 19 scalp electrodes (Fp1, Fp2, F7, F3, Fz, F4, F8, T3, C3, Cz, C4, T4, T5, P3, Pz, P4, T6, O1, and O2) placed according to the 10-20 International system. The scalp EEG was recorded at a sampling rate of 128 Hz using Galileo Suite NB Neuro digital EEG system. These recordings were collected from 115 subjects that include 67 male and 48 female ranging between 2.5 to 75 years of age. Two experts at Ramaiah Medical College and Hospital visually labelled the EEG as normal and epileptic. In total, 222 seizures were found from 58 hours of EEG which was collected from 115 subjects. Further, a 50 Hz notch filter

was applied on EEG to remove the power line noise. Next, independent component analysis was applied to remove the artefact's like eye blink, electrode displacement and muscle artefact's [72].

The determinant feature was extracted using matrix orders $N = 13, 16, 23$ and 32 and classified using SVM, K-NN, and MLP classifiers. Table 2.14 shows the classification results obtained using RMCH database. The highest sensitivity of 98.90%, specificity of 96.57%, accuracy of 97.56%, PPV of 95.47%, and NPV of 99.20% was reported using matrix order 32. We observe that the classification results increases as the matrix order increases. Both SVM and K-NN classifiers have shown the almost similar results for all the different matrix orders. However, the results obtained using K-NN were slightly lesser than other two classifiers. The better results obtained on RMCH database ensures the suitability of proposed methods on different EEG database.

2.5 Discussion

In this study, matrix determinant was proposed for the first time as the feature for epileptic EEG analysis. In total, eleven different classification problems using four different matrix orders were considered. The feature was evaluated using three supervised classifiers, namely SVM, K-NN and MLP with 10-fold cross-validation technique. Simulation results shows that information captured by EEG during epileptic activity which influences to rise in the matrix determinant acts as a biomarker to identify those events. In particularly, the change in the amplitude values during seizure activity was highlighted by higher determinant value. We observe that during the transition from normal

TABLE 2.14: Classification results using RMCH database

Classifier	Performance measures	Matrix order			
		N=13	N=16	N=23	N=32
SVM	SE (%)	97.48	97.68	98.45	98.52
	SP (%)	96.07	96.28	96.41	96.60
	CA (%)	96.77	96.98	97.43	97.56
	PPV (%)	94.45	95.02	95.23	95.47
	NPV (%)	98.13	98.28	98.84	98.36
K-NN	SE (%)	93.25	93.38	95.49	95.58
	SP (%)	95.41	95.43	96.00	96.57
	CA (%)	94.33	94.41	95.74	96.07
	PPV (%)	93.67	93.70	94.55	95.34
	NPV (%)	95.10	95.20	96.69	93.38
MLP	SE (%)	97.90	97.70	98.60	98.90
	SP (%)	95.50	96.20	96.30	96.50
	CA (%)	96.70	96.80	97.30	97.50
	PPV (%)	94.50	95.00	95.10	95.00
	NPV (%)	98.40	98.30	98.90	99.20

to pre-ictal state, determinant feature decreases and significantly increases for seizure activity.

Virtual EEG database of 230s was created using normal (set A) and epileptic (set E) EEG recordings for clinical validation using the same database. Fig. 2.9 shows the clinical validation results of the virtual EEG. It was classified by calculating matrix determinant feature (order $N = 13$) followed by SVM classifier. Initially, SVM classifier was trained with the targets 0 and 1 for normal and epileptic activities respectively. Furthermore, results shown in Fig. 2.9 were validated by experts to ensure that classification results were accurate.

During the experimental study, properties of matrix determinants were examined (refer to Fig. 2.3). The properties 1 and 2 were verified, whereas properties 3 to 5 were not encountered. Hence, this infers the suitability of

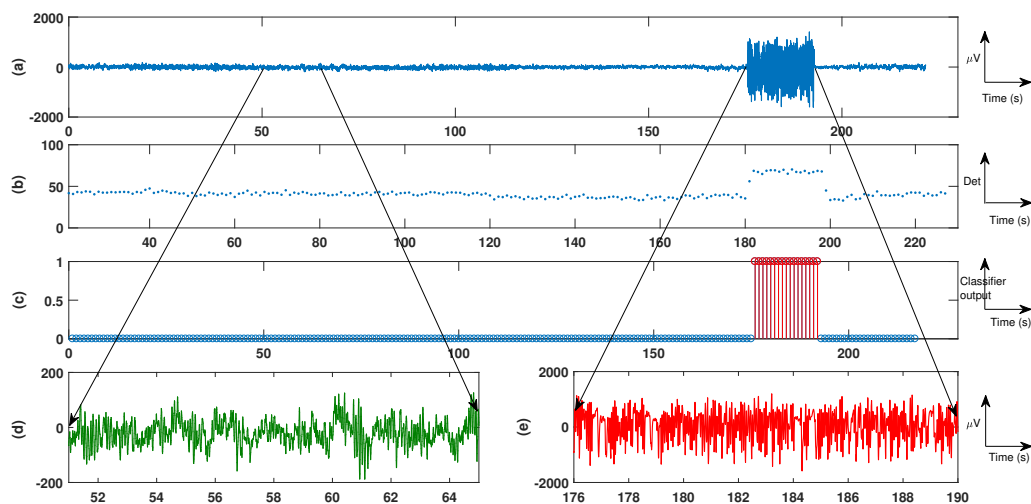


FIGURE 2.9: A representative example of EEG validated using the matrix determinant feature. (a) An epileptic EEG of duration 230s. (b) Each point shows matrix determinant calculated using the matrix order $N=13$. (c) SVM classifier output, targets 0 and 1 represents normal and epileptic states respectively. (d) Normal EEG from 51s to 65s. (e) Epileptic EEG from 176s to 190s.

the proposed feature for pattern recognition. As a future expansion, proposed algorithm will be tested on long-term EEG recordings with more number of patient data.

Fig. 2.10 shows the receiver operating characteristic curve and the area under the curve for binary classification problems using University of Bonn and RMCH data. The highest area under the curve of 0.9972 and 0.9852 was attained using University of Bonn and RMCH database.

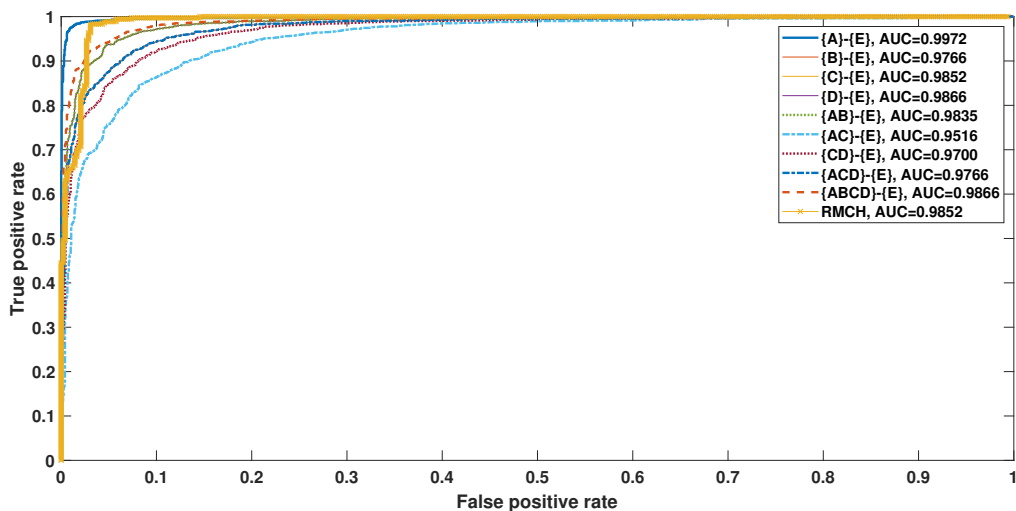


FIGURE 2.10: Receiver operating characteristic curve with area under the curve for binary classification problems. Only the best results of each classification problem is shown.

TABLE 2.15: Comparison of proposed determinant feature results with state-of-the-art methods using University of Bonn database.

Classification problem	Authors	Method	Accuracy (%)
{A}-{E}	[41]	EMD and genetic programming	98.64
	[52]	EMD and SVM	99.00
	[28]	DSTFT and MLP	99.80
	[53]	Weighted complex networks and SVM	100
	[73]	Wavelet and PNN	99.72
	[38]	Time frequency analysis and ANN	100
	[74]	Permutation entropy and SVM	93.55
	[34]	TQWT and K-NN	100
	[46]	DTCWT and CVNN	99.50
	[44]	ATFFWT and LS-SVM	100
[75]	Optimal orthogonal wavel and LS-SVM	100	

	[76]	Local binary pattern and BayesNet	99.00
	[77]	EMD and linear programming boosting	100
	[78]	DWT and MLPNN	100
	[27]	ApEn and ANN	99.60
	[9]	Entropies and Fuzzy classifier	99.00
	[21]	WPT based entropies and ANN	99.70
	Proposed	Matrix determinant and MLP	99.45
{B}-{E}	[53]	Weighted complex networks and SVM	99.76
	[74]	Permutation entropy and SVM	93.55
	[44]	ATFFWT and LS-SVM	82.88
	[28]	DSTFT and MLP	99.30
	Proposed	Matrix determinant and MLP	96.06
{C}-{E}	[53]	Weighted complex networks and SVM	96.00
	[44]	ATFFWT and LS-SVM	99.00
	[34]	TQWT and K-NN	99.50
	[74]	Permutation entropy and SVM	88.00
	[28]	DSTFT and MLP	98.50
	Proposed	Matrix determinant and MLP	97.60
{D}-{E}	[52]	EMD and SVM	93.00
	[28]	DSTFT and MLP	94.90
	[53]	Weighted complex networks and SVM	93.70
	[76]	Local binary pattern and BayesNet	95.50
	[74]	Permutation entropy and SVM	79.94
	[44]	ATFFWT and LS-SVM	98.50
	[34]	TQWT and K-NN	98.00
	[58]	LMD and SVM	98.10
	[43]	EMD and linear programming boosting	97.00
	Proposed	Matrix determinant and MLP	97.60
{AB}-{E}	[53]	Weighted complex networks and SVM	96.40
	Proposed	Matrix determinant and MLP	97.10
{AC}-{E}	Proposed	Matrix determinant and MLP	96.50

{CD}-{E}	[53]	Weighted complex networks and SVM	94.50
	Proposed	Matrix determinant and MLP	96.85
{ACD}-{E}	[41]	EMD and genetic programming	98.61
	[53]	Weighted complex networks and SVM	96.50
	Proposed	Matrix determinant and MLP	96.00
{ABCD}-{E}	[41]	EMD and genetic programming	98.89
	[46]	DTCWT and	99.13
	[38]	Time frequency analysis and ANN	97.73
	[34]	TQWT and K-NN	99.00
	[74]	Permutation entropy and SVM	86.16
	[44]	ATFFWT and LS-SVM	99.20
	[58]	LMD and SVM	98.87
	[52]	EMD and SVM	96.00
	[28]	DSTFT and MLP	98.10
	[53]	Weighted complex networks and SVM	94.00
	[78]	DWT and MLPNN	99.60
	[77]	EMD and linear programming boosting	99.20
	Proposed	Matrix determinant and MLP	97.20
{A}-{C}-{E}	Proposed	Matrix determinant and MLP	94.75
{AB}-{CD}-{E}	[41]	EMD and genetic programming	98.33
	[46]	DTCWT and CVNN	97.79
	[38]	Time frequency analysis and ANN	97.72
	[34]	TQWT and K-NN	98.60
	[78]	DWT and MLPNN	95.60
	[58]	LMD and SVM	98.40
	[52]	EMD and SVM	93.00
	[77]	EMD and linear programming boosting	97.60
Proposed	Matrix determinant and MLP	96.50	

Table 2.15 shows the comparison results between proposed matrix determinant and other state-of-the-art approaches. A novel genetic programming approach derived from EMD attained 98% overall classification accuracy using CGP and 10-fold cross-validation technique [41]. In [43], TQWT and bootstrap aggregating (Bagging) based approach showed 100% accuracy. This study decomposed EEG signal up to 29 sub-bands to select significant difference between normal and epileptic. [47] have used DWT followed by ApEn and showed a CA of 100% for classification problem {A}-{E}. [28] have proposed a novel feature extraction approach using DSTFT and MLP classifier and attained a CA of 98.1%. An interesting observation made from the studies reported by [28, 38, 41, 42, 43, 45, 48, 49, 50, 52, 58, 59, 77] was that they have applied one of the following preprocessing or decomposition technique EMD, LMD, DWT, SPWVD, TQWT, DTCWT and DSTFT on EEG signals to attain better performance. However, the proposed approach showed similar results without using any of the decomposition techniques ensuring lower computational cost. It is known that the introduction of any preprocessing procedure and decomposition technique leads to the additional computational burden which was evident from the studies reported [22, 36, 47].

Table 2.16 shows the execution time required to estimate the features at 1 s segmentation length for both the database. It is evident from Table 2.16 that the proposed feature proves to be superior regarding execution time as compared to other features reported in the literature.

The main findings of the proposed study are:

1. Eleven classification problems were considered to ensure the suitability of the matrix determinant feature for the detection of epileptic seizures.

TABLE 2.16: Execution time (sec) required to extract the features

Feature	University of Bonn	RMCH
DWT-ApEn [47]	82.31	9.21
ApEn [27]	57.58	6.44
Sample entropy [9]	34.71	3.88
Wavelet packet log energy entropy [21]	14.43	1.63
Wavelet packet entropy [36]	7.68	1.12
Matrix determinant	2.43	0.26

The accuracy of more than 96% was attained for all the classification problems, and average accuracy of 99.45% was achieved for the classification problem {A}-{E}.

2. The studies proposed by [28, 38, 41, 42, 43, 45, 48, 49, 50, 52, 58, 59] have applied decomposition techniques to achieve 100% accuracy for the classification problem {A}-{E}, whereas the proposed study reached accuracy of 99.45% without the help of any EEG signal decomposition method.
3. The proposed method shows the classification accuracy of 97.56% using RMCH database that is considered to be larger database than University of Bonn.
4. Classification was performed using both equal and unequal number of observations, to the best of authors knowledge no studies have reported such results. Training duration of all three classifiers for unequal number observations was found to be more.
5. Experimental results show the improvement in performance measures as the matrix order or a segmentation length increase.

6. The performance measure NPV was found to be less for an unequal number of observations for the classification.
7. Descriptive analysis showed the clear discrimination between non-epileptic and epileptic EEG for all the four matrix orders.
8. Computational time required to extract matrix determinant feature found to be very less as compared to features like ApEn, sample entropy, and permutation entropy.
9. Histogram of epileptic EEG in polar coordinates shows the same spread between 0 to 2π , whereas not in the case of normal EEG.
10. Bivariate analysis for binary classification of an equal number of observations proves the less overlap or correlation between set E and other EEG datasets.
11. Finally, the validation of proposed algorithm on University of Bonn and RMCH database implies the generalization and robustness of the novel determinant feature.

Despite the use of the widely used University of Bonn and our own RMCH EEG database in this work, it is still essential to validate on the more extensive database. As a future work, matrix determinant will be explored on other problems like sleep detection, depth of anesthesia etc. Further, we will explore the deep neural network for classification of epileptic seizures.

2.6 Conclusion

A novel matrix determinant feature was proposed in this study for the classification of epileptic seizures EEG signals. In total, eleven classification problems were formed using University of Bonn database and algorithm was validated on RMCH database. Initially, the EEG time series were sequentially arranged to form a square matrix of order, say, $N = 13, 16, 23$ and 32 , and matrix determinant were computed. The proposed feature was examined using descriptive analysis, bivariate histogram analysis and histogram plot in polar ordinates. The efficacy of the algorithm was evaluated using SVM, K-NN and MLP classifiers with 10-fold cross-validation. Experimental results show the highest classification accuracy of 99.45% (using University of Bonn database) and 97.56% (using RMCH database) and consistent performance for all the classification problems using all the three classifiers. The performance of the proposed approach was compared with several state-of-the-art feature extraction methods employed in the detection of an epileptic seizure. Hence, the proposed approach would be useful for the recognition of epileptic seizures from normal EEG in real-time.

Author credit statement

SR and NS formulated the problem statement. SR involved in writing codes, simulations, and paper writing. NS validated the results and reviewed the manuscript. PLK and ASH involved in clinical validation, clinical discussion and review process.

Acknowledgment

Authors would like to thank Dr. R.G. Andrzejak, for providing permission to use EEG database for research work. The authors are grateful to doctors of Institute of Neuroscience, Ramaiah Medical College, and Hospitals, Bengaluru, India, for valuable discussion and providing EEG recordings for research purpose.

CHAPTER 3

Automated detection of epileptic seizures
using successive decomposition index and
support vector machine classifier in
long-term EEG

S Raghu, Natarajan Sriraam, Shyam Vasudeva Rao, Alangar Sathyaranjan
Hegde, Pieter L Kubben

Neural Computing and Applications, 32: 8965-8984

Year: 2019

<https://doi.org/10.1007/s00521-019-04389-1>

Abstract

Epilepsy is a commonly observed long-term neurological disorder that impairs nerve cell activity in the brain and has a severe impact on people's daily lives. Accurate seizure detection in the long-term electroencephalogram (EEG) signals has gained vital importance in the diagnosis of patients with epilepsy. Visual interpretation and detection of epileptic seizures in long-term EEG is a time-consuming and burdensome task for neurologists. Therefore, in this study, we propose a computationally efficient automated seizure detection model using a novel feature called successive decomposition index (SDI). We observed that the SDI feature was significantly higher during the epileptic seizure as compared to normal EEG. The performance of the proposed method was evaluated using three databases, namely the Ramaiah Medical College and Hospital (DB1), CHB-MIT (DB2) and the Temple University Hospital (DB3) consisting of 58 hours, 884 hours, and 408 hours of EEG respectively. Experimental results revealed the sensitivity - false detection rate - median detection delay of 97.53%-0.4/h-1.5 sec, 97.28%-0.57/h-1.7 sec, and 95.80%-0.49/h-1.5 sec for DB1, DB2, and DB3 respectively using the support vector machine classifier. The proposed method significantly outperformed previously presented methods (wavelets and other feature extraction methods) while being computationally more efficient. Further, to the best of the author's knowledge, present study is the first study that was tested on three different EEG databases and showed consistent results leading to the generalization and robustness of the algorithm. Hence, the proposed method is an efficient tool for neurologists to detect epileptic seizures in long-term EEG.

3.1 Introduction

Epilepsy is the fourth most common neurological disorder and affects 65 million people of all ages around the world [1, 2, 79]. It is a chronic disorder that causes unprovoked recurrent seizures and characterized by unpredictable seizures that leads to health problems [2, 14, 79]. Epilepsy is treated using medication, surgery, vagus nerve stimulation, deep brain stimulation of the anterior nucleus of the thalamus [4], responsive neurostimulation, and dietary therapy [1, 5]. In epilepsy patients, seizure traces can be identified using electroencephalogram (EEG), electrocorticography (ECoG), stereo-EEG and non-invasive imaging techniques (e.g., PET, SPECT, and fMRI). Epilepsy patients undergo pre-surgical investigation prior to surgery that determines the area where the seizure begins. Long-term EEG is the potential brain parameter for the pre-surgery examination that concludes the need for surgery. In the EEG time series, the appearance of traces of spikes or sharp waves does indicate the reflection of seizure activities. The routine EEG shows the temporal and spatial information regarding brain activity, which is used to diagnose, monitor, and localize the epileptogenic focus. Interpreting long-term EEG for presurgical evaluation lasting several hours to days is a time-consuming and burdensome task since epileptic activities present in a small percentage of the entire data. However, robust seizure detection remains a challenging problem, due to the absence of adequate seizures EEG for training and testing. These challenges have motivated for development of automated seizure detection algorithm using three databases [2, 9, 79]. Thus, our study focuses on introducing an automated system using a novel feature and support vector

machine (SVM) classifier that is competent in recognizing the seizure onset quickly with better sensitivity and less detection delay. We expect that such system support the neurologist to overcome visual inspection and avoid human errors.

EEG is the gold standard for the classification of seizures and the diagnosis of epilepsy in terms of cost and safety. [2, 6, 7, 8, 9, 10]. The morphological shape of seizure EEG are spikes (20-70 ms), sharp waves (70-200 ms), and spike-and-wave discharges (a spike followed by a slow wave) referred to as epileptic waves [1, 12, 13]. In other words, seizure onset is characterized by a sudden change in frequency and the appearance of a new rhythm. Spikes and sharp wave EEG in a specific area of the brain relates to focal seizure, whereas spike-and-wave discharges, which widely spread over both sides of the brain are referred to as generalized seizures. Therefore, proposing a discriminating feature that is capable of separating normal and epileptic seizures is the most essential and challenging procedure.

3.1.1 Related work

Many studies have proposed different algorithms over the years using the University of Bonn EEG database [21, 27, 36, 66, 80, 81, 82, 83]. The recurrent Elman neural network (RENN) showed a classification accuracy of 100% using approximation entropy [27]. Time-domain, frequency domain, time-frequency domain, and entropy-based techniques have been reported in the literature [21, 27, 36, 80]. Shannon's and wavelet entropy [36], log-energy and norm entropies derived from wavelet packet decomposition [21], spectral

entropy, [81], sigmoid entropy [83] and variations of entropies [80] have been applied for the seizure detection related studies.

Several studies have been proposed using different databases for epileptic seizure detection [84, 85, 86, 87, 88, 89]. Gotman introduced a wavelet decomposition based algorithm that showed the sensitivity of 76% with 1/h [2]. Zhou et al. proposed multichannel EEG signal classification using the fuzzy feature and tested with several sets of real EEG data [90]. Multichannel fusion based seizure detection was introduced with two different schemes [91]. The first concatenated EEG feature vectors were independently obtained from the various EEG channels to form a single feature vector. The second approach was to combine independent decisions of different EEG channels to create an overall decision. Classification results showed that the feature fusion method performed better than the decision fusion approach. A hybrid model for epileptic seizure detection with genetic algorithm and particle swarm optimization showed a classification accuracy of 99.38 % using the SVM classifier [92]. Another hybrid method was proposed using fuzzy entropy-based features obtained from EEG signals in the fractional Fourier transform and wavelet packet decomposition domain [93]. A self-organizing map-based spatial clustering of entropy topography revealed that the critical electrodes shared the same cluster long time before the seizure onset [94]. A binary magnetic optimization algorithm using wavelet-based features was introduced in [95]. The algorithm proposed in [96] focused on reducing the epileptic seizure detection time while maintaining high accuracy, and locate the brain hemisphere,

which is affected by seizure activity. Automated detection of focal EEG signals using empirical wavelet transform and least-squares support vector machine (LS-SVM) showed the maximum accuracy of 82.53% [97]. Different entropies were investigated in normal, pre-ictal and epileptic EEGs and fuzzy classifier showed the highest accuracy of 98.1% [80]. Further, Acharya et al. [18] provided an extensive review on the application of entropies for seizure detection. Weighted permutation entropy based study showed an accuracy of 99.0% using the SVM classifier [98].

The physiology-based seizure detection system was proposed using sample entropy and statistical features on two datasets [8]. The results showed 86.69% of spike detection and 99.77% of seizure detection for dataset I and 91.18% of spike detection and 99.22% of seizure detection for dataset II using the SVM classifier. Short-term Fourier transforms (STFT) based scheme was introduced using an adaptive threshold technique and tested on 159 patients [99]. Patient-specific seizure onset detection method was proposed using wavelet decomposition and SVM classifier [88]. In this study, 36 pediatric subjects were considered, and the quantitative algorithm detected 131 of 139 seizures within 8 ± 3.2 sec of seizure onset. In [100], spatial and spectral features were used to train the SVM classifier and tested for 916 hours of EEG from 24 patients. The algorithm detected 96% of seizures from 173 seizures with a median detection delay of 3 sec and 2 false detections per 24-hour duration. Improved classification results were obtained in psychogenic non-epileptic seizures and vasodepressor syncope generalized epileptic seizures from non-epileptic using time domain, frequency domain and then combining

all features across channels [87]. Features were selected using a relief ranking algorithm that yielded the classification accuracy of 95% using a Bayesian network. A brief review was provided on the features such as time domain, frequency domain, nonlinear measures, time-frequency domain and application of entropies for seizure detection [18, 22].

The patient-independent neonatal seizure detection system was developed using the SVM classifier and validated for 267 hours of EEG from 17 newborns [85]. This system achieved the average detection rate of 89%, 96%, and 100% with one, two, and four false detections per hour respectively. In [101], prediction of epileptic seizures from intracranial EEG showed the sensitivity about 90-100% with the false positive rate of about 0-0.3 times per day using features derived from heart rate variability. Combined seizure index derived from wavelet coefficients revealed the sensitivity of 90.5%, the false detection rate of 0.5/h, and median detection delay of 7 sec [102]. A patient-specific early seizure detection algorithm using spectral parameters, time domain parameters, and wavelet analysis detected 14 of the 25 seizures before seizure onset with a median pre-onset time of 51 sec, and the false positive rate of 0.06/h using recurrent neural network [103]. A simple threshold-based scheme was introduced using the minimum variance modified fuzzy entropy (MVMFzEn) feature that obtained 100% classification accuracy [19].

Quantitative analysis of non-convulsive seizures in intensive care unit showed the mean sensitivity and mean false detection rate of 90.4% and 0.066/h respectively [104]. Relative amplitude and relative fluctuation index features with improved wavelet neural network classifier showed the sensitivity, specificity and false detection rate of 96.72%, 98.91 %, and 0.27/h respectively

[105]. Age-independent seizure detection algorithm using the SVM classifier was proposed using 78 patients with 592 seizures [84]. The area under the curve of 0.90 and 0.93 was obtained for neonatal and adults EEG with the application of feature baseline correction. Further, the assessment of epileptic seizures was performed using three significant features, namely pattern-match regulation static, maximum local frequency and amplitude variation [106]. Greene et al. make use of multi-features from different domains for neonatal seizure detection [10]. The fuzzy rule-based system was proposed for seizure detection in intracranial EEG [107]. Various features were used for the detection of temporal lobe epilepsy from scalp EEG [108]. The long-term audio and video EEG was used for detection of focal EEG seizures [109]. Mirowsaki et al. presented a study of prediction patterns for seizure prediction [86]. Further, wavelet transforms based approaches gained much attention towards EEG analysis due to its temporal and spatial analysis of signal [21, 47, 79, 107, 110].

Table 3.1 reports the information about various EEG databases that were used in the state-of-the-art epileptic seizure detection algorithms. All the studies have recorded the EEG using the International 10-20 system electrode placement. The CHB-MIT [88, 100], and the University of Bonn [33] databases are available in the public domain. In all the studies reported in Table 3.1, a notch filter was applied to EEG signals to attenuate power line noise.

The thorough literature survey confirms that existing approaches found to have its limitations towards attaining good sensitivity, less false detection rate, low detection delay and being less computational complexity. Further,

TABLE 3.1: Information on different EEG databases that were used in the state-of-the-art epileptic seizure detection studies in the past.

Author	EEG database center	No. of subjects	No. of electrodes	Length of EEG data	Sampling frequency (Hz)	EEG system	Band pass filter (Hz)
[91]	Royal Brisbane and Women's Hospital, Brisbane, Australia	8	20	4.82	256	Medelec Profile System	0-70
[34]	Neonatal Intensive Care Unit, Dept. of Neonatology, SSKM, Kolkata, India	12	6	~11 h	125 & 2000	NicOne 5.3	0.5 - 35
[100, 111]	CHB - MIT, USA	23	21	969 h	256	-	0.5 - 30
[99]	Epilepsy Center Erlangen (University Hospital Erlangen, Germany)	159	64	25,278 h	256	NATUS Europe	0.08-86
[112]	National Institute of Neurology and Neurosurgery Rhode Island Hospital	12	21	62 h	200	Nihon Kohden EEG 1200	0 - 70
[21, 80] [27, 81]	University of Bonn, Germany	5	1	0.65 h	173.61	-	0.53 - 40
[28]	CHB - MIT, USA	21	21	884 h	256	-	0.5 - 30
[103]	Thomas Jefferson University, Dartmouth University	25	20-32	~500 h	200	Grass-Telefactor Beehive LTM	0.3 - 70
[86, 105]	Epilepsy Center of the University Hospital of Freiburg, Germany	21	6	286 h	256	Neurofile NT digital video-EEG	4 - 30
[102]	Vancouver General Hospital, Canada	14	15	75.8 h	256	-	0.1 - 100
[84]	Maastricht University Hospital, Netherlands	78	19	~132 h	250	-	0.5-32
[87]	Department of Clinical Neurophysiology and Epilepsies in St. Thomas Hospital, London	11	21	-	250	-	-
[85]	Neonatal Intensive Care Unit of Cork University Maternity Hospital, Ireland	55	8	267.9	256	Viasys NicOne	0.5-13
[106]	Allegheny General Hospital, Pittsburgh, PA	55	-	~1208	-	-	-
[108]	Universitair Ziekenhuis Gasthuisberg, Leuven, Belgium	-	19	-	250	Brainlab digital EEG system	0.5-30

the existing algorithms have validated their algorithm on a single database. In order to obtain the generalization of seizure detection, the algorithm must be tested on several databases with a good number of epileptic seizure events.

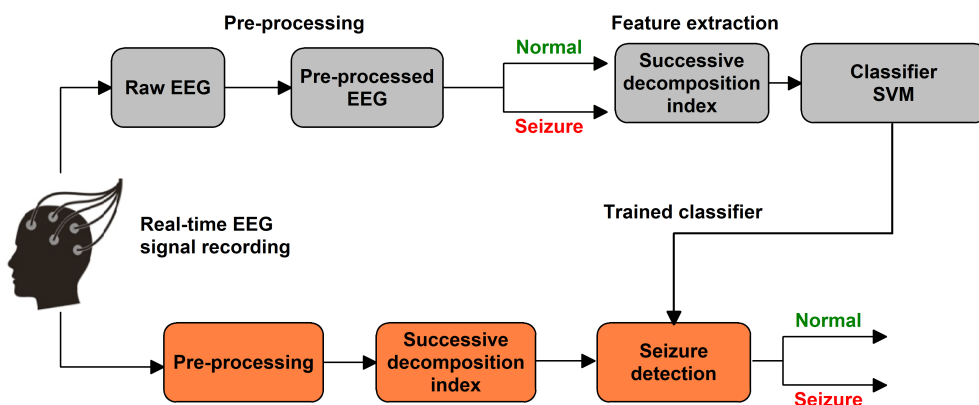


FIGURE 3.1: The general framework of the proposed automated epileptic seizure detection algorithm.

Hence, the proposed study attempts to overcome the above limitations through the application of a novel feature and SVM classifier using three different databases.

3.1.2 Proposed methodology

The proposed technique includes EEG data acquisition followed by pre-processing, segmentation of each channel at a constant window length, estimation of successive decomposition index (SDI) and classification. Fig. 3.1 shows the flow of the proposed automated seizure detection method. Initially, EEG recordings were preprocessed for noise and artifact removal. EEG was segmented into a constant non-overlapping window length of 1 sec and SVM classifier was used to classify SDI feature. Furthermore, the proposed algorithm applied to three datasets that consist of a good number of epileptic seizure events to validate its performance.

The rest of our paper was organized as follows. In Section 2, materials and methods were discussed in detail. Experimental results were presented in Section 3, and the salient features of the proposed study were reported in Section 4. Finally, the concluding remarks were reported in Section 5.

3.2 Materials and Methods

3.2.1 Clinical data

The experimental study was conducted on three EEG databases, namely the **DB1**-Ramaiah Medical College and Hospital (RMCH), **DB2**-Children's Hospital Boston-Massachusetts Institute of Technology (CHB-MIT), and **DB3**-Temple University Hospital which will be described briefly.

3.2.1.1 DB1

EEG recordings of DB1 were collected from the Institute of Neuroscience, RMCH, Bengaluru, India after appropriate ethical clearance. It includes 58 hours of 19 channel scalp EEG from 115 subjects (male-67, female-48) ranging from 2.5 to 75 years old. Among 115 subjects, 38 were suffering from epilepsy and 77 were healthy subjects. EEG signals were recorded using the International 10-20 system electrode placement at a sampling rate of 128 Hz. These EEG recordings were made from the following electrode placements: Fp1, Fp2, F7, F3, Fz, F4, F8, T3, C3, Cz, C4, T4, T5, P3, Pz, P4, T6, O1, and O2. Experts at the local hospital visually marked the epileptic and normal events of patient recordings. The subjects used for the study were suffering

from either one of the following seizures: focal seizures, generalized seizures, absence seizures, clonic seizures, tonic seizures, and myoclonic seizures.

3.2.1.2 DB2

The second database used in this study was obtained from the CHB-MIT [88] EEG database from Physionet repository which is available in the public domain ¹. DB2 consists of 844 hours of data from the 23 patients recorded at a sampling rate of 256 Hz. It was recorded with 23 channels using the International 10-20 system bipolar montage. It contains 23 channels, namely FP1-F7, F7-T7, T7-P7, P7-O1, FP1-F3, F3-C3, C3-P3, P3-O1, FZ-CZ, CZ-PZ, FP2-F4, F4-C4, C4-P4, P4-O2, FP2-F8, F8-T8, T8-P8, P8-O2, P7-T7, T7-FT9, FT9-FT10, FT10-T8, and T8-P8. This database includes 23 pediatric patients with the mean age of 9.9 ± 5.5 years.

3.2.1.3 DB3

The third and final database was obtained from the TUH EEG resource ² [113, 114]. This dataset consists of focal non-specific, generalized non-specific, simple partial, complex partial, absence, tonic, tonic-clonic, and myoclonic seizure from 316 subjects. These EEGs were recorded with the same as electrode configuration of DB1 at a sampling rate of 250 Hz. In total, 222 seizures from 316 subjects were considered from massive EEG recordings.

Table 3.2 shows the detailed information on all three databases. DB2 and DB3 recordings were already annotated with seizure start and end time.

¹<http://www.physionet.org/pn6/chbmit>

²https://www.isip.piconepress.com/projects/tuh_eeg/index.shtml

TABLE 3.2: Database details considered for the proposed study.

	DB1	DB2	DB3
Open source database	No	Yes	Yes
Sampling frequency (Hz)	128	256	250
Electrode position	10-20	10-20	10-20
No. of subjects	Male	67	5
	Female	48	18
	Total	115	23
Age range	Male	3-60	3-22
	Female	2.5-75	1.5-19
Total duration (hours)	58	884	408
No. of channels	19	23	19
No. of seizures	162	182	222
File format	ASCII	EDF	EDF

DB1: RMCH, **DB2:** CHB-MIT, **DB3:** TUH

3.2.2 Preprocessing

EEG recordings of DB1 were filtered using a notch filter (50 Hz) followed by a Butterworth bandpass filter (0.5-40 Hz) to attenuate noise and artifacts (eye blink and muscular). The power spectral density analysis confirmed the attenuation of 50 Hz power line noise after notch filter implementation. In the next step, filtered EEG was passed through the independent component analysis (ICA) algorithm to separate the eye blinks, and muscular artifacts [72]. Finally, experts annotated the preprocessed EEG as normal and epileptic seizures to develop a seizure detection algorithm.

3.2.3 Successive decomposition index

Wavelet-based studies have performed better in the past using different mother wavelets and the level of decomposition [21, 80, 103, 110]. However, the selection of the best wavelet and decomposition level for EEG analysis requires a thorough investigation in terms of classification results and computation time. In [21, 42, 47, 79, 93, 97, 110, 115], suitable wavelet, and decomposition levels were concluded by considering the results obtained from different mother wavelets and levels of decomposition.

The proposed SDI feature was derived by the motivation of the discrete wavelet transform (DWT). As we know, in the first level of DWT, the signal is passed to low pass filter and high pass filter. In the next levels, the output of low pass filter is simultaneously passed through a set of low pass and high pass filters. Finally, the coefficients are considered from different sub-bands to extract the features for classification. Whereas, in our proposed study, there is no restriction on levels of decomposition. The single coefficient from the last level is considered for further analysis.

The transition in the EEG from the normal to epileptic seizure activity is associated with the significant changes in the shape of the EEG signal. Therefore, capturing such an abrupt transition is essential to detect epileptic seizure activities.

Consider the EEG time series $x = \{x_1, x_2, x_3, x_4, \dots, x_n\}$, where n is the total number of the EEG samples (in one window) in the time series x . Here, we define two terms X^+ (average of $|x|$) and X^- (difference average of x).

The terms X^+ is given by:

$$X^+ = \frac{1}{n} \sum_{i=1}^n |x_i| \quad (3.1)$$

The coefficient X^+ is mean of the absolute of x .

In the next step, X^- is calculated by the iterative process. In the first level ($x^{(1)}$), EEG samples are arranged into $n/2$ non-overlapping pairs as shown below.

$$x^{(1)} = \left\{ \frac{x_1 - x_2}{2}, \frac{x_3 - x_4}{2}, \dots, \frac{x_{n-3} - x_{n-2}}{2}, \frac{x_{n-1} - x_n}{2} \right\} \quad (3.2)$$

The new coefficients of level 1, i.e. $x^{(1)}$ of length $n/2$ (n is updated in each level) after decomposition is represented as:

$$x^{(1)} = \{x_1^{(1)}, x_2^{(1)}, \dots, x_{n/2-1}^{(1)}, x_{n/2}^{(1)}\} \quad (3.3)$$

In general, the difference average can be written as follows:

$$X_i^L = \left(x_{2i-1}^L - x_{2i}^L \right) / 2 \quad (3.4)$$

Here, i goes from 1 to n , L is the number of levels of decomposition required to estimate the X^- and it is calculated by $L = 3.33 \log_{10}(n)$. The coefficient obtained in the last level of decomposition is taken as X^- . Number of coefficients in each level is given by $n/2^L$.

In the next step, defining two new terms X^{++} , and X^{--} using X^+ and X^- as follows:

$$X^{++} = \frac{X^+ + X^-}{2} \quad (3.5)$$

$$X^{--} = \frac{X^+ - X^-}{2} \quad (3.6)$$

The coefficients X^{++} and X^{--} gives the relation between X^+ and X^- . The square matrix A is formed using the four coefficients X^+ , X^- , X^{++} , and X^{--} as follows:

$$A = \begin{bmatrix} X^+ & X^{--} \\ X^- & X^{++} \end{bmatrix} \quad (3.7)$$

In our previous study [89], matrix determinant showed a good classification results for detection of epileptic seizure. Therefore, in this study, SDI was estimated by finding determinant [64] of the square matrix A .

$$SDI = \log_{10} \left(\frac{n}{L} (X^+ X^{++} - X^- X^{--}) \right) \quad (3.8)$$

The term n/L is a scalar parameter. The coefficient X^+ is much greater than the other three coefficients. SDI was arrived at by successively decomposing the EEG signal into the final level. Hence, the proposed parameter was labeled as SDI. We speculate that the SDI better tracks the transitions in the EEG of the time series along with the amplitudes of the EEG samples. Since the

proposed parameter follows linear relation in every step, SDI of epileptic EEG is expected to be higher as compared to normal EEG (refer to Section 3.1). The rationale behind using the determinant of all four coefficients has been explained in the discussion section.

3.2.4 Classifier

SVM is a supervised machine learning algorithm and it classifies the data by finding the best hyperplane that differentiates the two classes very well [23]. It was selected based on the reliable performance reported in previous studies for seizure detection [8, 25, 65, 80, 84, 85, 92, 97, 101]. The radial basis kernel function was chosen based on preliminary results and hyperparameters were determined using the optimization technique [25]. SVM classifier was trained with the class labels of 0 and 1 for normal and epileptic seizures EEG respectively. The training and testing were performed separately for each database using leave-one-subject-out cross-validation method. In this method, EEG data from one subject was used for testing and remaining were used for training. The procedure was repeated until all the subjects were used for training and testing.

3.2.5 Performance metrics

The performance of the epileptic seizure detection algorithm using SDI feature and SVM classifier was evaluated in terms of sensitivity, false detection rate, median detection delay and F measure [9, 47, 88].

- *Sensitivity*: the number of correctly identified epileptic seizure events.

- *False detection rate*: percentage of false detection during normal EEG over a period of data.
- *Median detection delay*: an average delay between expert marking and algorithm detection.
- *F measure*: The F measure is the harmonic mean of precision and recall. The recall is the same as sensitivity and precision is positive predictive value.

3.3 Results

3.3.1 Analysis of SDI feature

According to the behavior of the SDI feature discussed earlier (refer to Section 2.3), a seizure onset can be captured by the significant increase in its values. A Wilcoxon rank sum test exhibit $p < 0.05$ and z-score of -70.51 between normal and epileptic EEG. Further, descriptive statistics such as mean \pm standard deviation, upper quartile, lower quartile, and inter-quartile range between normal and epileptic showed a significant difference. Fig. 3.2 represents the boxplot of SDI derived from normal and epileptic seizures EEG for each channel. From the boxplot, the excellent discrimination between two activities was noticeable in each channel.

Fig. 3.3a shows the epileptic EEG example from DB1 and Fig. 3.3b shows the image derived using SDI values for corresponding channels. As can be seen, a significant increase in the SDI during seizure activity that is between 1110 sec and 1171 sec. The topographical map describes the distribution of

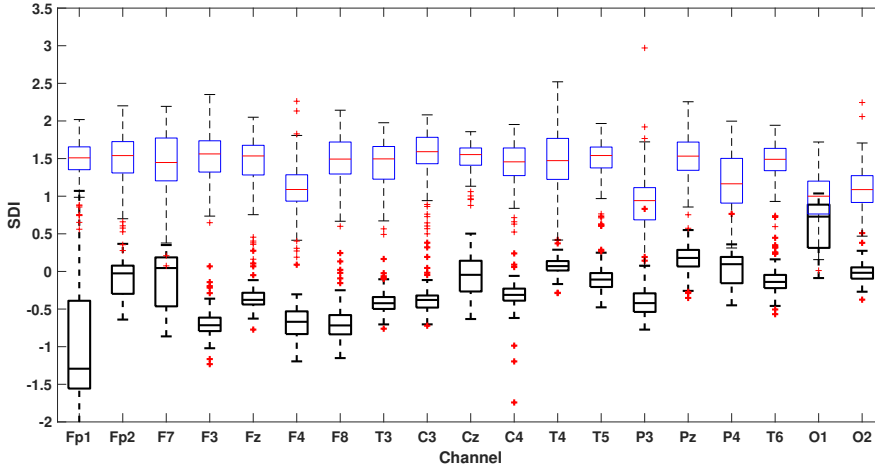
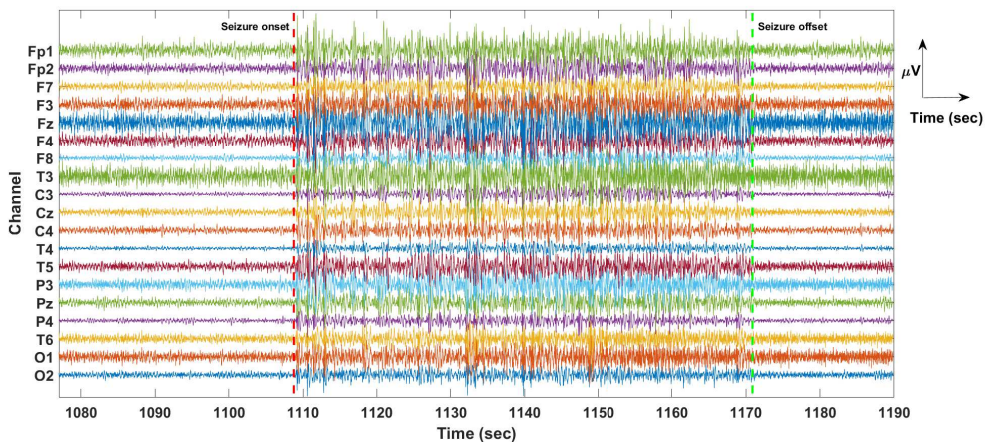


FIGURE 3.2: Boxplot derived from SDI correspond to normal (black boxes) and epileptic seizures EEG (blue boxes). The red + indicates the outliers which are beyond the whiskers. A Wilcoxon rank sum test showed $p < 0.05$ between normal and epileptic seizures SDI in each channel.

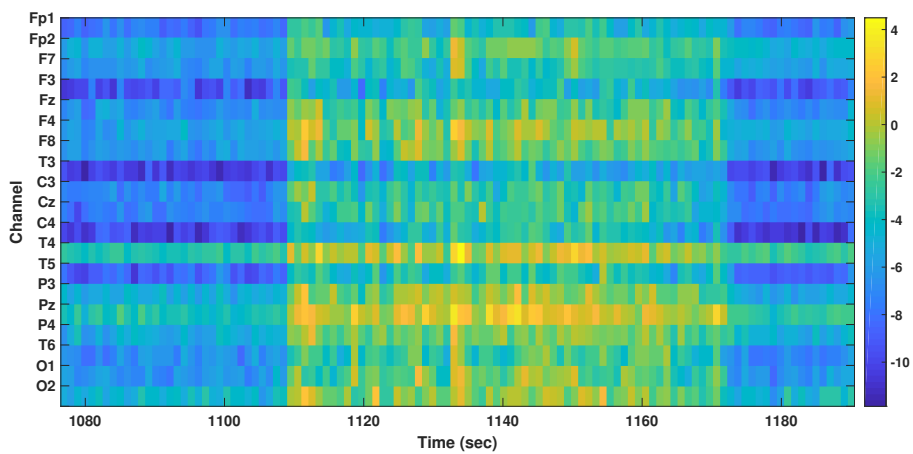
electrical activity across the brain by considering electrodes potential [116]. In this study, the SDI value of each channel was mapped onto the topoplot using the International 10-20 system electrode placement. Figs. 3.3c and 3.3d show the topographical map derived from SDI for the EEG shown in Fig. 3.3a. It is clear from the topoplot that the seizure onset started at 1110 sec and continued till 1171 sec. Refer to **Appendix A** for EEG and corresponding SDI values obtained for DB2 and DB3.

3.3.2 Seizures detection results

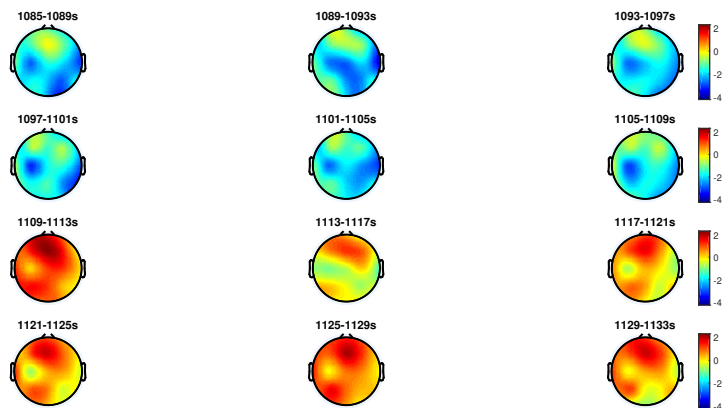
Fig. 3.4 presents the EEG, SDI and SVM classifier output corresponding to randomly selected channels F7, T3, T5, and P3. The seizure onset is at 1110 sec and offset is at 1171 sec according to the neurologist. As shown in the



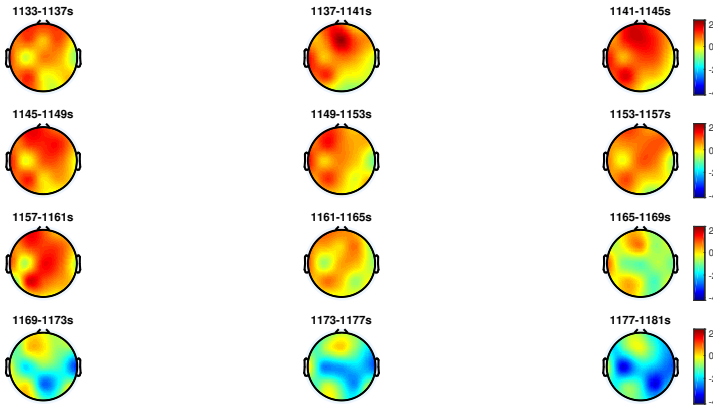
(a)



(b)



(c)



(d)

FIGURE 3.3: (a) Epileptic seizure EEG example from DB1. The red marker indicates the beginning of the seizure onset and green marker its end. (b) Image derived from SDI for the EEG as shown in Fig. 3.3a. The x-axis, and y-axis represent time and channel respectively. The colormap represents the SDI values. (c) & (d) The topographical map for the same EEG between 1085 to 1181 sec derived from SDI.

middle panel of the Fig. 3.4, SDI was found to be significantly higher during epileptic activities that is well discriminated from normal EEG. Thus, the epileptic seizure activity was identified correctly shortly after the onset by the SVM algorithm as shown in the lower panel of the Fig. 3.4 in red color. Applying the proposed algorithm to DB1, results showed the mean sensitivity of 97.53% with the mean false detection rate of 0.4/h, median detection delay of 1.5 sec and an F measure of 97.22%.

The study was extended on DB2 and DB3 to validate the efficiency, generalization capability, and robustness of SDI for seizure detection. Table 3.3 shows epileptic seizure detection results using all the three databases. Experimental results revealed that the mean sensitivity of 97.28%, mean false detection rate of 0.57/h, median detection delay of 1.7 sec and an F measure of

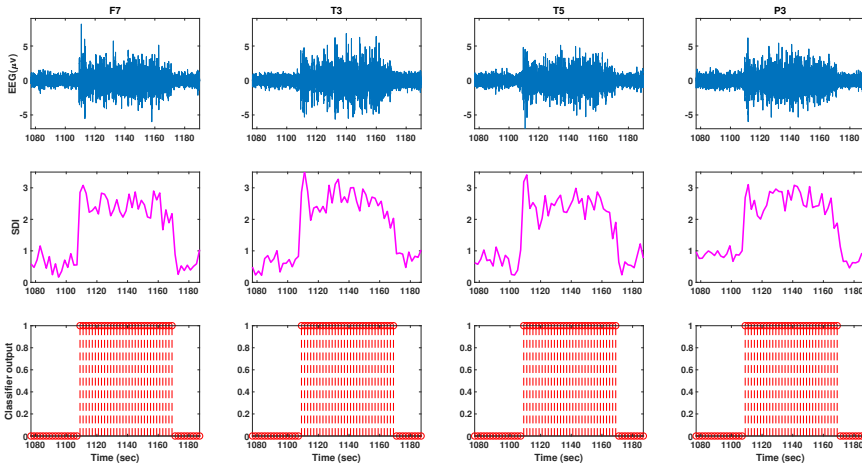


FIGURE 3.4: EEG, SDI, and SVM classifier output corresponding to different channels. The seizure starts at 1110 sec and ends at 1171 sec. Classifier output 0 and 1 represent normal and seizure activity respectively. **First row:** EEG, **Second row:** SDI, and **Third row:** classifier output.

96.29% for DB2. From DB3, 106 and 210 subjects with epilepsy and normal subjects were selected respectively from the huge EEG resource. The mean sensitivity of 95.80%, mean false detection rate of 0.49/h, median detection delay of 1.5 sec and an F measure of 94.70% were obtained. Fig. 3.5 shows the receiver operating characteristic curve obtained for the seizure detection algorithm for all the three databases. The area under the curve of 0.9811, 0.9756, and 0.9623 was obtained for DB1, DB2, and DB3 respectively.

TABLE 3.3: Results of epileptic seizure detection using the proposed method.

Database	Sensitivity (%)	False detection rate (/h)	Median detection delay (sec)	F measure (%)
DB1	97.53	0.40	1.5	97.22
DB2	97.28	0.57	1.7	96.29
DB3	95.50	0.49	1.5	94.70

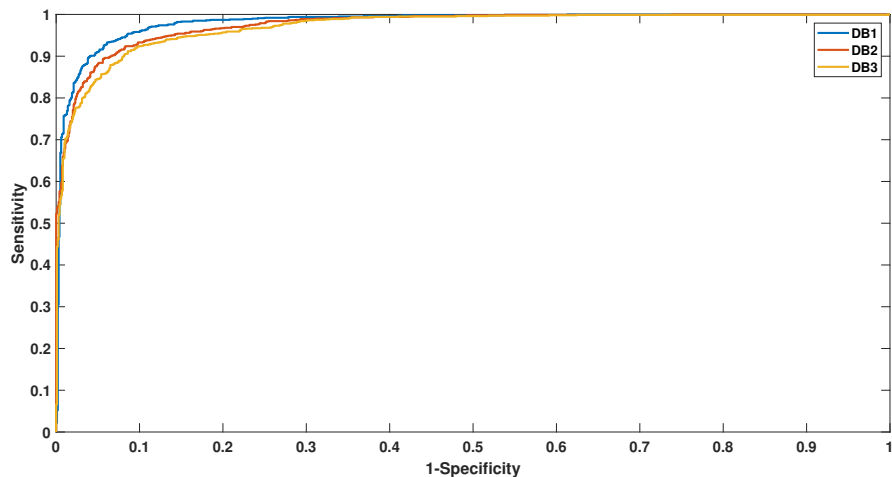


FIGURE 3.5: Receiver operating characteristic curve obtained from all the three databases. The area under the curve of 0.9811, 0.9756, and 0.9623 was obtained for DB1, DB2, and DB3 respectively.

3.3.3 Automated detection using GUI

To provide an automated seizure detection, we have developed a graphical user interface (GUI) in MATLAB 2017b using *APP Designer*. The GUI tests the EEG by feeding its SDI feature into the trained model (refer to Fig. 3.1). The screenshot of the automated seizure detection tool is displayed in Fig. 3.6. The detailed function of each component in the GUI is given in Table 3.8 (refer to **Appendix B**). The GUI video is available at <https://bit.ly/2O7xDxN>. The sample EEG was shown in Fig. 3.6 includes an epileptic seizure event that was correctly detected using our algorithm. Finally, the results obtained using GUI were validated by experts.

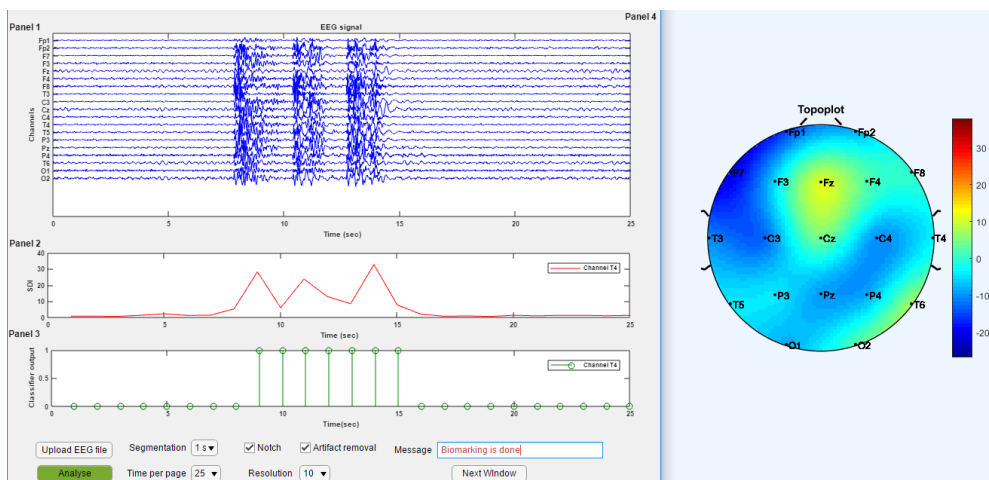


FIGURE 3.6: Screenshot of automated seizure detection implemented in MATLAB. **Panel 1:** Axes show EEG of all 19 channels that include two seizure events. **Panel 2:** Figure shows the SDI of the selected channel T4. **Panel 3:** Figure shows the classifier output of the channel T4. **Panel 4:** The topoplot designed for every 1 sec of EEG.

3.4 Discussion

The foremost importance of our real-time automated seizure detection algorithm was to achieve better performances regarding sensitivity, false detection rate, and median detection delay. Hence, to meet the objective, we have proposed the seizure detection algorithm using SDI and SVM classifier. It was observed that SDI increases significantly during the epileptic activity that confirms the suitability of SDI for identifying brain activities. Experimental results showed the highest sensitivity of 97.53%, the false detection rate of 0.4/h, median detection delay of 1.5 sec, and an F measure of 97.22% among the three databases, which provide evidence for clinical implementation in real-time.

The rationale behind using the determinant of all four coefficients has been

TABLE 3.4: Sensitivity obtained using linear classifiers for all the three databases.

Classifier	DB1 (%)	DB2 (%)	DB3 (%)
Linear regression	94.00	75.36	86.46
Linear discrimination	63.63	89.80	86.34
Linear SVM	95.12	88.36	88.35

explained here. During the initial simulation, it was observed that alone X^+ was more susceptible to outliers. The coefficient X^- was obtained by successively decomposing the EEG time series where it retained the high-frequency component. This formed the basis for estimation of SDI where it calculates the determinant by taking all four coefficients. The net impact was that the SDI was not susceptible to more outliers that significantly improved the classification results. Thus SDI outperformed over other feature extraction methods.

3.4.1 Classification results using other classifiers

Table 3.4 shows the comparison results of the proposed study using three linear classifiers, namely linear regression, linear discrimination, and linear SVM classifiers. Among all the three databases, the results obtained using radial basis kernel function based SVM classifier (refer to Table 3.3) was superior as compared to the results of linear classifiers. Further, it was observed that the false detection rate was too high using linear classifiers.

3.4.2 Comparison with wavelet decomposition

Wavelet decomposition of EEG signals using different mother wavelets and decomposition levels have been widely used for seizure detection [21, 47, 79,

107, 110]. The majority of the studies have used different mother wavelets, namely Haar, Symlets, Coiflets, and Meyer and varied the decomposition levels until 8. In order to compare the computational time of different wavelets against SDI, above mentioned wavelets were decomposed till 8th level followed by estimation of wavelet energy using DB1. Wavelet energy was considered as a feature due to the reason that it has shown superior performance. Fig. 3.7 shows the computation time required for feature extraction using different mother wavelets. In total, the mean time was calculated from 10 trials. As the results demonstrated, the computation time taken from the SDI approach was 1.25 sec that was less than all wavelet-based results. Besides, Coiflets and Meyer wavelets at the 6th level of decomposition showed the highest sensitivity of 96.2%. On the other hand, the lowest sensitivity of 89.6% was attained for Symlets wavelet at the 8th level of decomposition. The sensitivity of 96.2% achieved by Coiflets and Meyer wavelets at the 6th level was slightly less than the sensitivity of 97.53% shown by SDI. Interestingly, the highest sensitivity by Coiflets and Meyer wavelets at the 6th level was achieved at the highest computation time of 10.50 sec among all. However, the computation time taken by SDI was only 1.25 sec that was less in comparison with results obtained using wavelets. Hence, as compared to the SDI method, the wavelet-based approach required the selection of mother wavelet and decomposition level for better results at the cost of computational time.

3.4.3 Comparison with state-of-the-art approaches

Table 3.5 shows the comparison of the proposed method against existing methods that used different databases. As compared to the studies [88, 99, 105,

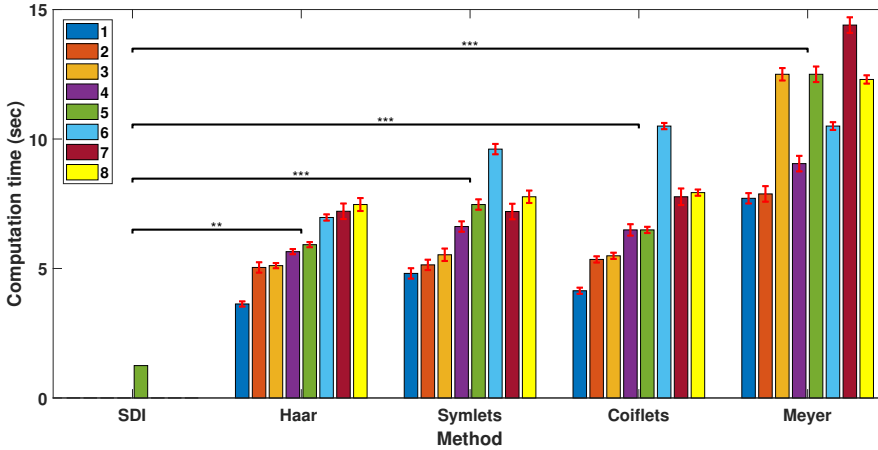


FIGURE 3.7: Computation time (sec) required for estimation of wavelet energy using wavelet decomposition and SDI on DB1. The legends in each color show the level of decomposition. The SDI results are presented for the last level of decomposition. $p < 0.05(*)$, $p < 0.01(**)$, $p < 0.001(***)$.

117], the highest sensitivity of 97.53% was achieved in our study. Similarly, the lowest median detection delay of 1.5 sec was obtained in our method that was lower than other studies reported in Table 3.5. Further, the false detection rate of 0.40/h was better as compared to studies [85, 100, 102, 117]. Attention must be taken while comparing the performance between various approaches since researchers have used different EEG databases.

In order to compare the performance and examine the efficiency of SDI feature, we perform a comparative study using other existing feature extraction methods. The features considered for the comparative study include: spectral entropy [81], approximate entropy [27], sample entropy and statistical features [8], log energy entropy derived from wavelet packet decomposition [21], and wavelet entropy [36] have been implemented on DB1 and classified using the

TABLE 3.5: Performance comparison of state-of-the-art epileptic seizure detection algorithms. The results of our method are highlighted in bold.

Author	Method	Classifier	Sensitivity (%)	Median detection delay (sec)	False detection rate (/h)
[88]	Wavelet decomposition, morphology, and Spatial features	SVM	94.24	8	15/60h
[100]	Spatial features	SVM	96	3	2/24h
[102]	Combined seizure index	Threshold	90.5	7	0.5/h
[103]	Spectral parameters, time domain, wavelet analysis parameters, and complexity measures	RENN	100	4	0.023/h
[104]	Signal amplitude variation and regularity statistics	Quantitative analysis	90.4	-	0.06/h
[85]	Multi-features	SVM	89	-	1/h
[99]	STFT and statistical features	Adaptive threshold	89.9	-	0.19/h
[105]	Relative amplitude and relative fluctuation index	Improved wavelet neural networks	96.72	-	0.27/h
[117]	HRV	Multivariate statistical process control	91	-	0.7/h
Proposed	SDI	SVM	97.53	1.5	0.40/h

SVM classifier. Table 3.6 shows the performance comparison in terms of computational time required for feature extraction and classification results. Even though the sensitivity of the other feature extraction methods was close to SDI, our method outperformed other methods in terms of computation time. It has almost 2.13% improvement in sensitivity as compared to [36] and 2.23% as compared to [81] and [21]. Further, approximate entropy [27] was found to be computationally expensive as reported in [21]. The false detection rate was superior in the proposed method as compared to the other features reported in Table 3.6. Overall, we observed the best performance by SDI against other existing feature proposed for seizure detection.

The spectral [81], approximate [27], sample [8], log energy [21], and wavelet [36] entropy methods have been implemented on all three databases and classified using the SVM classifier. Fig. 3.8a showed an F measure obtained for different entropies and SDI. The highest F measure was obtained using the SDI feature for all the three databases. The least F measure of

TABLE 3.6: Performance comparison of SDI with other feature extraction methods on DB1 using the SVM classifier. The best performances are highlighted in bold.

Method	Computation time (sec)	Sensitivity (%)	Median detection delay (s)	False detection rate (/h)
Spectral entropy	14.01	95.30	1.5	0.70
Approximate entropy	159.76	93.20	1.6	0.95
Wavelet entropy	6.02	95.40	1.5	0.64
Sample entropy and statistical features	13.98	94.21	1.55	0.88
Wavelet packet decomposition and log energy entropy	8.33	95.30	1.5	0.64
SDI	1.25	97.53	1.5	0.40

93.20% (approximate entropy), 92.10% (sample entropy) and 91.00% (sample entropy) was observed for DB1, DB2, and DB3 respectively.

The algorithms proposed in [28, 31, 88, 118] have used the same EEG recordings from DB2, and the results are reported in Table 3.7. The highest sensitivity and less detection delay were achieved in our study as compared to the other methods reported in Table 3.7. An improvement of 1.28% in sensitivity and 12.3 sec in mean detection delay was achieved in comparison to [31]. The false detection rate of 0.13/h in [31, 118] was better than ours, but the other two performances were better in our method. These comparisons underline that proposed method is a robust method for seizure detection.

In our previous study [19], classification of epileptic seizure was performed based on a threshold parameter derived using MVMFzEn. EEG recordings from 20 channels were taken into consideration to estimate the MVMFzEn followed by a threshold. However, in the proposed study, the decision was made based on the individual channel information. Our previous study [19] was implemented using only 38 subjects but, present study was extended the validation on 115 subjects.

Several non-linear entropy measures developed from the concepts of chaos

TABLE 3.7: Performance comparison for different methods using DB2. The best performances are highlighted in bold.

Author	Method	Sensitivity (%)	Median detection delay (sec)	False detection rate (/h)
[88]	Wavelet decomposition, morphology, spatial features and SVM	94.24	8	15/60h
[100]	Spatial features and SVM	96	3	2/24h
[31]	Lacunarity and Bayesian linear discriminant analysis	96.25	13.8	0.13/h
[28]	Multivariate feature and SVM	70	-	-
[118]	Sparse rational decomposition, the local Gabor binary patterns and SVM	91.13	-	0.35
Proposed method	SDI and SVM	97.53	1.5	0.40/h

and non-linear dynamics have been introduced for the recognition of epileptic EEG signals [27, 36, 47, 80, 81, 107]. Some of the entropy features, namely Shannon entropy, Renyi entropy, approximate entropy, sample entropy, permutation entropy, fuzzy entropy, and distribution entropy have been proposed and achieved promising results in the field of epilepsy detection. Further, resulting entropy of the EEG signal bounded in a range due to its nonlinear property. The detection of epileptic seizure would be possible using entropy measurements, whereas it would be difficult to identify the intensity of the seizure occurrence accurately due to the bounded entropy. However, the proposed SDI feature performs linear measurement showing the excellent reflection of variation in the EEG signal for the epileptic condition. Such a thing helps in identifying the intensity of epileptic activity in a specific EEG channel or the location of the brain.

3.4.4 Relative performance

We have compared the results of different entropies using the relative performance (RP) [21]. In this study, RP was measured using an F measure and computation time (sec). The RP can be written as:

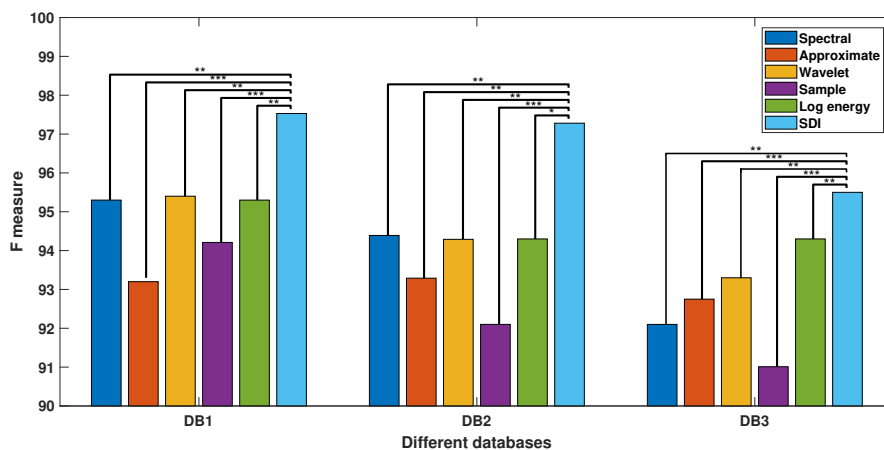
$$RP = \frac{(100 - Fmeasure)}{Computation\ time} \quad (3.9)$$

The higher the RP indicates better performance of the algorithm [21]. Best RP can be obtained with the higher F measure and less computation time. Fig. 3.8b shows the RP obtained for different entropies using all three databases. As can be seen, the SDI algorithm showed the highest RP as compared to the other entropies of all three databases.

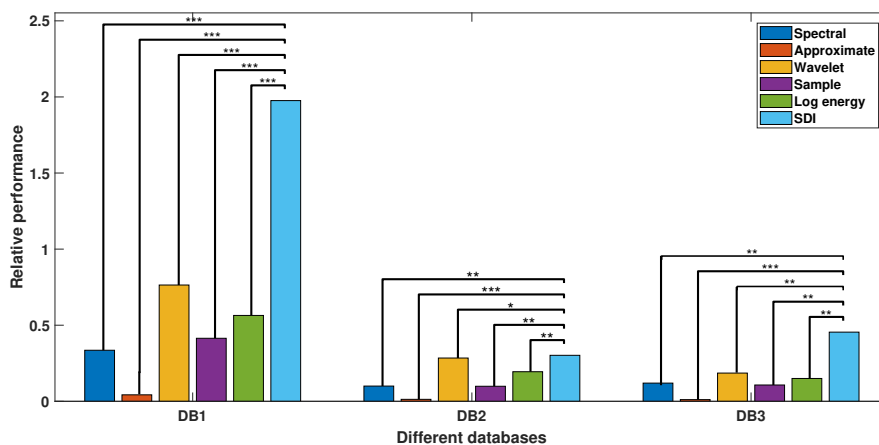
The complete study was conducted on MATLAB 2017b using 8GB RAM, CPU 2 GHz with an Intel i3 processor. The average/median computation time required to extract SDI for a 19 channels x 1 sec EEG epoch was about 281 μ /262 μ sec.

3.4.5 Limitations and future directions

The proposed method is yet to be implemented on a hardware platform. Although it performed well for seizure detection in MATLAB software, it must be implemented in hardware for real-time seizure detection. Further, parallel processing for feature extraction from multichannel EEG in real time would reduce the computation time that enhances the performance of the overall algorithm. The cross-database evaluation (using three or more databases) of the seizure detection will be implemented in future study.



(a) F measure



(b) Relative performance

FIGURE 3.8: Comparison results using different entropies on all three databases (a) F-measure (b) Relative performance. $p < 0.05$ (*), $p < 0.01$ (**), $p < 0.001$ (***).

3.4.6 Summary of the study

In summary, we have evaluated the SDI feature using three databases for automatic seizure detection in long-term EEG. Experimental results confirm that

seizure detection using SDI feature outperforms in terms of sensitivity, false detection rate, and median detection delay. Our conclusions are based on statistical analysis, classification results and comparison results. Also, MATLAB GUI was developed for automated seizure detection. Therefore, the proposed automated system for seizure detection can significantly reduce the neurologist burden that enhances the efficiency of medical diagnosis and the treatment of patients with epilepsy.

3.5 Conclusion

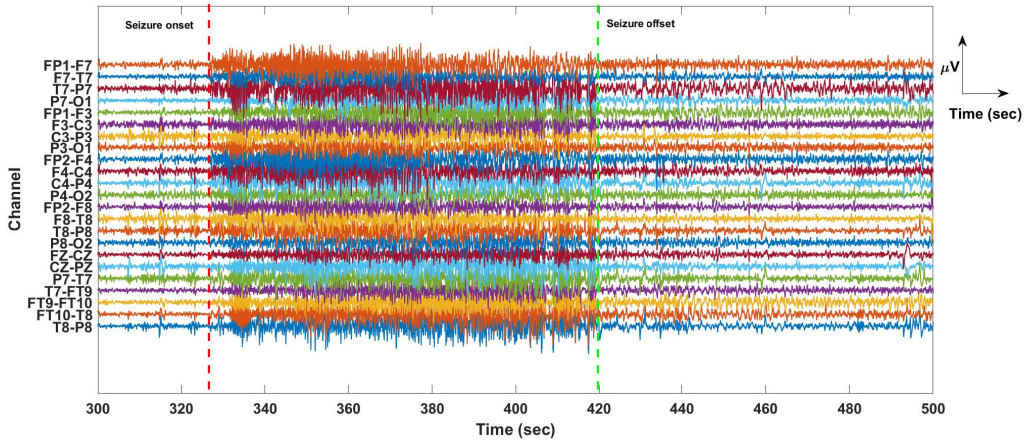
A novel feature called SDI was proposed and evaluated for real-time recognition of epileptic seizure in long-term EEG using three databases. It was observed that the SDI better tracks the transition in the EEG by reflecting the significant increase during seizure activity with less computation complexity. The significant difference ($p < 0.05$) was observed between normal and epileptic seizures EEG. Classification results revealed the sensitivity- false detection rate- median detection delay of 97.53%-0.4/h-1.5 sec, 97.28%-0.57/h-1.7 sec, 95.80%-0.49/h-1.5 sec using DB1, DB2 and DB3 respectively. The computation time analysis shows that SDI is faster among several feature extraction methods including wavelet-based features and other feature extraction methods. Experimental results obtained using SDI performed better than existing methods on all three databases proving the robustness, efficiency and general applicability of the proposed seizure detection algorithm. Hence, the proposed algorithm is the optimal choice to assist neurologists as a valuable diagnostic tool providing better and timely care for epilepsy patients.

Acknowledgment

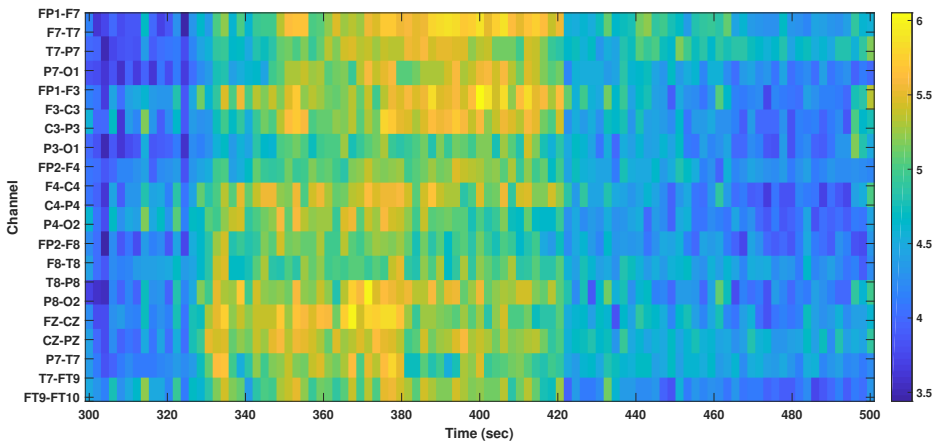
The authors are grateful to doctors of the Institute of Neuroscience, Ramaiah Medical College and Hospitals, Bengaluru, India, for valuable discussion and providing EEG recordings for research purpose. Authors also grateful to Dr. Ali Shoeb from CHB-MIT and team of the TUH for permitting to use their database for research. This research did not receive any specific grant from funding agencies in the public, commercial, or not-for profit sectors.

Appendix A

Fig. 3.9a illustrates the EEG from DB2 (subject no:chb01) and Fig. 3.9b shows its image representation derived from SDI feature. An epileptic seizure activity begins at 327 sec and ends at 420 sec, Fig. 3.9b shows a significant increase of SDI during seizure activity. Similarly, Fig. 3.10a shows the epileptic EEG from DB3 (subject no.:1217, session:s03, and file:a02) and Fig. 3.10b presents an image representation of the corresponding SDI feature.



(a)

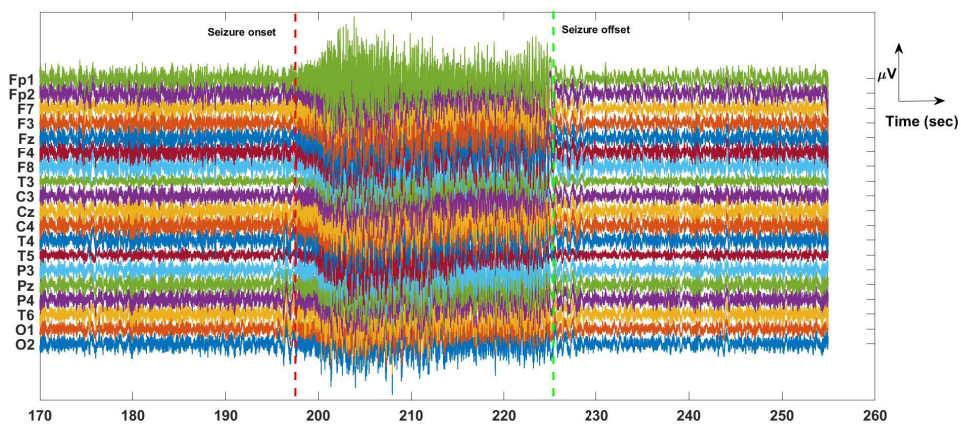


(b)

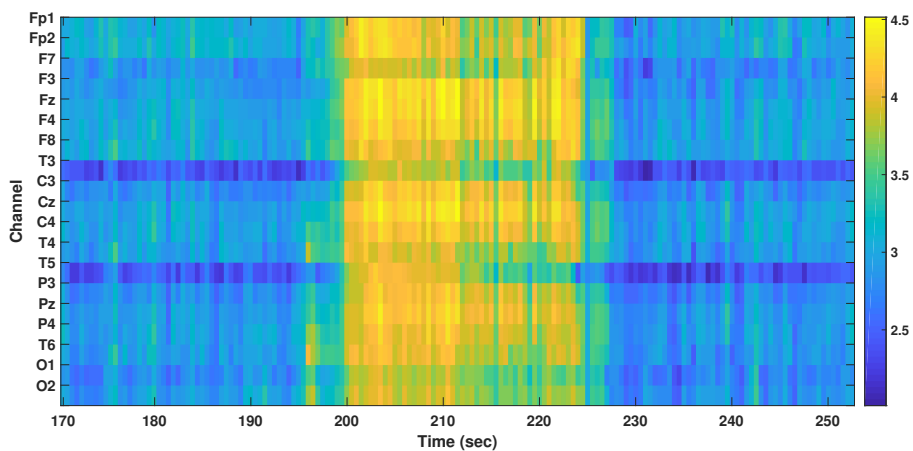
FIGURE 3.9: **(a)** Epileptic EEG example collected from DB2 which consist of 23 bipolar channels and display shows the EEG between the time duration of 300 secs to 500 secs. **(b)** Image derived from SDI for the EEG as shown in Fig. 3.9a. The x-axis and y-axis represent time and channel respectively. The colormap represents the SDI values.

Appendix B

Table 3.8 shows the functions of MATLAB GUI components.



(a)



(b)

FIGURE 3.10: (a) Epileptic EEG example collected from DB3 which consist of 19 channels and EEG displayed between the time duration of 170 secs to 255 secs. (b) Image derived from SDI for the EEG as shown in Fig. 3.10a. The x-axis and y-axis represent time and channel respectively. The colormap represents the SDI values.

TABLE 3.8: Functions of MATLAB GUI components.

GUI Components	Function
Load EEG file	It loads the EEG file from the folder
Panel 1	Display EEG
Panel 2	Display SDI of selected channel
Panel 3	Display classifier output of the channel shown in Panel 2
Panel 4	Display topoplot for every 1 sec of EEG
Segmentation	Window length for feature extraction (default: 1 s)
Time per page	Duration of EEG displayed in one page (default: 70 s)
Notch	Checked box shows EEG with 50 Hz line noise (default: Notch applied)
Artifact removal	Checked box shows EEG with artifacts (default: ICA applied)
Resolution	Sensitivity for EEG display (default: 10 μ s)
Previous window	Display previous window EEG (previous 70 s)
Next window	Display next window EEG (next 70 s)

CHAPTER 4

Performance evaluation of DWT based
sigmoid entropy in time and frequency
domains for automated detection of epileptic
seizures using SVM classifier

S Raghu, Natarajan Sriraam, Yasin Temel, Shyam Vasudeva Rao, Alangar
Satyaranjandas Hegde, Pieter L Kubben

Computers in Biology and Medicine, 110:127-143

Year: 2019

<https://doi.org/10.1016/j.compbiomed.2019.05.016>

Abstract

The electroencephalogram (EEG) signal contains useful information on physiological states of the brain and has proven to be a potential biomarker to realize the complex dynamic behavior of the brain. Epilepsy is a brain disorder described by recurrent and unpredictable interruption of healthy brain function. Diagnosis of patients with epilepsy requires monitoring and visual inspection of long-term EEG by the neurologist, which is found to be a time-consuming procedure. Therefore, this study proposes an automated seizure detection model using a novel computationally efficient feature named sigmoid entropy derived from discrete wavelet transforms. The sigmoid entropy was estimated from the wavelet coefficients in each sub-band and classified using a non-linear support vector machine classifier with leave-one-subject-out cross-validation. The performance of the proposed method was tested with the Ramaiah Medical College and Hospital (RMCH) database, which consists of the 58 Hours of EEG from 115 subjects, the University of Bonn (UBonn), and CHB-MIT databases. Results showed that sigmoid entropy exhibits lower values for epileptic EEG in contrary to other existing entropy methods. We observe a seizure detection rate of 96.34%, a false detection rate of 0.5/h and a mean detection delay of 1.2 s for the RMCH database. The highest sensitivity of 100% and 94.21% were achieved for UBonn and CHB-MIT databases respectively. The performance comparison confirms that sigmoid entropy was found to be better and computationally efficient as compared to other entropy methods. It can be concluded that the proposed sigmoid entropy could be used as a potential biomarker for recognition and detection of epileptic seizures.

4.1 Introduction

Epilepsy is a neurological disorder that affects the brain and will have a profound influence on patients' daily lives. A sudden discharge of electrical activity in the brain causes temporary brain dysfunction, which is referred to as seizure and recurrent seizures lead to epilepsy [2, 119]. The World Health Organization (WHO) estimated that epilepsy affects 50 million people worldwide [119]. The electroencephalogram (EEG) signals have proven to be a potential biomarker for detection and recognition of epilepsy [2]. A thorough inspection of the long-term EEG recordings is necessary to recognize the abnormal EEG patterns, which are found to be time-consuming, costly and leading to human errors. Though several automated, computer-aided algorithms for seizure detection were proposed earlier, there is still scope for identifying better biomarkers for real-time seizure detection.

Neurological disorders cause changes in EEG patterns, which could be used as a marker for the diagnosis. It was shown that non-linear methods could provide potential markers for EEG analysis over conventional methods [2, 120, 121] however, several limitations exist which needs to be solved. To design an automated seizure detection system, it is essential to extract features that describe the morphology of the epileptic seizures from EEG signals in a better manner. Studies have reported that the best feature significantly improves the algorithm performance [80, 84, 122]. Thus, we propose a novel feature named sigmoid entropy derived from the sigmoid function that offers a significant nonlinear behavior to capture robust markers for seizure detection.

For epileptic seizure detection, studies based on non-linear entropy have

shown significant results in terms of sensitivity as compared to other known EEG derived features. It can be observed from the literature that variations of entropy methods have been applied for seizure detection [27, 47, 80, 84, 115, 122, 123, 124, 125, 126]. Different entropy methods such as approximation entropy (ApEn), sample entropy, phase entropy 1 and phase entropy 2 have been used for the automatic detection of normal, pre-ictal, and the ictal conditions [80]. Among the seven different classifiers described in [80], fuzzy classifier showed the highest accuracy of 98.1%. Permutation entropy was used to identify the changes in EEG signals during absence seizures [123, 125]. A method based on discrete wavelet transforms (DWT), and ApEn obtained 100% classification accuracy using an artificial neural network [47]. Srinivasan et al. showed a classification accuracy of 100% between normal and epileptic EEG using ApEn and artificial neural network classifier [27]. Optimized sample entropy with extreme learning machine method showed a high accuracy of 99.0% [124]. Fuzzy entropy and support vector machine (SVM) based approach for the detection of epileptic seizures showed acceptable results [126]. Acharya et al. [18] gave a systematic review of the application of various entropy methods to differentiate normal, interictal, and ictal EEG signals. A patient non-specific algorithm showed a specificity of 99.9%, sensitivity of 87.5% and a false positive rate 0.9/h [127].

In [98], weighted permutation entropy showed distinguishable band for seizure and normal EEG segments. An accuracy of 99.0% was achieved using SVM classifier between healthy subjects (with eyes open and closed) and epileptic patients [98]. Automated threshold-based detection of epileptic

seizures was proposed using a novel feature called minimum variance modified fuzzy entropy [19]. In this study, relative energy was used as a membership function to estimate fuzzy entropy and an accuracy of 100% was obtained using the threshold method. In [19, 98], lower entropy was observed for epileptic seizures EEG, which were in contrary to other entropy methods proposed in [21, 27, 36, 47]. Wavelet packet transforms followed by log energy and norm entropy showed an accuracy of 99.7% using recurrent Elman neural network [21]. Further, Renyi, spectral, Shannon and wavelet entropy methods were explored for the classification of epileptic seizures [36, 66, 81, 110]. The above-mentioned entropy-based studies demonstrated promising classification results for epileptic seizure detection.

On the other hand, a framework using DWT and SVM was proposed for the epileptic focus localization problem [42]. In this study, seven commonly used wavelet families (Coiflets, Daubechies, Discrete Meyer, Haar, Biorthogonal, Reverse biorthogonal, Symlets) were considered for the EEG signal decomposition. An accuracy of 88.0% was obtained using optimal frequency bands and wavelet coefficient features. Statistical features extracted from wavelet decomposed EEG were classified using the relevance vector machine (RVM) classifier [128]. Similarly, statistical features estimated from DWT showed an accuracy of 97.83% using combined neural network model [129]. Faust et al. [130] proposed a review on wavelet-based EEG processing for seizure detection. Further, signal energy [131], Eigenvalues [9], and 21 different features [132] were investigated for the classification of epileptic seizures and promising results were reported. Transfer learning semi-supervised learning fuzzy system based model was found to be computationally intensive for

solving real-time seizure detection [133]. A deep convolution neural network-based approach was introduced recently for automated seizure detection using EEG signals [39, 134]. The SVM classifier has been extensively used for epileptic seizure detection due to its efficient generalization ability and promising results [42, 58, 132, 135].

A number of studies [21, 42, 43, 47, 79, 82, 93, 97, 110, 129, 130, 131, 135, 136, 137] have employed wavelet transforms for seizure detection and have reported promising results. Therefore, in this study, EEG signal was decomposed using DWT with five different wavelet functions.

The thorough literature survey suggests that the classification results could be further improved through an optimal selection of the feature extraction method and classifier. It is essential that the algorithm computation time should be very short for real-time seizure detection. Hence, in this study, in order to achieve better performance over existing methods, a novel feature referred to as sigmoid entropy derived from DWT coefficients was introduced. A SVM model was later employed to classify seizure and non seizure patterns.

The rest of the paper is organized as follows. In Section 2, a brief description of the sigmoid entropy and the database used for the study is described. The results of the study are presented in Section 3 and performance comparison is discussed in Section 4. Finally, Section 5 concludes the paper.

4.2 Methodology

4.2.1 Proposed method

Fig. 4.1 depicts the block diagram of the proposed seizure detection algorithm that uses a DWT based sigmoid entropy and SVM classifier. The EEG recordings were pre-processed using a notch filter and a bandpass filter to remove any noise. An independent component analysis was performed to remove any artifacts. The EEG was segmented into 1 s length to maintain the stationarity of the signal. Further, the EEG signal was decomposed using DWT consisting of five different mother wavelets. Subsequently, sigmoid entropy was estimated in both time and frequency domain using amplitude and power spectral density of the EEG signal. Finally, the extracted features were classified using SVM classifier with the segment and event-based approaches and the performance of the algorithm was evaluated using three databases.

4.2.2 Clinical data

In this study, three EEG databases were used to validate the proposed seizure detection algorithm. The first database was obtained from the Ramaiah Medical College and Hospitals (RMCH), Bengaluru, India. Ethical clearance was obtained from the RMCH ethics committee to study EEG recordings for research purpose. The unipolar scalp EEG was recorded using 19 electrodes placed according to the International 10-20 system of configuration at a sampling rate of 128 Hz using Galileo Suite-EB Neuro EEG system. The database

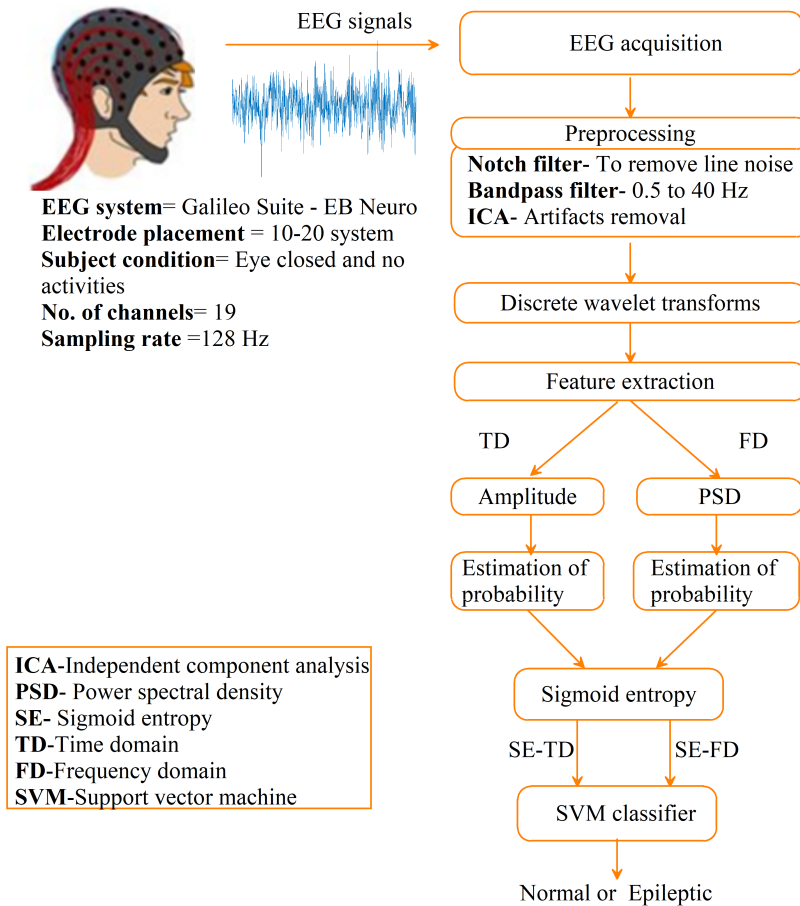


FIGURE 4.1: Block diagram of the proposed seizure detection algorithm using DWT based sigmoid entropy and SVM classifier for the RMCH database.

comprises of 115 subjects, which include 67 male and 48 female, ranging between 2.5 to 75 years of age. Among the 115 subjects, 38 were suffered from epilepsy and 77 were healthy subjects. The scalp EEG was recorded from the following electrode positions: Fp1, Fp2, F7, F3, Fz, F4, F8, T3, C3, Cz, C4, T4, T5, P3, Pz, P4, T6, O1, and O2. Two experts with the same display setting were visually labeled the EEG recordings as normal and epileptic events. The seizure activities with a minimum duration of 6 s and a maximum of any

period were considered for the study.

The second database used in our study was a publicly available database from the University of Bonn (UBonn) ¹ [33]. The EEG recordings were obtained from Five different patients who have undergone presurgical evaluations. The EEG recordings in UBonn database were divided into five sets (A-E), each set consisting of 100 single channel EEG segments of 23.6 s duration recorded at a sampling rate of 173.61 Hz. Each subset A, B, C, D, and E represent the states of normal with eyes open, normal with eyes closed, pre-ictal, post-ictal and ictal respectively. For this study, classification problems, namely {A}-{E}, {ACD}-{E}, {ABCD}-{E}, and {AB}-{CD}-{E} were formed using five different subsets [9, 47, 89, 137].

The third database was collected from CHB-MIT [88], an open-source EEG available in Physionet repository ². This database consists of 844 hours of EEG recordings, which comprises of 182 seizures recorded from 23 patients. The recordings were obtained from 23 channels placed according to 10-20 International system bipolar montage electrode placement and recorded at a sampling rate of 256 Hz. One can refer to [88, 100] for more details on the EEG database and patient information.

4.2.3 Preprocessing

For the RMCH database, EEG was pre-processed using suitable signal processing techniques. A 50 Hz notch filter was used to attenuate the power line interference. Further, EEG time series were filtered using a bandpass filter

¹http://epileptologie-bonn.de/cms/front_content.php?idcat=193&lang=3&changelang=3

²<http://www.physionet.org/pn6/chbmit>

with the lower and a higher cut-off frequency of 0.5 Hz and 40 Hz respectively. An independent component analysis was applied to the EEG signal to remove artifacts such as eye blinks, chewing, muscular artifacts, etc [138]. In our study, filtering techniques were not employed on UBonn and CHB-MIT databases as the available data was already pre-processed.

4.2.4 Discrete wavelet transform

DWT is a spectral analysis technique that provides a multi-resolution and time-frequency analysis of non-stationary EEG signal [139, 140]. DWT has been used extensively for seizure detection and promising results were achieved [21, 42, 43, 47, 79, 82, 93, 97, 110, 129, 130, 131, 135, 136]. DWT comprises pairs of low pass filter (approximation coefficients) and high pass filter (detail coefficients). At each level of DWT, the signal is simultaneously passed through a set of low pass filter and high pass filter followed by downsampler (refer to Fig. 4.2). The selection of the decomposition level depends on the dominant frequency components of the signals [79, 92, 139, 140].

The wavelet ψ^i can be obtained from the following relationship [139]:

$$\psi^{2i} = \frac{1}{\sqrt{2}} \sum_{k=-\infty}^{\infty} h(k) \psi^i \left(\frac{t}{2} - k \right) \quad (4.1)$$

$$\psi^{2i+1} = \frac{1}{\sqrt{2}} \sum_{k=-\infty}^{\infty} g(k) \psi^i \left(\frac{t}{2} - k \right) \quad (4.2)$$

Here, i is the modulation parameter, k is the translation parameter, ψ^i is the mother wavelet, $h(k)$ is the low pass filter and $g(k)$ is the high pass filter

associated with the scaling function and the mother wavelet function [139, 140].

The wavelet coefficient $c_{j,k}^i$ (j is the dilation parameter) corresponding to a signal $s(t)$ can be obtained as [139],

$$c_{j,k}^i = \int_{-\infty}^{\infty} s(t) \psi_{j,k}^i(t) dt \quad (4.3)$$

Based on the previous studies reported on seizure detection [47, 79, 82, 93, 97, 110, 130, 131, 135, 136], we have selected five most commonly used wavelets, namely Haar, Coiflets (Coif4), Discrete Meyer (Dmey), Biorthogonal (Bior3.1) and Reverse Biorthogonal (Rbio3.1). These studies have proved that above-mentioned mother wavelets were well suited for EEG signal analysis.

Fig. 4.2 shows the structure of wavelet decomposition of an EEG signal up to the fifth level. The decomposition levels until the fourth, fifth, and fifth levels were considered for RMCH, UBonn, and CHB-MIT databases respectively. The levels of decomposition selected were different as each database has a different sampling frequency. The EEG sub-bands were selected, ensuring different frequency ranges as it would reveal information associated with that EEG band. The frequency ranges of approximation and detail coefficients in each level were given in Table 4.1.

4.2.5 Sigmoid entropy

The latest improvements in non-linear dynamics theory or chaos theory provided a new concept to analyze EEG time series due to its high versatility. It is

TABLE 4.1: Information about EEG sub-bands and frequency range of wavelet decomposition of EEG signal for RMCH ($f_s=128$ Hz), UBonn ($f_s=173.71$ Hz) and CHB-MIT ($f_s=256$ Hz)

Decomposition level	Sub-bands	Frequency range of sub-bands	Frequency range (Hz)		
			RMCH	UBonn	CHB-MIT
1	A1	0- $f_s/4$	0-32	0-43.4	0-64
	D1	$f_s/4$ - $f_s/2$	32-64	43.4-86.8	64-128
2	A2	0- $f_s/8$	0-16	0-21.7	0-32
	D2	$f_s/8$ - $f_s/4$	16-32	21.7-43.4	32-64
3	A3	0- $f_s/16$	0-8	0-10.85	0-16
	D3	$f_s/16$ - $f_s/8$	8-16	10.85-21.7	16-32
4	A4	0- $f_s/32$	0-4	0-5.43	0-8
	D4	$f_s/32$ - $f_s/16$	4-8	5.42-10.85	8-16
5	A5	0- $f_s/64$	-	0-2.70	0-4
	D5	$f_s/64$ - $f_s/32$	-	2.70-5.43	4-8

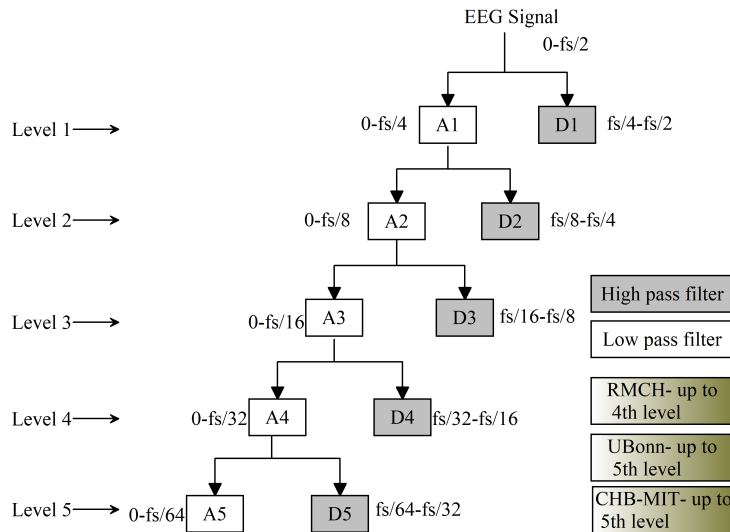


FIGURE 4.2: Structure of wavelet decomposition of EEG up to the fifth level.

a well-known fact that EEG contains nonlinear elements, which is a reflection of the neuronal activity in the brain. The sigmoid function is one of the most

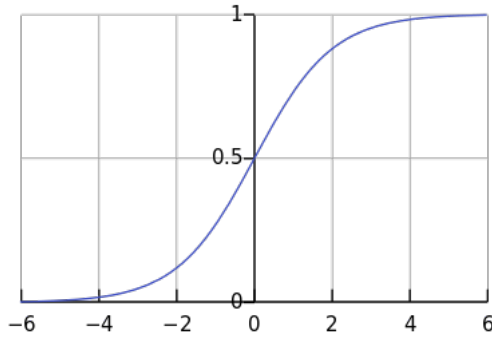


FIGURE 4.3: Sigmoid function with the output between 0 and 1.

widely used activation functions in neural networks. The advantage of this activation function is, unlike the linear function is that its output is always in the range of 0 and 1. Therefore, we propose sigmoid entropy to analyze EEG time series data by exploiting the nonlinear characteristics of the sigmoid function.

4.2.5.1 Definition

A sigmoid function is a particular case of the logistic function having “S” shaped curve (refer to Fig. 4.3) defined by (4.4)

$$\sigma(t) = \frac{1}{1 + e^{-t}} \quad (4.4)$$

4.2.5.2 Sigmoid entropy

The sigmoid function is used as a feature for epileptic seizure detection as it is widely used in the artificial neural networks as a nonlinear complex function. Assuming that n is the number of possible states that the amplitude of wavelet decomposed EEG are quantized into and p_i the probability of each

state is $p = \{p_i\}$, $0 \leq p_i \leq 1$ and $\sum_{i=1}^n p_i = 1$. In this study probability of the occurrence of EEG signal is calculated using the histogram method by specifying bin ranges. The bin range of $0.05 \mu v$ was considered for all the three databases.

Now by replacing t with p in (4.4), where $p = \{p_1, p_2, p_3, \dots, p_n\}$, (4.4) becomes

$$\sigma(p) = \frac{1}{1 + e^{-p}} \quad (4.5)$$

Expanding (4.5) becomes

$$\sigma(p) = \frac{1}{1 + e^{-p_1} + e^{-p_2} + e^{-p_3} + \dots + e^{-p_n}} \quad (4.6)$$

The amount of information captured by (4.6) is referred to as sigmoid entropy (H_s) for time domain and (4.6) can be written as

$$H_s = \frac{1}{1 + \sum_{i=1}^n e^{-p_i}} \quad (4.7)$$

Similarly, sigmoid entropy for the frequency domain is calculated using

$$H_s = \frac{1}{1 + \sum_{i=1}^n e^{-p_{f_i}}} \quad (4.8)$$

Where p_f is probability values derived from power spectral density (PSD) of the wavelet decomposed EEG signal that was calculated using the periodogram method.

The dynamic range of the sigmoid entropy lies between 0 and 1. According to the characteristics of the sigmoid function, maximum entropy of '1' infers less variation of the signal and more variation or fluctuation of the signal indicated to low entropy.

4.2.5.3 Property of sigmoid entropy

The property of sigmoid function is defined as [141], If $\sigma(t) = \frac{1}{1+e^{-t}}$, then differential equation is $\sigma'(t) = \sigma(t)(1 - \sigma(t))$. Similarly, the property of sigmoid entropy can be written as,

$$\text{if } H(p) = \frac{1}{1 + \sum_{i=1}^n e^{-p}}, \text{ then } H'(p) = H(p)(1 - H(p))$$

4.2.5.4 Additivity property

Shannon entropy [142] and Tsallis entropy [143] are well known extensive and non-extensive entropy measures respectively. Given two independent systems A and B , where H_A and H_B are their entropy values, respectively, for which the joint probability density must satisfy the following properties.

1. **Shannon entropy:** $H(A \cup B) = H(A) + H(B)$ that meets the additive property for $H = - \sum_{i=1}^n p_i \log_2(p_i)$ [142]
2. **Tsallis entropy:** Tsallis brings out the non-extensive entropy equation as follows [143]

$$S_q = \frac{1 - \sum_{i=1}^n (p_i)^q}{q - 1} \quad (4.9)$$

where, n is the number of possible states of the system, and q is the entropy index, and it defines the degree of non-extensive. The pseudo

additivity property of the Tsallis entropy is given as [143]

$$H(A \cup B) = H(A) + H(B) + (q - 1)H(A)H(B) \quad (4.10)$$

3. **Sigmoid entropy:** As similar to the Shannon and Tsallis entropy, additivity property for sigmoid entropy can be written as:

$$H_s(A \cup B) = H_s(A) + H_s(B) - \delta(H_s(A)H_s(B)) \quad (4.11)$$

where $\delta = (n - 1) + (1 - \text{erf}(\text{erf}(\sum_{i=1}^n p_i = 1)))$. We consider the *erf* function because sigmoid function resembles Gaussian error function shape [60]. The *erf* function is calculated for *erf*(1) since $\sum_{i=1}^n p_i = 1$.

Thus, δ can be rewritten as $\delta = (n - 0.7750)$.

Hence, (4.11) can be rewritten as follows:

$$H_s(A \cup B) = H_s(A) + H_s(B) - (n - 0.7750)(H_s(A)H_s(B)) \quad (4.12)$$

4.2.6 Classification

The classification of epileptic seizures was performed using the SVM classifier as the good performance was reported in previous studies [25, 42, 47, 65, 89, 128, 135]. SVM uses kernel method to transform the feature set that draws an optimal boundary between possible outputs [23]. The preliminary study reveals better performance using radial basis function kernel and the same was implemented for further analysis.

In order to find the best wavelet and a decomposition level for seizure detection on the RMCH database, a segment-based and event-based classification approach was employed as reported in [98]. The optimal decomposition level and wavelet were identified from a segment-based approach employed for event-based classification approach. The SVM classifier was implemented with leave-one-subject-out cross-validation method for the RMCH database.

To evaluate the segment-based approach, we have used performance measures, namely sensitivity, specificity, accuracy, and F measure [21, 47, 80]. F-measure is the harmonic mean of precision and recall. The recall is the same as sensitivity and precision is the positive predictive value (PPV).

$$Sensitivity = \frac{TP}{TP + FN} \quad (4.13)$$

$$Specificity = \frac{TN}{TN + FP} \quad (4.14)$$

$$Accuracy = \frac{TP + TN}{TP + FP + TN + FN} \quad (4.15)$$

$$Fmeasure = 2 \cdot \frac{\text{precision} \cdot \text{recall}}{\text{precision} + \text{recall}} \quad (4.16)$$

$$PPV = \frac{TP}{TP + FP} \quad (4.17)$$

$$NPV = \frac{TN}{TN + FN} \quad (4.18)$$

where, TP is true positive, FN false negative, TN is true negative and FP is false positive.

Further, the performance of the event-based seizure detection on the RMCH database was evaluated using seizure detection rate (SDR), false detection rate (FDR) and mean detection delay (MDD) [100].

- *SDR*: Number of correctly detected epileptic seizure events
- *FDR*: Percentage of false seizure detections per hour
- *MDD*: Mean time difference between seizure occurrence and algorithm detection

Similarly, UBonn database was evaluated using a segment-based approach with 10-fold cross-validation and the performance was assessed in terms of sensitivity, specificity, accuracy and F measure. Further, PPV and negative predictive value (NPV) were used to compare the results with existing methods (refer to Table 4.6) obtained using UBonn database.

Cohen's Kappa coefficient is a statistical method that measures between two raters [144]. In our study, two raters were an epileptic seizure and normal EEG. Kappa determines if there is an agreement between two raters by chance with a percentage. Table 4.2 shows cell probabilities for two raters. The predictions A and B represent the epileptic seizure and normal EEG respectively. In other words, these predictions can be obtained from the confusion matrix.

To compute Kappa, first, we need to calculate the observed level of agreement (P_o) and expected agreement (P_e), which is given by [144]

$$P_o = \frac{P_{AA} + P_{BB}}{P_T} \quad (4.19)$$

TABLE 4.2: Calculation of Kappa values

		Rater #2	
		Prediction of A Value	Prediction of B Value
Rater #1	Prediction of A Value	P_{AA}	P_{AB}
	Prediction of B Value	P_{BA}	P_{BB}

$$P_e = \left(\frac{P_{AA} + P_{AB}}{P_T} * \frac{P_{AA} + P_{BA}}{P_T} \right) + \left(\frac{P_{AB} + P_{BB}}{P_T} * \frac{P_{BA} + P_{BB}}{P_T} \right) \quad (4.20)$$

where,

$$P_T = P_{AA} + P_{AB} + P_{BA} + P_{BB} \quad (4.21)$$

Finally, the Kappa coefficient is calculated as [144]

$$K = \frac{P_o - P_e}{1 - P_e} \quad (4.22)$$

The Kappa is always less than or equal to 1. The Kappa coefficient with a value of 1 implies perfect agreement and any value less than 1 can be interpreted as follows: Poor agreement (< 0.2), Fair agreement (0.2-0.4), Moderate agreement (0.4-0.6), Good agreement (0.6-0.8), and Very good agreement (0.8-1).

4.2.7 Alarm for seizure detection

Tawfik et al. [98] have proposed channel fusion based seizure detection by combining the results obtained from different channels to determine the seizure onset. Similarly, Zandi et al. [137] have proposed seizure alarm method, when at least three different channel alarms occur within a duration of 5 s. Bogaarts

et al. [84] have applied both epochs based and event-based seizure classification. Their mechanism helped to reduce the false alarm and improve the sensitivity.

In our study, to improve the performance of the algorithm, post-processing of the SVM classifier in the event-based approach was employed as reported in [84, 98, 137]. Fig. 4.4 depicts the procedure of alarm for seizure detection. The channels were marked as seizure if at least three channels classifier output was 1; otherwise, those channels were marked as non-seizure. The reason behind choosing three channels for the decision making was that a minimum of three channels was associated with seizures in case of focal seizures.

4.3 Results

4.3.1 Spectrogram analysis

Fig. 4.5 shows the EEG (channel T5) from the RMCH database and its spectrogram analysis before and after pre-processing. Figs. 4.5a & c shows raw EEG and filtered EEG signal respectively. The line noise at 50 Hz can be observed in Fig. 4.5b and spectrogram of filtered EEG are shown in Fig. 4.5d. Spectrogram analysis revealed that PSD during epileptic activity was found to be higher resulting in better discrimination as compared to the normal activity. Therefore, good discrimination in terms of amplitude and PSD for epileptic activity was achieved. These influenced to derive the DWT based sigmoid entropy both in time and frequency domains.

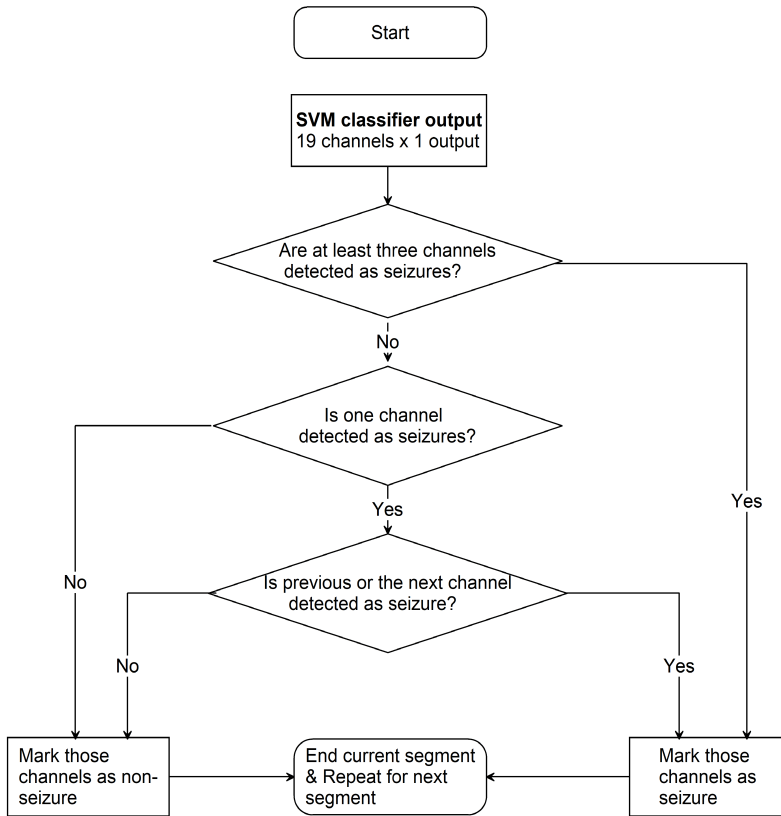


FIGURE 4.4: The flow chart of alarm for seizure detection. During the preliminary visual marking and training phase of SVM, it was seen that the minimum duration of seizure activities was found 6 s. Therefore, when the consecutive segments are marked as seizures for a minimum of 6 sec, then it is considered as one seizure event. This mechanism helped us to reduce the false detections that arise due to artifacts and non-epileptic activities.

4.3.2 Analysis of sigmoid entropy using synthetic signal

We explore the sigmoid entropy to observe the changes in EEG signal under different conditions. A synthetic signal was created which comprises of three parts of 5 s duration each with different probability density functions [145]: (A) Gaussian distribution with zero mean and standard deviation of 1, (B)

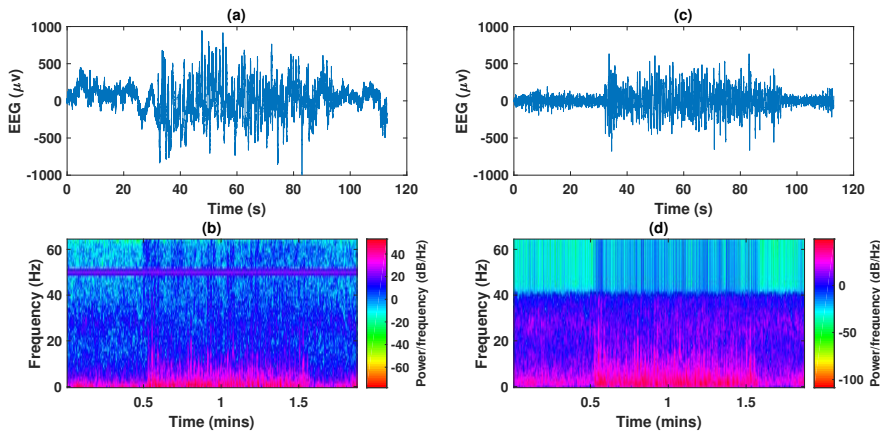


FIGURE 4.5: An example of EEG (channel T5) from the RMCH database and its analysis. **(a)** Raw EEG with 50 Hz line noise. **(b)** The spectrogram showing the presence of line noise at 50 Hz and an increase in power value during seizure activity. **(c)** EEG after applying a notch filter and bandpass filter (refer 2.2 for filter specifications). **(d)** The spectrogram showing line noise is removed at 50 Hz and bandpass filtered between 0.5 - 40 Hz. The spectrogram was plotted with the following specifications: Window=Hamming, Window length=128, Number of overlap samples=120, Number of DFT points=128, and Sampling rate= 128 Hz.

normal EEG signal from channel T5, (C) epileptic EEG from channel T5. Fig. 4.6 shows the analysis of sigmoid entropy for the synthetic signal. The following were the facts derived from the synthetic signal analysis:

1. Entropy was less for Gaussian distribution and further less for epileptic EEG.
2. Entropy was maximum for normal EEG.
3. The transition from one distribution to another was clearly seen.

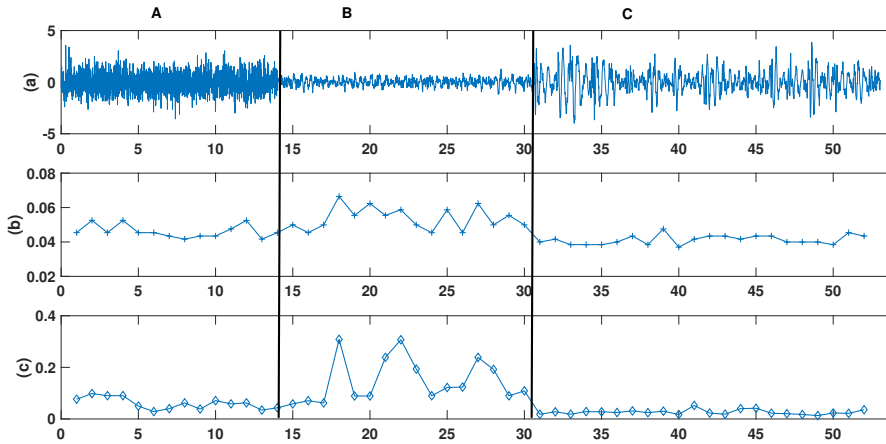


FIGURE 4.6: **(a)** A synthetic signal. **(b)** Sigmoid entropy in the time domain. **(c)** Sigmoid entropy in the frequency domain.

4.3.3 Segment-based approach classification results

The segmentation length of 1 s was applied for feature extraction and seizure detection. The EEG signal was decomposed up to the fourth level using Haar, Coif4, Dmey, Bior3.1, and Rbio3.1 mother wavelets for RMCH database. An example of decomposed EEG in D1, D2, D3, D4, and A4 sub-bands are shown in Fig. 4.7. Fig. 4.8 shows the Boxplot of sigmoid entropy in time and frequency domains derived from DWT. In Fig. 4.8 the black and green boxes indicate the distribution of the sigmoid entropy values of normal and epileptic EEG respectively. Boxplot analysis showed good discrimination in terms of median, quartile, upper quartile and interquartile range for all the wavelets.

In order to find the best decomposition level and wavelet, we employed the segment-based classification approach [84, 98, 137]. The optimal decomposition level and wavelet obtained in segment-based approaches were employed

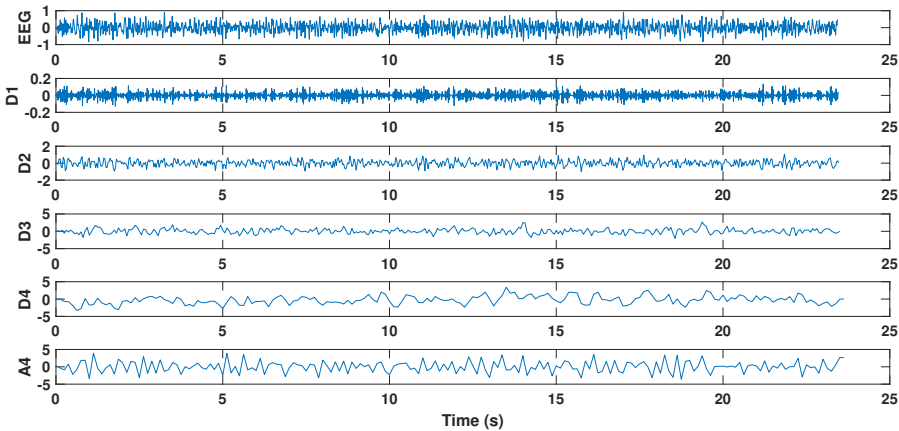


FIGURE 4.7: Wavelet decomposition of a sample EEG up to the fourth level using Bior3.1 wavelet. The EEG displayed in the following order from top to bottom: EEG, D1, D2, D3, D4, and A4 sub-bands.

for event-based classification approach. Fig. 4.9 shows the classification results achieved using the segment-based approach. The sensitivity of 100% was seen in the D1 sub-band using Coif 4, Dmey, Bior3.1, and Rbio3.1 wavelets. However, sensitivity obtained in the D1 sub-band using Haar wavelet was very close to other wavelets. Further, again sensitivity of 100% was seen in the D2 sub-band using Haar, Coif 4, Dmey, and Bior3.1 wavelets. The highest sensitivity of 99.72% was achieved in the D3 sub-band using Dmey, Bio3.1 and Rbio3.1 wavelets. Similarly, Dmey and Bio3.1 wavelets in D4 sub-bands showed 100% sensitivity. The maximum sensitivity of 99.97% seen in the A4 sub-band using Dmey wavelet. The results showed that all the wavelets were capable of producing good sensitivity (i.e., seizure detection) using sigmoid entropy. The specificity of 100% was obtained in D2 (Rbio3.1), D3 (Haar, Coif4, and Bior3.1, and Rbio3.1), and D4 (Haar, Coif4, and Bio3.1) sub-bands. The least sensitivity and specificity obtained was 92.28% in (Rbio3.1)

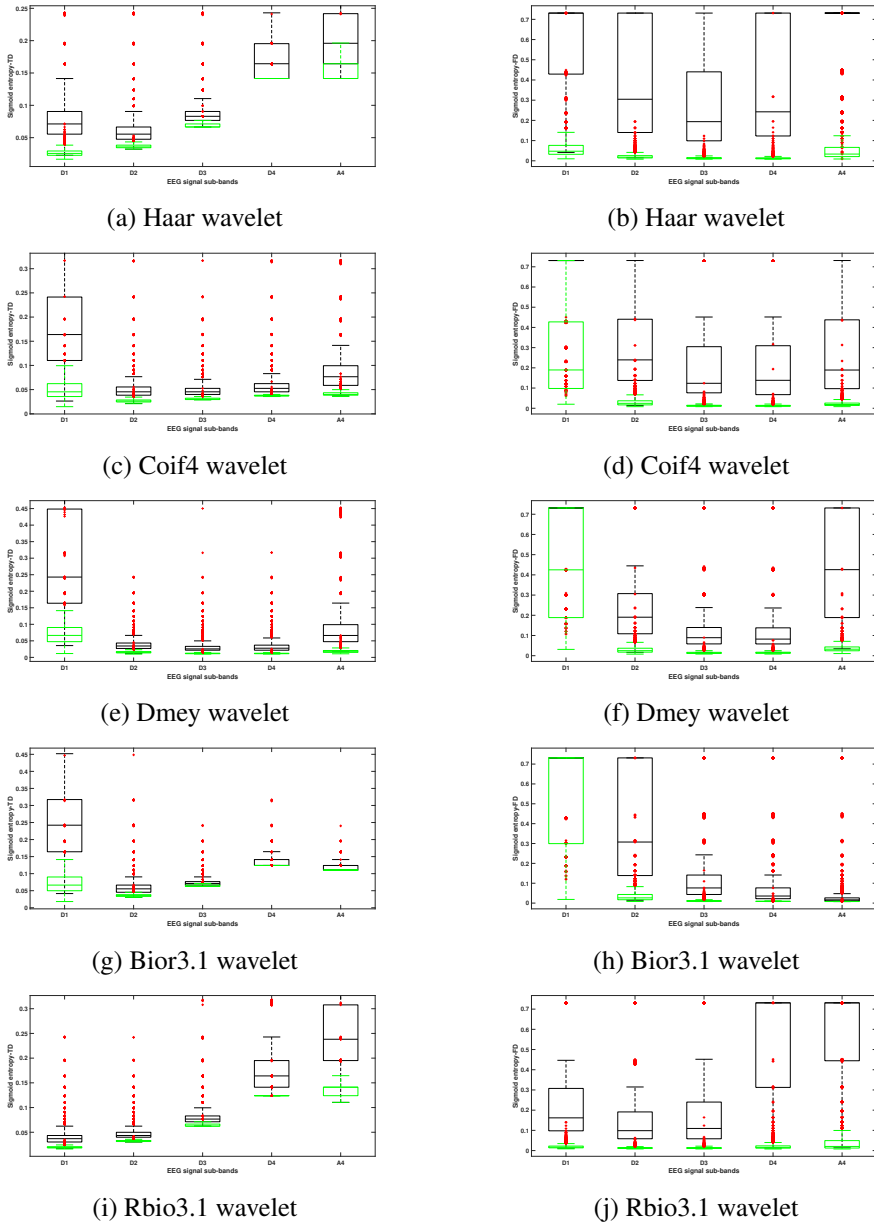


FIGURE 4.8: The boxplot of sigmoid entropy in the time domain (left column) and frequency domain (right column). The box displayed in Black boxes and Green boxes represents normal and epileptic EEG respectively. The data points displayed using + are whiskers. Wilcoxon rank sum test showed $p < 0.05$ between normal and epileptic EEG sigmoid entropy for all the wavelets and decomposition level.

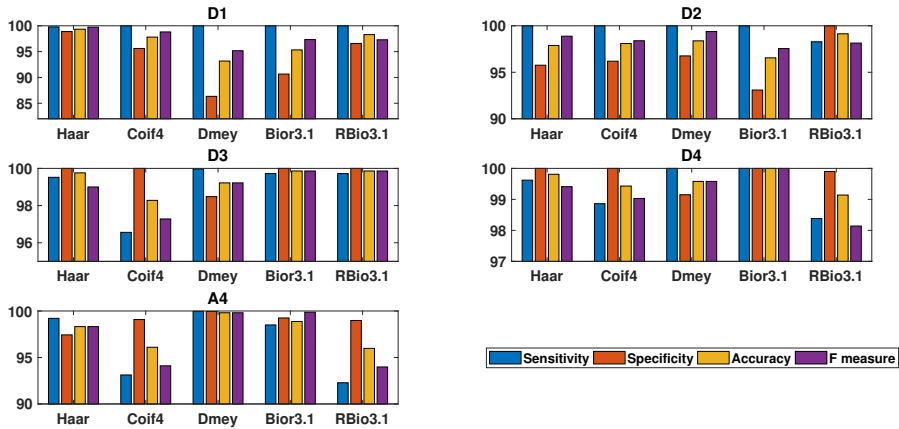


FIGURE 4.9: Classification results using a segment-based approach the RMCH database. The results are grouped wavelet wise for each sub-band.

and 86.34% in D1 (Dmey) respectively. The highest sensitivity, specificity, and accuracy of 100% was achieved using Bior3.1 wavelet in D4 sub-band.

In Fig. 4.9, the last bar shows the F-measure for the same. The least F-measure were 93.05% (Dmey), 96.45% (Bior3.1), 98.10% (Coif4), 99.10% (Rbio3.1) and 95.80% (Rbio3.1) in EEG sub-bands D1, D2, D3, D4, and A4 respectively. Among all the sub-bands and wavelets, highest sensitivity, specificity, accuracy, and F-measure of 100% was achieved using Bior3.1 wavelet in D4 sub-band. Therefore, the segment-based approach showed that Bior3.1 wavelet in D4 sub-band is the optimal choice for the event-based approach.

4.3.4 Event-based approach classification results

For the event-based approach, Bior3.1 wavelet in D4 sub-band was employed as it showed superior performance (Section 3.3). Fig. 4.10 presents EEG, sigmoid entropy in time and frequency domains and classifier output corresponding to different channels of an epileptic patient data obtained from RMCH database. According to the visual identification of the EEG by experts, the seizure starts at 32 s and ends at 93 s. As shown in the right panel of Fig. 4.10, the seizure was detected immediately after the onset at 32 s (in F4, T3, and T5) and with some delay in channels Cz and P3. On applying the proposed method to the complete epileptic data, which consist of 162 seizures, SDR of 96.34% along with the MDD of 1.2 s and FDR of 0.5/h was observed. Thus, the proposed method was capable of capturing the seizure onsets shortly after its occurrence reducing the detection delay. Nearly 60% of the seizure onsets across each channel were detected within 1 s, and remaining were identified within 2 s.

4.3.5 Results using UBonn database

The proposed method was applied to one of the gold standard EEG database obtained from the UBonn [33] to evaluate the generalization and efficiency of the algorithm. The sigmoid entropy feature extracted from the UBonn database was classified using the segment-based approach with 10-fold cross-validation. Since the sampling frequency of UBonn database was 173.71 Hz, EEG was decomposed up to the fifth level. For UBonn database, the following sub-bands were considered: D1 ($fs/4$ - $fs/2$), D2 ($fs/8$ - $fs/4$), D3 ($fs/16$ - $fs/8$),

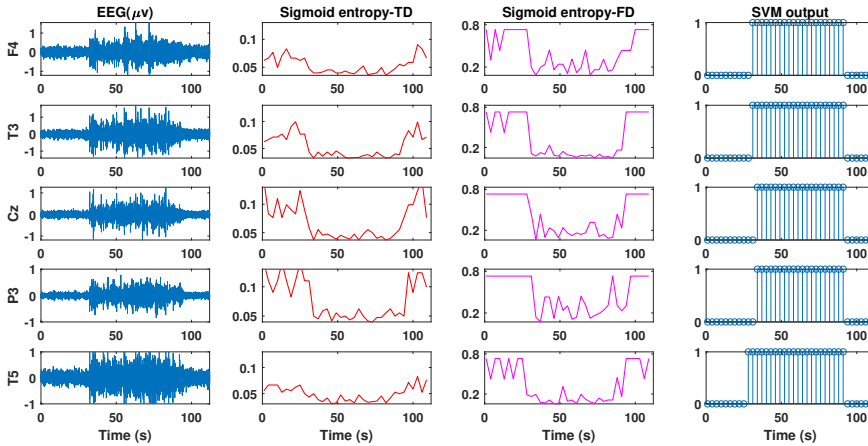


FIGURE 4.10: The EEG, sigmoid entropy in time and frequency domain and classifier output corresponding to different channels of an epilepsy patient. The seizure starts at 32 s and ends at 93 s. The description of data showed in this figure as follows: **First column:** EEG of different channels, **Second column:** Sigmoid entropy in the time domain, **Third column:** Sigmoid entropy in the frequency domain, and **Fourth column:** SVM classifier output.

D4 (fs/32-fs/16), D5 (fs/64-fs/32) and A5 (0-fs/64). The frequency content within the sub-bands are as follows: 43.4-86.8 Hz, 21.7-43.4 Hz, 10.85-21.7, 5.42-10.85 Hz, 2.70-5.43 and 0-2.70 Hz for D1, D2, D3, D4, D5, and A5 respectively.

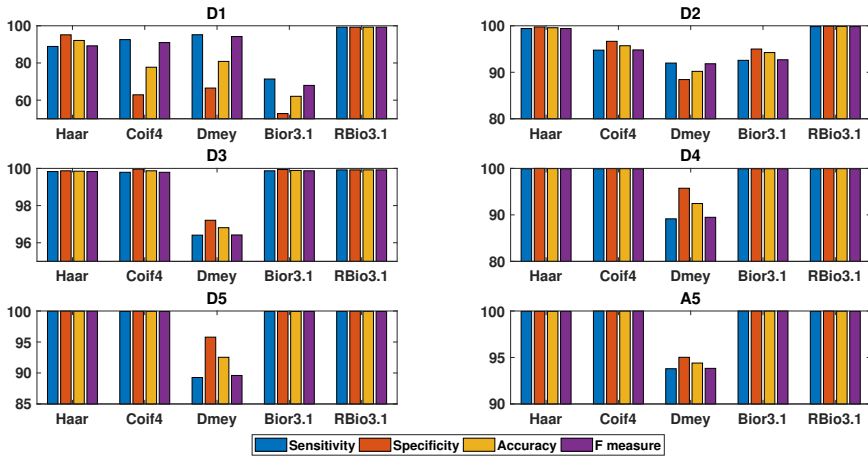
Fig. 4.11(a) shows the classification results obtained for the UBonn database for the case {A}- {E}. The highest sensitivity of 99.28% (Rbio3.1), 99.83% (RBio3.1), 99.92% (Rbio3.1), 99.92% (all except for Dmey), 100% (Coif4 and Bior3.1) in D1, D2, D3, D4, and A4 sub-bands were obtained respectively. All the four performance measures showed 100% in sub-band A5 using Haar and Rbio3.1 wavelets. One can observe that results in D3, D4, and D5 sub-bands using all the wavelets were close to 100% except in Dmey wavelet. The results obtained in D1 sub-band was less as compared to other wavelets except

for Rbio3.1 wavelet. Dmey wavelet in all the sub-bands except D1 showed poor performance against other wavelets. The interesting fact observed was that the performance measures achieved using Rbio3.1 wavelet in all the bands were greater than 99.24%. Further, Bior3.1 wavelet showed similar results to Rbio3.1 wavelet in D3, D4, D5, and A5 sub-bands.

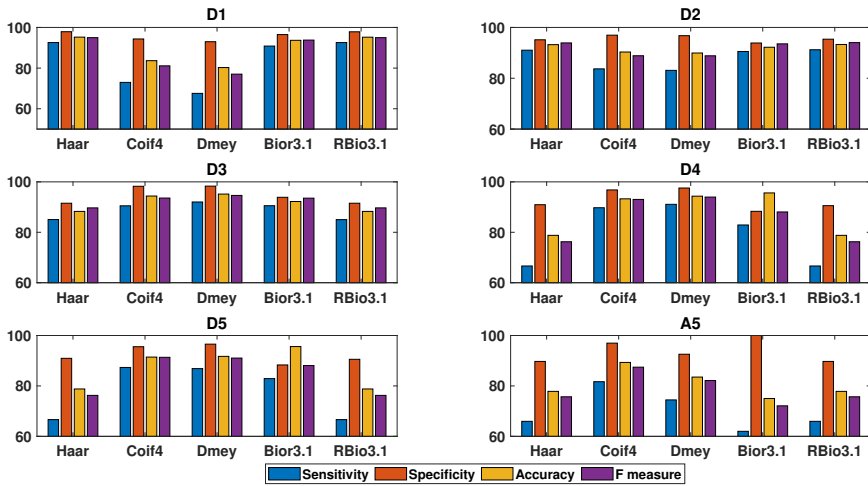
Fig. 4.11(b) shows the results obtained for classification problem {ACD}-{E}. The highest classification accuracy of 95.61% was achieved using Bio3.1 wavelet in sub-band D4. Further, Haar wavelet in sub-band D1, Coif4 in sub-band D3, Dmey in sub-band D3, and Rbio3.1 in sub-band D1 showed the highest accuracy of 95.24%, 94.38%, 95.16%, and 95.21% respectively. The highest classification accuracy of 96.23% was obtained using Haar wavelet in sub-band D2 for classification problem {ABCD}-{E} (refer to Fig. 4.11(c)). The 3-class classification problem {AB} -{CD}-{E} showed the highest accuracy of 90.89% using Rbio3.1 wavelet in sub-band D2 (refer Fig. 4.11(d)).

4.3.6 Results using CHB-MIT database

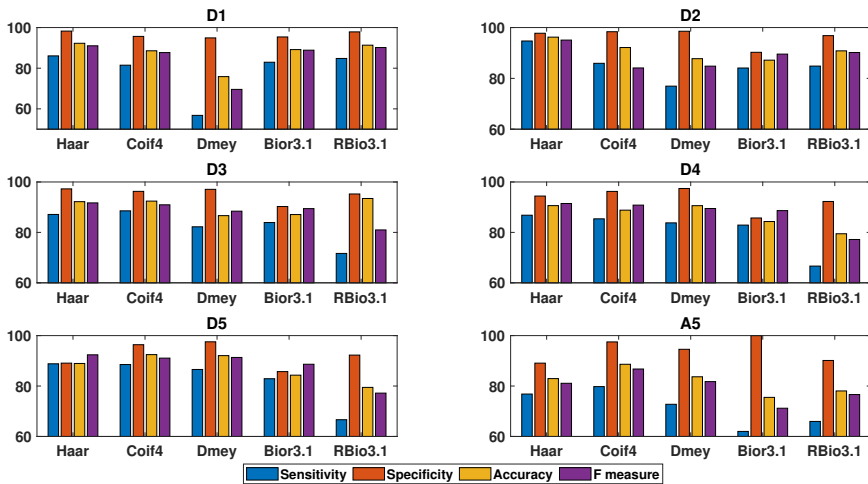
The proposed method was tested on one of the largest EEG database CHB-MIT [88] available in the open source. The classification methodology adopted for the RMCH database was applied to this database also. Fig. 4.12 shows the classification results obtained for CHB-MIT database. Good results were obtained in D1 to D4 sub-bands using all the wavelets. The highest accuracy of 88.48% (D3), 90.65% (D1), 90.78% (D4), 91.53% (D1), and 94.38% (D1) was obtained using Haar, Coif4, Dmey, Bio3.1, and Rbio3.1 wavelets respectively. Among all the wavelets, the highest sensitivity of 94.21% was obtained in sub-band D3 using Rbio3.1 wavelet. The highest sensitivity of 100 % was



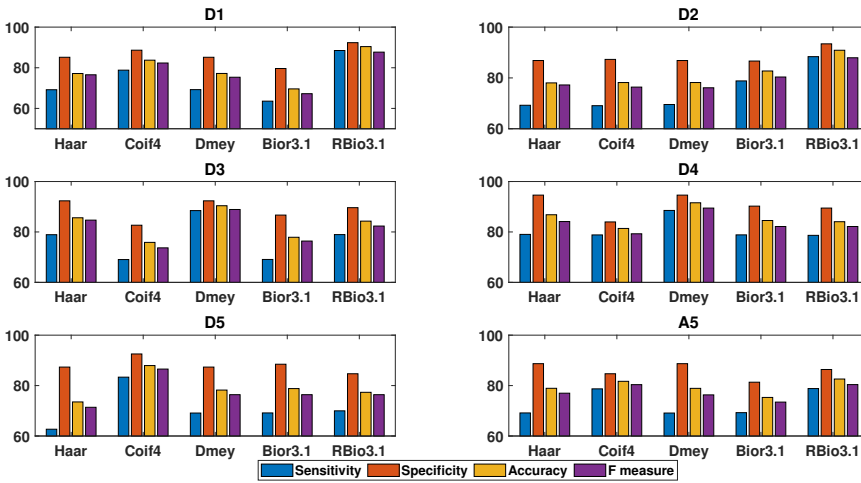
(a)



(b)



(c)



(d)

FIGURE 4.11: Classification result using segment-based classification approach for UBonn database. (a) Classification problem {A}-{E}. (b) Classification problem {ACD}-{E}. (c) Classification problem {ABCD}-{E}. (d) Classification problem {AB}-{CD}-{E}. The results are grouped wavelet wise for each sub-band.

seen in many sub-bands and wavelets. Notably, the classification results obtained using sub-bands D5 and A5 were less as compared to other sub-bands.

UBonn and CHB-MIT databases exhibited higher sigmoid entropy for normal EEG similar to the RMCH database. Hence, it shows that sigmoid entropy performs fairly better on different databases exhibiting good generalization for seizure detection.

4.3.7 Analysis of Cohen's Kappa Coefficient

Table 4.3 shows the Kappa coefficient obtained from all the three databases. The highest Kappa of 1 (very good agreement) was obtained for Bio3.1 wavelet in sub-band D4 using the RMCH database. It was observed that the Kappa coefficients obtained for the RMCH belonged to the very good agreement range

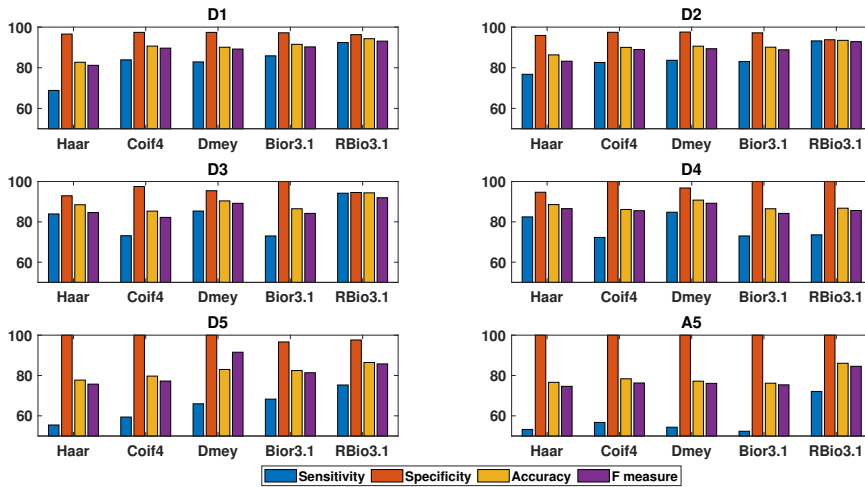


FIGURE 4.12: Classification results using CHB-MIT database. The results are grouped wavelet wise for each sub-band.

of (0.8 to 1). Further, the Kappa coefficient of 1 was obtained for many sub-bands and wavelets for the UBonn database. The results obtained for class A-E are only reported in Table 4.3. Finally, the highest Kappa coefficient of 0.940 was achieved for Rbio3.1 wavelet in sub-band D4 for the CHB-MIT database. Notably, the least Kappa coefficients were obtained for CHB-MIT as compared to the RMCH and UBonn databases. Overall, the Kappa coefficients obtained from all the databases belong to either good or very good agreement category.

4.4 Discussion

The primary aim of the proposed method was to enhance the SDR, FDR, and MDD for real-time seizure detection. In that context, a novel feature referred

TABLE 4.3: Cohen's Kappa Coefficient obtained for all the three databases

Database	Sub-band	Haar	Coif4	Dmey	Bior3.1	Rbio3.1
RMCH	D1	0.972	0.961	0.921	0.934	0.962
	D2	0.965	0.963	0.967	0.958	0.972
	D3	0.982	0.972	0.984	0.987	0.989
	D4	0.982	0.981	0.984	1.00	0.980
	A4	0.942	0.932	0.980	0.975	0.952
UBonn	D1	0.922	0.853	0.868	0.716	0.985
	D2	0.997	0.945	0.895	0.932	1.00
	D3	0.985	0.982	0.952	0.989	0.982
	D4	1.00	1.00	0.923	1.00	1.00
	D5	1.00	1.00	0.926	1.00	1.00
	A5	1.00	1.00	0.948	1.00	1.00
CHB-MIT	D1	0.812	0.892	0.884	0.903	0.932
	D2	0.843	0.894	0.891	0.890	0.923
	D3	0.869	0.842	0.884	0.843	0.940
	D4	0.857	0.789	0.883	0.843	0.836
	D5	0.752	0.774	0.812	0.802	0.834
	A5	0.742	0.762	0.746	0.762	0.846

Interpretation of Kappa values: Poor agreement (< 0.2), Fair agreement (0.2-0.4), Moderate agreement (0.4-0.6), Good agreement (0.6-0.8), and Very good agreement (0.8-1)

to as sigmoid entropy using DWT in both time and frequency domains was proposed and evaluated on three EEG databases.

The seizure detection algorithm using weighted permutation entropy proposed in [98] reports a lower measure for epileptic seizure EEG as compared to normal EEG signal. Further, similar results were obtained in [19] using minimum variance modified fuzzy entropy. In resemblance to [98] and [19], sigmoid entropy measure also exhibited lesser entropy for epileptic EEG than

TABLE 4.4: Performance comparison of the studies that are used entropy methods

Authors	Feature extraction	Classifier	Database	Results
[80]	ApEn, Sample entropy, Phase Entropy 1 and 2	Fuzzy classifier	UBonn	Accuracy= 98.1%
[124]	Optimized sample entropy	Extreme learning machine	UBonn	Accuracy= 99.0%
[47]	DWT based ApEn	Artificial neural network	UBonn	Accuracy= 100%
[126]	Fuzzy entropy	SVM	UBonn CHB-MIT	Accuracy= 100% Sensitivity=98.27% Accuracy= 98.31%
[36]	Wavelet entropy	Recurrent Elman networks	UBonn	Accuracy= 99.75%
[21]	Wavelet packet based log energy entropy	Recurrent Elman networks	UBonn	Accuracy= 99.7%
Proposed	DWT based sigmoid entropy	SVM	UBonn CHB-MIT	Sensitivity= 96.34% Sensitivity=100% Sensitivity=94.21%

normal EEG in our study.

4.4.1 Performance comparison with other entropy methods

Table 4.4 shows the performance comparison of the studies that use entropy methods for the classification of seizures. The studies [21, 36, 47, 80, 124] have used a single database to test their proposed algorithm. Whereas, in the proposed study, three different databases have been studied to test the algorithm. It can be seen from Table 4.4 that the results are shown by our study were better for the UBonn database.

In order to compare the performance of the sigmoid entropy with other entropy methods, the three most widely used Shannon, Renyi, and Tsallis entropy were tested on all the three databases. An entropy index of 2 was set for both Renyi entropy and Tsallis entropy [80]. Different entropy was estimated using Bior3.1 wavelet in D4, Rbio3.1 wavelet in A5, and Rbio3.1 in D3 sub-bands for the RMCH, UBonn, and CHB-MIT databases respectively (These were concluded as superior in Section 3).

Fig. 4.13 shows the performance comparison of four entropy methods using the RMCH, UBonn, and CHB-MIT databases. On all the three databases,

sigmoid entropy showed the highest classification results as compared to other entropy methods (refer to Fig. 4.13). Further, for UBonn database, sensitivity for Shannon and Renyi entropy was the same as our method, but not for other measures. However, the classification results of other entropy methods were very much close to the results of sigmoid entropy.

The seizure detection algorithm must be computationally efficient for quick detection of seizure activity. Therefore, we ran the algorithm for ten trials and mean time (s) was calculated that includes preprocessing (T_P), DWT (T_{DWT}), feature extraction (T_{FE}) and classification (T_{CL}) using SVM. The total computation time (CT) required to execute a complete algorithm can be expressed as:

$$CT(s) = T_P + T_{DWT} + T_{FE} + T_{CL} \quad (4.23)$$

The complete experiment was implemented in MATLAB 2017b using 8GB RAM, CPU 2 GHz with an Intel I3 processor. The performance results may differ from machine to machine based on the system configuration.

Fig. 4.13 shows the computation time taken to execute the algorithm for each entropy. The proposed sigmoid entropy displayed lesser computation time than other existing entropy methods for the RMCH (10.02 s), UBonn (24.52 s), and CHB-MIT (366.05 s) databases. Relative performance (RP) was used to compare the efficiency of the sigmoid entropy against other entropy measures [21]. It is defined as the ratio of the F measure to the computation time (s), and it can be expressed as:

$$RP = \frac{F_{measure}}{CT} \quad (4.24)$$

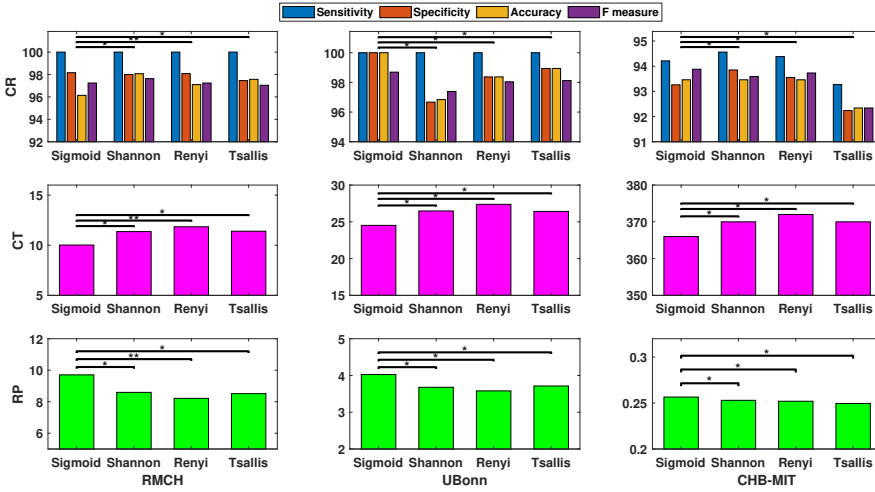


FIGURE 4.13: Performance comparison of sigmoid entropy results with other entropy methods. **First row:** Classification results (CR). **Second row:** Computation time (CT) in seconds. **Third row:** Relative performance (RP) of the algorithm. **Left column:** RMCH, **Middle column:** UBonn, and **Right column:** CHB-MIT. $p < 0.05(*)$, $p < 0.01(**)$, $p < 0.001(***)$.

The higher the RP better the performance of the algorithm. Fig. 4.13 shows the RP obtained for four entropy methods. Sigmoid entropy exhibits slightly better performance as compared to the other three entropy methods for all the three databases. Hence, it confirms that sigmoid entropy is better and computationally efficient as compare to other entropy methods.

4.4.2 Performance comparison using long term EEG

Table 4.5 shows a comparison study with other existing methods. The studies considered for the comparison are based on the criteria that the algorithms have used long-term multichannel EEG and reported SDR, FDR, and MDD. The proposed algorithm attained a good sensitivity of 96.34%, which is comparable to [88] and [122] and higher than other studies reported in Table 4.5.

Our method shows significant improvement in MDD (1.2 s), which is better than the results reported in [137, 146, 147, 148]. The FDR of 0.5/h was achieved that was almost similar to other studies.

TABLE 4.5: Performance comparison of epileptic seizure detection methods

Authors	Duration of EEG (h)	Number of subjects	Number of channels	Number of seizures	Feature extraction	Classifier	SDR (%)	FDR (/h)	MDD (s)
[146]	652	28	24	126	Wavelet transform, energy amplitude and variance	Bayes network	78	0.86	9.8
[147]	525	21	16	88	Wavelet transform, energy, amplitude, variance, cross-correlation, relative derivative	Bayes network	81	0.60	16.9
[99]	22,278	159	19	794	Moving window STFT, averaged and integrated power	Adaptive thresholding	87.3	0.22	-
[137]	76	14	15	63	Combined seizure index	Cumsum thresholding	90.5	0.51	8.02
[148]	236	26	28	79	Regularity index, combined seizure index	Cumsum thresholding	91	0.33	7
[135]	509	21	18	161	Wavelet transform, relative energy, fluctuation index, coefficient of variation and relative amplitude	SVM	94.46	0.58	-
[88]	844	23	18	163	Spectral energy, spatial features, temporal features	SVM	96	0.083	3
[122]	440	23	23	150	Harmonic wavelet packet transform fractal dimension, spatial and temporal features	RVM	96	0.1	1.34
Proposed	58	115	19	162	Sigmoid entropy	SVM	96.34	0.5	1.2

4.4.3 Performance comparison using UBonn database

We have evaluated the generalization of our algorithm on UBonn database. Table 4.6 shows the performance comparison of the studies conducted using UBonn database. The studies considered for the comparison that have reported the performance measures, namely sensitivity, specificity, accuracy, PPV, and NPV. Few studies have attained lesser performance measures despite employing DWT with more number of features. Noticeably, the proposed method showed better results on all measures using DWT.

Fig. 4.14 shows the performance comparison using radar chart for the studies conducted using UBonn database that was reported in Table 4.6. In the

radar chart, the best method spans a larger Pentagon. Our seizure detection method exhibited the largest area (red pentagon in Fig. 4.14) as compared to other studies.

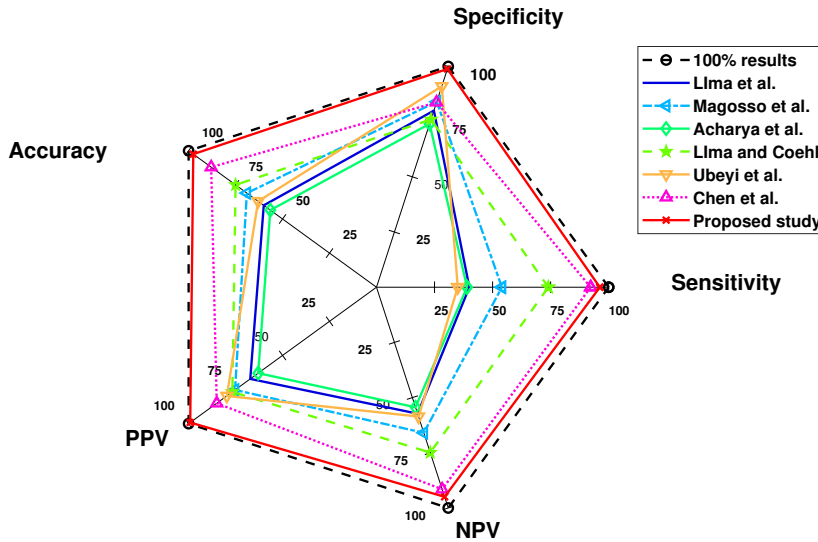


FIGURE 4.14: The performance comparison using radar chart for the UBonn database. The outermost dotted black line indicates the 100% performance. The Pentagon represents the performance of each method in a different color.

4.4.4 Significant findings of the study

The significant findings of the study are listed below:

1. This study introduced DWT based sigmoid entropy in time and frequency domains that were derived from the sigmoid function for the detection of epileptic seizures.

TABLE 4.6: Performance comparison of the studies conducted using UBonn database

Authors	Method	Sensitivity (%)	Specificity (%)	Accuracy (%)	PPV (%)	NPV (%)
[128]	DWT + Statistical features and RVM	40	80	60	67.19	57.28
[131]	DWT + Signal energy	54	84	69	75.28	65.95
[9]	Wavelet packet decomposition + Eigenvalues and Gaussian mixture model	39	74	56.5	62.97	54.38
[132]	Wavelets + 21 features and SVM	74	76	75	76.71	74.91
[129]	Wavelet + Statistical features and Combined neural network	35	91	63	79.67	58.6
[42]	DWT + 9 features and SVM	92.24	83.76	88	85.03	91.52
Proposed	DWT +Sigmoid entropy and SVM	100	100	100	100	100

2. The proposed algorithm was tested on three databases, namely RMCH, UBonn, and CHB-MIT for its generalization and robustness.
3. Five commonly used wavelets, namely Haar, Coif4, Dmey, Bior3.1, and RBio3.1, were examined and compared with different decomposition levels. Among five different wavelets, Bio3.1 in D4 sub-band, Rbio3.1, and Haar in A5 sub-band, Rbio3.1 in D3 sub-band was found to be the best choice for RMCH, UBonn, and CHB-MIT databases respectively. Further, Dmey wavelet showed the least performance for UBonn database.
4. The classification results obtained in D5 and A5 sub-bands using CHB-MIT database was less as compared to other sub-bands.
5. The results reveal that the transition from normal to epileptic activity in the brain can be better described using sigmoid entropy.
6. Sigmoid entropy measure for epileptic EEG was found to be lower than normal EEG, which is similar to the methods proposed in [19, 98].

7. It has been proven that non-extensive Tsallis entropy is better than Shannon entropy only when proper entropy index q was chosen. However, no such selection is required for the estimation of sigmoid entropy.

4.4.5 Limitations and future directions

During the simulation, it was observed that the bin ranges should be set properly during the probability estimation of the signal. Improper selection of such parameter leads to *not a number* or *infinity* in a MATLAB platform. As a future direction, the proposed algorithm will be tested on more number of EEG recordings. Further, sigmoid entropy will be explored on EEG signals obtained for different conditions such as detection of the level of alcohol, drowsiness detection, and anesthesia depth level detection. In addition, a deep learning based approach will be introduced to all the three databases.

4.5 Conclusion

In this paper, a novel feature referred to as sigmoid entropy was proposed for the detection of epileptic seizures in the EEG signals. Sigmoid entropy was estimated by decomposing the EEG signal using DWT. Experimental results showed that sigmoid entropy was capable of capturing the transitions in the EEG that reflected the abnormal activity in the brain. The results showed that the sigmoid entropy value was lower for epileptic activity as compared to normal EEG. The best wavelet and decomposition level (sub-band) was identified using five wavelets. Among five different wavelets, Bio3.1 (sub-band D4), Rbio3.1 and Haar (sub-band A5), and Rbio3.1 (sub-band) D3 was found to be the best choice for the RMCH, UBonn, and CHB-MIT databases respectively.

The classification results showed an SDR of 96.34%, MDD of 1.2 s and FDR of 0.5/h for the RMCH database. Further, the highest sensitivity of 100% and 94.21% were obtained using UBonn and CHB-MIT databases respectively. Our experimental results conclude that sigmoid entropy can be used to analyze the brain dynamics to understand the epileptic seizures behavior with less computational complexity.

Acknowledgment

The authors are grateful to doctors of the Institute of Neuroscience, Ramaiah Medical College and Hospitals, Bengaluru, India, for valuable discussion and providing EEG recordings for research purpose. Authors are also grateful to Dr. R. G. Andrzejak and CHB-MIT team for giving access to use their EEG databases in the public domain for research. The authors would also like to thank the anonymous reviewers for their helpful comments and suggestions that greatly improved the quality and clarity of the manuscript.

CHAPTER 5

Complexity analysis and dynamic characteristics of EEG using MODWT based entropies for identification of seizure onset

S Raghu, Natarajan Sriraam, Yasin Temel, Shyam Vasudeva Rao, Pieter L Kubben

The Journal of Biomedical Research, 34(3): 211-225

Year: 2019

<http://www.jbr-pub.org.cn/article/doi/10.7555/JBR.33.20190021>

Abstract

In this paper, complexity analysis and dynamic characteristics of electroencephalogram (EEG) signal based on maximal overlap discrete wavelet transform (MODWT) has been exploited for the identification of seizure onset. Due to the fact that wavelet-based studies were well suited for classification of normal and epileptic seizure EEG, we have applied MODWT which is an improved version of discrete wavelet transform (DWT). The selection of optimal wavelet sub-band and features play a crucial role to understand the brain dynamics in epilepsy patients. Therefore, we have investigated MODWT using four different wavelets, namely Haar, Coif4, Dmey, and Sym4 sub-bands until 7 levels. Further, we have explored the potentials of six entropies, namely sigmoid, Shannon, wavelet, Renyi, Tsallis, and Stein's unbiased risk estimator (SURE) entropies in each sub-band. The sigmoid entropy extracted from Haar wavelet in sub-band D4 showed the highest accuracy of 98.44% using support vector machine classifier for the EEG collected from Ramaiah Medical College and Hospitals (RMCH). Further, the highest accuracy of 100% and 94.51% was achieved for the University of Bonn (UBonn) and CHB-MIT databases respectively. The findings of the study showed that Haar and Dmey wavelets found to be computationally economical and expensive respectively. Besides, in terms of dynamic characteristics, MODWT results revealed that highest energy present in sub-bands D2, D3, and D4 and entropies in those respective sub-bands outperformed other entropies in terms of classification results for RMCH database. Similarly, using all the entropies, sub-bands D5 and D6 outperformed other sub-bands for UBonn and CHB-MIT databases

respectively. In conclusion, the comparison results of MODWT outperformed DWT.

5.1 Introduction

Epilepsy is the neurological disorder that causes an uncontrolled and involuntary movement characterized unprovoked seizures [14]. A seizure occurs when a burst of electrical impulses in the brain escapes their normal limits [149]. Epilepsy is the fourth most common neurological disease and 2.2 million people or 7.1 for every 1,000 people of the world suffering [1, 149]. Depending on where the seizure starts, they are portrayed as being focal onset, generalized onset or unknown onset. Electroencephalogram (EEG) contains abundant information on neural, physiological and pathological conditions of brain disorders. It is essential to identify the distinctive parameter that is capable of revealing the dynamic characteristics of the brain in epilepsy patients. However, manual inspection of immense EEG data recorded over a long time found to be a time-consuming and tiresome task by experts in hospitals. Further, the manual inspection between different experts may produce odd results which tend to wrong classification. Therefore, it is essential to develop the automated model which is the optimal selection of features and classifier. To address the above-mentioned limitations, we propose the automated seizure onset detection model using maximal overlap discrete wavelet transform (MODWT) based entropies and support vector machine (SVM) classifier. Hence, timely detection and diagnosis of epilepsy patients gain prioritized clinical attention around the world.

In recent years, extensive research on epileptic seizures has been done using discrete wavelet transform (DWT). Wavelet-based methods found to be outperformed in terms of time-frequency resolution, denoising, different temporal scales and robustness to outliers [150]. DWT with the statistical features [42, 128, 129], signal energy [131], Eigenvalues [9], and 21 different features [132] have reported promising results. Normal, pre-ictal and ictal EEGs were studied using wavelet packet transform with log and norm entropies [21]. In [47], complexity analysis of EEG was explored in different sub-bands of DWT using approximate entropy. DWT and SVM based algorithm showed better results for long-term EEGs [135]. In our recent study [19], 100% accuracy was reported using minimum variance modified fuzzy entropy on 38 patients. Further, approximate entropy, Phase entropy 1 and 2, and sample entropy [80], weighted permutation entropy [98], Renyi, spectral and Shannon entropies [36, 66, 81] and wavelet entropy [110] have been explored for epileptic seizure studies. Acharya et al. have reviewed the application of different entropies for seizure detection and reported advantages and shortcomings [18].

Spike-wave-discharge onset was identified using MODWT coefficients for absence seizure detection [151]. In [152], MODWT and log-normal distribution based model was evaluated using random forest classifier. In this study, the authors did not analyze the energy distribution and different wavelets were not varied. Epileptic seizure prediction was performed using MODWT and nonlinear similarity index [153]. This study showed the best performance in the beta (10-30Hz) frequency band. An extensive analysis between MODWT and DWT for functional brain network construction demonstrated the optimal ways of choosing the wavelet method, filters, and decomposition level

[150]. The results suggested that MODWT outperformed DWT and produces fewer variable estimates than DWT. MODWT correlation coefficients measure exhibited good spatial correspondence between intracranial and scalp EEG [154]. MODWT sub-bands have yielded an accuracy of 99.26% using feed-forward artificial neural networks [155].

The literature survey suggests that most of the studies [21, 27, 66, 80, 152] have conducted on one of the oldest publicly available University of Bonn EEG database [33]. Very few studies have investigated MODWT on EEG signals and entropy index of Renyi, Tsallis and SURE entropy have varied. In addition, the dynamic characteristics of EEG have not been studied for different sub-bands and entropies for epileptic EEG. MODWT is the modified version of DWT without down-sampling in each decomposition level and it is a highly redundant, and nonorthogonal transform [156, 157]. Elimination of down-sampling in MODWT avoid the loss of information and enhances the time-frequency resolution on each scale. Therefore, in our study, MODWT was selected for EEG decomposition with Haar, Coif4, Dmey, and Sym4 wavelets. The measure of entropy used to quantify the uncertainty of the signal either in the time or frequency domain. In order to reveal the dynamic characteristics and complexity analysis of EEG signal sigmoid, Shannon, Wavelet, Renyi, Tsallis, and Stein's unbiased risk estimator (SURE) entropies were implemented in our study. Hence, the goal of the study is to identify the computationally efficient optimal combination of MODWT sub-band with entropies using the SVM classifier for the detection of seizure onset.

Fig. 5.1 depicts the flow of the proposed epileptic seizure detection algorithm. The proposed method has been divided into five stages. **Stage 1:**

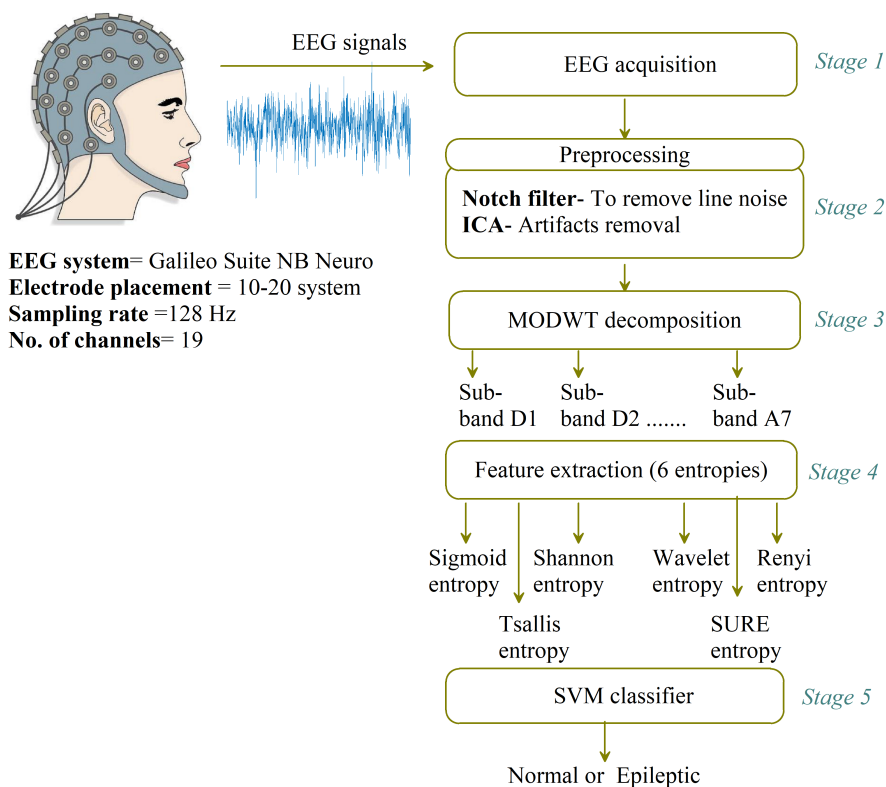


FIGURE 5.1: Block diagram of the proposed algorithm.

Recordings of EEG at the hospital. **Stage 2:** The raw EEG signals were pre-processed to eliminate line noise and artifacts. **Stage 3:** The EEG signals were decomposed using MODWT with four different wavelets. **Stage 4:** Six entropies were extracted from each sub-band. **Stage 5:** Finally, the entropies were classified using SVM classifier.

The rest of the paper has been organized as follows. In Section 2, a brief introduction of EEG data, pre-processing, MODWT and feature extraction methods were described. The experimental results are presented in Section 3 followed by a discussion in Section 4. Finally, Section 5 concludes the importance of the proposed study.

5.2 Materials and Methods

5.2.1 EEG recordings

The proposed algorithm was validated on three databases, namely Ramaiah Memorial College and Hospitals (RMCH), University of Bonn (UBonn), and Children's Hospital Boston- Massachusetts Institute of Technology, (CHB-MIT) EEG recordings.

5.2.1.1 Ramaiah Memorial College and Hospitals

The EEG recordings used in our study were obtained from the RMCH, Bengaluru, India after ethical clearance was obtained to use the EEG for research purpose [19]. This unipolar EEG was recorded using 19 scalp electrodes (Fp1, Fp2, F7, F3, Fz, F4, F8, T3, C3, Cz, C4, T4, T5, P3, Pz, P4, T6, O1, and O2) placed according to the International 10-20 system configuration at a sampling rate of 128 Hz using Galileo Suite NB Neuro digital EEG system. The complete database comprises of 115 subjects (67 male and 48 female) ranging between 2.5 to 75 years of age with average age of 40 ± 20.3 years. Two experts at RMCH visually marked EEG as normal and epileptic segments. In total, 162 seizures were found from approximately 58 hours of EEG which was collected from 115 subjects. In total, RMCH database consists of approximately 4.36 hours of epileptic seizures data and approximately 53 hours of normal EEG. The length of the recording duration of each patient varied from 20 minutes to 3 hours.

5.2.1.2 University of Bonn

The second database used in our research was collected from publicly available EEG recordings from the UBonn ¹ [33]. These recordings were recorded from five different subjects under-going presurgical evaluations. UBonn recordings were converted from multi-channel to single channel EEG by original researcher [33]. UBonn EEG was divided into five sets (A-E), each set consisting of 100 single channel EEG segments of 23.6 s duration recorded at a sampling rate of 173.61 Hz. Each subset corresponds to normal with the eye open (set A), normal with eye closed (set B), pre-ictal (set C), post-ictal (set D) and ictal state (set E). In our present study, four classification problems, namely {A}-{E}, {ACD}-{E}, {ABCD}-{E}, and {AB}-{CD}-{E} between epileptic and non-epileptic groups were considered based on the previous studies [9, 47, 89, 137].

5.2.1.3 CHB-MIT

The last and third EEG database was collected from CHB-MIT [88] open-source available in Physionet repository ². This is one of the largest databases consists of 844 hours of EEG recordings with 182 seizures from the 23 patients. This EEG was recorded using the 10-20 International system bipolar montage electrode placement with 23 channels at a sampling rate of 256 Hz. One can refer to the [88, 100] for more details on the EEG database and patient information.

¹http://epileptologie-bonn.de/cms/front_content.php?idcat=193&lang=3&changelang=3

²<http://www.physionet.org/pn6/chbmit>

5.2.2 Preprocessing

The patients EEG collected from RMCH database was preprocessed using suitable signal processing techniques. A 50 Hz notch filter was implemented to eliminate power line interference. Further, EEG was filtered using a band-pass filter between 0.5 Hz to 40 Hz. In order to eliminate the artifacts (eye blink, muscle artifacts, and electrode displacement) from EEG independent component analysis was applied [138].

5.2.3 Maximal overlap discrete wavelet transform

The MODWT is an improved version of DWT [156, 157]. The MODWT is a linear filtering method that decomposes the signal into coefficients over a set of scales. The MODWT differs from DWT in terms of flexible time-frequency representation, highly redundant, non-orthogonal, and eliminates down sampling at each level of decomposition [152]. Further, MODWT is well-defined for all sample sizes N , whereas DWT requires N to be a multiple of 2^J for J levels.

The input data are samples of a function $f(x)$ evaluated at N many time points. The function can be expressed as a linear combination of the scaling function $\phi(x)$ and wavelet $\psi(x)$ at varying scales and translations [156, 157]:

$$f(x) = \sum_{k=0}^{N-1} C_k 2^{-J_0/2} \phi(2^{-J_0}x - k) + \sum_{j=1}^{J_0} f_j(x) \quad (5.1)$$

where $f_j(x) = \sum_{k=0}^{N-1} d_{j,k} 2^{-j/2} \mu(2^{-j}x - k)$ and J_0 is the number of levels of wavelet decomposition. The first sum is the coarse scale approximation of

the signal, and the second sum with $f_j(x)$ are the details at successive scales. MODWT returns the N -many coefficients $\{c_k\}$ and the $(J_0 \times N)$ -many detail coefficients $\{d_{j,k}\}$ of the expansion. Number of decomposition level is given by $J_0 + 1$. In MODWT, detail coefficients are produced at each level and scaling coefficients are returned only for the final level.

The MODWT partitions the energy across the various scales and scaling coefficients are as follows [156, 157]:

$$\|X\|^2 = \sum_{j=1}^{J_0} \|W_j\|^2 + \|V_{J_0}\|^2 \quad (5.2)$$

where X is the input data, W_j are the detail coefficients at scale j , and V_{J_0} are the final-level scaling coefficients.

The selection of wavelet function and decomposition level plays a significant role in analyzing EEG signals using MODWT that depends on the dominant frequency distribution in each sub-band. In [130, 152], EEG was decomposed till level 6 using Haar wavelet, but other wavelets were not investigated. Therefore, in this study, four different mother wavelets, namely Haar, Coif4, Dmey, and Sym3 have been used to decompose EEG till level 7 (RMCH and UBonn) and level 10 (CHB-MIT) to identify the optimal combination for seizure onset detection.

5.2.4 Feature extraction

The entropy of EEG reflects the amount of uncertainty or randomness the signal [80]. The measure of entropy used to quantify the uncertainty of the signal

either in the time or frequency domain. In order to reveal the dynamic characteristics and complexity analysis of the EEG signal, the following six entropies were investigated in our study. Most studies have reported the results using a single entropy index for Renyi, Tsallis, and SURE entropies. Whereas, in our study, these entropies were varied with different entropy index. The segmentation length of 1 sec was used to extract the features.

5.2.4.1 Sigmoid entropy

In our recent study, sigmoid entropy has been proposed for the identification of seizure onset [83]. As we know that, a sigmoid function is a particular case of the logistic function having “S” shaped curve. EEG contains non-linear elements that are the indication of the neuronal activity of epileptiform discharges. The sigmoid function is non-linear activation function the output always bounded to be in range (0,1). Due to the fact that EEG is a non-linear signal, we are introducing sigmoid entropy by bringing the concept of probabilities to the sigmoid function.

As we know that sigmoid function is defined as [141]

$$\sigma(t) = \frac{1}{1 + e^{-t}} \quad (5.3)$$

In our study, assuming that n is the number of possible states that the amplitude of the EEG are quantized into and p_i the probability of each state is $p = \{p_i\}$, $0 \leq p_i \leq 1$ and $\sum_{i=1}^n p_i = 1$. The probability of occurrence of EEG signal is calculated using histogram method by specifying bin ranges (0.05 microvolts based on the preliminary study).

Now by replacing t with p in (5.3), where $p = \{p_1, p_2, p_3, \dots, p_n\}$, (5.3) becomes

$$\sigma(p) = \frac{1}{1 + e^{-p}} \quad (5.4)$$

Expanding (5.4) becomes

$$\sigma(p) = \frac{1}{1 + e^{-p_1} + e^{-p_2} + e^{-p_3} + \dots + e^{-p_n}} \quad (5.5)$$

The amount of sigmoid entropy ($H_{SigmoidEn}$) captured by (5.5) can be written as [83]

$$H_{SigmoidEn} = \frac{1}{1 + \sum_{i=1}^n e^{-p_i}} \quad (5.6)$$

The dynamic range of the sigmoid entropy lies between 0 and 1. According to the characteristics of the sigmoid function, maximum entropy of ‘1’ would infer the less variation of the signal [83]. In contrast, more variation or fluctuation of the signal may indicated by low entropy.

5.2.4.2 Shannon entropy

Shannon entropy is most widely used probability based entropy for EEG signals [142] and it is given by

$$H_{ShanEn} = - \sum p_i \log_2(p_i) \quad (5.7)$$

Where p_i is the probabilities of occurrence of possible states in decomposed EEG signal s .

5.2.4.3 Wavelet entropy

Wavelet entropy is a non-normalized Shannon entropy estimated from wavelet co-efficients and it is given by [142, 158],

$$H_{WaveEn} = - \sum s_i^2 \log_{10}(s_i^2) \quad (5.8)$$

5.2.4.4 Renyi entropy

Renyi entropy is a generalization of Shannon entropy, which quantifies diversity, uncertainty or randomness of a system. It includes other entropy measures as special cases.

Renyi entropy of order α is defined as [159],

$$H_{RenyiEn} = \frac{1}{1 - \alpha} \log_2 \left(\sum_{i=1}^n p_i^\alpha \right) \quad (5.9)$$

Where p_i is the probabilities of decomposed EEG signal s , α is the order or entropy index ($\alpha \geq 0$), in our study $\alpha = 2, 3$, and 5 was chosen.

5.2.4.5 Tsallis entropy

Tsallis entropy is a non-extensive generalization of Boltzmann–Gibbs entropy [143]. For a set of probabilities $\{p_i\}$, Tsallis entropy is defined as

$$H_{TsallisEn} = \frac{1}{1 - \alpha} \left(1 - \sum_{i=1}^n p_i^\alpha \right) \quad (5.10)$$

where α is the entropy index which is positive parameter. In our study α was chosen to be 1.5, 3 and 5.

5.2.4.6 Sure entropy

SURE entropy is measuring tool for quantifying properties related to information for an accurate representation of a signal and it defined as [160]

$$H_{SureEn} = n - \#\{i \text{ such that } |s_i| \leq \varepsilon\} + \sum_i \min(s_i^2, \varepsilon^2) \quad (5.11)$$

where, s_i is the decomposed EEG signal and ε is a positive threshold value or entropy index. In our study, ε was varied as 1, 3, and 5.

5.2.5 Classification

The classification of epileptic seizures was performed using the SVM classifier due to its better performance in previous studies [25, 42, 47, 65, 89, 128, 135]. SVM uses kernel method to transform the feature set that draws an optimal boundary between the possible outputs [23]. The preliminary study reveals the better performance using radial basis function kernel as compared to other kernel functions and the same was implemented for further analysis. SVM classifier was implemented using leave-one-out-subject cross-validation to achieve the robustness of the method. Further tuning parameters were set as follows: Kernel function = radial basis function, Kernel Scale = auto, Box Constraint = 1, and Standardize = true. The performance of the proposed seizure detection technique was evaluated using sensitivity, specificity, and accuracy.

$$Sensitivity = \frac{TP}{TP + FN} \quad (5.12)$$

$$Specificity = \frac{TN}{TN + FP} \quad (5.13)$$

$$Accuracy = \frac{TP + TN}{TP + FP + TN + FN} \quad (5.14)$$

where, TP is true positive, FN false negative, TN is true negative and FP is false positive.

5.3 Results

In this section, we have investigated the effect of different wavelet methods and decomposition length on (i) energy content in each sub-band of EEG (ii) variation of entropy in each sub-band distinguishing between normal and epileptic EEG (iii) classification results. Fig. 5.2 shows the example of epileptic EEG collected from RMCH database with seizure onset and offset. As discussed in the previous section, we have applied 7 level MODWT on EEG signals configured using Haar, Coif4, Dmey, and Sym4 wavelets. Basically, these results help to understand the EEG brain dynamics in terms of energy distribution, the behavior of entropy and classification results in each sub-band. The EEG signal and its coefficients corresponding to each sub-band using Haar wavelet depicted in Fig. 5.3. It is clear that the length of the decomposed signal in each level is the same as the original EEG. Further, energy and entropies are estimated in each sub-band.

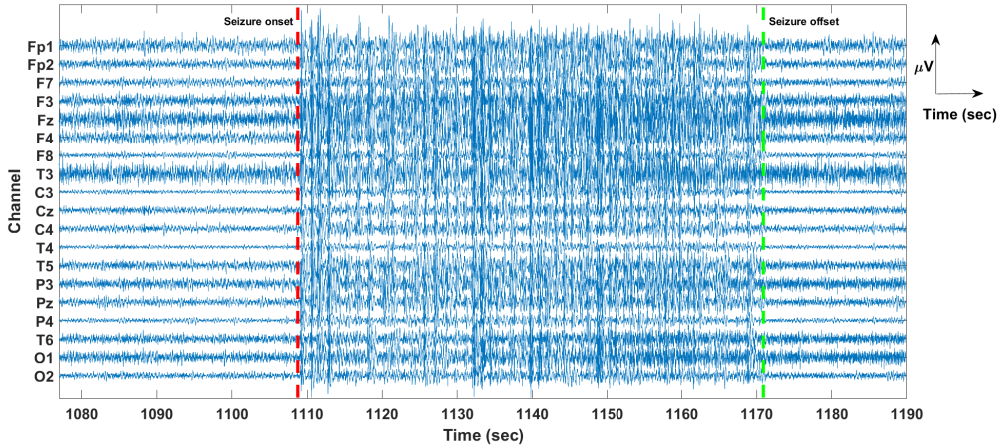


FIGURE 5.2: An example of epileptic seizure EEG from RMCH database. The red marker indicates the beginning of the seizure onset and green marker its end.

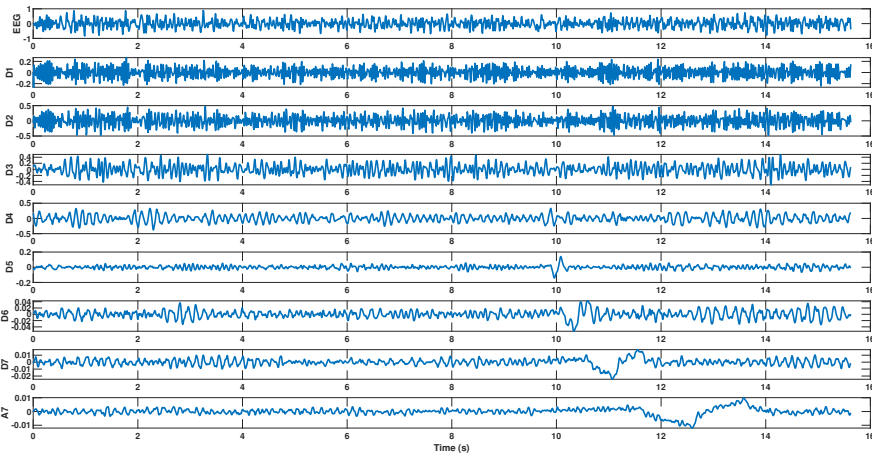


FIGURE 5.3: An illustrative example of decomposed EEG using MODWT.

5.3.1 Effect of decomposition level on energy

Fig. 5.4 demonstrates the distribution of energy in each sub-band decomposed using MODWT configured with Haar, Coif4, Dmey, and Sym4 wavelets. We

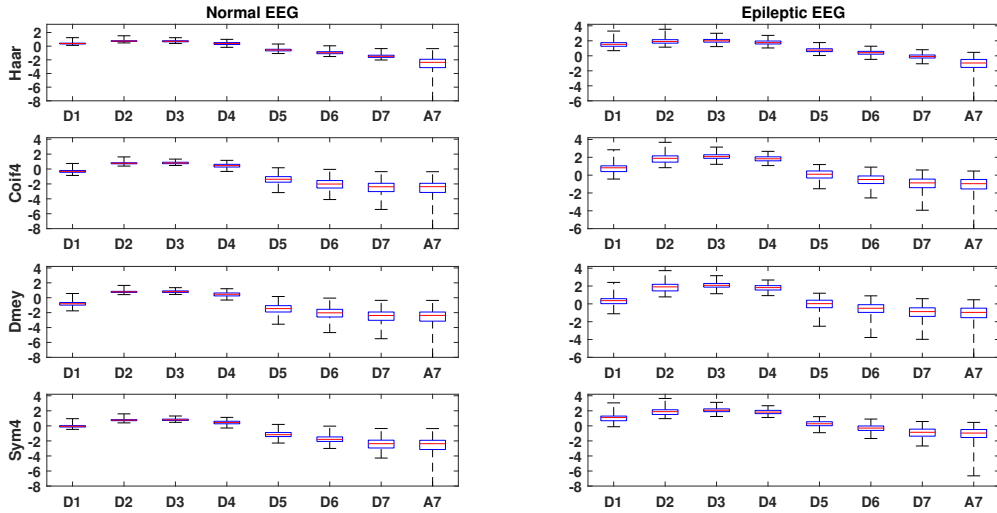


FIGURE 5.4: Boxplot describing distribution of energy in MODWT EEG over different scales.

have investigated the energy distribution in every sub-band for annotated normal and epileptic EEG using different mother wavelet functions. We observe $p < 0.01$ in all the sub-bands except for sub-band A7 in level 7. We found that energy content in the levels 2 (sub-band D2), 3 (sub-band D3), and 4 (sub-band D4) was significantly high as compared to the other levels for all the wavelets. In all the wavelets, least energy was found to be in sub-band A7. In addition, the range of distribution was very less in sub-bands D2, D3, and D4. It shows that the level of decomposition has an effect on the amount of information revealed contained in EEG signals.

5.3.2 Effect of MODWT decomposition length entropies

In this section, we have demonstrated the behavior of entropies when decomposed using MODWT. Fig. 5.5 shows the effect of MODWT decomposition length on entropies for different decomposition levels and wavelets. In Fig. 5.5(a), sigmoid entropy exhibited lower for epileptic and higher for normal EEG. We observe that sigmoid entropy increases as the function of decomposition length and lies between 0 to 1. In contrast to sigmoid entropy, Shannon entropy and wavelet entropies behaved quite different. That means, higher and lower entropies were obtained for epileptic and normal EEG respectively.

Fig. 5.5(b) depicts the entropies obtained for Renyi entropy ($\alpha = 2, 3,$ and 5). Renyi entropy was found to be increasing as entropy index α goes higher. Similar observation was seen for SURE entropies for $\epsilon = 1, 3,$ and 5 (refer to Fig. 5.5(d)). Tsallis entropy was seen to be decreasing as the entropy index $\alpha = 1.5, 3,$ and 5 increases (refer to Fig. 5.5(c)). It was understood that the behavior of Tsallis entropy is opposite to Renyi and SURE entropies with respect to entropy indexes. In all the entropies, more transition of entropies from sub-band D4 to D5 was observed for Coif4 and Dmey wavelets (refer second and third column of Fig. 5.5). Collectively, entropies were higher in sub-bands D2, D3, and D4 for all the entropies except for sigmoid. It was clear that entropies start decreases as decomposition length goes down (reverse in case of sigmoid). Smooth transition in entropies over decomposition length between sub-bands was observed in case of Haar and Sym4 wavelets. The higher time complexity in case of Dmey wavelet was observed as compared to the other three wavelets. Wilcoxon rank sum test showed $p < 0.01$ between normal and epileptic EEG entropies for all the wavelets and sub-bands except

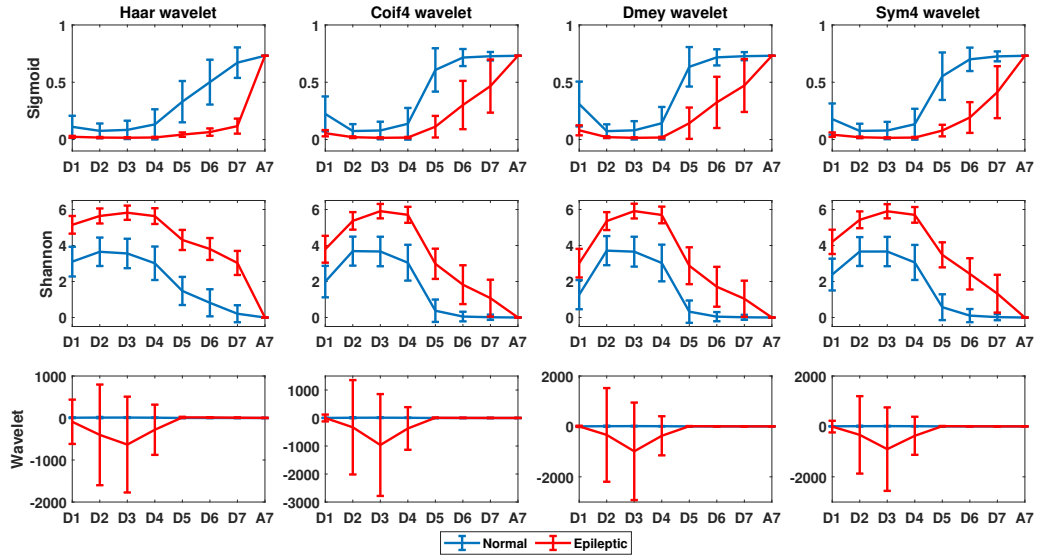
for sub-band A7.

5.3.3 Classification results using RMCH database

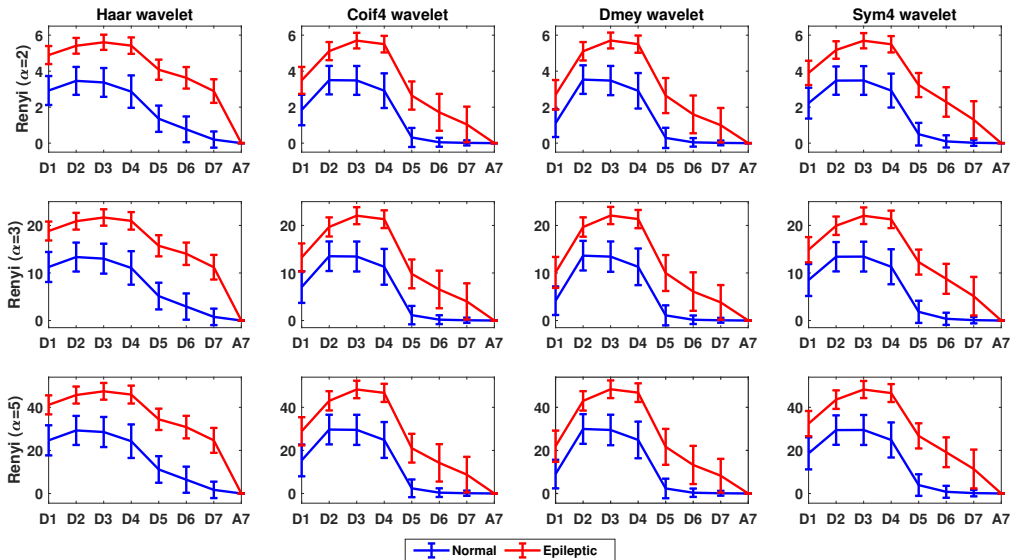
Fig. 5.6 shows the classification accuracy using MODWT with different entropies (sigmoid, Shannon, and wavelet) for different decomposition levels and mother wavelets. Sigmoid entropy with Haar wavelet in sub-band D4 showed the highest classification accuracy of 98.44%. In addition, Haar wavelet in sub-band D3 (98.20%) and Sym4 wavelet in sub-band (97.96%) showed the best performance. The results obtained in other sub-bands were close to the best performance.

In the case of Shannon entropy, the highest classification accuracy of 98.02%, 97.44%, 97.08%, and 97.74% obtained in sub-band D4 using Haar, Coif4, Dmey and Sym4 wavelets respectively. Wavelet entropy showed the highest accuracy of 96.80% in sub-band D4 using Haar wavelet. In the case of wavelet entropy, poor performance was observed in Coif4 and Dmey wavelets. The least classification accuracy was observed in sub-band A7 for sigmoid and Shannon entropy. However, wavelet entropy showed the least performance in sub-band D1.

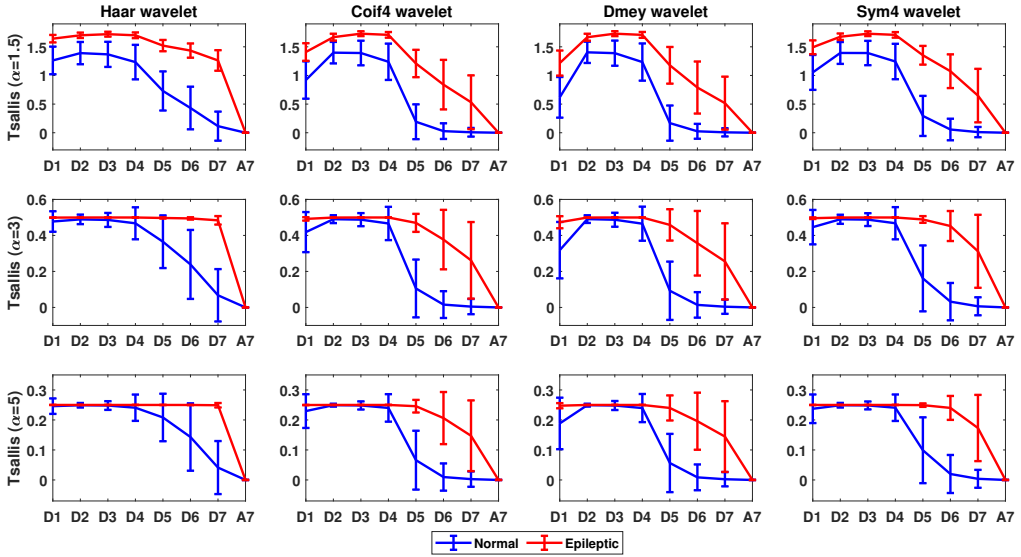
Fig. 5.7 depicts the classification accuracy obtained for Renyi entropy using different entropy indexes. Again, Haar and Sym4 wavelets performed better in sub-bands D3 and D4. We observe that accuracy slightly decreases as the entropy index increases. The best results of 97.73% were obtained in D4 sub-band using Haar wavelet for Renyi entropy with $\alpha = 2$. Similar classification results observed for Tsallis entropy (refer to Fig. 5.8) using $\alpha = 1.5$ and 3. However, Tsallis entropy with $\alpha = 5$ performed worse in D1, D2, D3, and D4



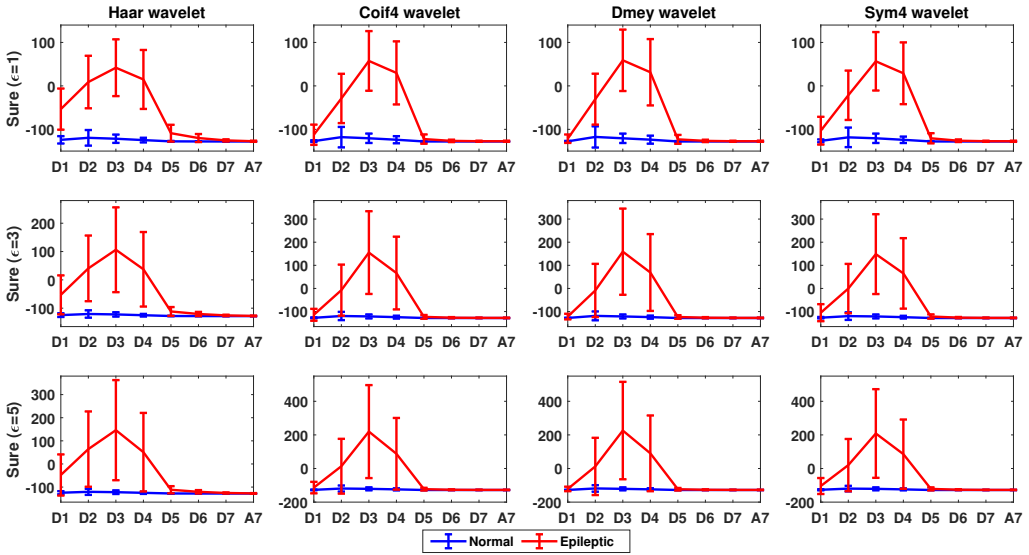
(a)



(b)



(c)



(d)

FIGURE 5.5: Effect of MODWT decomposition length on entropies. **(a) First row:** Sigmoid entropy, **Second row:** Shannon entropy, **Third row:** Wavelet entropy. **(b) First row:** Renyi entropy ($\alpha = 2$), **Second row:** Renyi entropy ($\alpha = 3$), **Third row:** Renyi entropy ($\alpha = 5$). **(c) First row:** Tsallis entropy ($\alpha = 1.5$), **Second row:** Tsallis entropy ($\alpha = 3$), **Third row:** Tsallis entropy ($\alpha = 5$). **(d) First row:** Sure entropy ($\epsilon = 1$), **Second row:** Sure entropy ($\epsilon = 3$), **Third row:** Sure entropy ($\epsilon = 5$). In all the sub figures, **First column:** Entropies of Haar wavelet. **Second column:** Entropies of Coif4 wavelet. **Third column:** Entropies of Dmey wavelet. **Fourth column:** Entropies of Sym4 wavelet.

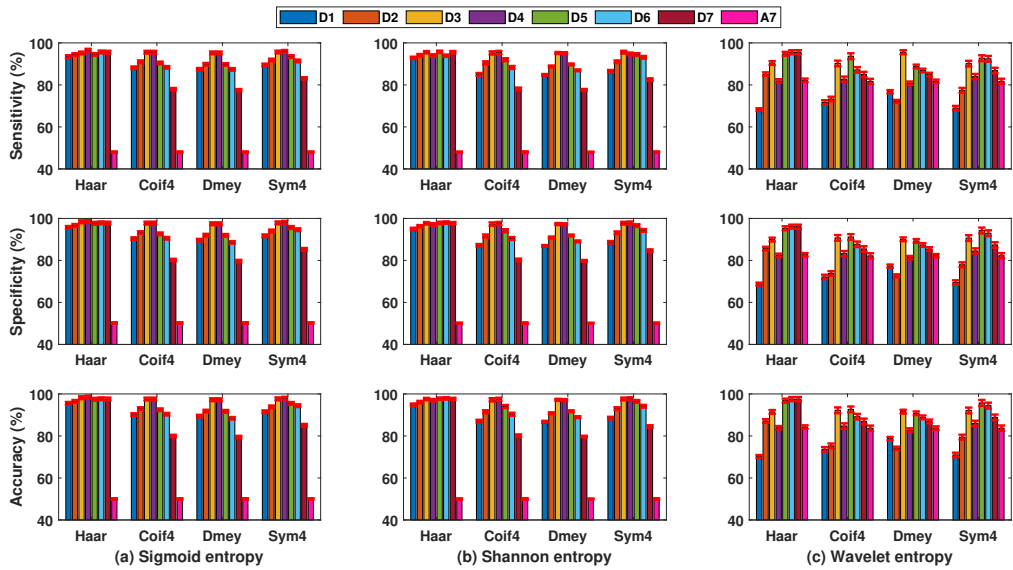


FIGURE 5.6: Classification results shown by MODWT based entropies for different decomposition levels and wavelets. **Left column:** Sigmoid entropy, **Middle column:** Shannon entropy, **Right column:** Wavelet entropy. Legend indicates the decomposition levels of MODWT.

sub-bands and highest of 97.31% obtained in D7 sub-band using Haar wavelet. SURE entropy with $\epsilon = 1, 3$, and 5 produced accuracy of 97.87%, 97.99%, 97.75% in sub-band D4 using Haar wavelet respectively. Not much difference in the results was observed for higher ϵ in all the wavelets. Across these results, SURE entropy with $\epsilon = 5$ was better in terms of results when compared with higher entropy index among other entropies. Collectively, results in sub-band D4 were excellent among all the entropies and wavelets. Quantitatively, lower decomposition levels appear to provide better classification results which are acceptable for clinical use. In terms of revealing dynamic characteristics, complexity and classification results, MODWT configured using Haar wavelet-based sigmoid entropy outperformed other entropies.

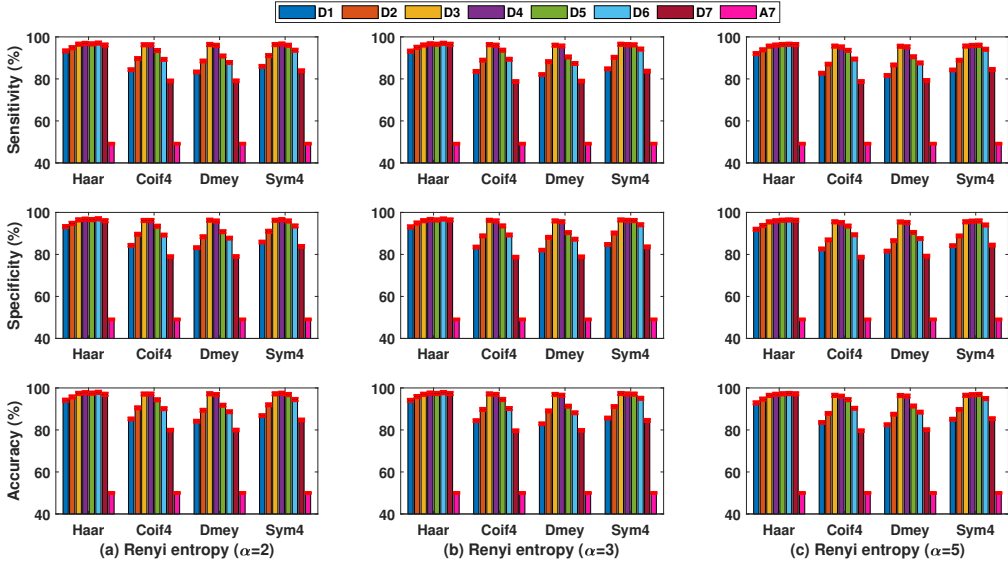


FIGURE 5.7: Classification results shown by MODWT based Renyi entropy for different decomposition levels and wavelets. **Left column:** Renyi entropy ($\alpha = 2$), **Middle column:** Renyi entropy ($\alpha = 3$), **Right column:** Renyi entropy ($\alpha = 5$). Legend indicates the decomposition levels of MODWT.

5.3.4 Classification results using UBonn database

UBonn EEG data was classified using 10-Fold cross-validation for classification problems, namely $\{A\}-\{E\}$, $\{ACD\}-\{E\}$, $\{ABCD\}-\{E\}$, and $\{AB\}-\{CD\}-\{E\}$. The experiment was conducted using all four wavelets and variants of entropies as similar to RMCH. Only the best results (Haar wavelet) using all the four wavelets are presented in Fig. 5.10. Both Sigmoid and Shannon entropies showed the highest specificity, sensitivity and accuracy of 100% using Haar wavelet in sub-band D5 for classification problem $\{A\}-\{E\}$ (refer to Fig. 5.10a). Further, Renyi entropy with $\alpha = 2$, Tsallis entropy with $\alpha = 1.5$ and SURE entropy with $\epsilon = 5$ showed best results among different entropy index values. The sensitivity obtained by wavelet and SURE entropies

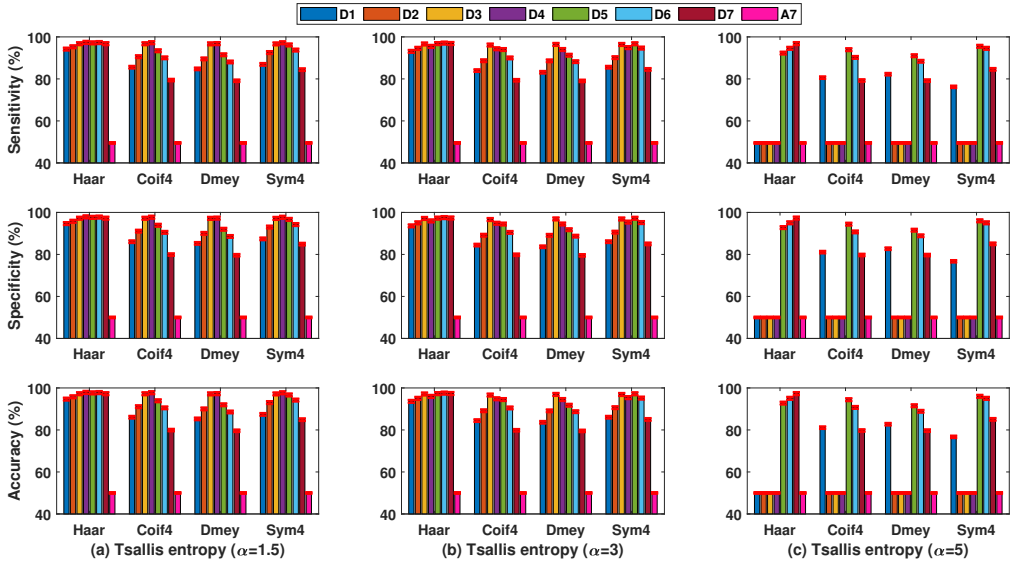


FIGURE 5.8: Classification results shown by MODWT based Tsallis entropy for different decomposition levels and wavelets. **Left column:** Tsallis entropy ($\alpha = 1.5$), **Middle column:** Tsallis entropy ($\alpha = 3$), **Right column:** Tsallis entropy ($\alpha = 5$). Legend indicates the decomposition levels of MODWT.

was higher in sub-band A7 as compared to the other sub-bands. However, poor specificity was shown by same entropies in sub-band A7.

For the classification problem $\{ACD\}$ -E, the good results were achieved using sub-bands D1 to D5, and highest accuracy of 96.43% in sub-band D2 (refer to Fig. 5.10b). The highest accuracy of 94.06% was shown by sub-band D5 using sigmoid entropy for classification problem $\{ABCD\}$ -E (refer to Fig. 5.10c). Tsallis entropy with $\alpha = 3$ and 5 showed poor performance in all the sub-bands except for D4 and D5. Similarly, for three class classification problem $\{AB\}$ - $\{CD\}$ -E, all the entropies showed accuracy of around 91.00% in sub-bands D1 and D2 (refer to Fig. 5.10d). We observe accuracy was decreasing as the decomposition level of MODWT goes deeper. Notably,

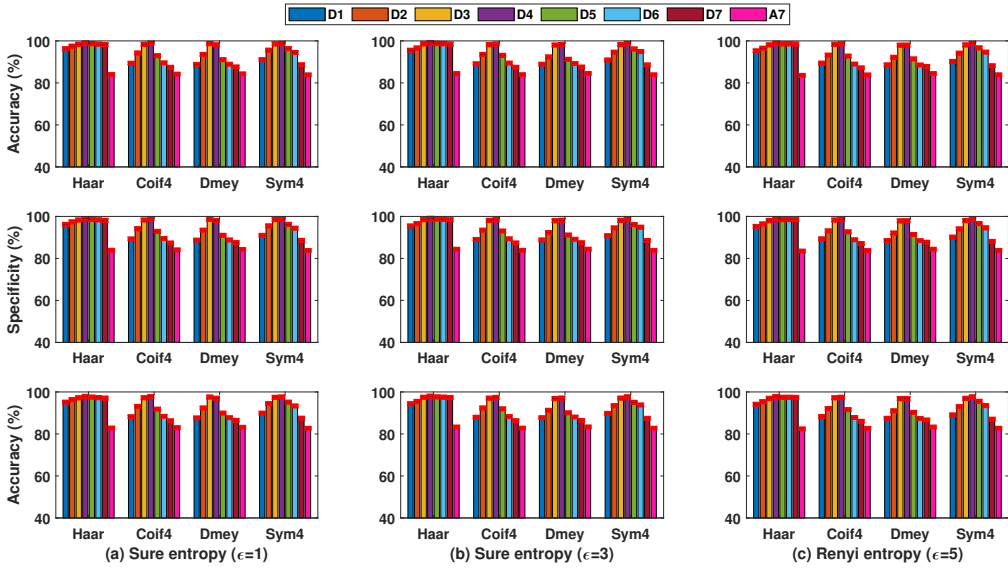
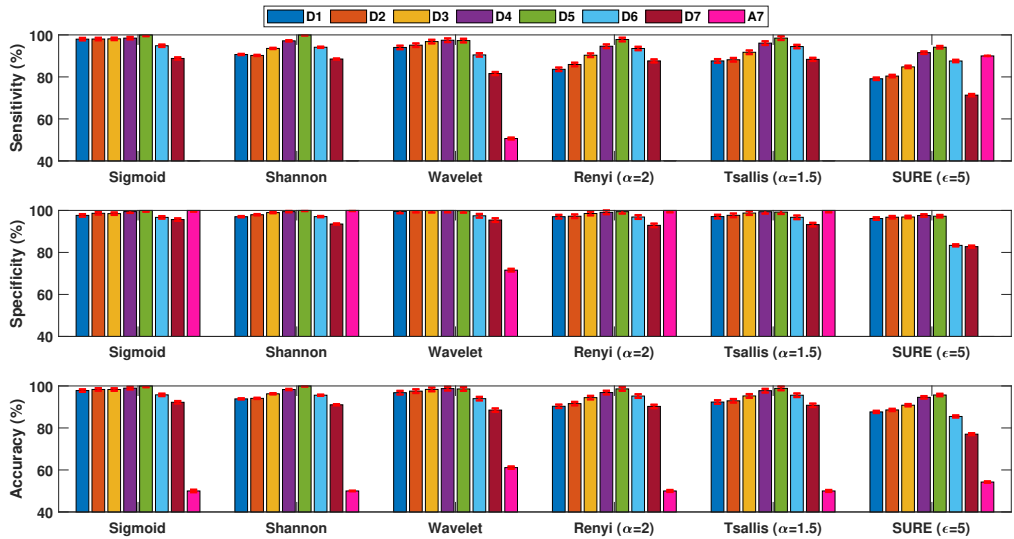


FIGURE 5.9: Classification results shown by MODWT based Sure entropy for different decomposition levels and wavelets. **Left column:** Sure entropy ($\epsilon = 1$), **Middle column:** Sure entropy ($\epsilon = 3$), **Right column:** Sure entropy ($\epsilon = 5$). Legend indicates the decomposition levels of MODWT.

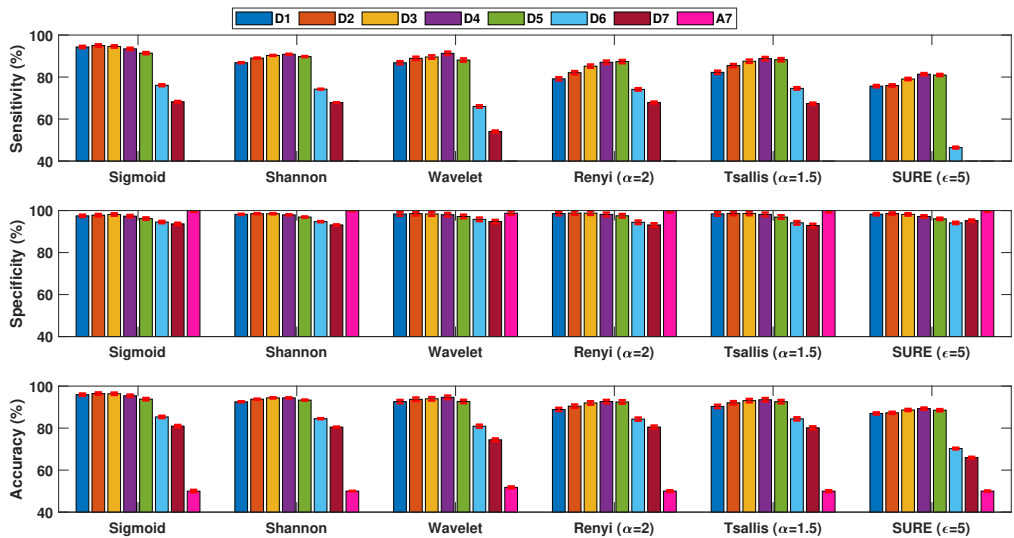
good sensitivity was seen in sigmoid entropy using sub-band A7 but not in other entropies. In contrast, good specificity was observed in all the entropies in sub-band A7 except for sigmoid entropy. Overall, sigmoid and Shannon entropies outperformed other entropies in terms classification results using the wavelets and sub-bands.

5.3.5 Classification results using CHB-MIT database

Fig. 5.11 depicts the classification results obtained for CHB-MIT database using Haar wavelet (found to be best) using all the six entropies. Due to the higher sampling rate of 256 Hz, CHB-MIT database was decomposed until level 10. Interestingly, all the entropies using Haar wavelet in sub-band

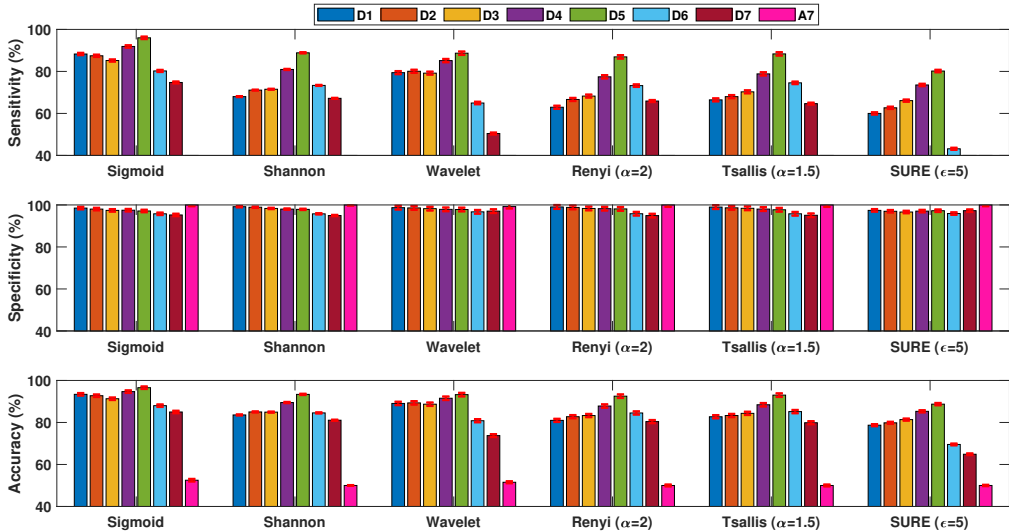


(a)

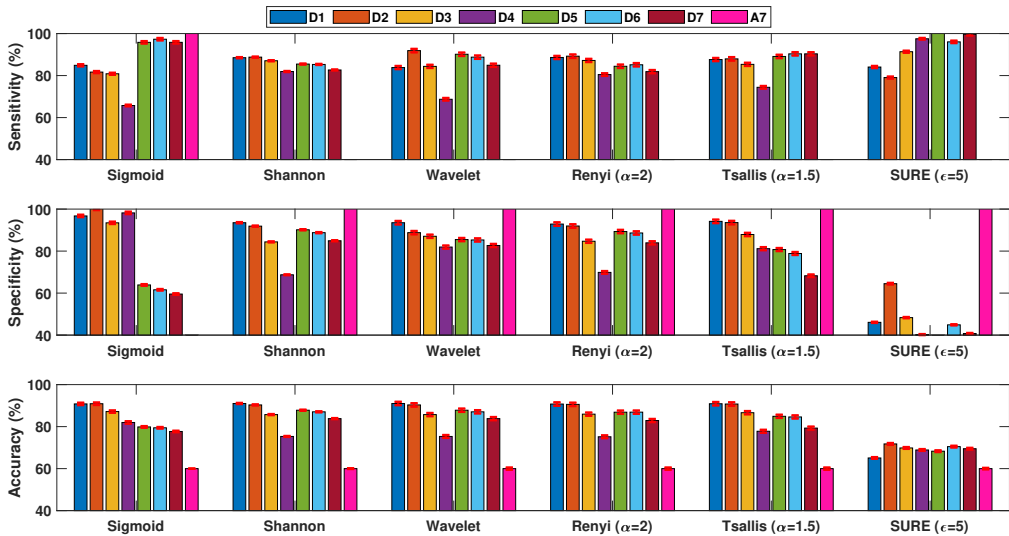


(b)

D6 performed better leading highest sensitivity specificity and accuracy of 96.62%, 96.67%, and 94.51% respectively. Again, as similar to RMCH and UBonn databases, the least results obtained in sub-band A10 (i.e last level)



(c)



(d)

FIGURE 5.10: Classification results shown by MODWT based entropies with Haar wavelet for UBonn database. Legend indicates the decomposition levels of MODWT. Classification problem (a) {A}-{E}, (b) {ACD}-{E}, (c) {ABCD}-{E}, and (d) {AB}-{CD}-{E}

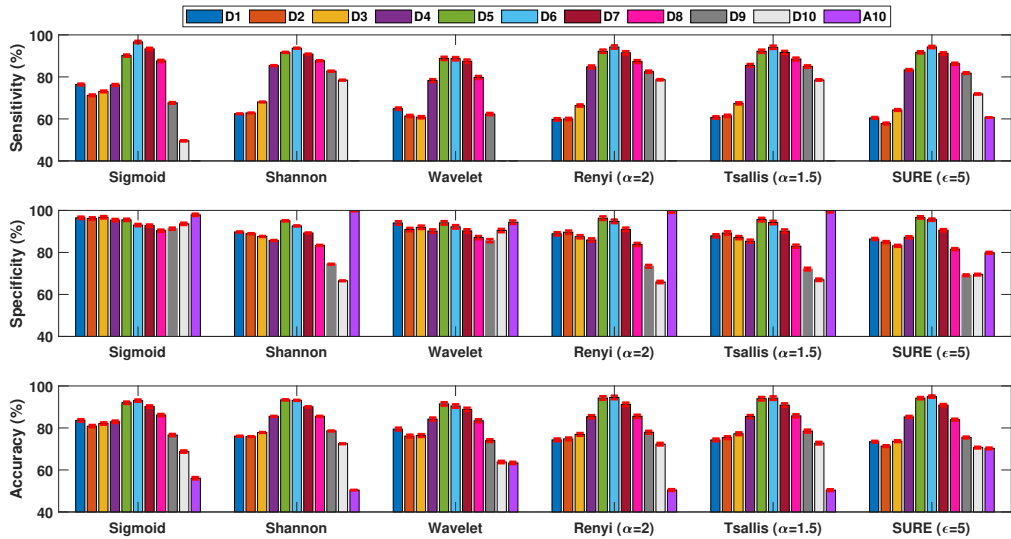


FIGURE 5.11: Classification results shown by MODWT based entropies for CHB-MIT database. Legend indicates the decomposition levels of MODWT.

using all the entropies. Further, results obtained in sub-bands D5 and D7 were close to D6. The above results conclude that the proposed method performs better on different EEG databases.

5.4 Discussion

In this paper, we have investigated the complexity analysis and dynamic characteristics of EEG signals using MODWT and six entropies for identification of seizure onset. To carry out this objective, EEG signals were decomposed using MODWT until level 7. Further, six entropies were estimated in each sub-band to classify using SVM classifier.

As we have already discussed, MODWT is an improved version of DWT

without orthogonality. MODWT does not apply the decimation and the coefficients in each level remain the same length being non-decimated DWT [156]. MODWT offers several advantages over the DWT which are discussed here. The redundancy property of the MODWT facilitates the arrangement of the decomposed coefficients at each level with the original time series, thus enables comparison between the original series and its decomposition [156, 157]. The coefficients of MODWT multiresolution analysis are associated with zero phase filters which result in a more asymptotically efficient wavelet variance estimator than the DWT [156]. Further, it is transform invariant, since a shift in the signal does not change the pattern of the wavelet transform coefficients. Finally, MODWT is energy conserving, it is well suited for analyzing the scale dependence of variability [156, 157]. With the influence of the above facts, MODWT outperformed DWT in terms of classification results.

5.4.1 Performance comparison with DWT

We have compared the results of MODWT versus DWT using same wavelets and features to highlight the advantages of MODWT. The performance of the MODWT results was compared using the RMCH database. The EEG signals were decomposed into 5 levels and results from the best sub-bands were reported in Fig. 5.12. The classification results showed that MODWT outperformed DWT. The Wilcoxon rank sum test delivered the statistical difference of $p < 0.01$ between the accuracy of MODWT and DWT for sigmoid and wavelet entropy. In addition, $p < 0.05$ shown for other entropies, thus it indicates MODWT based features greatly improve the classification results.

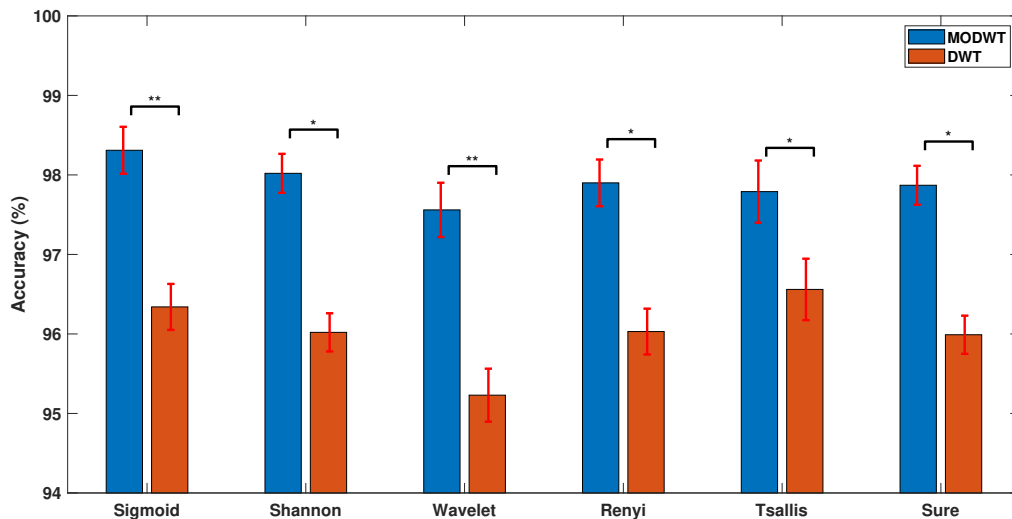


FIGURE 5.12: Performance comparison between entropies derived from MODWT and DWT. $p < 0.05$ (*), $p < 0.01$ (**), $p < 0.001$ (***) .

Above analysis is evident that the property of MODWT over DWT has an advantage of capturing more significant information from EEGs.

5.4.2 Performance comparison with other existing methods

Table 5.1 shows the comparison results with other existing methods. The studies considered for the comparison based on the criteria that the EEG time series have been decomposed using either DWT or MODWT. One should notice that the EEG recordings used in their study are different and exact comparison cannot be performed. The studies [122, 152] that have used EEG recordings from the UBonn yielded accuracy close to 100% due to the clean EEG provided in the database. In [152], the highest classification accuracy of 100% was shown

TABLE 5.1: Performance comparison of epileptic seizure detection methods

Author	EEG database	Duration of EEG (h)	Number of subjects	Number of channels	Number of seizures	Feature extraction	Classifier	Results (%)
[152]	UBonn	1.29	5	Not specified*	100 seizure files	MODWT+LND scale parameter and shape parameter	Random forest	Accuracy= 100
[153]	Epilepsy Center of the University Hospital of Freiburg, Germany	509	421	18	161	MODWT+ nonlinear similarity index	Threshold	Accuracy= 91.9
[135]	Epilepsy Center of the University Hospital of Freiburg, Germany	509	21	18	161	DWT+ relative energy, fluctuation index, coefficient of variation and relative amplitude	SVM	Accuracy= 94.86
[122]	CHB-MIT	884	23	23	182	Harmonic wavelet packet transform fractal dimension, spatial and temporal features	Relevance vector machine	Sensitivity= 96 Accuracy= 99.8
[146]	UBonn	1.29	5	Not specified*	100 seizure files			
[146]	Epilepsy Telemetry Unit at the Montreal Neurological Institute and Hospital	652	28	24	126	DWT+ energy, amplitude and variance	Bayes network	Sensitivity= 78
[147]	Compumedics, Melbourne, Australia	525	21	16	88	DWT+ energy, amplitude, variance, crosscorrelation, and relative derivative	Bayes network	Sensitivity= 79
[137]	Vancouver General Hospital, Germany	76	14	15	63	DWT+ Combined seizure index	Adaptive thresholding	Sensitivity= 90.5
[99]	Epilepsy Center University of Erlangen, Germany	22,278	159	19	794	Moving window STFT, averaged and integrated power	Adaptive thresholding	Sensitivity= 89.9
Proposed	RMCH, Bengaluru, India	58	115	19	162	MODWT+ Sigmoid entropy	SVM	Accuracy= 98.44
	UBonn	1.29	5	Not specified*	100 seizure files	MODWT+ Sigmoid entropy	SVM	Accuracy= 100
	CHB-MIT	884	23	23	182	MODWT+ Renyi entropy	SVM	Accuracy=94.51

* The multi-channel EEG was converted into single channel segments

using Sym8 wavelet using MODWT. The study also showed MODWT outperformed DWT in terms of classification results and computation time. Further, the wavelet-based nonlinear similarity index showed better performance in beta (10-30 Hz) frequency band [153]. The results reported in [122, 137, 146, 147] have shown DWT is suits well for seizure detection but MODWT has not explored. However, the proposed study using MODWT and six entropies showed excellent results. In particular, MODWT with sigmoid entropy outperformed other entropies among all the four wavelets.

5.4.3 Performance comparison of computational time

Fig. 5.13 depicts the computational time required for pre-processing, MODWT, feature extraction and classification procedure of the proposed technique using

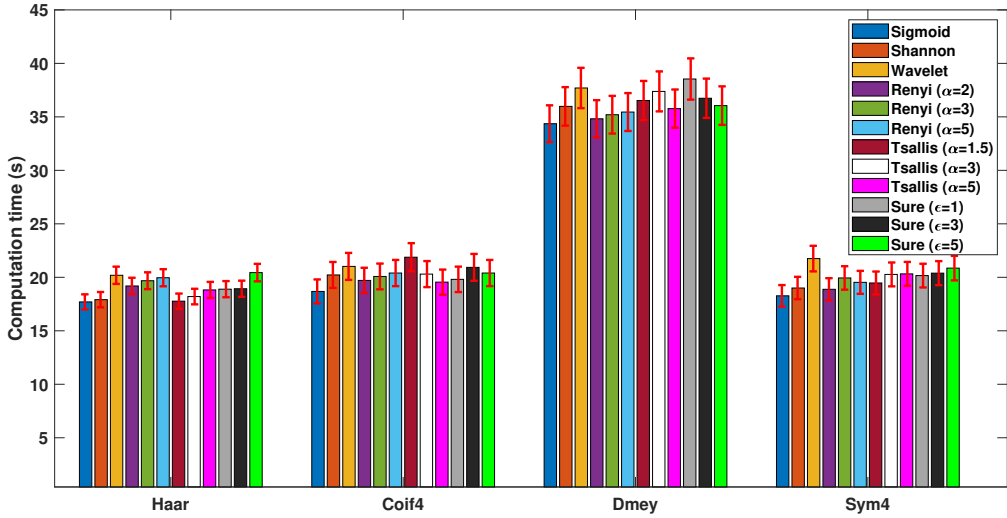


FIGURE 5.13: Computational time (s) between different entropies using MODWT for RMCH database.

RMCH database. The results considered for comparison that was performed better among different sub-bands in respective entropies and wavelets. Individually, the computational time taken by sigmoid entropy in all the wavelets was found to be slightly less. Further, wavelet entropy was slightly computationally expensive when compared with other entropies. Overall, Haar wavelet and Dmey wavelets were computationally economically and expensive respectively. The proposed method was implemented on MATLAB 2016b using 8GB RAM, CPU 2 GHz with an Intel I3 processor.

The overall performance of the proposed technique was assessed using relative performance [21]. Relative performance is defined as the ratio of the classification accuracy to the computation time (s) and it is given by

$$Relative\ performance = \frac{Accuracy}{Computation\ time} \quad (5.15)$$

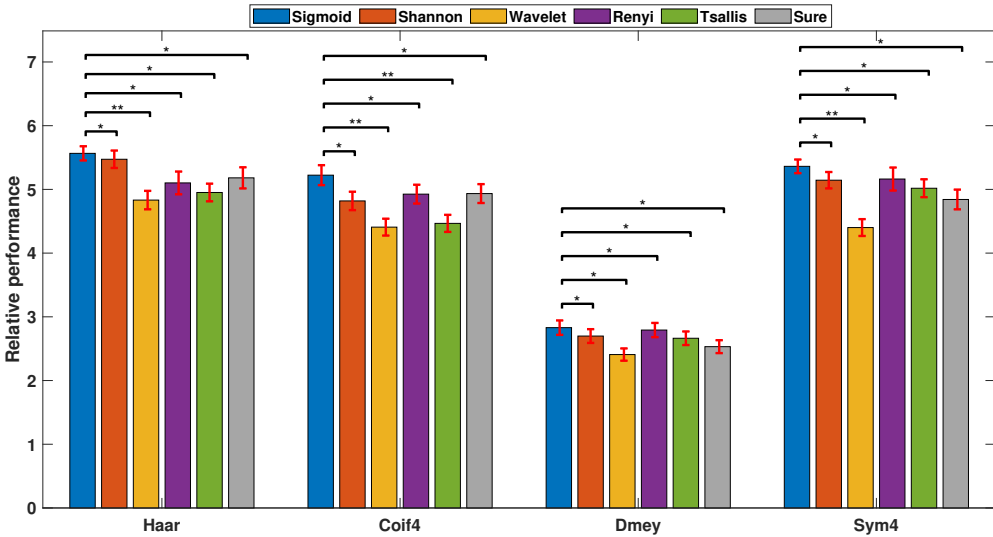


FIGURE 5.14: Relative performance obtained for best results among four wavelets and entropies. $p < 0.05(*)$, $p < 0.01(**)$, $p < 0.001(***)$

It can be speculate from the above equation that efficiency of the model indicated by higher relative performance. Fig. 5.14 shows the best relative performance obtained among all the wavelets and entropies. We observe that sigmoid entropy using Haar wavelet yielded better relative performance among all. Further, Dmey wavelet showed least relative performance when compared to other wavelets.

5.4.4 Significant findings of the study

The salient features and contributions of proposed study are summarized as follows:

1. The application of MODWT revealed significant information about epileptic EEG in different wavelets sub-band and entropies.

2. The proposed study was validated on three databases including our own database (RMCH) and two open sources UBonn and CHB-MIT. To the best of authors knowledge, no studies have used three databases to validate their studies.
3. The energy content in the sub-bands D2, D3 and D4 were significantly high as compared to the other levels for all the wavelets in case of RMCH database.
4. Sigmoid entropy exhibited lower for epileptic and higher for normal EEG. However, we observe contrast results for other entropies as higher and lower for epileptic and normal EEG respectively.
5. Renyi and SURE entropies were found to be increasing as entropy index α and ϵ goes higher respectively.
6. Tsallis entropy was seen to be decreasing as the entropy index increases.
7. Haar wavelet in sub-band D4 and D5 showed the highest classification accuracy among all the wavelets and entropies for RMCH and UBonn databases respectively.
8. In case of CHB-MIT database, Haar wavelet in sub-band D6 showed better results as compare to other wavelets and sub-bands due to the different sampling frequency of EEG signal. Interestingly, all the entropies performed better using CHB-MIT database.
9. In most of the cases, least classification accuracy was observed using the last level of approximation coefficients A7 (for RMCH and UBonn)

and A10 (CHB-MIT). However, wavelet entropy showed slightly better results in the same band for all the three databases.

10. The dynamic characteristics revealed by the proposed study suggest that entropies based features behave differently in each sub-band of MODWT. Collectively, sub-bands D2, D3, and D4 reveal salient information of the brain which is essential for seizure onset detection for RMCH database.
11. Similarly, sub-bands D5 and D6 outperformed other sub-bands for UBonn and CHB-MIT databases respectively.
12. Overall, our study suggests that entropy index values of Renyi, Tsallis, and SURE entropies must be selected carefully.

As a future expansion, the study will be extended on larger EEG databases using best MODWT sub-band and entropy. Further, deep learning neural network will be explored along with the classification of seizure types.

5.5 Conclusion

In this paper, complexity analysis and dynamic characteristics of epileptic EEG was studied using MODWT based entropies and classified using SVM classifier. Experimental results suggest that sigmoid entropy outperformed other entropies using all the wavelets. Collectively, results demonstrate that different mother wavelets have an impact on computational time, but not much on classification results in the same sub-band. Extensive insight into the wavelet analysis on RMCH database showed that energy content in the sub-bands D2,

D3 and D4 is high and highest classification accuracy shown by same. Furthermore, the entropies in sub-bands D2, D3, and D4 is significantly high for all the entropies except for sigmoid entropy. Sigmoid entropy produced the highest classification results of 98.44% using Haar wavelet in sub-band D4 for RMCH database. Further, the highest accuracy of 100% and 94.51% was achieved for UBonn and CHB-MIT databases respectively. We observe that Haar and Dmey wavelets found to be computationally economical and expensive respectively. The proposed study suggest that entropy index in Renyi, Tsallis, and SURE entropies must be chosen properly.

Acknowledgment

The authors are grateful to doctors of Institute of Neuroscience, Ramaiah Medical College and Hospitals, Bengaluru, India, for valuable discussion and providing EEG recordings for research purpose.

CHAPTER 6

Adaptive median feature baseline correction for improving recognition of epileptic seizures in ICU EEG

S Raghu, Natarajan Sriraam, Erik D Gommer, Danny M W Hilkmann, Yasin
Temel, Shyam Vasudeva Rao, Pieter L Kubben

Neurocomputing, 407:385-398

Year: 2020

<https://doi.org/10.1016/j.neucom.2020.04.144>

Abstract

Automated classification of epileptic seizures surrogates the manual interventions required for analyzing long-term electroencephalographic (EEG) signals and helps to speed up the treatment in epilepsy patients. Developing a patient independent algorithm is a great challenge due to the differences in EEG characteristics. Feature distribution among many subjects results in inter-subject variability, which leads to poor classification performance. Therefore, in order to overcome this limitation, we have proposed a novel adaptive median feature baseline correction (AM-FBC) method to update the feature distribution. Two recently proposed features referred to as successive decomposition index (SDI) and matrix determinant (MD) were extracted from 40 intensive care unit patients EEG at a segmentation length of 4 s with 50% overlap. We have investigated the influence of outliers removal and correction, AM-FBC, and post-processing of classifier output to improve the seizure detection results. The classification was performed using a support vector machine classifier with leave-one-subject-out cross-validation. With the application of above-mentioned methods, the highest area under the curve (AUC) of 0.9663 (sensitivity(S^+) = 0.9661, specificity(S^-) = 0.8446) and 0.9812 (S^+ = 0.9822, S^- = 0.8705) was achieved using SDI and MD features respectively. Further, the AUC of 0.9593 (S^+ =0.9069, S^- = 0.8695) was achieved when both SDI and MD features were used with the application of the outliers correction method. The findings of the study suggest (1) Outliers correction method does not improve results (2) AM-FBC enhances the results (3) Post-processing method improved the classification results at least 2 to 5% and reduced false

detections (4) Lowering the outlier removal factor showed good AUC at the cost of loss of feature samples.

6.1 Introduction

Epilepsy is a neurological disorder that affects the brain cortical network that in turn affects one's daily life [149]. It is a chronic disease that causes unprovoked recurrent seizures and is characterized by unpredictable seizures that leads to health problems [2, 79, 149]. It is the fourth most common neurological disorder, which affects 65 million people of all ages around the world [1]. In certain critical situations, epilepsy patients undergo pre-surgical investigation prior to surgery that determines the localization and nature of a seizure. Seizures are a common occurrence in traumatic brain injury patients in the intensive care unit (ICU) [161]. Although estimates of the overall incidence of seizures in the ICU vary, the risk of seizures is higher than in patients at other hospital departments, perhaps with the exception of the emergency department [161]. One of the goals of therapy in the ICU is to suppress seizures to obtain a better patient outcome [161]. Monitoring the long-term electroencephalographic (EEG) signals that belong to epilepsy patients is essential for pre-surgical evaluation, which is found to be a tedious and time-consuming process due to the need for visual interpretation. Accordingly, a reliable patient independent real-time epileptic seizure detection model helps towards long-term monitoring of patients with epilepsy. The high variability in time-varying EEG characteristics between subjects leads to poor classification performance [20, 162]. Therefore, we propose an adaptive median feature baseline correction (AM-FBC) method to reduce the inter-subject variability by

making use of median values of extracted features.

Several patient independent automatic detection of epileptic seizure algorithms have been proposed in recent years. A patient-specific model using wavelet packet based combined seizure index revealed the sensitivity of 90.5%, a false detection rate of 0.51/h and median detection delay of 7 s [137]. A threshold based seizure detection method was proposed using the minimum variance modified fuzzy entropy showed classification accuracy of 100% [19]. Another threshold-based decision-making algorithm for artifact removal showed good results using a support vector machine (SVM) [30]. Subasi et al. [163] have compared the performance of principal component analysis, independent component analysis (ICA) and linear discrimination analysis for seizure detection using the SVM classifier. A patient-specific seizure detection algorithm using wavelet decomposition and SVM classifier [88] detected 131 of 139 seizures. Another patient-specific algorithm using spectral parameters, time domain parameters, and wavelet analysis predicted 14 of the 25 seizures [103]. The changes in absence seizure were classified using permutation entropy [123].

Acharya et al. [80] showed the highest accuracy of 98.1% using fuzzy classifier when classified using approximation entropy (ApEn), sample entropy, phase entropy 1 and phase entropy 2. Further, the application of different entropy methods has been reviewed to differentiate normal, interictal, and ictal EEG signals [18]. In [39, 57, 164], normal, pre-ictal, and seizure activities were classified using the convolution neural network. Automatic epileptogenic zone recognition and localization on scalp EEG using long-term

recurrent convolutional network showed the sensitivity, specificity, and accuracy of 84.0%, 99.0%, and 99.0% respectively [165]. Wave2Vec was proposed to learn the deep representation of epileptic seizures temporal data [166]. Different transformation techniques like discrete cosine transformation, singular value decomposition, discrete wavelet transformation (DWT) were studied for epileptic seizure detection [167]. Improved correlation-based feature selection method with random forest classifier achieved an accuracy of 100.0% between normal and epileptic [168]. Mahalanobis-similarity-based feature extraction method using extreme learning machine classifier showed an accuracy of 97.53% [169]. Classification of epileptic and non-epileptic EEG events using time domain and frequency domain features achieved an accuracy of 95.0% using Bayesian network [87]. Different algorithms for analysis of epilepsy [22] and wavelet-based EEG processing [130] for seizure detection have been reviewed. Different entropy methods like log energy and norm entropy [21], approximate entropy [27, 170], weighted permutation entropy [98], Renyi, spectral, Shannon and wavelet entropy [36, 66, 81], sample and permutation entropy [171], and sigmoid entropy [83] have been successfully used for seizure detection. K-nearest neighbor entropy estimator, log energy entropy, Shannon entropy, and Poincaré plot parameters were extracted from Empirical mode decomposition (EMD) [172]. Intrinsic mode functions from empirical wavelet transform has been studied to improve time–frequency representation of non-stationary signals in [173, 174, 175]. Time–frequency localization of scaling functions and design of three-band biorthogonal linear phase wavelet filter banks has been studied for classification of seizure and seizure-free EEG signals [176, 177].

In a recent study [162], feature normalization procedure based on median decaying memory (MDM) showed promising improvements towards seizure detection. In this method, in order to correct the feature baseline, initial 5 s of non-seizure EEG segment was used. The same approach was applied in [20] using 1 minute EEG to update the baseline to evaluate seizure detection performance in 17 ICU patients. Five feature normalization techniques, namely MDM, mean memory, standard deviation memory, peak detector, and signal range was applied to a line length feature that proved MDM was outperformed [178]. Bogaarts et al. [179] have proposed an algorithm to improve the area under the curve from 0.767 to 0.902 using average non-seizure feature values (ANSFV) and an optimal threshold for feature baseline correction (FBC) and a Kalman filter to classifier output for post-processing. This feature normalization based patient independent approach showed the AUC of 0.90 and 0.93 for neonatal and adult patients respectively [84]. Further, Temko et al. [180] proposed post-processing of the SVM classifier output using a central linear moving average filter (MAF). Ahmed et al. [181] suggested a post-processing approach using the MAX operator and MAF that significantly improved the seizure detection results.

SVM classifier have been widely used for seizure detection studies [20, 25, 65, 84, 88, 163, 179, 180, 181]. In our recent study, successive decomposition index (SDI) showed the highest sensitivity of 97.53% using the SVM classifier [182]. Further, matrix determinant (MD) was evaluated on eleven classification problems derived from University of Bonn database [89]. These two features have been tested on the Ramaiah Medical College and Hospitals, CHB-MIT, Temple University Hospital databases in our previous studies [89,

182]. Therefore, in this paper, we have used these two novel features (SDI and MD) to validate against new EEG recordings using the most widely used and suitable SVM classifier for seizure detection [89, 182].

The significant contributions of our study are: (1) We have proposed a novel approach called AM-FBC to reduce the inter-subject variability in feature distribution (2) Effect of outliers removal and correction (3) Effect of post-processing to improve the seizure detection performance (4) Two recently proposed novel features, namely SDI and MD were tested against new EEG recordings.

Fig. 6.1 depicts the flow of the proposed algorithm for the epileptic seizure detection. The raw EEG recordings were pre-processed using a notch filter and bandpass filter followed by artifacts removal. The two features (SDI and MD) were classified using the SVM classifier with leave-one-subject-out cross-validation followed by post-processing.

The goal of this paper is to evaluate both the SDI and MD features and the effects of baseline correction, outlier removal and correction, and post-processing of the SVM classifier output on classification performance. We hypothesize that the application of the above-mentioned methods would improve the performance of seizure detection using ICU EEG in epilepsy patients.

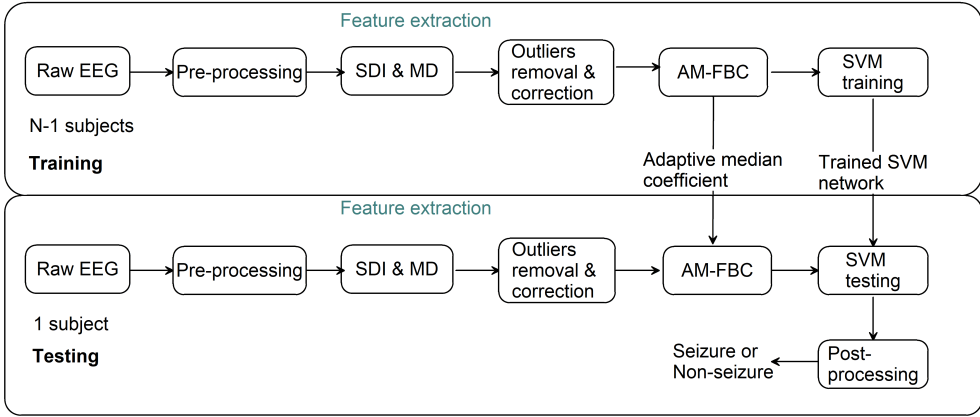


FIGURE 6.1: The flow of the proposed seizure detection algorithm. The SVM classifier was trained using $(N - 1)$ subjects and tested on the left out subject. The adaptive median coefficient estimated from the trained subject was used to correct the feature baseline of the test subject.

6.2 Materials and methods

6.2.1 Clinical EEG recordings

The clinical data for the study were obtained from the Department of Clinical Neurophysiology, Maastricht University Medical Centre (MUMC+), Maastricht, The Netherlands for research purpose after approved by the hospital ethics committee. The dataset consists of 40 EEG registrations (22 female and 18 male) from an ICU with the age ranges between 22 and 89 years with a mean age of 54.47 years. The 19 unipolar electrodes Fp1, Fp2, F7, F3, Fz, F4, F8, T3, C3, Cz, C4, T4, T5, P3, Pz, P4, T6, O1, and O2 were placed according to International 10-20 system electrode configuration. The scalp EEG was recorded using BrainLab EEG recording system at a sampling rate of 250 Hz using a common average montage. In total, 21 hours of EEG (mean duration

0.5243 hours) consist of 1273 seizure epochs that varied per subject from 1 to 228 with a minimum and maximum seizure duration of 12 s and 1949 s respectively. The minimum duration of seizure epoch was considered 10 s as per the International Federation of Clinical Neurophysiology [183]. Experts at MUMC+ Hospital annotated the seizure and non-seizure epochs. The EEG data was not scored in accordance to type of seizures. But in many seizures, the majority of the channels were involved, so most seizures were generalized. Table A6.3 shows the EEG database details used for the proposed study.

6.2.2 Pre-processing

A 50 Hz IIR notch filter was applied to eliminate the power line noise at 50 Hz and the EEG signals were bandpass filtered between 0.5 to 32 Hz. Further, ICA was applied to filtered EEG to eliminate the artifacts like eye blinks, muscle artifacts, and electrode movements [72]. The ICA toolbox available in EEGLab was used to remove the artifacts [116].

6.2.3 Feature extraction

In this study, two features, namely SDI [182] and MD [89] reported recently by our group were used for seizure detection. One can refer to [89, 182] for more details on these novel feature extraction methods. Both features were extracted at a segmentation length of 4 s with 50% overlap.

6.2.3.1 Successive decomposition index

Consider the EEG time series $x = \{x_1, x_2, x_3, x_4, \dots, x_n\}$, where n is the total number of the EEG samples in the time series x . Since the sampling

frequency is 250 Hz, n becomes 1000 (4s x 250 samples).

In order to define SDI coefficients, first, we define two terms X^+ and X^- which are average of $|x|$ and difference average of x respectively. The coefficient X^+ is given by [182],

$$X^+ = \frac{1}{n} \sum_{i=1}^n |x_i| \quad (6.1)$$

In the subsequent step, the second coefficient X^- was calculated by the iterative process. In the first level ($x^{(1)}$), EEG samples were arranged into $n/2$ non-overlapping pairs as shown below [182],

$$x^{(1)} = \left\{ \frac{x_1 - x_2}{2}, \frac{x_3 - x_4}{2}, \dots, \frac{x_{n-3} - x_{n-2}}{2}, \frac{x_{n-1} - x_n}{2} \right\} \quad (6.2)$$

Here, if n is not a power of 2 then zeros can be padded towards the end of the x which does not affect on results. After decomposition, $x^{(1)}$ of length $n/2$ (n is updated in each level) is represented as [182],

$$x^{(1)} = \{x_1^{(1)}, x_2^{(1)}, \dots, x_{n/2-1}^{(1)}, x_{n/2}^{(1)}\} \quad (6.3)$$

It can be simplified and written as follows,

$$X_i^L = (x_{2i-1}^L - x_{2i}^L) / 2 \quad (6.4)$$

The coefficient remained in the last level ($L = 3.33 \log_{10}(n)$) of decomposition was taken as X^- .

Our next aim was to define two new terms X^{++} , and X^{--} using X^+ and X^- as follows [182],

$$X^{++} = \frac{X^+ + X^-}{2} \quad (6.5)$$

$$X^{--} = \frac{X^+ - X^-}{2} \quad (6.6)$$

The square matrix A was formed using the four coefficients X^+ , X^- , X^{++} , and X^{--} as follows [182],

$$A = \begin{bmatrix} X^+ & X^{--} \\ X^- & X^{++} \end{bmatrix} \quad (6.7)$$

The basis for forming a square matrix and estimating determinant of same for seizure detection was given in [89]. Thus, SDI was calculated using determinant of the square matrix A [182].

$$SDI = \log_{10} \left(\frac{n}{L} (X^+ X^{++} - X^- X^{--}) \right) \quad (6.8)$$

The term n/L is a scalar parameter. Our previous study [182] has proven that SDI better tracks the seizure activity in EEG along with the amplitudes of the EEG samples.

6.2.3.2 Matrix determinant

Our recent study [89] has proven that the amount of information captured by matrix determinant during epileptic activity increases its measure to acts as a biomarker to identify those events.

The EEG time series were arranged sequentially to form a square matrix by considering the total elements in the square matrix represent a segmentation length. Let the EEG time series be $x = \{x_1, x_2, x_3, x_4, \dots, x_n\}$ and apply absolute square i.e. $x = |x|^2$. The absolute was taken because positive and negative EEG samples gets vanishes when their magnitude is same. Defining the matrix with an order of $N(N = r = c)$ and sequentially arrange x into matrix form as follows [89],

$$A = \begin{bmatrix} x_1 & x_2 & \dots & x_r \\ x_{r+1} & x_{r+2} & \dots & x_{r+r} \\ x_{2r+1} & x_{2r+2} & \dots & x_{2r+r} \\ \cdot & \cdot & \dots & \cdot \\ x_{(r-1)r+1} & x_{(r-1)r+2} & \dots & x_{(r-1)r+r} \end{bmatrix} \quad (6.9)$$

where r and c are the square matrix order.

The matrix determinant feature was estimated as follows [89],

$$MD = \log_{10} |A| \quad (6.10)$$

In our study, the square matrix was formed with an order of 32 to estimate the determinant feature.

6.2.4 Outliers removal and correction

An outlier is a data sample that is distinctly separate from the rest of the data [25, 184]. It may be due to variability in the measurement, electrode displacement, fluctuation in data and it may indicate the experimental error. As reported in [25, 184, 185, 186], it can be noted that the outliers removal improves the classification results for EEG signal classification without losing much diagnostic information. In this study, we have applied outliers removal using Tukey's range test and outliers were replaced using different methods (refer to Table 6.1). According to Tukey's range test [185], an outlier is an observation which is outside the range of $[Q1 - k * IQR, Q3 + k * IQR]$, where k is a non-negative integer. Where, $Q1$ is 25th percentile, $Q3$ is 75th percentile and inter quartile range (IQR) is the difference between $Q3$ and $Q1$. In our study, k was varied as 0.5, 1, 1.5, 2 and 3 to study the effect of outliers removal on classification results with respect to the percentage of loss of feature samples. For outliers correction approach, three methods for detecting outliers, namely mean, median and quartiles were used. The detected outliers were replaced using spline and nearest methods [187].

6.2.5 Adaptive median feature baseline correction

The high variability in time-varying EEG characteristics between patients leads to poor classification performance [20, 162]. Therefore, AM-FBC was proposed using the median values of features SDI and MD. AM-FBC was applied individually for each feature and the procedure is give below:

1. Consider the features of all the subjects $f(sub_1, sub_2, \dots, sub_n)$ from training data. Here, sub_1, sub_2 are subjects and f is a feature (f may be SDI or MD).
2. Calculate the $f(Median_{seizure})$ and $f(Median_{non-seizure})$ of all the training subjects using seizure and non-seizure feature respectively. The length of the $f(Median_{seizure})$ and $f(Median_{non-seizure})$ are the same as a number of subjects.
3. Estimate global median ($f(Median_{global})$) using median values of seizure and non-seizure.

$$f(Median_{global}) = Median\{f(Median_{seizure}) f(Median_{non-seizure})\} \quad (6.11)$$

4. Now estimate the median of single subject $f(Median_{sub i})$, where $i = 1, 2, 3, \dots, n$ subjects.
5. Now finding the adaptive median coefficient (λ) using $f(Median_{global})$ and $f(Median_{sub i})$.

$$\lambda = f(Median_{global}) - f(Median_{sub i}) \quad (6.12)$$

6. Now correct the feature baseline of $sub i$ using λ as follows:

$$f_{new i} = \lambda + f_{sub i} \quad (6.13)$$

7. Repeat step 4 to step 6 for all the training subjects (n).

8. Repeat step 4 to step 6 for the testing subjects using the $f(\text{Median}_{global})$ calculated from the training data.

The λ can be either negative or positive depends on the inter-subject median variability.

6.2.6 Classification

The classification of the proposed method was performed using the SVM classifier due to its better performance in previous studies [25, 42, 65, 89, 128, 135, 170]. During the simulation, the radial basis function kernel showed better performance in terms of classification results. The classifier was assessed using leave-one-subject-out cross-validation to achieve the robustness of the method. The trained SVM classifier was tested on each single left out subject and the process repeated so that all the subjects have been used for testing. Further, SVM classifier tuning parameters were set as follows in MATLAB 2018b: Kernel function = radial basis function, Kernel Scale = 1, Box Constraint = 1, and Standardize = true.

The simulations were performed on MATLAB 2018b using 8GB RAM, CPU 2 GHz with an Intel i3 processor.

6.2.7 Post-processing

As reported in [180, 181], post-processing was performed using a 5-tap MAF to the SVM classifier output. This helps to reduce the random noise without disturbing the sharp step response during seizure activity. The filtered output [0, 1] was compared with a threshold of 0.5 to make the final decision as seizure and non-seizure. After the threshold, the decision was made as seizure

and non-seizure if the threshold was greater than and less than of 0.5 respectively. Post-processing of the classifier output helps to reduce the false alarms in real-time seizure detection for ICU patient monitoring.

6.2.8 Performance measures

The algorithm performance was calculated by the mean results across all the 40 subjects using leave-one-subject-out cross validation. The algorithm was assessed using performance parameters, namely sensitivity, specificity, the area under the curve (AUC) and false detection rate (FDR).

$$\text{Sensitivity } (S^+) = \frac{TP}{TP + FN} \quad (6.14)$$

$$\text{Specificity } (S^-) = \frac{TN}{TN + FP} \quad (6.15)$$

where, TP is seizure detected as seizure, FN is seizure detected as non-seizure, TN is non seizure detected as non-seizure and FP is non-seizure detected as seizure. The area under the receiver operating characteristic (ROC) curve was reported using sensitivity and 1-specificity. An FDR was calculated by using the ratio of a total number of false detections to the total duration of the data in hours in all the epochs.

6.2.9 Classification scenarios

The proposed seizure detection approach was evaluated using 10 different classification scenarios (CS) in terms of outliers removal and correction, AM-FBC, and post-processing and same is depicted in Table 6.1.

TABLE 6.1: Different classification scenarios considered for the study

Classification scenario	Outliers removal and correction	AM-FBC	Post- processing
1	No	No	No
		No	Yes
2	No	Yes	No
		Yes	Yes
3	Replace (Nearest- Mean)	Yes	No
		Yes	Yes
4	Replace (Spline-Median)	Yes	No
		Yes	Yes
5	Replace (Spline-Quartile)	Yes	No
		Yes	Yes
6	Yes ($k=3$)	Yes	No
		Yes	Yes
7	Yes ($k=2$)	Yes	No
		Yes	Yes
8	Yes ($k=1.5$)	Yes	No
		Yes	Yes
9	Yes ($k=1$)	Yes	No
		Yes	Yes
10	Yes ($k=0.5$)	Yes	No
		Yes	Yes

Note: CS3 to CS5 are outliers correction and CS6 to CS10 are outliers removal methods.

Spline and nearest are outlier correction methods. Median, Mean and Quartile are outlier detect methods.

6.3 Results

6.3.1 Analysis of AM-FBC

Fig. 6.2 shows the example of the raw EEG signal, pre-processed EEG and spectra of channel Fp2 from subject 2. The SDI and MD values for all the 40 subjects were shown using the boxplot in Figs. 6.3a & c respectively. The inter-subject variability in SDI and MD features can be observed in most of the subjects (high variability in subjects 3, 4, 10, 16, 22, 25, 27, 28, 31, 32, 33, 34, 35, 36, 37 38 and 39), which leads to poor classification performance. In order to correct the feature baseline among different subjects, we have applied a novel AM-FBC (refer to 2.5) and results are shown in Figs. 6.3b & d for

each subject. We observe that the SDI and MD features baseline was brought to a common range (indicated in a horizontal line) after applying AM-FBC. We observe some overlap between seizure and non-seizure in SDI and MD features for subjects 4, 10, 12, 16, 21, 25, 27, 28, 30, 33, 34, 35 and 39, which degrades the classification results. After AM-FBC for both SDI and MD seizure and non-seizure features were significantly different ($p < 0.05$) when tested using a Wilcoxon rank sum test.

Fig. 6.4 shows the resultant features median values before and after AM-FBC. In Fig. 6.4, the smooth line shows the median values for actual SDI and MD features. It can be seen that high variation of median values among different subjects. In addition, the overlap between seizure and non-seizure median values can be observed for both the features before the AM-FBC. The other line with a circle and plus shows the corrected median values after applying AM-FBC.

6.3.2 Influence of post-processing

The effect of post-processing of the SVM classifier output is depicted in Fig. 6.5. The post-processing mechanism involves a 5-tap MAF, thresholding, and binary decision. Figs. 6.5b & c shows the SDI and MD features respectively for the EEG shown in Fig. 6.5a. As one can observe that the false alarms in Fig. 6.5d are high as compared to the ground truth results in Fig. 6.5g. The SVM classifier output was smoothed using a 5-tap MAF for each channel and applied a threshold at 0.5 as described in [85]. As a result of filtering, the false detections were reduced (refer to Fig. 6.5f) and the output was closely

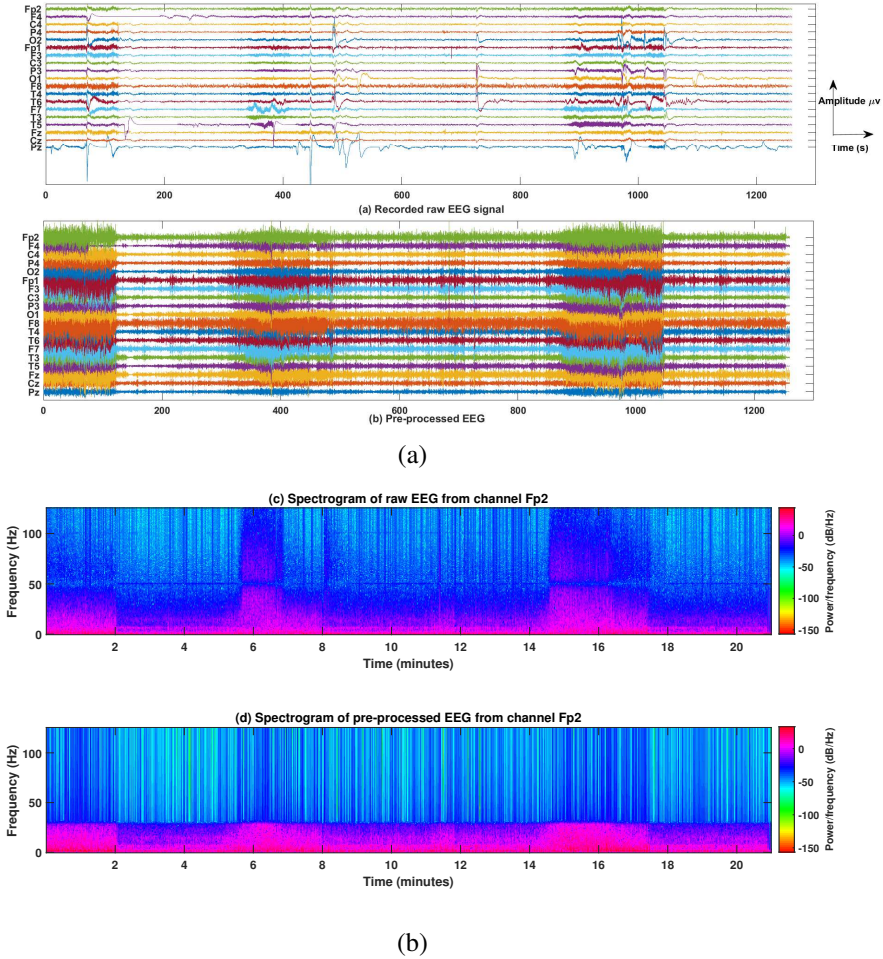


FIGURE 6.2: **(a)** Raw EEG from subject 2. **(b)** Pre-processed EEG using a notch filter, bandpass filter and ICA for artifacts removal. **(c)** Spectrogram of raw EEG from channel Fp2. **(d)** Spectrogram of pre-processed EEG from channel Fp2.

matched with ground truth labels (refer to Fig. 6.5g). The post-processing approach significantly improved the classification results ($p < 0.05$) for seizure detection (refer to Fig. 6.8).

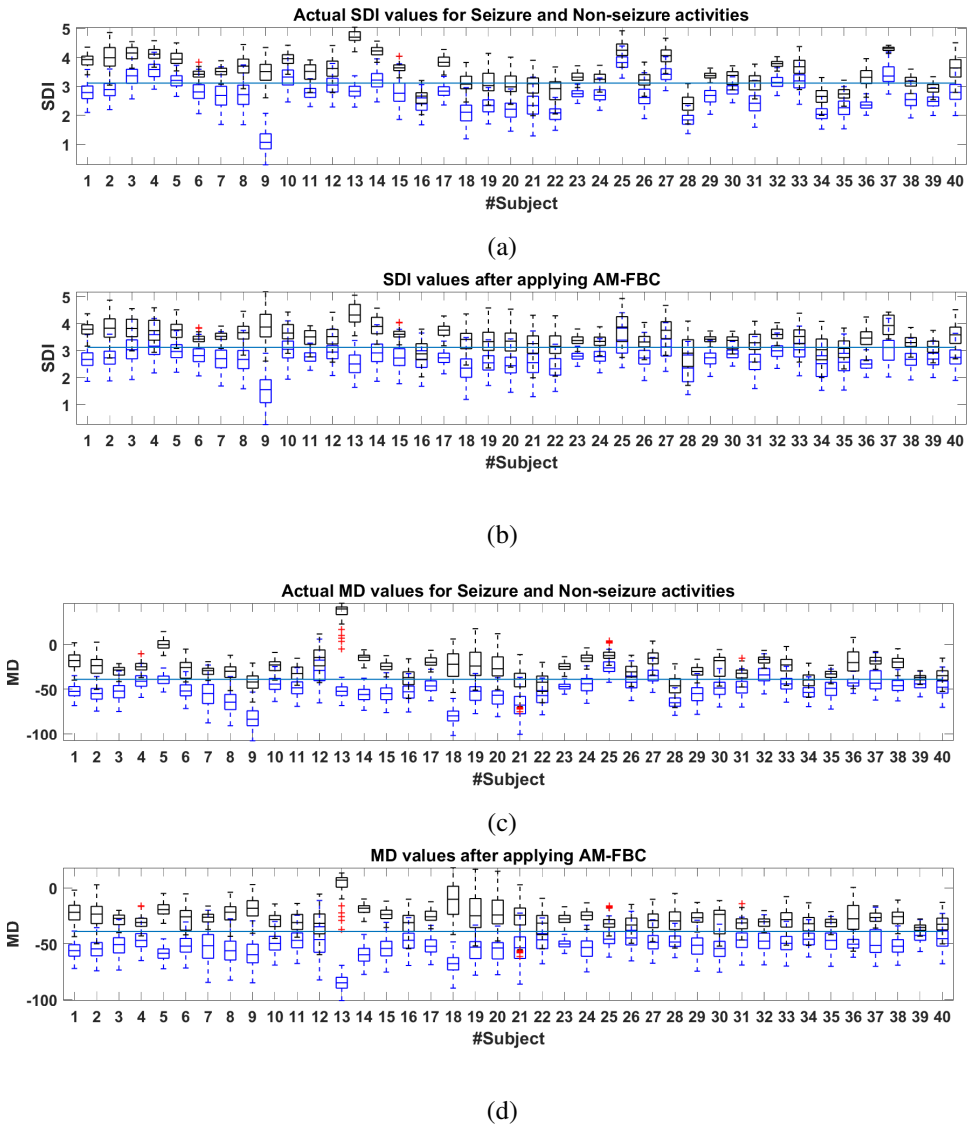


FIGURE 6.3: The boxplot of SDI and MD features for each subject before and after AM-FBC. The boxplot with black boxes indicates seizure and blue boxes indicates non-seizure. The red + indicates the outliers which are beyond the whiskers. The horizontal blue line was drawn as a reference threshold using median values.

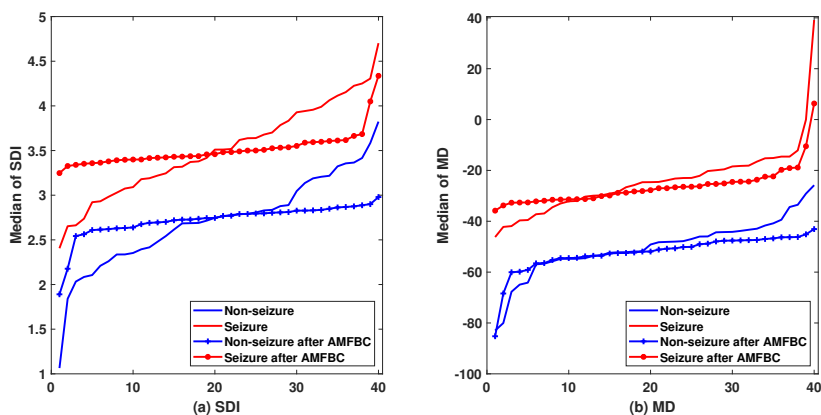


FIGURE 6.4: Median values of SDI and MD before and after AM-FBC. The x-axis is the median values that are sorted for better understanding.

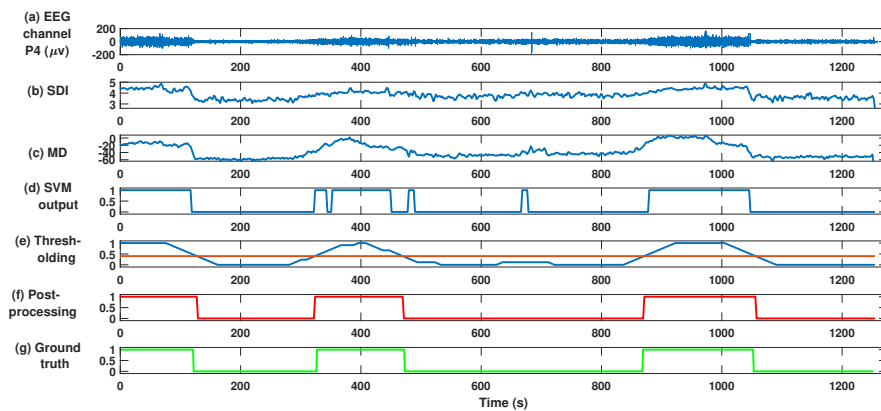


FIGURE 6.5: Effect of post-processing for seizure detection. (a) EEG signal belongs to channel P4. (b) & (c) Corresponding SDI and MD values of channel P4 respectively. (d) SVM classifier output. (e) The smoothed output after a 5-tap MAF was applied on classifier output when classified using both SDI and MD. The threshold (red line) was set to 0.5 to make a binary decision. (f) Binary decision after applying thresholding to smoothed output. (g) Ground truth, where 0 and 1 indicate non-seizure and seizure respectively.

6.3.3 Seizure classification results

Fig. 6.6 shows the ROC curve for different classification scenarios. The best ROC was obtained when both SDI and MD features were classified and post-processing was applied. The estimated area under the ROC curve for each classification scenario is reported in Fig. 6.7. In the case of both SDI and MD features together, outliers removal was excluded due to an imbalance number of feature segments in SDI and MD.

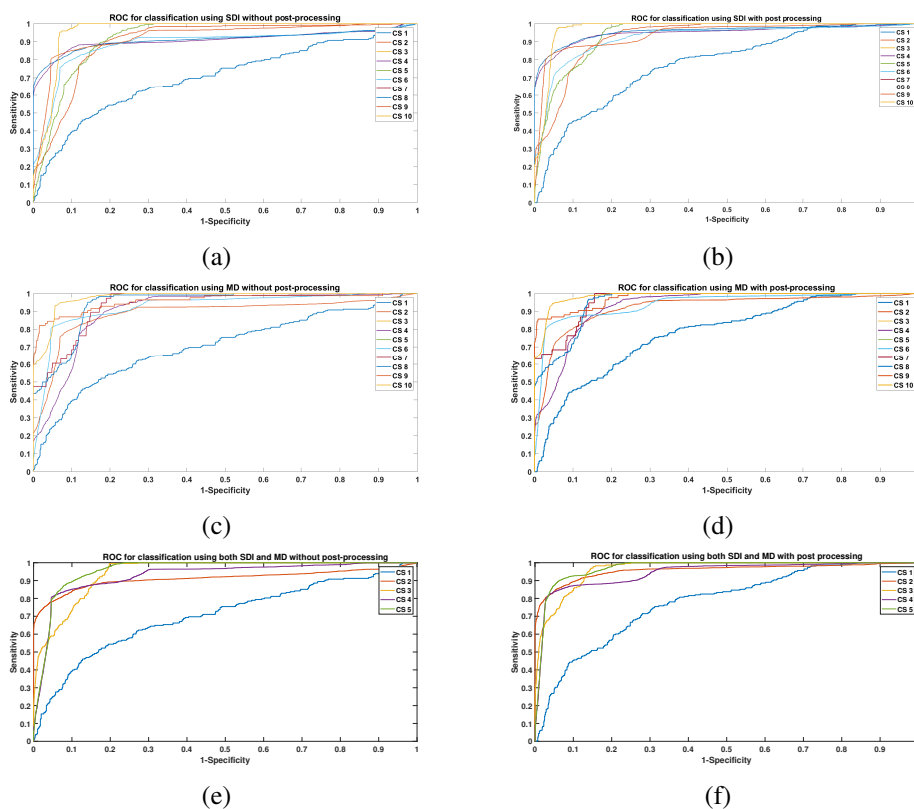


FIGURE 6.6: The ROC curve for different classification scenarios for the proposed method. (a) & (b) The ROC curve of SDI, (c) & (d) The ROC curve of MD, (e) & (f) The ROC curve when both SDI and MD was used for classification. **Left column:** The ROC curve without post-processing, **Right column:** The ROC curve with post-processing. The CS indicates classification scenario.

First, we discuss the classification results obtained using SDI feature. The AUC of 0.6064 ($S^+=0.2307$, $S^-=0.9820$) was achieved when outliers removal, AM-FBC, and post-processing techniques (CS1) were not applied. These poor results were due to the inter-subject variability of SDI feature. In CS2, the AUC of 0.9062 ($S^+=0.8573$, $S^-=0.8567$) was achieved with AM-FBC, without the outliers removal and post-processing. It was evident that AM-FBC has a significant contribution to classification results. Further, applying post-processing in CS2, the AUC increased to 0.9428 ($S^+=0.8722$, $S^-=0.8770$). Hence, it was proven that the application of AM-FBC and post-processing greatly improves seizure detection and reduces the FDR.

In next CS3, CS4 and CS5, outliers were detected using median, mean and quartiles methods respectively and filled using spline and nearest methods [187]. Application of outliers correction methods resulted in the AUC of 0.9388, 0.9445, and 0.9445 for CS3, CS4, and CS5 respectively when post-processing was used. Interestingly, no distinct difference in terms of classification results was observed with outliers and outliers correction methods (CS2 to CS4). The AUC of 0.9072 ($S^+=0.8578$, $S^-=0.8566$) and 0.9437 ($S^+=0.8734$, $S^-=0.8764$) were obtained without and with post-processing respectively when $k = 3$ (CS6) for outliers removal which was same as the presence of outliers (CS2). Using the $k = 2, 1.5, 1$ and 0.5 , for CS7, CS8, CS9, and CS10 the AUC of 0.9470 ($S^+=0.8742$, $S^-=0.8758$), 0.9525 ($S^+=0.8805$, $S^-=0.8776$), 0.9627 ($S^+=0.8984$, $S^-=0.8805$), and 0.9663 ($S^+=0.9661$, $S^-=0.8446$) was obtained respectively. We observe that the AUC increases as the k value decrease that implies more loss the feature samples. Even though the highest AUC was achieved for CS10 ($k = 0.5$), the S^- drops to 0.8446 which is not a

good sign.

Similar observations were made when the MD feature was used for classification. The AUC of 0.9332, 0.9000, 0.9475, 0.9476 was obtained for CS2 to CS5 respectively with post-processing. Further, the highest AUC of 0.9757 ($S^+=0.9791$, $S^-=0.8636$) and 0.9812 ($S^+=0.9822$, $S^-=0.8705$) was achieved with $k = 0.5$ (CS10) for without and with post-processing respectively.

The AUC was increased to 0.9158 and 0.9556 without and with post-processing respectively when both SDI and MD features (CS2) were used for classification. Further, the AUC of 0.9619 ($S^+=0.9434$, $S^-=0.8561$), 0.9592 ($S^+=0.9062$, $S^-=0.8702$), and 0.9593 ($S^+=0.9069$, $S^-=0.9069$) were obtained for CS3, CS4, and CS5 respectively using post-processing which was better as compared to results obtained using SDI and MD alone.

Fig. 6.8 shows the comparison of AUC obtained in case of with and without outliers removal, AM-FBC, and post-processing on SDI and MD features. The overall results from different CS conclude that the application of outliers removal and correction, AM-FBC and post-processing plays a significant role ($p < 0.05$) in improving classification results.

6.4 Discussion

6.4.1 Effect of outliers removal

We have investigated the effect of outliers on classification results and loss of diagnostic information. In order to accomplish this task, we have considered the CS 6 to 10 and corresponding AUC. The percentage of the feature samples lost after outliers removal was taken into account for the analysis. Fig. 6.9

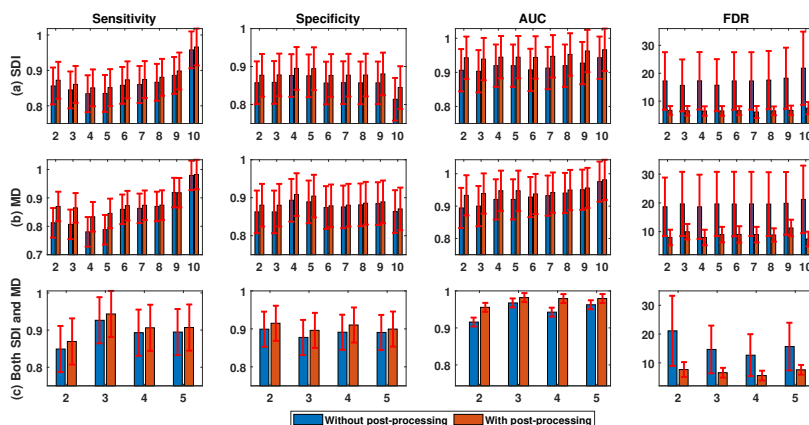


FIGURE 6.7: Classification results in different CS obtained using the proposed seizure detection approach. **First row (a):** SDI results, **Second row (b):** MD results, **Third row (c):** Results when both SDI and MD were combined. **First column:** Sensitivity (S^+), **Second column:** Specificity (S^-), **Third column:** AUC, and **Fourth column:** FDR. The X-tick labels indicate different classification scenarios.

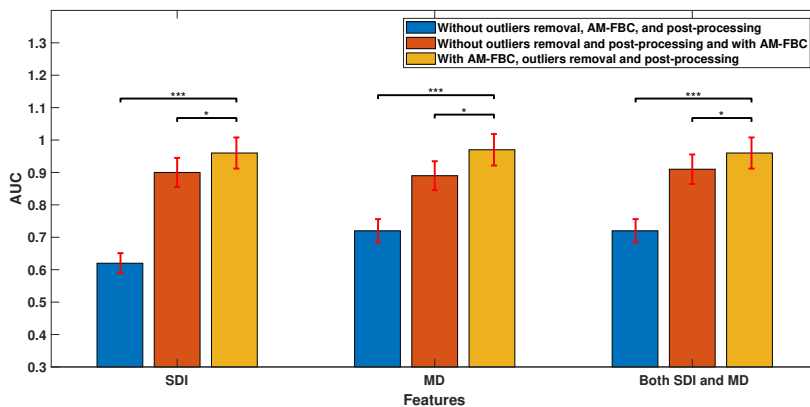


FIGURE 6.8: Significance comparison in terms of with and without outliers removal, AM-FBC, and post-processing on SDI and MD features. $p < 0.05(*)$, $p < 0.01(**)$, $p < 0.001(***)$.

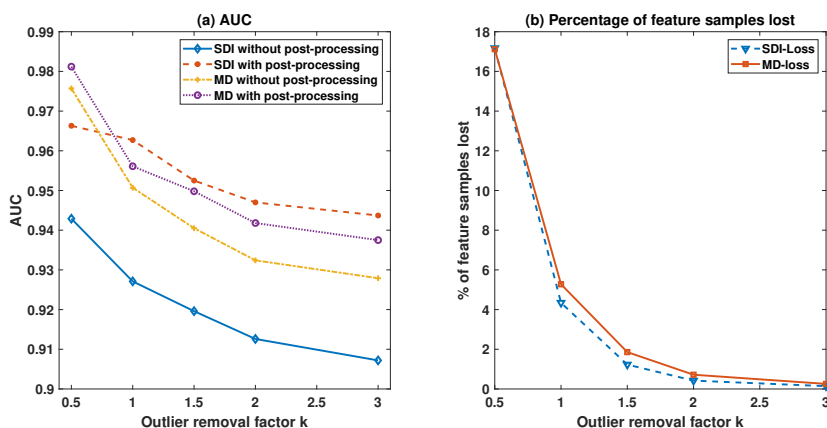


FIGURE 6.9: (a) Effect of outliers removal on classification results (AUC). (b) Percentage of feature samples lost. The x-axis varied with different k values such as 0.5, 1, 1.5, 2 and 3.

shows the effect of outlier removal on AUC and percentage of feature samples lost. As it can be seen, the highest AUC of 0.9663 and 0.9812 was obtained for $k = 0.5$ using SDI and MD features respectively. However, 17% of the feature samples were lost as compared to the original feature set. Similarly, a minimum of 0.3% of samples were lost for $k = 3$ and showed AUC of 0.9023. We observe that as the outlier removal factor k increases, the AUC and percentage of loss of feature samples decreases. In other words, the lower the k , the higher the classification results and loss of diagnostic information. As an optimal setting, $k = 1.5$ can be used for real-time application as that was resulted in the AUC of 0.958 with 1% of samples lost. It concludes that outliers removal factor must be chosen carefully in order to avoid losing diagnostic information.

6.4.2 Effect of a moving average filter

The length of the MAF for post-processing needs to be chosen properly. If the length of the filter is higher, it tends to a delay in seizure detection and short seizures will be missed out. The lower length of the filter will not improve the classification results but ideal for lower detection delay. In our study, it needs a delay of 10 s (5th order filter x segmentation length of 4 s = 20 s, due to 50% overlap it becomes 10 s data) to produce classification output of MAF. The 10 s criteria is the same as a minimum seizure duration considered as per International Federation of Clinical Neurophysiology (refer to 6.2.1) [183]. Hence, our classification results suggest that a 5-tap MAF would be ideal to avoid limitations such as higher detection delay and lower classification performance.

6.4.3 Effect of threshold in post-processing

With the goal of achieving an acceptable trade-off between sensitivity and specificity, threshold must be fixed accordingly. Fig. 6.10 shows graph of sensitivity and specificity versus different threshold for post-processing. The higher the sensitivity for lower threshold value results in poor specificity and in contrary for higher threshold values. In order to achieve the good trade-off between sensitivity and specificity, a threshold of 0.5 found to be optimal selection. Further, a threshold of 0.5 provides an equal justification to both the classes (seizure and non-seizure) being a mid-point.

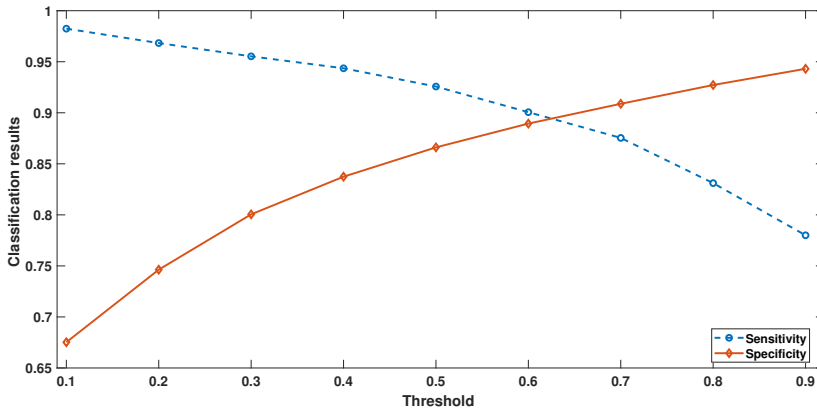


FIGURE 6.10: Effect of threshold in post-processing on sensitivity and specificity. Threshold was varied between 0.1 to 0.9.

6.4.4 Comparison with other studies

The comparison was restricted to the studies that have used either or both FBC and post-processing for seizure detection. Ahmed et al. [181] have proven that the post-processing of the SVM classifier output improved the seizure detection rate. Similarly, Temko et al. [180] have used the central linear MAF followed by logical OR operation with collar technique to increase the seizure detection rate and reduce the false detection. In [180, 181], post-processing was applied using a 9-tap and 15-tap MAF respectively, which leads to a delay in the final decision of seizure detection. Further, Bogaarts et al. have used a Kalman filter for post-processing in his three studies [20, 84, 179] proving the need for post-processing and a Kalman smoother for features before classification. Logesparan et al. [178] have proven MDM was better among five methods and improved classification results seen in [20]. In [162], bitwise logical OR operator was applied on classification output which was obtained from DWT based 65 features. In total, 55 [180, 181], 65 [162] and 103 [20, 84,

TABLE 6.2: Comparison between the state of the art seizure detection algorithms

Author	EEG database	Duration of EEG (h)	Number of subjects	Number of seizures	Feature extraction	FBC	Classifier	Post-processing	Results
[162]	National Society of Epilepsy (UK), Katholieke Universiteit Leuven (Belgium), and Freiburg University Hospital (Germany).	172	24 adults	47	DWT based Relative power	Normalization	Threshold	Bitwise logical OR operator	AUC = 0.83
[178]	CHB-MIT Neonatal Intensive Care Unit (NICU) of Cork University Maternity Hospital, Cork, Ireland	884	23	182	Line length	MDM	Threshold	No	AUC=0.93
[181]	MUMC, The Netherlands	261	17 neonates	821	55 features	No	SVM	MAF	AUC=0.71
[179]	MUMC, The Netherlands	25	39 term and pre-term new borns	360	103 features	ANSFV	SVM	Kalman filter	AUC=0.902 Sensitivity=0.801 Specificity=0.831
[20]	MUMC, The Netherlands Neonatal Intensive Care Unit (NICU) of Cork University Maternity Hospital, Cork, Ireland	4018	17 ICU patients	1362	103 features	MDM	SVM	Kalman filter	AUC=0.96
[180]	MUMC, The Netherlands	267	17 new borns	705	55 features	No	SVM	Central linear MAF	Sensitivity=89%
[84]	MUMC, The Netherlands	613	39 neonatal 39 adults	34898*	103 features	ANSFV	SVM	Kalman filter	AUC=0.93
Proposed	MUMC, The Netherlands	21	40 ICU patients	1273**	SDI and MD	AM-FBC	SVM	MAF	AUC=0.9663 (SDI) AUC=0.9812 (MD) AUC=0.9593 (Both)

*34898 Feature vectors derived from 10s epoch, ** 1373 seizure epochs of 10 s duration

[179] features were used that leads to the computational expense of the overall algorithm during feature extraction and classification. The results presented in Table 6.2 shows that the proposed method outperformed other state-of-the-art methods in terms of classification results.

In case of real-time seizure detection, latency of seizure detection also matters to avoid any damages caused to patient. As discussed in previous studies [85, 100, 137] latency of seizure detection is one of the key metric. The algorithm used to calculate the features and the subsequent classification of the data is possible within 4 seconds. Therefore, patient treatment can be considered on short notice.

6.4.5 Significant findings of the study

The significant findings and contributions of our study are summarized as follows:

1. A novel AM-FBC was proposed to overcome the inter-subject variability in feature distribution and a 5-tap MAF for post-processing of the SVM classifier.
2. We observed a significant difference in terms of median values of SDI and MD features before and after AM-FBC.
3. Outliers removal method outperformed outliers correction method.
4. The lower outlier removal factor (say $k = 0.5$) results in high loss of feature samples with improved classification results.
5. When outliers were removed with $k = 0.5$, specificity started decreasing as compared to results of $k = 1$.
6. The classification results revealed that the FDR reduces when post-processing was applied.
7. As compared to the studies [20, 84, 162, 179, 180, 181] that have used multiple features for seizure detection, our proposed algorithm has shown better classification results using a single feature leading to computationally efficient, which is an ideal for real-time application.
8. The MD performs better than SDI without post-processing and contrary with post-processing (refer to Fig. 6.9) revealing post-processing has more effect on SDI compared to MD.

9. We have already proven that SDI and MD were computationally efficient in our previous studies [89, 182]. AM-FBC and post-processing are simple steps leading to computationally efficient algorithms. Starting from pre-processing to post-processing for off-line seizure detection of a single subject takes on average 2.6 s.
10. Overall, the results of the study suggest that AM-FBC and post-processing has an effect on seizure classification results.

6.4.6 Clinical significance

This study mainly focuses on FBC to reduce the feature distribution variation using AM-FBC, which has major impact on improving the classification results. Developed algorithm will help to monitor the epilepsy patients admitted to ICU. Further, it reduces the manual intervention of experts for analyzing long term EEG signals.

6.4.7 Limitations and future direction

For this study, we only used short duration EEG recordings from MUMC. From this it is unknown if there are drawbacks using these classifiers for long-term recordings as in continuous recording on the ICU. Further, outliers removal results in loss of diagnostic information even though good classification results were obtained. Classification of artifacts and epileptiform activities was not done in our study where that has a significant contribution to reduce false detection. As a future expansion, long-term EEG recording will be used to validate the proposed algorithm. Further, deep learning neural network will be explored for seizure detection.

6.5 Conclusion

In this paper, we propose a novel algorithm called AM-FBC to correct the inter-subject variability in feature distribution for patient-independent seizure detection algorithm in ICU EEG. The results suggest that the application of AM-FBC, outliers removal and post-processing revealed the AUC of 0.9663 and 0.9822 using SDI and MD features respectively. Further, we found that the lower the outlier removal factor improved the seizure detection performance at the cost of loss of feature samples. This study has proven that two novel features SDI and MD were capable of detecting seizures on new EEG dataset leading to algorithm generalization and robustness.

Acknowledgment

The authors are grateful to the Department of Clinical Neurophysiology, MUMC+, Maastricht, The Netherlands for allowing us to use EEG recordings for research purpose

Appendix: Patient details

TABLE 6.3: EEG database details used for the study

Subject #	No. channels has seizures	Age (years)	Gender	Record length (h)	Number of seizure epochs	Mean duration of seizure (s)	Min duration of seizure (s)	Max duration of seizure (s)
1	4	68	M	0.3694	38	57.92	21	102
2	19	27	M	0.3472	21	125.19	121	184
3	2	33	F	0.3361	4	79.75	29	111
4	2	61	F	0.5861	29	85.72	39	157
5	5	56	F	0.8028	21	35.42	29	42
6	1	47	F	0.4111	1	115	115	115
7	4	84	M	0.7389	8	79.62	53	116
8	19	75	F	0.7361	56	62.35	24	135
9	9	22	M	0.4556	9	311	262	484
10	4	57	F	1.1333	8	950	26	1949
11	2	65	F	0.4528	4	55	38	76
12	19	65	M	0.6583	26	147.57	43	171
13	3	46	F	0.3278	3	31	31	31
14	2	76	M	0.5000	38	33.26	17	43
15	19	40	F	0.4639	52	80.43	38	194
16	19	49	F	0.3861	44	55.51	34	124
17	2	50	F	0.3444	4	132	131	134
18	4	40	M	0.4000	4	87.50	32	106
19	19	49	F	0.8028	43	55.5	34	124
20	19	49	F	1.5750	43	55.5	34	124
21	3	66	M	0.5500	12	140.33	124	150
22	3	29	M	0.3333	30	20.1	20	36
23	3	62	M	0.4556	9	112.33	106	117
24	12	43	M	0.7306	228	19.89	25	32
25	11	40	F	0.6472	44	59	24	119
26	5	71	M	0.3667	10	169	169	169
27	14	84	F	0.4500	224	44.43	18	82
28	19	71	F	0.3611	76	74.25	15	125
29	2	89	F	0.5167	14	84.71	49	135
30	3	79	F	0.5361	3	90	90	90
31	5	29	F	0.3111	9	13.77	13	16
32	3	59	M	0.4472	3	79	79	79
33	19	83	M	0.5194	114	17	12	29
34	7	46	F	0.7111	39	111.6	26	142
35	3	23	F	0.3417	15	45.2	39	52
36	19	46	F	0.3556	19	79	79	79
37	5	50	M	0.4639	10	12	12	12
38	19	27	F	0.3389	38	12	12	12
39	4	68	M	0.3722	8	164.5	150	179
40	3	62	M	0.3344	12	91.5	79	119

CHAPTER 7

Cross-database evaluation of EEG based classification of epileptic seizures driven by adaptive median feature baseline correction

S Raghu, Natarajan Sriraam, Erik D Gommer, Danny M W Hilkmann, Yasin
Temel, Shyam Vasudeva Rao, Alangar Sathyaranjan Hegde, Pieter L Kubben
Clinical neurophysiology, 131:1567-1578

Year: 2020

<https://doi.org/10.1016/j.clinph.2020.03.033>

Abstract

Objective: In long-term EEG signals, automated classification of epileptic seizures is desirable in diagnosing epilepsy patients, as it otherwise depends on visual inspection. Existing studies have validated their algorithms using cross-validation on the same database and no attempts have been made to extend their work on other databases to test the generalization capability of the developed algorithms. In this study, we present the algorithm for cross-database evaluation for classification of epileptic seizures using five EEG databases collected from different centers. The cross-database framework helps when sufficient epileptic seizures EEG data are not available to build automated seizure detection model.

Methods: Two features, namely successive decomposition index and matrix determinant were extracted at a segmentation length of 4 s (50% overlap). Then, adaptive median feature baseline correction (AM-FBC) was applied to overcome the inter-patient and inter-database variation in the feature distribution. The classification was performed using a support vector machine classifier with leave-one-database-out cross-validation. Different classification scenarios were considered using AM-FBC, smoothing of the train and test data, and post-processing of the classifier output.

Results: Simulation results revealed the highest area under the curve-sensitivity-specificity of 1-1-1, 0.89-0.99-0.82, 0.99-0.73-1, 0.95-0.97-0.85, 0.99-0.99-0.92 using the Ramaiah Medical College and Hospitals, CHB-MIT, Temple University Hospital, Maastricht University Medical Centre, and University of Bonn databases respectively.

Conclusions: We observe that the AM-FBC plays a significant role in improving seizure detection results by overcoming inter-database variation of feature distribution.

Significance: To the best of the author's knowledge, this is the first study reporting on the cross-database evaluation of classification of epileptic seizures and proven to be better generalization capability when evaluated using five databases and can contribute to accurate and robust detection of epileptic seizures in real-time.

7.1 Introduction

Epilepsy is the fourth most common neurological disorder, which affects 65 million people of all ages around the world [1, 2, 79]. A sudden discharge of electrical activity in the brain causes temporary brain dysfunction, which is referred to as a seizure and recurrent seizures lead to epilepsy [2, 119]. The EEG signal contains clinically related information on neural, physiological and pathological conditions of brain disorders. For epilepsy patients, long-term monitoring of EEG signals is essential for pre-surgical evaluation, which is found to be a challenging task as it requires manual intervention [7, 33, 79, 80, 188]. Automated seizure detection is desirable in long-term EEG because that surrogate the manual intervention and saves experts time, improves pre-surgical evaluation and speeds up the diagnosis process. Existing studies have validated their algorithm on the same database but not on other databases to prove the generalization capability of the algorithm. Seizure detection algorithm would be more benefited when it is validated on multiple

EEG databases with a good number of seizures events. Therefore, to overcome this gap, we present an algorithm for cross-database evaluation for classification of epileptic seizures using five EEG databases. Such cross-database approach also helps when insufficient epileptic seizures EEG data is available to build a seizure detection model.

7.1.1 Related background

Several studies have been proposed in the past for classification of epileptic seizures [2, 21, 37, 80, 89, 178, 179]. The EEG signals from neonatal and adult patients were considered to develop a patient-independent seizure detection model which belongs to the same database. It was reported in [20, 178], feature normalization procedure based on the median decaying memory (MDM) method increases the seizure detection performance. Another feature baseline correction (FBC) method called average non-seizure feature values (ANSFV) uses the first 3 min of the seizure and artifact-free EEG to correct the feature baseline [84, 179]. A patient-specific seizure onset detection model was proposed using wavelet decomposition based morphology and spatial features using Children's Hospital Boston-Massachusetts Institute of Technology (CHB-MIT) database [88].

Optimized deep neural network architecture was applied on EEG signals to perform binary, three-class, and five class classification of epileptic seizures [189]. Frequency–moment signatures based showed better seizure detection results using 12 patients EEG [190]. Spectral and temporal features extracted in five frequency bands classified using support vector machines (SVM) classifier [191]. Zheng et al. [192] proposed seizure prediction model using phase

synchronization information of intrinsic mode functions extracted by bivariate empirical mode decomposition. A prospective multi-center study was performed in three epilepsy monitoring units including 205 patients [193]. Further, the study was extended on retrospective EEG data of 310 patients and the publicly available CHB–MIT dataset. A multimodal automatic seizure detection algorithm showed the high sensitivity with full and reduced electrode montages [194]. Integrated power in the frequency band 2.5–12 Hz calculated from the short-time Fourier transform (STFT) approach using adaptive thresholding was applied on 194 temporal-lobe epilepsy patients [188].

Wavelet packet transforms (WPT) based combined seizure index (CSI) [102] and harmonic WPT [122] features based models were proposed for seizure classification. Discrete wavelet transforms (DWT) based statistical features model was introduced using the classifier using Bern-Barcelona dataset and the University of Bonn (UBonn) databases [42]. Rational STFT (DSTFT) based approach yielded good classification results using multi-layer perceptron (MLP) classifier. Matrix determinant feature using the SVM classifier was proposed using the Ramaiah Medical College and Hospitals (RMCH) and UBonn databases [89]. A threshold-based seizure detection method was proposed using the minimum variance modified fuzzy entropy [19]. Recently, deep learning algorithms have been used for classification of normal, pre-ictal, and seizure activities [39, 57, 164]. Further, promising results were obtained using entropies like approximate entropy [27, 47], weighted permutation entropy [98], log energy and norm entropy [21], sigmoid entropy [83], Renyi, spectral, Shannon and wavelet entropies [36, 66, 81, 110] for seizure detection. Acharya et al. [22] have reviewed articles related to computer-aided

diagnostic systems to automatically classify normal and abnormal activities using less number of features. A review on wavelet-based EEG processing for automated detection of epileptic seizures was reported in [130]. A systematic review on autonomic symptoms and signs during epileptic seizures which includes cardiovascular changes, respiratory manifestations, gastrointestinal symptoms, cutaneous manifestations, sexual and genital manifestations, and urinary symptoms was performed [195].

The post-processing of the classifier output has gained attention using a Kalman filter [179], a central linear moving average filter (MAF) [180], and MAX operator with a MAF [181] for seizure detection with improved performance. It was evident from the literature that the SVM classifier has been promising classification tool for epileptic seizure detection [20, 25, 65, 84, 88, 163, 179, 180, 181].

The proposed study used two features called successive decomposition index (SDI) and matrix determinant (MD), which were proposed by our group in [89, 182]. The SDI was evaluated on the RMCH, CHB-MIT and the Temple University Hospitals (TUH) databases in [182] and MD was tested on UBonn and RMCH databases in [89]. Further, adaptive median feature baseline correction (AM-FBC) was proposed in [196] to correct inter-subject variation in feature distribution for intensive care unit (ICU) EEG recordings that were collected from Maastricht University Medical Centre (MUMC). In the same study, post-processing of classifier output proven to be ideal to improve the classification results. Above-mentioned methods were used in the present study to propose a cross-database framework for seizure detection.

Even though multiple databases were used in [20, 42, 89, 122, 193] for

epileptic seizure classification, the cross-database framework was missing for the generalization ability of the algorithm. Therefore, the present study proposes cross-database evaluation using five EEG databases for classification of epileptic seizures driven by AM-FBC, smoothing of the train and test data and post-processing of the SVM classifier output.

7.1.2 Importance and contributions of proposed study

Importance of cross-database validation are: (1) Cross-database algorithm can be used when sufficient epileptic seizures EEG data is not available to build a seizure detection model on new EEG recordings, (2) Cross-database evaluation confirms the generalization capability of the developed algorithm.

The followings are the contributions of our study: (1) AM-FBC was used to reduce the inter-subject and inter-database variation in the feature distribution, (2) Studied the effect of smoothing of the train and test data, (3) Post-processing of the SVM classifier output, and (4) Most importantly, cross-database evaluation was proposed using five EEG databases.

7.2 Materials and methods

7.2.1 Proposed method

Fig. 7.1 depicts the flow of the cross-database evaluation for classification of the epileptic seizure using five ($N = 5$) databases. Initially, the EEG recordings were pre-processed and two features (SDI and MD) were extracted. First, FBC was applied to the subjects level and then to the database level. Smoothing of the train and test data was applied before the SVM classifier was

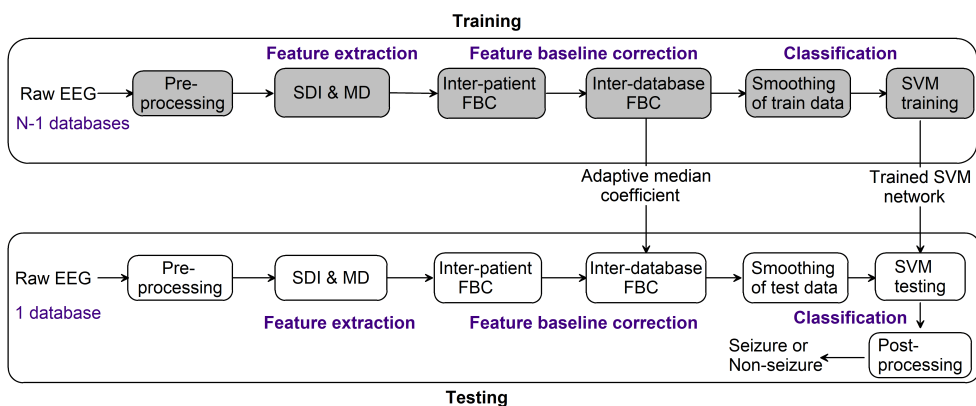


FIGURE 7.1: The flow of the cross-database framework evaluation for seizure detection using five ($N = 5$) databases. The SVM classifier was trained with $(N - 1)$ databases and tested on the left out database. First, the feature baseline correction (FBC) was applied separately on each database to correct the inter-patient variation. The adaptive median coefficient estimated from trained inter-database FBC was used to correct the feature baseline of the test database.

trained with leave-one-database-out cross-validation approach. The trained SVM classifier was tested on the left out database and post-processing was applied using a MAF. The same procedure was repeated five times until all the databases were used both training ($(N - 1)$ times) and testing (1 time).

7.2.2 Clinical EEG recordings

The cross-database evaluation was performed using five databases obtained from the RMCH, CHB-MIT, TUH, MUMC, and UBonn EEG recordings.

7.2.2.1 RMCH

The first EEG database used for the cross-database framework was from the RMCH, Bengaluru, India after ethical approval was obtained from the RMCH ethics committee to use these EEG recordings for research purpose. The

RMCH database was recorded using the International 10-20 system configuration at a sampling rate of 128 Hz using Galileo Suite NB Neuro digital EEG system. This unipolar EEG was recorded using the following 19 scalp electrodes: Fp1, Fp2, F7, F3, Fz, F4, F8, T3, C3, Cz, C4, T4, T5, P3, Pz, P4, T6, O1, and O2. Reference electrode placed at the ear was used as reference for unipolar EEG. Only EEG recordings from epileptic patients were used for this study, which consists of 115 subjects (67 male and 48 female) ranging between 2.5 to 75 years. Two experts at the RMCH visually marked EEG as non-seizure and seizure segments. The RMCH database consists of 162 seizures (approximately 4.36 hours of seizure data) from 115 subjects with the recording duration of each patient varied from 20 minutes to 3 hours.

7.2.2.2 CHB-MIT

The second database used for the cross-database framework was obtained from the CHB-MIT¹ EEG database which is available in Physionet repository [88, 100]. The CHB-MIT database is one of the largest open source EEG databases with 844 hours of data from the 23 patients recorded at a sampling rate of 256 Hz. The CHB-MIT database was recorded using the International 10-20 system bipolar montage electrode placement with the following 23 channels: FP1-F7, F7-T7, T7-P7, P7-O1, FP1-F3, F3-C3, C3-P3, P3-O1, FZ-CZ, CZ-PZ, FP2-F4, F4-C4, C4-P4, P4-O2, FP2-F8, F8-T8, T8-P8, P8-O2, P7-T7, T7-FT9, FT9-FT10, FT10-T8, and T8-P8.

¹<http://www.physionet.org/pn6/chbmit>

7.2.2.3 TUH

The third database was obtained from the TUH² EEG resource [113, 114], which includes EEG from focal non-specific, generalized non-specific, simple partial, complex partial, absence, tonic, tonic-clonic, and myoclonic seizure. This unipolar EEG signal was recorded using the International 10-20 system electrode configuration at a sampling rate of 250 Hz. For the study, 222 seizures from 316 subjects were considered from massive EEG recordings. The electrode placement in the TUH database was the same as in the RMCH database.

7.2.2.4 MUMC

The fourth database was obtained from the Department of Clinical Neurophysiology, MUMC, Maastricht, The Netherlands. The MUMC EEG database was used for research purpose after approved by the hospital ethics committee. This database consists of 40 routine EEG registrations recorded at the intensive care unit. The MUMC scalp EEG recordings were recorded using BrainLab EEG recording system at a sampling rate of 250 Hz using a common average montage using 19 unipolar electrodes. This database consists of 21 hours of EEG including 1273 seizure epochs with a minimum duration of 12 s and a maximum duration of 1949 s. Technician at the MUMC hospital annotated the seizure and non-seizure epochs and checked by a clinical neurophysiologist. The electrode placement in the MUMC database was the same as in the RMCH database.

²https://www.isip.piconepress.com/projects/tuh_eeg/index.shtml

7.2.2.5 UBonn

The fifth database used for the cross-database framework was a publicly available database from the UBonn³[33]. The UBonn EEG was recorded from five different subjects under-going pre-surgical evaluations. UBonn EEG recordings were divided into five subsets (set A, set B, set C, set D, and set E), each subset consists of 100 single-channel EEG segments of 23.6 s duration recorded at a sampling rate of 173.61 Hz. Each subset EEG in UBonn belongs to normal with eyes open (set A), normal with eyes closed (set B), pre-ictal (set C), post-ictal (set D) and ictal state (set E) conditions. Sets A and B contain recordings obtained through external surface electrodes and sets C–E were recorded using intracranial electrodes. In our study, set A to set D considered as non-seizure and set E considered as seizure activity [48, 80].

Table 7.1 provide detailed information on all the five databases used for cross-database evaluation. All the five EEG databases used in the study are belongs to retrospective data.

7.2.3 Pre-processing

Among the five databases, the three open source databases (CHB-MIT, TUH, and UBonn) were already pre-processed for artifacts. Initially, a 50 Hz IIR notch filter was applied to eliminate the power line noise and a bandpass filter was applied with a lower and higher cut-off frequency of 0.5 and 32 Hz respectively. In order to eliminate the artifacts like eye blinks, muscle artifacts, and electrode movements, independent component analysis (ICA) was applied

³http://epileptologie-bonn.de/cms/front_content.php?idcat=193&lang=3&changelang=3

TABLE 7.1: Details of different EEG databases used for cross-database evaluation

	RMCH	CHB-MIT	TUH	MUMC	UBonn
Open source database	No	Yes	Yes	No	Yes
Type of EEG	Scalp	Scalp	Scalp	Scalp	Scalp and Intracranial
Type of recording	Unipolar	Bipolar	Unipolar	Unipolar	Unipolar
Sampling frequency (Hz)	128	256	250	250	173.73
Electrode position	10-20	10-20	10-20	10-20	10-20
Number of subjects	115	23	316	40	5
Age range (years)	3-60	3-22	2-90	22-89	-
Total duration (hours)	58	884	408	21	3.24
Number of channels	19	23	19	19	1**
Number of seizures	162	182	222	1273*	100***

* 1273 seizure events

** Multichannel data was converted to a single channel

*** 100 seizures file each of 23.36 s duration

to the filtered EEG (only on RMCH and MUMC databases) [72, 186] using the ICA toolbox available in the EEGLab [116].

7.2.4 Feature extraction

In this study, we have used two features, namely SDI and MD that were recently proposed by our group in [89, 182]. These were validated using RMCH, CHB-MIT, TUH, and MUMC databases in our previous studies [89, 182, 196] and were extracted at a segmentation length of 4 s with 50% overlap in this study.

The procedure to estimate SDI and MD is given in **Appendix A** and **Appendix B** respectively.

7.2.5 Adaptive median feature baseline correction

Considering the fact that features have variations in the distribution in patient level and database level, FBC was applied in two stages. First, AM-FBC was

applied to update the feature distribution among the patients (scenario was dominant in MUMC database). Next, feature baseline was applied on five databases to correct the inter-database feature distribution variation. The AM-FBC was successfully implemented to update the feature baseline for inter-patient variation in our previous study [196] and better classification results were obtained.

7.2.5.1 Inter-patient FBC

The procedure to correct the feature baseline among patients is given here.

1. Let a typical feature of all the subjects be represented as $f(sub_1, sub_2, \dots, sub_n)$.
2. Calculate the $f(Median_{seizure})$ and $f(Median_{non-seizure})$ of all the training subjects using seizure and non-seizure feature respectively. The length of the $f(Median_{seizure})$ and $f(Median_{non-seizure})$ equals the number of subjects.
3. Estimate global median ($f(Median_{global})$) using median values of seizure and non-seizure.

$$f(Median_{global}) = Median\{f(Median_{seizure}) f(Median_{non-seizure})\} \quad (7.1)$$

4. Now estimate the median of a single subject $f(Median_{sub\ i})$, where $i = 1, 2, 3, \dots, n$ subjects.

5. Now calculate the adaptive median coefficient (λ) using $f(\text{Median}_{global})$ and $f(\text{Median}_{sub i})$.

$$\lambda = f(\text{Median}_{global}) - f(\text{Median}_{sub i}) \quad (7.2)$$

6. Now correct the feature baseline of $sub i$ using λ as follows:

$$f_{new_i} = \lambda + f_{sub i} \quad (7.3)$$

7. Repeat the step 4 to step 6 for all the subjects (n) using the $f(\text{Median}_{global})$.

The above procedure was applied to both SDI and MD features separately.

7.2.5.2 Inter-database FBC

The procedure to correct the feature baseline among databases is given in **Appendix C**.

7.2.6 Smoothing train and test data

Smoothing of the train and test data for classification purpose reported improved results in [20, 84, 179]. Therefore, in this study, we have applied a 5-tap MAF to the train and test data which reduces the random noise and improves the classification results [181].

7.2.7 Classification

The cross-database framework was evaluated using the SVM classifier due to its better performance reported in previous studies [25, 42, 47, 65, 89, 128,

135]. During the preliminary study, the radial basis kernel function showed better performance in terms of classification results. The proposed method was evaluated using leave-one-database-out cross-validation in which, the SVM classifier was trained using four databases and tested on the left out database. The procedure was repeated five times until all the databases were used for the testing phase. The SVM classifier was tuned as follows: Kernel function = radial basis function, Kernel Scale = 1 and Box Constraint = 1.

The experiment was performed in MATLAB 2018b using 8GB RAM, CPU 2 GHz with an Intel i3 processor.

The cross-database framework was assessed using performance parameters, namely sensitivity, specificity, and the area under the curve (AUC).

$$\text{Sensitivity } (S^+) = \frac{TP}{TP + FN} \quad (7.4)$$

$$\text{Specificity } (S^-) = \frac{TN}{TN + FP} \quad (7.5)$$

where, TP is seizure detected as seizure, TN is non-seizure detected as non-seizure, FN is seizure detected as non-seizure, and FP is non-seizure detected as seizure. The area under the receiver operating characteristic (ROC) curve was estimated using sensitivity and 1-specificity.

7.2.8 Post-processing

The post-processing of the classifier output has proven to be a better choice to reduce false detections and improve the classification results [180, 181, 196]. In our study, different tap lengths (2 to 10) of MAF were applied to the SVM

TABLE 7.2: Different classification scenarios used to evaluate cross-database framework

Classification scenario	FBC	Smoothing of train data	Smoothing of test data
1	No	No	No
2	No	Yes	No
3	No	Yes	Yes
4	Yes	No	No
5	Yes	Yes	No
6	Yes	No	Yes
7	Yes	Yes	Yes

Note: All the classification scenarios were evaluated with and without post-processing

classifier output to perform the post-processing as reported in [180, 181, 196]. The post-processing output $[0, 1]$ was assigned depending on a predefined threshold of 0.5 to classify as a seizure and non-seizure. The given EEG segment was classified as a seizure and non-seizure if the value was greater than or equal to and less than 0.5 respectively.

7.2.9 Classification scenarios

The proposed cross-database framework was evaluated using different classification scenarios (CS) in terms of AM-FBC, smoothing of the train and test data, and post-processing of the SVM classifier output. Table 7.2 depicts the 7 different CS used to evaluate the cross-database framework.

7.3 Results

7.3.1 Analysis of AM-FBC

After pre-processing, both SDI and MD features were extracted and AM-FBC was applied individually to correct the inter-patient variation in the distribution of the feature. Most inter-patient variation was seen in the MUMC database. Figs. 7.2a & b shows the SDI and MD feature distribution for all the five databases. We observe more variation in features distribution between databases. In the RMCH database, SDI feature values for seizure are below the SDI values of non-seizure from the other four databases. This is also the case for the MD feature values in the RMCH and MUMC databases which is referred to as inter-database feature distribution variation. Further, features from the MUMC database had more outliers due to noisy EEG recordings. In the next step, AM-FBC was applied to correct the feature baseline in inter-database. The inter-database AM-FBC results are depicted in Figs. 7.2c & d for SDI and MD features respectively. The Figs. 7.2c & d show that the features baseline has been brought to a uniform level after applying AM-FBC. A Wilcoxon rank sum test showed significance difference ($p < 0.05$) for each database between seizure and non-seizures activities. The median values of both the features before and after AM-FBC are depicted in Fig. 7.3. The high variation among the databases is reflected for both SDI and MD features. The median values after AM-FBC show less variation between the databases.

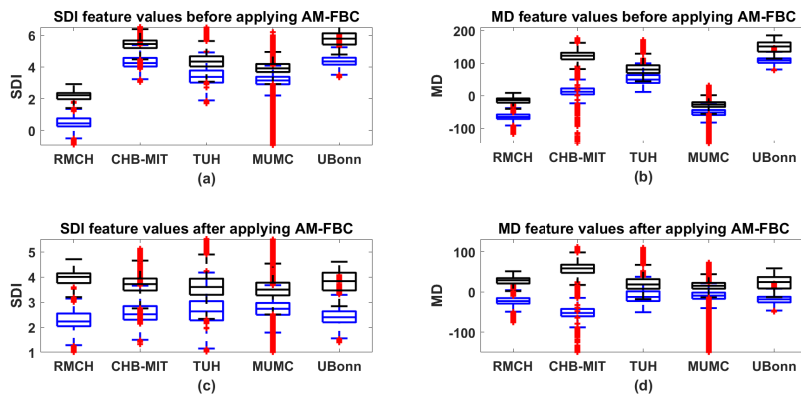


FIGURE 7.2: The boxplot of SDI and MD features for each database before and after applying AM-FBC. **(a)** SDI feature before applying AM-FBC. **(b)** MD feature before applying AM-FBC. **(c)** SDI feature after applying AM-FBC. **(d)** MD feature after applying AM-FBC. The boxplot with black boxes and blue boxes indicates seizure and non-seizure activities respectively. The red + indicates the outliers which are beyond the whiskers.

7.3.2 Cross-database results

Fig. 7.4 shows the ROC curve obtained from all the five databases under different CS. The ROC was grouped database wise, with and without post-processing of the classifier output. The area under the ROC curve obtained for the proposed study is reported in Fig. 7.5. The ROC curve obtained for the RMCH database was below the threshold line due to the effect of inter-database feature distribution variation. Overall, the best ROC curve was achieved when AM-FBC and smoothing of the test data were applied.

Fig. 7.5 shows the S^+ , S^- , and AUC obtained for cross-database evaluation. First, we discuss CS1, where AM-FBC, smoothing of train and test data and post-processing was not applied. The AUC of 0.08 ($S^+=0$, $S^-=0.90$), 0.99 ($S^+=0.99$, $S^-=0.99$), 0.97 ($S^+=0.98$, $S^-=0.94$), 0.83 ($S^+=0.41$, $S^-=0.98$),

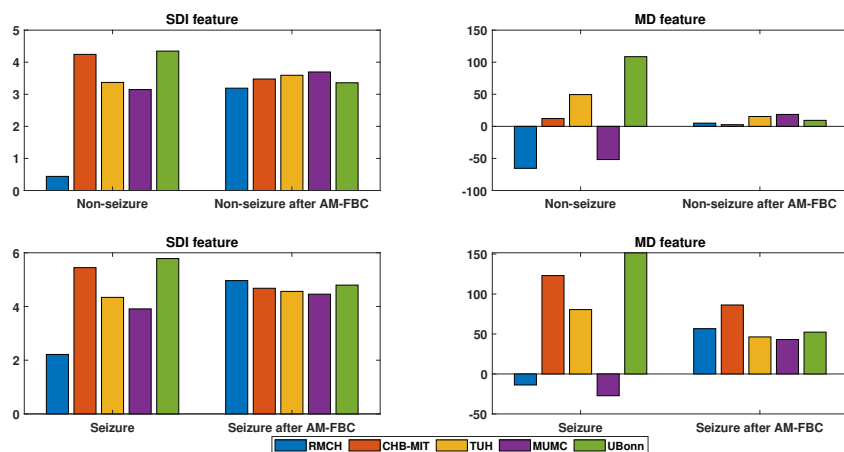
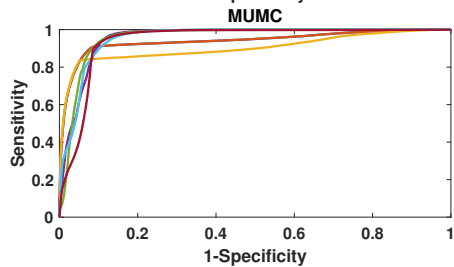
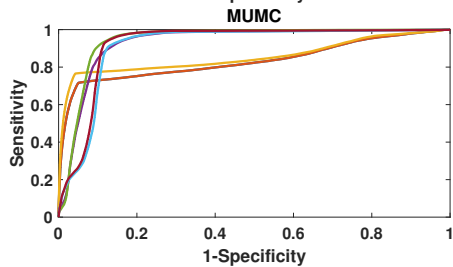
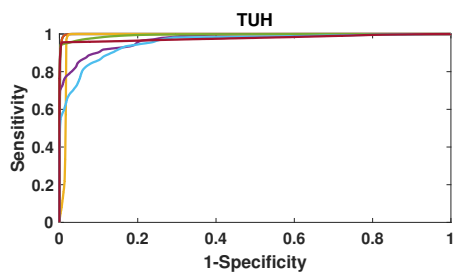
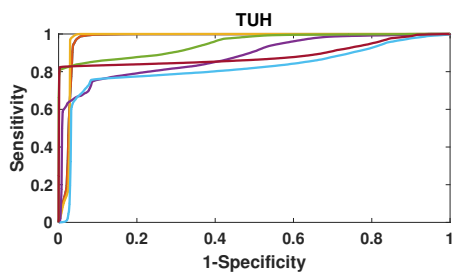
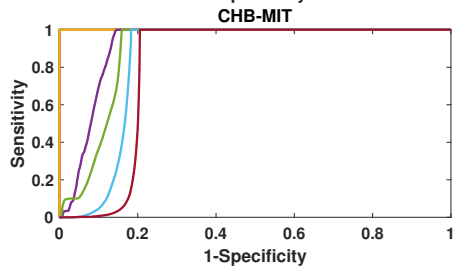
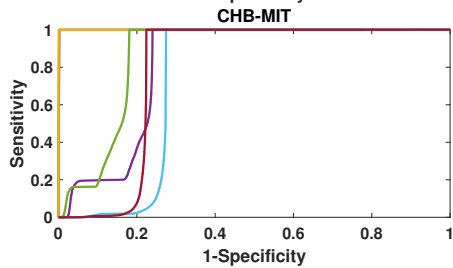
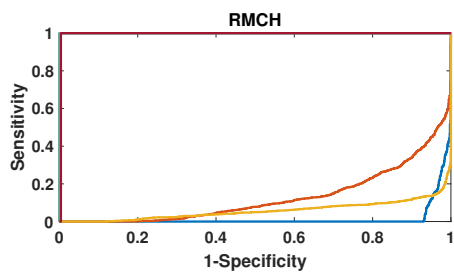
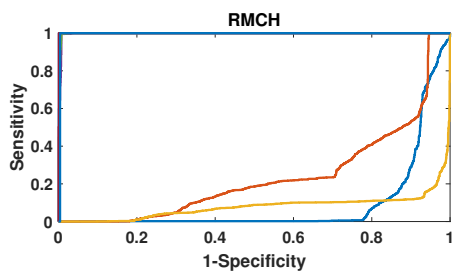


FIGURE 7.3: The median values of SDI and MD feature for each database before and after AM-FBC. Seizure and non-seizure features are plotted individually and grouped database.

and 0.87 ($S^+=1$, $S^-=0$) was obtained for the RMCH, CHB-MIT, TUH, MUMC, and UBonn databases respectively without post-processing. The AUC performance of 0.01, 1, 0.99, 0.93, and 0.91 was obtained using the RMCH, CHB-MIT, TUH, MUMC, and UBonn databases respectively when post-processing was applied. Further, similar results were seen in case of CS2 and CS3 for all the databases leading to the worse performance for the RMCH database. The S^+ closes to zero was obtained for the RMCH database due to reason that the seizure EEG feature values of RMCH database are below the non-seizure EEG feature values in the training databases (refer to Figs. 7.2a & b). This was the clear indication of effect of inter-database feature distribution variation.

Now, we have applied AM-FBC to correct the feature distribution variation in inter-database. The effect of AM-FBC is already shown in Figs. 7.2 & 7.3. The AUC of 0.99 ($S^+=0.98$, $S^-=0.98$), 0.81 ($S^+=0.99$, $S^-=0.75$), 0.88 ($S^+=0.65$, $S^-=0.96$), 0.93 ($S^+=0.92$, $S^-=0.84$), 0.97 ($S^+=0.98$, $S^-=0.90$)



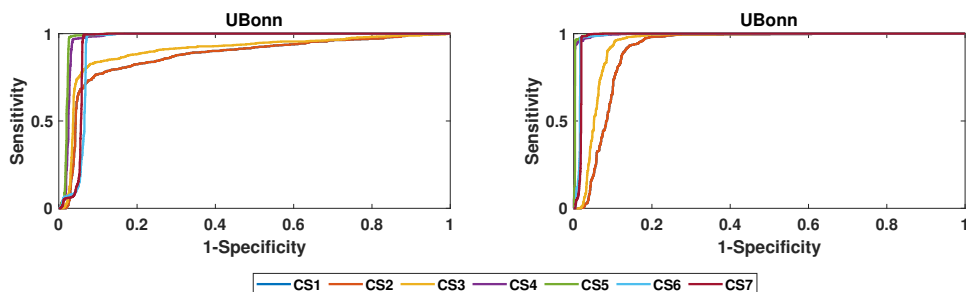


FIGURE 7.4: The ROC curve for cross-database evaluation under different CS for (a) RMCH, (b) CHB-MIT, (c) TUH, (d) MUMC, and (e) UBonn databases. **Left column:** ROC curve without post-processing, **Right column:** ROC curve with post-processing. In legend, CS indicates classification scenario (refer to Table 7.2 for details).

was achieved for the RMCH, CHB-MIT, TUH, MUMC, and UBonn databases respectively in CS4 without post-processing. Similarly, the AUC was increased to 1, 0.91, 0.91, 0.95, 0.99 for the RMCH, CHB-MIT, TUH, MUMC, and UBonn databases respectively when post-processing was applied. The influence of AM-FBC improved the S^+ and S^- for the RMCH, MUMC and UBonn databases respectively, which was worse in CS1 to CS3.

In CS4 to CS7, we have studied the effect of smoothing of the train and test data for the SVM classifier. The AUC of 1, 0.84, 0.95, 0.95, 0.98 was obtained for the RMCH, CHB-MIT, TUH, MUMC, and UBonn databases respectively when post-processing was applied in CS5. Overall, the highest classification results were obtained in CS6 when AM-FBC applied along with smoothing of test data. The highest AUC of 1 ($S^+=1$, $S^-=1$), 0.89 ($S^+=0.99$, $S^-=0.82$), 0.99 ($S^+=0.73$, $S^-=1$), 0.95 ($S^+=0.97$, $S^-=0.85$), 0.99 ($S^+=0.99$, $S^-=0.92$) was achieved for the RMCH, CHB-MIT, TUH, MUMC, and UBonn databases respectively in CS6 with post-processing. Finally, we have taken an average

of all the databases classification results to assess the performance of different CS (refer to Fig. 7.5f). The results showed that the AUC of 0.77, 0.79, 0.77, 0.93, 0.94, 0.96, and 0.94 for CS1 to CS7 respectively with post-processing which is being high for CS6.

The MAF length was varied between 2 to 10 to identify the optimal MAF length to reduce the false detections. It was observed that false detection rate decreases as the MAF length increases. For the optimal CS6 at the highest sensitivity, the average false detection rate (per hour) of 0.15, 2.5, 1, 1.7, and 1.1 was achieved for RMCH, CHB-MIT, TUH, MUMC, and UBonn databases respectively for MAF length of 10.

Overall, classification results showed that AM-FBC is essential to achieve the generalized results for all the databases. Further, the smoothing of the train and test data improved the classification results. The classification results suggest that the proposed cross-database approach has better generalization capability when evaluating using five databases.

7.4 Discussion

This study presents a cross-database evaluation for classification of epileptic seizures using SDI and MD features, AM-FBC, smoothing, and post-processing. The results showed that the highest AUC of 1, 0.89, 0.99, 0.95, and 0.99 using the RMCH, CHB-MIT, TUH, MUMC, and UBonn databases respectively.

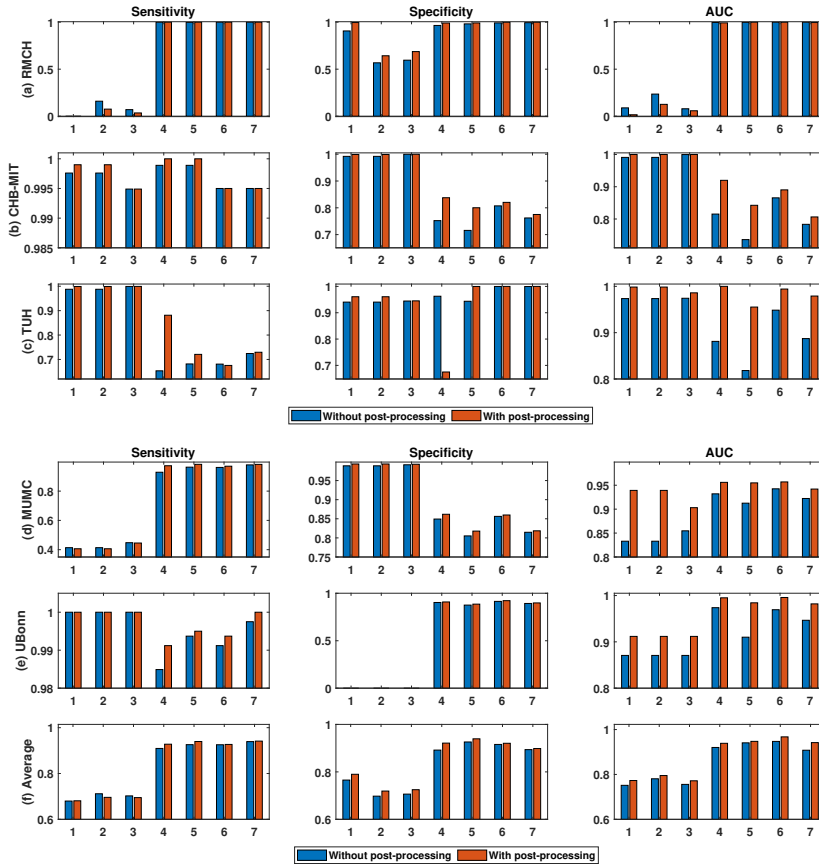


FIGURE 7.5: Cross-database evaluation results using different CS for (a) RMCH, (b) CHB-MIT, (c) TUH, (d) MUMC, (e) UBonn databases, (f) Average of all the five databases results. **First column: S^+ , Second column: S^- , Third column: AUC.** The x-tick labels indicate different classification scenarios.

7.4.1 Influence of FBC

The classification results obtained for CS1 to CS3 were not consistent for all the five databases. The S^+ obtained for the RMCH and MUMC were close to 0 and 0.44 respectively due to inter-database feature distribution variation. It can be clearly understandable from Figs. 7.2a & b that was due to the fact that the seizure EEG feature values of the RMCH and MUMC databases were

below the non-seizure EEG feature values of other databases. Similarly, the S^- was 0 for the UBonn without applying AM-FBC for CS1 to CS3 because non-seizure EEG feature values of the UBonn database were above the seizure EEG feature values of other four databases. Even though good performance was achieved for the CHB-MIT and TUH database in CS1 to CS3 (without FBC), the worse performance in terms of S^+ and S^- cannot be acceptable in real-time scenario. The influence of AM-FBC (refer to Figs. 7.2c & d) improved the classification results in case of CS4 to CS7 (refer to Fig. 7.5) proving that cross-database evaluation requires FBC.

The influence of AM-FBC on cross-database evaluation is depicted in Fig. 7.6 when tested on MUMC database and trained using the left out databases with CS6. Figs. 7.6b & c shows the SDI and MD features respectively for the EEG shown in Fig. 7.6a. As one can observe that the misclassification in Fig. 7.6e are high as compared to the ground truth results in Fig. 7.6d when AM-FBC was not applied. As a result of AM-FBC and smoothing (refer to CS6), proper classification was seen (refer to Fig. 7.6f) with few false alarms and it was corrected using post-processing (refer to Fig. 7.6h) that the output was closely matched with ground truth labels (refer to Fig. 7.6d).

7.4.2 Influence of MAF on false detection

In our study, the MAF length was varied between 2 to 10 to identify the optimal MAF length which influences on reducing the false detections. Fig. 7.7 shows the effect of MAF length on false detections for all the five databases. As it can be seen from Fig. 7.7 that the false detection rate decreases as the MAF length increases. The best results were achieved when MAF length was

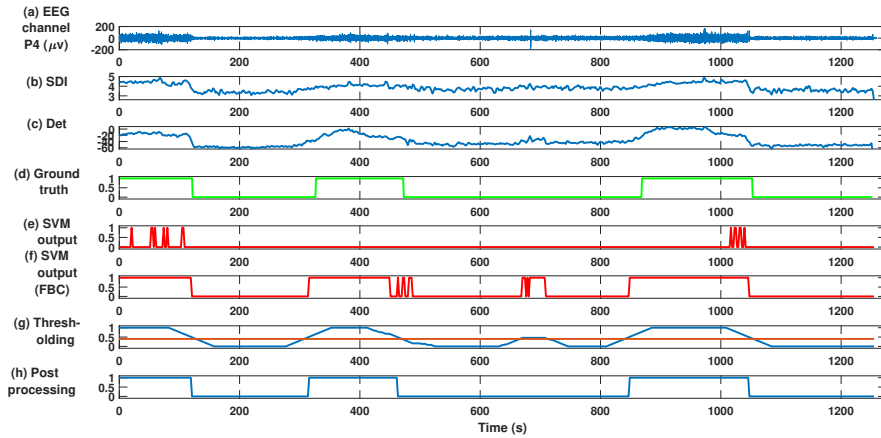


FIGURE 7.6: Effect of post-processing for seizure detection. **(a)** EEG signal belongs to channel P4. **(b) & (c)** Corresponding SDI and MD values of channel P4 respectively. **(d)** Ground truth, where 0 and 1 indicate non-seizure and seizure respectively. **(e)** SVM classifier output (without AM-FBC). **(f)** SVM classifier output after applying AM-FBC. **(g)** The smoothed output after a 5-tap MAF was applied on SVM classifier output (after AM-FBC). The threshold (red line) was set to 0.5 to make a binary decision. **(h)** Binary decision after applying thresholding to smoothed output.

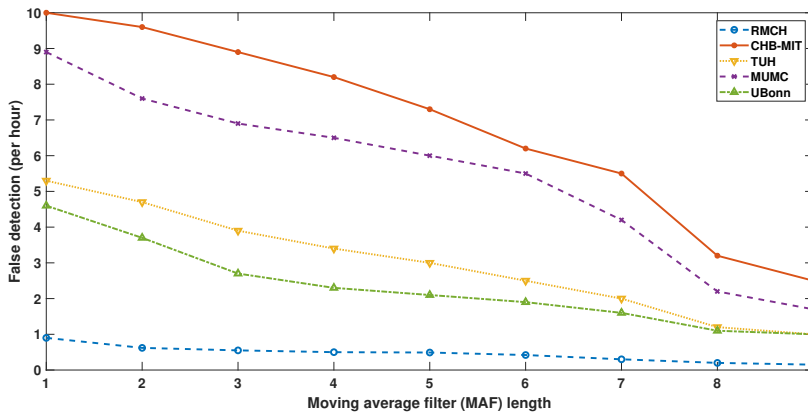


FIGURE 7.7: Effect of MAF length on false detections in post processing.

10 for CS6. The MAF length beyond 10 was not tested as it results in higher delay in detecting seizure epochs.

7.4.3 Comparison with other studies

It is worth noting that the exact comparison cannot be made as no studies have reported cross-database evaluation for classification of epileptic seizures. The results presented in Table 7.3 shows the comparison results of previously proposed methods with the proposed cross-database evaluation results and comparison was performed database wise. WPT based CSI showed the highest sensitivity of 90.5% from 14 patients [102]. Statistical features extracted from DWT coefficients have achieved an accuracy of 83.07% and 88.00% using the Bern-Barcelona dataset and UBonn databases respectively using the SVM classifier [42]. The fractal dimension and harmonic WPT feature-based model using the RVM classifier showed a sensitivity of 96.0% and 99.8% using the CHB-MIT and UBonn EEG databases respectively [122]. DSTFT based approach yielded a classification accuracy of 98.1% using MLP classifier.

The MDM FBC method showed an AUC of 0.93 using the CHB-MIT database [103] and 0.96 using the MUMC database [20]. The AUC of 0.92, 0.93, and 0.93 was achieved for neonatal, adult and combined dataset respectively [84]. Further, the ANFSV FBC method was implemented on 103 features using the MUMC database which showed the AUC of 0.92 [179]. Similarly, our previous study on the MUMC database using SDI feature showed the highest AUC of 0.98 with the help of the AM-FBC method [196]. However, in our present cross-database study using MUMC database, the highest AUC of 0.95 only achieved due to the different training data. A Kalman filter was applied to the SVM classifier output for post-processing, which improved

the classification results in [20, 84, 179]. In [180, 181, 196], improved performance was observed when a MAF was used for post-processing. In our previous study using the RMCH database [197], the highest accuracy of 98.44% was obtained using maximal overlap discrete wavelet transform (MODWT) based sigmoid entropy, but present cross-database approach showed even better performance on the same database due to the larger training dataset. The SDI and MD features have shown better performance using the RMCH, CHB-MIT, MUMC databases with leave-one-subject-out cross-validation when the algorithm was trained and tested on same database [89, 182, 196]. One can observe that the larger feature set have been used for classification of epileptic seizures in [20, 28, 82, 84, 88, 179, 180, 181], which could result in computational complexity.

7.4.4 Clinical significance

One of the challenges in designing the automated seizure detection algorithms is lack of annotated seizures EEG data. The algorithm proposed in our study combines EEG from five different databases and compensates for the feature distribution variation. Our results demonstrate that the new EEG recordings from same and/or different database can be validated without spending much time on designing a new algorithm. Hence, it is cost effective in terms of designing the new algorithm and speed up the treatment procedure.

7.4.5 Significant findings of the study

The significant findings and contributions of cross-database evaluation are summarized as follows:

TABLE 7.3: Comparison between the state of the art seizure detection algorithms and cross-database approach

EEG database	Number of subjects	Duration of EEG (h)	Number of seizures	Author	Feature extraction	FBC	Classifier	Post-processing	Results
CHB-MIT	23	884	182	[122]	Harmonic wavelet packet transform fractal dimension, spatial and temporal features	No	RVM	No	$S^+ = 96.0\%$
				[103]	Line length	MDM	Threshold	No	AUC=0.93 $S^+ = 98.27\%$ A= 98.31%
				[126]	Fuzzy entropy	No	SVM	No	$S^+ = 94.24\%$
TUH	316	408	222	[88]	Wavelet based features	No	SVM	No	$S^+ = 97.28\%$
				[182]	SDI	No	SVM	No	$S^+ = 94.0\%$
				[19]	MVMFZ	No	Threshold	No	$S^+ = 95.80\%$
UBonn	5	3.24	100	[80]	Entropies	No	Fuzzy classifier	No	A=99.00%
				[82]	Optimal orthogonal wavelet based features	No	LS-SVM	No	A=100%
				[198]	Weighted complex networks	No	SVM	No	A=100%
RMCH	115	58	162	[21]	Wavelet packet transform based log energy entropy	No	REN	No	A=99.70%
				[118]	DSTFT	No	MLP	No	A=99.80%
				[89]	MD	No	SVM	No	A=97.56%
MUMC	39 term and pre-term new born	25	360	[179]	103 features	ANSFV	SVM	Kalman filter	AUC=0.90
				[20]	103 features	MDM	SVM	Kalman filter	AUC=0.96
				[84]	103 features	ANSFV	SVM	Kalman filter	AUC=0.93
MUMC	39 neonatal	613	34898 ¹	[196]	SDI and MD	AM-FBC	SVM	MAF	AUC=0.96 (SDI) AUC=0.98 (MD)
Neonatal Intensive Care Unit (NICU) of Cork University Hospital, Cork, Ireland	17 new borns	267	705	[181]	55 features	No	SVM	Central linear MAF	$S^+ = 89\%$
				[180]	55 features	No	SVM	MAF	AUC=0.71
National Society of Epilepsy (UK), Katholieke Universiteit Leuven (Belgium), and Freiburg University Hospital (Germany).	24 adults	172	47	[178]	DWT based Relative power	Normalization	Threshold	Bitwise logical OR operator	AUC = 0.83
Proposed									
RMCH	115	58	162						AUC=1
CHB-MIT	23	884	182						AUC=0.89
TUH	316	408	222		SDI and MD	AM-FBC	SVM	MAF	AUC=0.99
MUMC	40 ICU patients	21	1273 ³						AUC=0.95
UBonn	5	3.24	100 ⁴						AUC=0.99

¹ 34898 Feature vectors derived from 10s epoch, ²1373 seizure epochs of 10 s duration, ³1273 seizure events, ⁴100 seizures file each of 23.36 s duration, A= Accuracy

1. This is the first study reporting cross-database evaluation for automated classification of epileptic seizures.
2. The S^+ and S^- of 0 was obtained for the RMCH and UBonn databases respectively without the application of AM-FBC.

3. AM-FBC on inter-patient and inter-database level proved its need to perform the cross-database evaluation.
4. AM-FBC along with smoothing of the test data outperformed other CS on all the five databases.

7.4.6 Future direction

As a future study, a deep learning technique will be implemented on these five databases to perform the cross-database evaluation. The classification results could be further improved by adding a few significant features and optimizing the algorithm. The proposed study will be validated on new EEG databases to improve the algorithm performance. Mixing the whole data could be an interesting future task to improve the generalization of the algorithm. Further, a mobile-based seizure alert system will be introduced using the proposed cross-database evaluation algorithm.

7.5 Conclusion

To the best of authors knowledge, we are the first to present a cross-database evaluation for automated classification of epileptic seizures. Inter-subject and inter-database variation in the feature distribution was corrected using AM-FBC. With the application of AM-FBC, smoothing, and post-processing, the highest AUC of 1, 0.89, 0.99, 0.95, and 0.99 was achieved using the RMCH, CHB-MIT, TUH, MUMC, and UBonn databases respectively. AM-FBC along with smoothing of the test data outperformed other CS. It can be concluded that the cross-database approach has better generalization capability when

evaluated using five databases. Finally, cross-database framework helps when sufficient epileptic seizures EEG data is not available to build a seizure detection model.

Acknowledgment

The authors are grateful to the Department of Clinical Neurophysiology, MUMC+, Maastricht, The Netherlands, and RMCH, Bengaluru, India for providing EEG recordings for research purpose. Authors also grateful to Dr. Ali Shoeb from CHB-MIT and Dr. R. G. Andrzejak from UBonn and team of TUH for permitting to use their database for research.

Appendix A. Successive decomposition index

Defining the EEG time series $x = \{x_1, x_2, x_3, x_4, \dots, x_n\}$, where n is the total number of the EEG samples in the time series x or segmentation length ($n = fs * s$). First, to define SDI coefficients, we define two terms X^+ and X^- , which are average of $|x|$ and difference average of x respectively. The first coefficient X^+ is given by [182],

$$X^+ = \frac{1}{n} \sum_{i=1}^n |x_i| \quad (7.6)$$

The second coefficient X^- was calculated by the iterative process by arranging the EEG samples into $n/2$ non-overlap pairs that give first level ($x^{(1)}$)

coefficients, as shown below [182],

$$x^{(1)} = \left\{ \frac{x_1 - x_2}{2}, \frac{x_3 - x_4}{2}, \dots, \frac{x_{n-3} - x_{n-2}}{2}, \frac{x_{n-1} - x_n}{2} \right\} \quad (7.7)$$

Zeros can be padded towards the end of the x , if n is not a power of 2. After decomposition, $x^{(1)}$ of length $n/2$ (n is updated in each level) is represented as [182],

$$x^{(1)} = \{x_1^{(1)}, x_2^{(1)}, \dots, x_{n/2-1}^{(1)}, x_{n/2}^{(1)}\} \quad (7.8)$$

It can be further simplified as follows,

$$X_i^L = (x_{2i-1}^L - x_{2i}^L) / 2 \quad (7.9)$$

The coefficient obtained in the last level ($L = 3.33 \log_{10}(n)$) of decomposition considered as X^- .

Now, our goal is to define two new terms X^{++} , and X^{--} as follows [182],

$$X^{++} = \frac{X^+ + X^-}{2} \quad (7.10)$$

$$X^{--} = \frac{X^+ - X^-}{2} \quad (7.11)$$

The square matrix A was formed using the four coefficients X^+ , X^- , X^{++} , and X^{--} as follows [182],

$$A = \begin{bmatrix} X^+ & X^{--} \\ X^- & X^{++} \end{bmatrix} \quad (7.12)$$

Our previous study [89] showed that the determinant of a square matrix can be used for a biomarker to detect seizure activities. Therefore, determinant [64] of the square matrix A was used to calculate a SDI feature [182].

$$SDI = \log_{10} \left(\frac{n}{L} (X^+ X^{++} - X^- X^{--}) \right) \quad (7.13)$$

The term n/L is a scalar parameter. Our previous study [182] showed that SDI better tracks the seizure activity in EEG along with the amplitudes of the EEG samples.

Appendix B. Matrix determinant

Recently, we have shown that MD can be used as a biomarker for classification of epileptic seizures [89, 196].

Initially, the EEG time series were arranged sequentially to form a square matrix with the total elements in the square matrix represent a segmentation length. Let the EEG time series be $x = \{x_1, x_2, x_3, x_4, \dots, x_n\}$ and apply absolute square i.e. $x = |x|^2$.

Now, define the square matrix with an order of $N(N = r = c)$ and sequentially arrange x into matrix form as follows [89],

$$A = \begin{bmatrix} x_1 & x_2 & \dots & x_r \\ x_{r+1} & x_{r+2} & \dots & x_{r+r} \\ x_{2r+1} & x_{2r+2} & \dots & x_{2r+r} \\ \cdot & \cdot & \dots & \cdot \\ x_{(r-1)r+1} & x_{(r-1)r+2} & \dots & x_{(r-1)r+r} \end{bmatrix} \quad (7.14)$$

The MD feature was calculated as follows [89],

$$MD = \log_{10} |A| \quad (7.15)$$

In our study, we have used a square matrix with an order of 32 to estimate the MD feature. In our previous studies [89, 182, 196], the MD feature was applied on RMCH, UBonn, and MUMC databases and has shown better classification results.

Appendix C. Inter-database FBC

The procedure to correct the feature baseline among databases is given here.

1. Consider the features of all the databases $f(DB_1, DB_2, \dots, DB_n)$ from the training data. Here, DB_1, DB_2 are databases and f is a feature.
2. Calculate the $f(Median_{seizure})$ and $f(Median_{non-seizure})$ of all the training databases using seizure and non-seizure features respectively. The length of the $f(Median_{seizure})$ and $f(Median_{non-seizure})$ equals the number of databases.
3. Estimate global median ($f(Median_{global})$) using median values of seizure and non-seizure features.

$$f(Median_{global}) = Median\{f(Median_{seizure}) f(Median_{non-seizure})\} \quad (7.16)$$

4. Now estimate the median of a single database $f(Median_{DB_i})$, where $i = 1, 2, 3, \dots, n$ databases.

5. Now calculate the adaptive median coefficient (λ) using $f(\text{Median}_{global})$ and $f(\text{Median}_{DB_i})$.

$$\lambda = f(\text{Median}_{global}) - f(\text{Median}_{DB_i}) \quad (7.17)$$

6. Now correct the feature baseline of DB_i using λ as follows:

$$f_{new_i} = \lambda + f_{DB_i} \quad (7.18)$$

7. Repeat step 4 to step 6 for all the training databases ($n - 1$).
8. Repeat step 4 to step 6 for the testing database using the $f(\text{Median}_{global})$ calculated from the training database.

The λ can be either negative or positive depends on the inter-subject median variation. The AM-FBC should be applied individually to each feature.

CHAPTER 8

A convolutional neural network based framework for classification of seizure types

S Raghu, Natarajan Sriraam, Yasin Temel, Shyam Vasudeva Rao, Pieter L
Kubben

*2019 41st Annual International Conference of the IEEE Engineering in Medicine
and Biology Society (EMBC), Berlin, Germany, 2019, pp. 2547-2550.*

Year: 2019

<https://ieeexplore.ieee.org/abstract/document/8857359>

Abstract

Epileptic seizures are caused by a disturbance in the electrical activity of the brain and classified as many different types of epileptic seizures based on the characteristics of EEG and other parameters. Till now research has been conducted to classify EEG as seizure and non-seizures, but the classification of seizure types has not been explored. Thus, in this paper, we have proposed the 8-class classification problem in order to classify different seizure types using convolutional neural networks (CNN). This research study suggests a CNN based framework for classification of epileptic seizure types that include simple partial, complex partial, focal non-specific, generalized non-specific, absence, tonic, and tonic-clonic, and non-seizures. EEG time series was converted into spectrogram stacks and used as input for CNN. To the best of authors knowledge, ours is the very first study that classified the seizures types using the computational algorithm. The four CNN models, namely AlexNet, VGG16, VGG19, and basic CNN model was applied to study the performance of 8-class classification problem. The proposed study showed a classification accuracy of 84.06%, 79.71%, 76.81%, and 82.14% using AlexNet, VGG16, VGG19 and basic CNN models respectively. The experimental results suggest that the proposed framework could be helpful to the neurology community for recognition of seizures types.

8.1 Introduction

Epileptic seizures are caused by a disturbance in the electrical activity of the brain and there are many different types of epileptic seizure [13, 14]. Epileptic seizures are divided into focal seizures, generalized seizures, and unknown seizures depending on how and where they begin in the brain. Focal seizures can start in one area or group of cells on one side of the brain. Depending on a person's level of awareness during their seizures focal seizures are again classified as simple partial and complex partial seizures [15, 16]. Generalized seizures affect both sides of the brain or groups of cells on both sides of the brain at the same time [13]. Generalized seizures are again divided into absence, tonic, atonic, clonic, tonic-clonic, myoclonic seizures. Generalized seizures are classified based on motor symptoms and non-motor symptoms that involve movement [13, 15, 16]. Motor symptoms include jerking movements (clonic), muscles becoming tense or rigid (tonic), muscles becoming weak or limp (atonic), and brief muscle twitching (myoclonic) [13, 15, 16]. When the beginning and where the seizure starts is not known is referred to as unknown seizures [15, 16]. As such, seizure classification has been done based on motor symptoms, level of awareness and electroencephalogram (EEG) signals. In this study, we have classified seizures types using EEG alone without using motor symptoms, level of awareness and video EEG.

Locating epileptic activity in a continuous EEG recording lasting several days or weeks is exhausting, demanding and time-consuming task. Special attention is required to develop computer-aided algorithms to recognize and classify seizure types. Such automated procedure will help the neurologist to

enhance their clinical decisions.

A limited number of studies have been conducted on seizure detection using convolutional neural networks (CNN). Short-time Fourier transforms (STFT) based images were classified using CNN for prediction of seizures using intracranial and scalp EEG [199]. This study achieved the sensitivity of 81.4%, 81.2%, 82.3% on three different datasets. Pyramidal 1-dimensional CNN was used for binary classification of seizure vs. non-seizure and normal vs. ictal using University of Bonn database [200]. Classification of seizure and non-seizure using deep neural networks showed an F-measure accuracy of 95% [201]. Real-time seizure detection using video-EEG recordings and CNN showed the area under the curve of 78.33% [202]. A threshold based automated detection of epileptic seizures using minimum variance modified fuzzy entropy achieved 100% accuracy [19]. Classification of focal and non-focal EEG signals showed good results using multi-features when classified using support vector machine classifier [25, 65]. Further, many studies have proposed using log energy and norm entropy [21], matrix determinant [89] and other methods.

Acharya et al. [203] proposed 13-layer deep CNN and accuracy of 88.67% showed using University of Bonn database EEG recordings. CNN model was used to distinguish ictal, preictal, and interictal segments using Freiburg (accuracy of 96.70%) and CHB-MIT (accuracy of 97.50 %) databases [56]. Robust features were learned by images based representation of EEG spectrogram in three frequency bands (0-7, 7-14, and 14-49 Hz) for seizure detection [204]. Optimized deep learning for EEG big data was proposed for seizure prediction using the Internet of Things [205]. Deep CNN architecture on TUH databases

showed the sensitivity of 30.83% and specificity of 96.86% [206]. Application of CNN for four-class motor imagery classification have shown 68% accuracy [207]. It can be inferred from the literature that no studies have been proposed for classification of seizure types. This research study suggests a CNN based framework for classifying the EEG derived seizure types with 8-class pattern classification.

8.2 Methodology

8.2.1 EEG recordings

The proposed study was implemented on the EEG collected from Temple University Hospital database [114]. These EEG recordings were recorded according to 10-20 International system electrode placement and a sampling rate of 250 Hz. The recordings consist following 19 unipolar channels EEG: Fp1, Fp2, F7, F3, Fz, F4, F8, T7, C3, Cz, C4, T8, P7, P3, Pz, P4, P8, O1, and O2. The TUH database is annotated with different types of seizures based on following three manifestations: Electrographic, Electroclinical, and Clinical. The database consists of simple partial seizure (SP), complex partial seizure (CP), focal non-specific seizure (FN), generalized non-specific seizure (GN), absence seizure (AB), tonic seizure (TN), and tonic-clonic seizure (TC). The complete details of the database used in the study are summarized in Table 8.1. The remaining EEG files were considered as non-seizure (NS) events which was already labeled. Remember not all the NS events were considered for study due to the imbalance data challenge of CNN. In total, 31 hours of EEG data from 239 subjects were considered for the study.

TABLE 8.1: Database information

Seizure Type	Number of patients	Seizure Events	Duration (s)
SP ^a	8	48	2580.41
CP ^a	31	196	11726.68
FN ^b	47	440	22868.44
GN ^b	55	110	8960.49
AB ^a	13	39	2076.55
TN ^a	12	17	1180.135
TC ^a	8	20	551.63
NS ^a	65	310 ^c	59509.35

^a Manifestation: Electroclinical

^b Manifestation: Electrographic

^c Number of Non Seizure events

8.2.2 Preprocessing

The primary requirement of CNN is 2-dimensional inputs, thus EEG time series were converted into image shape by taking STFT. In order to avoid the insignificant information at the high beta band, bandpass filter with a range of 0.1 to 44 Hz was applied to EEG time series. Further, the spectrogram of the EEG was computed using a Kaiser window of length 63 with a shape parameter of 1, 75% overlapping, and an FFT length of 256. Finally, the spectrogram of all the 19 channels was vertically concatenated to form the final image (refer to Fig.8.1A). In order to overcome the imbalance dataset challenge of CNN, we have used an overlapping technique to generate balanced samples for training phase [199].

8.2.3 Convolutional neural network

Convolutional neural network (CNN) have gained attention due to its self-feature learning capability and excellent classification results on extremely multi-class problems. In CNN, each convolution block consists of a convolution layer (Conv) with rectified linear unit (ReLU) activation function, pooling layer (pool) and batch normalization. In this study, three pretrained CNN models (AlexNet [208], VGG16 [209], and VGG19 [209]) and basic CNN models was applied to solve 8-class problem. Using the transfer learning approach, the pretrained models were retrained for our dataset by replacing the final layers [210].

The dimension of the final spectrogram image was 420 x 560 which was the same used for our network. For pretrained models, images were rescaled to 227 x 227, 224 x 224 and 224 x 224 for AlexNet, VGG16, and VGG19 CNN respectively. The generalized CNN architecture for the proposed study is shown in Fig. 8.1. One can refer to [209, 211] for detailed information on VGG16 and VGG19 network configuration. Basic CNN model was formed using three Conv blocks followed by a fully connected layer and an output layer. Each block consists of a batch normalization, a Conv layer with ReLU activation function, and a max pooling layer. All the CNN models were trained using stochastic gradient descent with momentum optimizer using 70% of images (70% of total seizures). The remaining 30% of the images (30% of total seizures) were used for the validation of trained CNN model. The learning rate was varied as 0.001, 0.0001, and 0.00001 during the training phase and best results were reported. The performance of the study was evaluated in terms of classification accuracy.

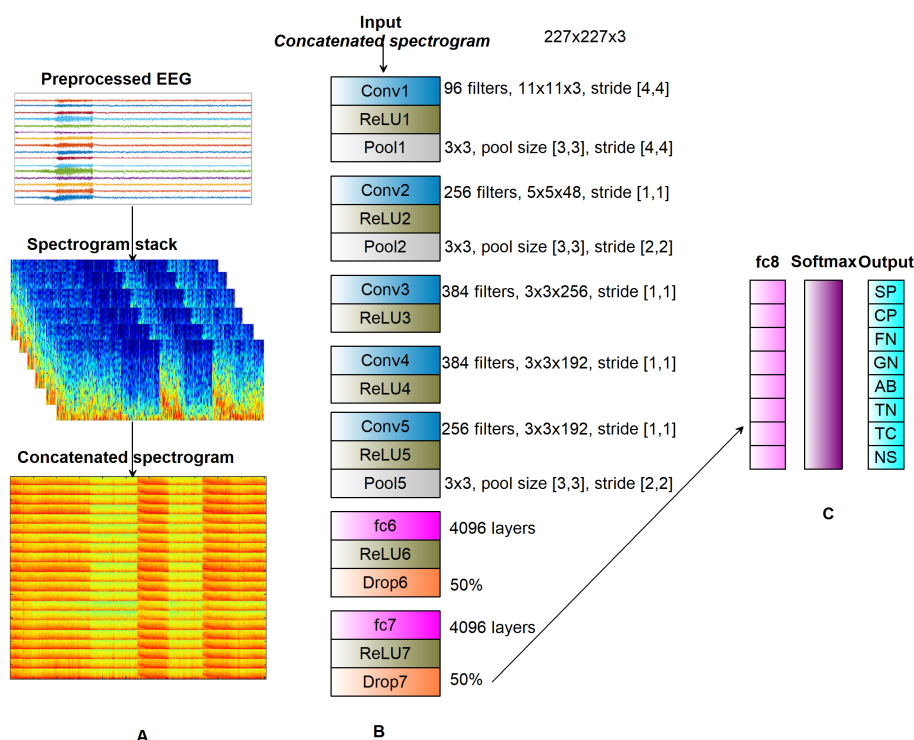


FIGURE 8.1: Generalized CNN architecture used in the study. The illustrations **A** and **C** were common for all the four CNN models and **B** was varied as AlexNet, VGG16, and VGG19, and basic CNN. **A** Generation of spectrogram stack and concatenated the 19 channel spectrogram to generate a single image. **B** This illustrates the AlexNet CNN configuration of the proposed study. For other CNN models, **B** was replaced by VGG16, and VGG19, and basic network. **C** It consists of fully connected layer (fc), softmax activation function followed by output layer.

8.3 Results and Discussion

The spectrogram stack was created using multichannel EEG as described in Fig. 8.1. The balanced dataset was created using an overlapping technique to overcome imbalance dataset challenge. CNN was trained and tested using 70% and 30% of the images respectively. CNN evaluation results using

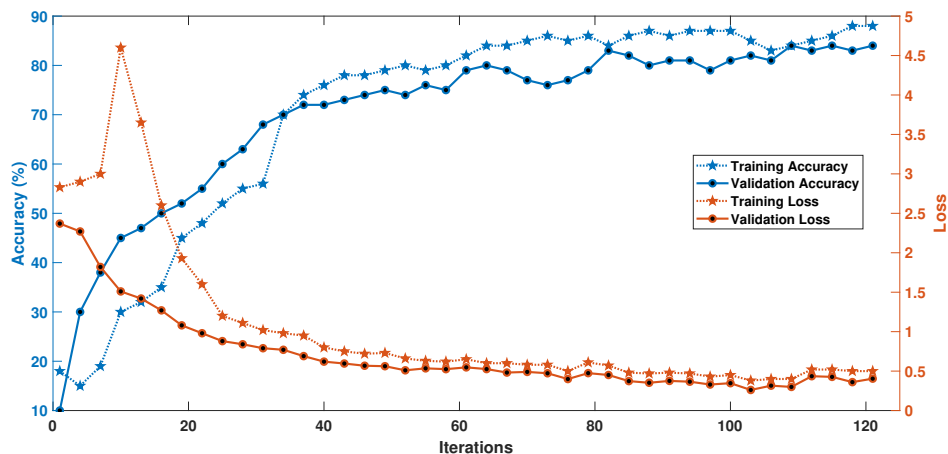


FIGURE 8.2: AlexNet CNN architecture evaluation during training and validation phase in terms of accuracy and loss.

AlexNet is shown in Fig. 8.2. We observe that highest training and testing accuracy was 89.12% and 84.02% respectively. Further, CNN parameters were tuned in terms of learning rate and momentum for best performance. Fig. 8.2 shows classification accuracy as a function of momentum. It can be seen that highest classification results of 84.06% 79.71%, 76.81%, and 82.14% were obtained for AlexNet, VGG16, VGG19, and basic CNN models respectively for the momentum of 0.95.

Table 8.2 summarizes the classification results obtained using different CNN models. The classification results were observed for different learning rates. The proposed study shows highest classification results of 84.06% (AlexNet) 79.71% (VGG16), 76.81% (VGG19), and 82.14% (basic CNN) with learning rate of 0.0001, 0.0001, 0.00001 and 0.001 respectively. With the less training duration, AlexNet CNN showed better performance as compared to other three CNN models. AlexNet, VGG16, and VGG19 showed the least

performance when CNN was trained with a learning rate of 0.001. However, with the same learning rate, basic CNN showed the best performance against other learning rates. The number of epochs and iterations taken by basic CNN were more as compared to other CNN models. The VGG16 and VGG19 CNN models were found to be expressive in terms of training time. Overall, AlexNet CNN showed better performance with the accuracy of 84.06%.

The major contributions of the proposed study are:

1. Arrangement of spectrogram of multichannel EEG into a single image (vertically concatenate) to gather the brain dynamics significant information.
2. Generation of balanced dataset for CNN using overlapping technique.
3. Basic model outperformed as compared to the other optimized pretrained models. It can be further improved for better results.
4. Notably, classification of seizure types alone using EEG without the aid of video EEG and motor symptoms.
5. To the best of authors knowledge, it is the first study on epileptic seizures EEG to solve the 8-class classification problem.

The experiment was conducted on MATLAB 2018a with Intel core i7 CPU@2.20GHz and single GPU for parallel computation. As a future score, the experiment will be extended on complete TUH data to enhance the classification results. Further, other CNN models will be evaluated with different filter size, batch size, and other network tuning parameters.

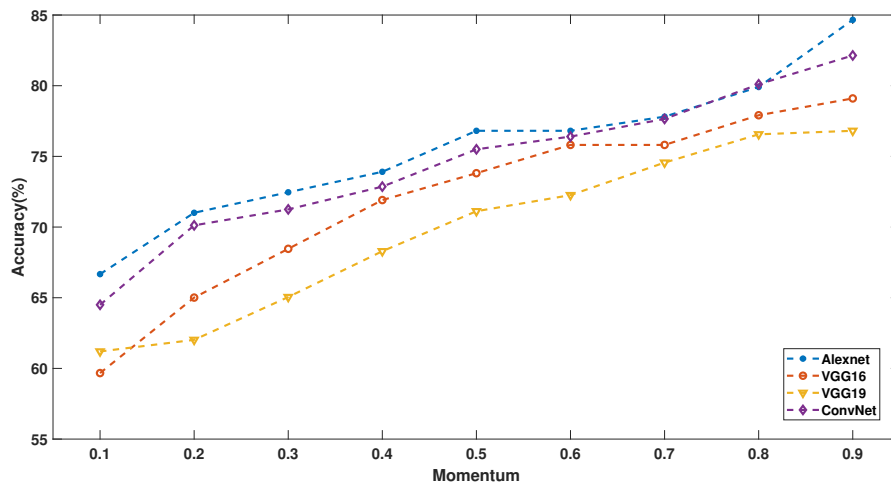


FIGURE 8.3: Evaluation of all the four CNN models using momentum vs. accuracy.

8.4 Conclusion

In this study, we have performed the 8-class classification problem to classify seizure types using CNN. In order to solve the problem, EEG time series were converted into spectrogram stacks for CNN input. The experimental results revealed the classification accuracy of 84.06%, 79.71%, 76.81%, and 82.14% using AlexNet, VGG16, VGG19 and basic CNN models respectively. To the best of authors knowledge, the proposed study is first of its kind to solve classification of seizure types using EEG alone.

TABLE 8.2: Classification results using different CNN models

CNN model	Accuracy (%)	Training time (s)	Epochs	Iterations	Learning rate
AlexNet	11.12	10	2	21	0.001
	84.06	51	8	114	0.0001
	78.26	67	10	147	0.00001
VGG16	11.36	6	3	16	0.001
	79.71	109	5	78	0.0001
	76.36	226	12	195	0.00001
VGG19	10.14	24	2	18	0.001
	72.46	101	5	75	0.0001
	76.81	234	11	174	0.00001
Basic CNN	82.14	43	20	270	0.001
	78.37	87	39	540	0.0001
	75.17	94	30	650	0.00001

Acknowledgment

The authors would like to thank Temple University Hospital, Pennsylvania, USA, for permitting to use their database for research.

CHAPTER 9

EEG based multi-class seizure type classification using convolutional neural network and transfer learning

S Raghu, Natarajan Sriraam, Yasin Temel, Shyam Vasudeva Rao, Pieter L
Kubben

Neural Networks, 124:202-212

Year: 2020

<https://doi.org/10.1016/j.neunet.2020.01.017>

Abstract

Recognition of epileptic seizure type is essential for the neurosurgeon to understand the cortical connectivity of the brain. Though automated early recognition of seizures from normal electroencephalogram (EEG) was existing, no attempts have been made towards the classification of variants of seizures. Therefore, this study attempts to classify seven variants of seizures with non-seizure EEG through the application of convolutional neural networks (CNN) and transfer learning by making use of the Temple University Hospital EEG corpus. The objective of our study is to perform a multi-class classification of epileptic seizure type, which includes simple partial, complex partial, focal non-specific, generalized non-specific, absence, tonic, and tonic-clonic, and non-seizures. The 19 channels EEG time series was converted into a spectrogram stack before feeding as input to CNN. The following two different modalities were proposed using CNN: (1) Transfer learning using pre-trained network, (2) Extract image features using pretrained network and classify using the support vector machine classifier. The following ten pretrained networks were used to identify the optimal network for the proposed study: Alexnet, Vgg16, Vgg19, Squeezenet, Googlenet, Inceptionv3, Densenet201, Resnet18, Resnet50, and Resnet101. The highest classification accuracy of 82.85% (using Googlenet) and 88.30% (using Inceptionv3) was achieved using transfer learning and extract image features approach respectively. Comparison results showed that CNN based approach outperformed conventional feature and clustering based approaches. It can be concluded that the EEG

based classification of seizure type using CNN model could be used in pre-surgical evaluation for treating patients with epilepsy.

9.1 Introduction

Epileptic seizures are caused by a disturbance in the electrical activity of the brain, which is classified into focal, generalized, and unknown [13, 14]. Accurate classification of epileptic seizure type plays a crucial role in the treatment and disease management of epilepsy patients [17]. Focal seizures start on one side of the brain and depending on the patient level of awareness during a seizure, it is again classified as simple partial and complex partial seizures [15, 16]. Generalized seizures affect both sides of the brain at the same time and again divided into absence, tonic, atonic, clonic, and tonic-clonic, myoclonic seizures [13]. Generalized seizures are classified based on motor symptoms and non-motor symptoms that involve movement [13, 15, 16]. Motor symptoms include jerking movements (clonic), muscles becoming tense or rigid (tonic), muscles becoming weak or limp (atonic), and brief muscle twitching (myoclonic) [13, 15, 16]. Unknown seizures are the one when the beginning and where the seizure starts is not known [15, 16].

Epileptic seizure type affects the choice of drugs and patient safety [17]. Most of the work reported in the literature focused on the application of machine learning towards automated seizure detection. There is a huge demand to extend the application of machine learning especially convolution neural networks (CNN) for multi-class seizure type classification. As we know that manual inspection of long-term electroencephalogram (EEG) recordings, lasting several days or weeks is a time-consuming task. Special attention is

required to develop an automated algorithm for classification of multi-class seizure type. Therefore, in this study, we have classified seizure type using EEG alone without using motor symptoms, level of awareness and video EEG. Such automated procedure may help the neurological community to improve clinical decision making and identify the optimal treatment for epilepsy patients.

The application of CNN towards the classification of epileptic seizures have been implemented in recent studies [56, 199, 200, 201, 202, 203]. In a recent study by Acharya et al. [203], a 13-layer deep CNN showed an accuracy of 88.67% using the University of Bonn database. Plot EEG image-based study using CNN showed a true positive rate of 74.0% between seizure and non-seizures EEG activities [212]. Seizure prediction using intracranial and scalp electroencephalogram signals achieved a sensitivity of 81.4%, 81.2%, and 75.0% using the Freiburg Hospital intracranial EEG dataset, the Boston Children's Hospital-MIT scalp EEG dataset, and the American Epilepsy Society seizure prediction challenge dataset respectively [213]. Neonatal seizure detection using deep CNN with 26 neonates achieved the seizure detection rate of 77.0% [214]. Signal transforms using empirical mode decomposition and classification using CNN showed an accuracy of 98.9% when classifying between focal and non-focal signals [215]. In the same study, an accuracy of 99.5% for classifying non-seizure vs. seizure recordings, 96.5% between healthy, non-focal and seizure recordings, 95.7% when classifying healthy, focal and seizure recordings was obtained. A CNN based model showed the highest accuracy of 96.7% and 97.5% using the Freiburg and CHB-MIT databases respectively [56]. Another study using the University of Bonn

database was proposed using pyramidal 1-dimensional CNN for binary classification of seizure vs. non-seizure and normal vs. ictal [200]. Similarly, an F-measure of 95.0% was achieved between the classification of seizure and non-seizure using deep neural networks [201]. Video-EEG recordings were classified using CNN showed the area under the curve of 78.33% for real-time seizure detection [202]. A recent study using machine learning for 7-class seizure type classification showed an F1 score of 0.907 without using non-seizure EEG signals [17]. The sensitivity of 30.83% and specificity of 96.86% was achieved using deep CNN architecture on the TUH database [206]. Seizure detection was performed using the robust features learned from images based representation of EEG spectrogram in three frequency bands (0-7, 7-14, and 14-49 Hz) [204]. Internet of Things based optimized deep learning for seizure prediction was proposed using EEG big data [205].

Adaptive structure of a multi-layer back-propagation network was proposed for automatic epileptic seizure detection using five epilepsy patients EEG data [216]. A reliable classifier architecture was obtained by applying fast Fourier transform (FFT) and auto-regressive based features to wavelet neural networks classifier [217]. A supervised multi-spiking neural network architecture showed a classification accuracy in the range of 90.7%-94.8% which was better than single-spiking neural network [218]. A continuous neural networks based model showed a maximum correct classification percentage of 97.2% for two-class problem [219]. A review was given on recent supervised and unsupervised methods to train deep spiking neural networks and compared them in terms of accuracy and computational cost [220].

Other than CNN, recent studies have focused on automated detection of

epileptic seizures using different feature extraction methods and machine learning algorithms. The features like log energy and norm entropy [21, 25, 37, 65], sigmoid entropy [83], matrix determinant [89], approximation entropy [27], sample and phase entropy [80], and permutation entropy [125] have been explored for seizure detection. Multi-features based classification of focal and non-focal EEG signals was performed using the support vector machine (SVM) classifier [25, 65]. Optimal configuration of multi-layer perceptron was performed using different transfer functions, training functions and mean square error for classification of epileptic seizures [66].

It is clear from the literature that no successful studies (in terms of classification results) have been proposed for the classification of multi-class seizure type in the presence of non-seizure EEG signals. Therefore, this study suggests a CNN based framework using transfer learning and extract image features using pretrained networks for classifying the EEG derived seizure type. To the best of the author's knowledge, this is the first of its kind study using deep learning for classification of multi-class seizure type.

9.2 Methodology

9.2.1 EEG recordings

The multi-class seizure type classification was implemented using the EEG signals collected from the Temple University Hospital (TUH) open-source database [113]. This scalp EEG signal recordings were recorded according to the International 10-20 system electrode placement at a sampling rate of 250 Hz. The TUH database consists of simple partial seizure (SP), complex

TABLE 9.1: EEG database details used for the proposed study.

Seizure Type	Description	Number of patients	Seizure events	Duration (h)
SP ^a	Partial seizures during consciousness; Type specified by clinical signs only	18	63	1.2
CP ^a	Partial seizures during unconsciousness; Type specified by clinical signs only	31	210	8.2
FN ^b	Focal seizures which cannot be specified by its type	63	542	22.56
GN ^b	Generalized seizures which cannot be further classified into one of the groups below	75	231	12.5
AB ^a	Absence discharges observed on EEG; the patient loses consciousness for a few seconds (Petit Mal)	21	63	1.3
TN ^a	Stiffening of the body during a seizure (EEG effects disappears)	19	29	1.3
TC ^a	At first stiffening and then jerking of the body (Grand Mal)	15	25	0.8
NS ^a	EEG without any type of seizure events	110	540 ^c	35.6

Manifestation: ^aElectroclinical, ^bElectrographic and ^cNumber of Non-seizure events

partial seizure (CP), focal non-specific seizure (FN), generalized non-specific seizure (GN), absence seizure (AB), tonic seizure (TN), tonic-clonic seizure (TC), and myoclonic seizures. In our study, we ignore the myclonic seizures because of its very low count. The recordings consist of following 19 unipolar channels EEG: Fp1, Fp2, F7, F3, Fz, F4, F8, T7, C3, Cz, C4, T8, P7, P3, Pz, P4, P8, O1, and O2. The EEG recordings were annotated with different type of seizures based on Electrographic, Electroclinical, and Clinical manifestations [114]. The description of the TUH database used in the study is summarized in Table 9.1. The EEG files other than seizure type labels were considered as non-seizure (NS) and not all the NS events were considered for the study due to the imbalance data challenge of CNN. For the experiment, 83.46 hours of EEG data from 352 subjects were considered for the study. The subjects suffering from more than one type of seizures were excluded from the study.

9.2.2 Preprocessing

The EEG signals were passed through a bandpass filter with a cut-off frequency of 0.1 to 44 Hz. Since CNN expects 2-dimensional input for its analysis, the EEG signals were converted into an image using short-time Fourier transforms (STFT). The following specifications were set to compute the STFT: Kaiser window of length 63 with a shape parameter of 1, 75% overlap, and an FFT length of 256. The spectrogram of all the 19 channels was vertically concatenated to form the final image (refer to Figs. 9.1 & 9.2). In order to overcome the imbalance dataset challenge of CNN, we have used an overlap technique to produce balanced samples or images for the training phase [199].

9.2.3 Convolutional neural network

CNN has been found to be an ideal for image-based classification due to its self-feature learning capability and excellent classification results on multi-class classification problems. A CNN consists of a convolution layer (Conv) with rectified linear unit (ReLU) activation function, pooling layer (Pool) and batch normalization. Further, at the final layers, it consists of fully connected (fc), drop out, softmax and classification output layers. Conv layer have filters which detects different patterns in image (spectrogram) such as edges, shapes, textures, and objects. In this study, ten pretrained CNN models, namely Alexnet, Vgg16, Vgg19, Squeezenet, Googlenet, Inceptionv3, Densenet201, Resnet18, Resnet50, and Resnet101 were used to identify the best model for the proposed 8-class problem [208, 209, 221]. The proposed

method was evaluated using the following two methods: (1) Transfer learning using pretrained network, (2) Extract image features using pretrained network.

9.2.3.1 Transfer learning using pretrained network

Transfer learning is the process of taking a pretrained deep learning network and fine-tuning it to learn a new task [210]. Fig. 9.1 shows the flow of the multi-class seizure type classification based on the transfer learning using pretrained network. Transfer learning was performed by using the following steps:

1. Create the spectrogram image data using EEG signals.
2. Choose a pretrained network.
3. Replace the final layers with new layers adapted to the new data set.
4. Specify the new number of classes (in our study 8-class) in training images.
5. Resize images, specify training options (Solver name or training options, initial learning rate, number of epochs, mini-batch size, validation data, and validation frequency) and train the network.
6. Test trained network by classifying test or validation images.

Table 9.2 shows ten different pretrained networks used for the study [221] along with network depth, number of layers, required image input size, and final three layers replaced for the each pretrained networks. In order to identify the suitable model, the learning rate (LR) was varied as 1e-3, 1e-4, 1e-5

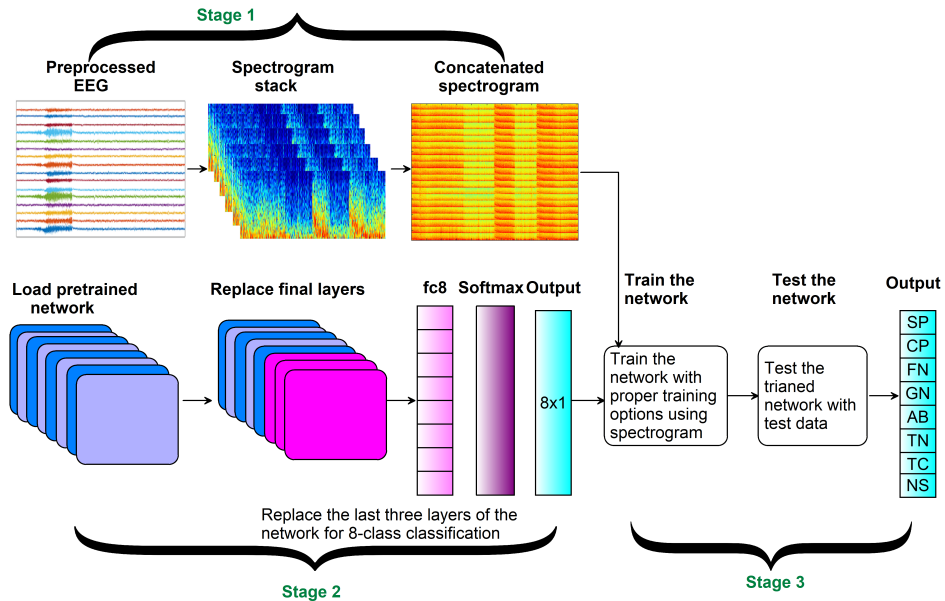


FIGURE 9.1: Flow of the multi-class seizure type classification based on transfer learning using pretrained network. **Stage 1:** Generation of spectrogram stack and concatenated the 19 channels spectrogram to generate a single image. **Stage 2:** Load the pretrained networks and replace the final three layers for 8-class classification. **Stage 3:** Train the network using spectrogram data (70%) and test with the remaining data (30%).

and $1e-6$ and three solvers were used, namely stochastic gradient descent with momentum (sgdm), root mean square propagation (rmsprop), and adaptive moment estimation (adam) optimizer.

9.2.3.2 Extract image features using pretrained network

In this method, we have used a pretrained network as a feature extractor by using the layer activation's as features and classified using the SVM classifier [222]. Feature extraction is the easiest and fastest way to use the representational power of pretrained deep networks because it only requires a single pass

TABLE 9.2: Different pretrained networks used for the study.

Pretrained network	Depth	Number of layers	Image input size	Final three layers replaced
Alexnet	8	25	227 x 227	fc8, prob, output
Vgg16	16	41	224 x 224	fc8, prob, output
Vgg19	19	47	224 x 224	fc8, prob, output
Squeezenet	18	68	227 x 227	pool10, prob, ClassificationLayer_predictions
Googlenet	22	144	224 x 224	loss3-classifier, prob, output
Inceptionv3	48	316	299 x 299	predictions, predictions_softmax, ClassificationLayer_predictions
Densenet201	201	709	224 x 224	fc1000, fc1000_softmax, ClassificationLayer_fc1000
Resnet18	18	72	224 x 224	fc1000, prob, ClassificationLayer_predictions
Resnet50	50	177	224 x 224	fc1000, fc1000_softmax, ClassificationLayer_fc1000
Resnet101	101	347	224 x 224	fc1000, prob, ClassificationLayer_predictions

through the data. The flow of extract image features using pretrained network approach is depicted in Fig. 9.2. In this method, features were extracted from all the layers and classified using the SVM classifier for all the ten pretrained networks [222]. In pretrained networks, deeper layers contain higher-level features, which are constructed using the lower-level features of earlier layers [222, 223]. Further, earlier layers typically extract fewer, shallower features, have the higher spatial resolution, and a larger total number of activation's [222, 223].

9.2.4 Classification methodology

In both the methods, the dataset was divided into 70% and 30% for training and testing phase respectively. The SVM classifier was trained using a radial

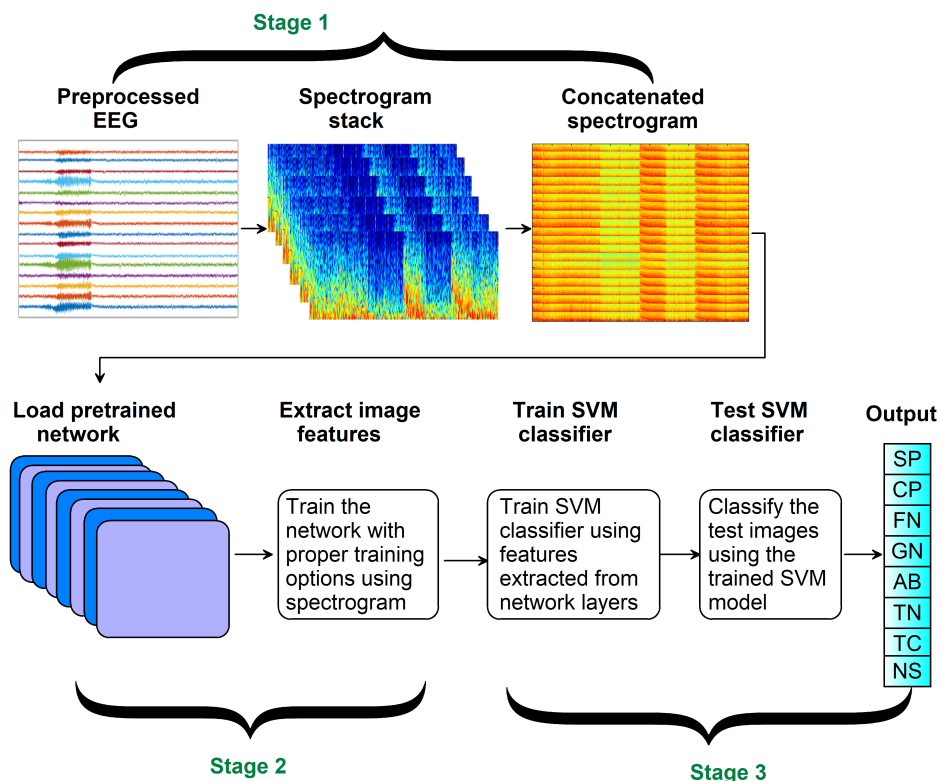


FIGURE 9.2: Flow of the multi-class seizure type classification based on extract image features using pretrained network. **Stage 1:** Generation of spectrogram stack and concatenated the 19 channel spectrogram to generate a single image. **Stage 2:** Load the pretrained networks and extract the image features from specified layers. **Stage 3:** Train the SVM classifier using features extracted from layers and test the SVM model using the features extracted from the test images.

basis kernel function. The performance of the model was assessed using classification accuracy. The experiment was repeated for 10 times and average results were reported.

9.3 Results

In this section, we discuss the classification results obtained using both transfer learning and extract image features approach. Fig. 9.3 depicts the classification accuracy obtained using transfer learning approach. The experiment was conducted using different solvers and LR. The highest accuracy of 77.66% (LR=1e-4), 76.60% (LR=1e-5), 74.47% (LR=1e-4) was achieved using sgd, rmsprop, and adam solvers respectively using Alexnet model. The rmsprop using LR of 1e-5 showed the highest accuracy of 67.02% and 65.96% using Vgg16 and Vgg19 respectively. Squeezenet outperformed with LR of 1e-4 against other LR's using all the three solvers. Googlenet showed the highest accuracy of 74.74% (LR=1e-3), 78.72% (LR=1e-4), and 82.85% (LR=1e-4) using sgd, rmsprop, and adam solvers respectively. Inceptionv3 network with LR of 1e-3 achieved the highest accuracy of 71.28%, 70.21%, and 68.21% using sgd, rmsprop, and adam solvers respectively. Densenet201 network with LR of 1e-4 using adam solver showed the highest accuracy of 75.53%. For Resnet50 and Resnet101, LR of 1e-3 outperformed other LR's using all the three solvers and Resnet18 using rmsprop and LR of 77.66% showed the highest accuracy. Overall, LR of 1e-4 performed better in most of the solvers and pretrained networks. Finally, Googlenet showed the highest accuracy of 82.85% using LR of 1e-4 and adam solver.

Fig. 9.4 shows the predictions and their probabilities in descending order obtained using Googlenet. As it can be seen, TN and TC seizure type prediction probabilities are high as compared to other types prediction. Fig. 9.5

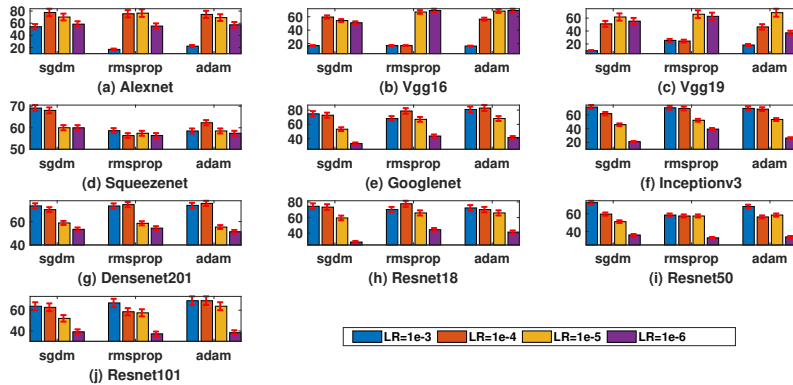


FIGURE 9.3: Classification accuracy obtained for transfer learning using pretrained network approach. The results are grouped solver wise for each pretrained network.

depicts the validation images with predicted labels and predicted probabilities using Googlenet. Predicted probability shows how well probability of an event (seizure type) is calculated from available data. The seizure types AB, FN, GN, CP, and SP showed the prediction probabilities greater than 80%.

Fig. 9.6 depicts the classification accuracy obtained using the extract image features approach. The image features were extracted from every layer and classified using the SVM classifier. As it can be observed, the classification accuracy gets improved in deeper layers of the pretrained networks due to higher-level features. However, the performance of the Densenet201 (refer to Fig. 9.6g) started fluctuating in deeper layer features. In contrary, Squeezenet and Googlenet (refer to Figs. 9.6d & e) did not show better performance in earlier layers. The remaining pretrained networks were capable of maintaining the less fluctuating accuracy in deeper layers features. The highest classification accuracy of 76.60%, 83.83%, 81.82%, 85.11%, 74.47%, 88.30%, 85.11%, 86.17%, 86.17%, and 87.23% was achieved using features extracted

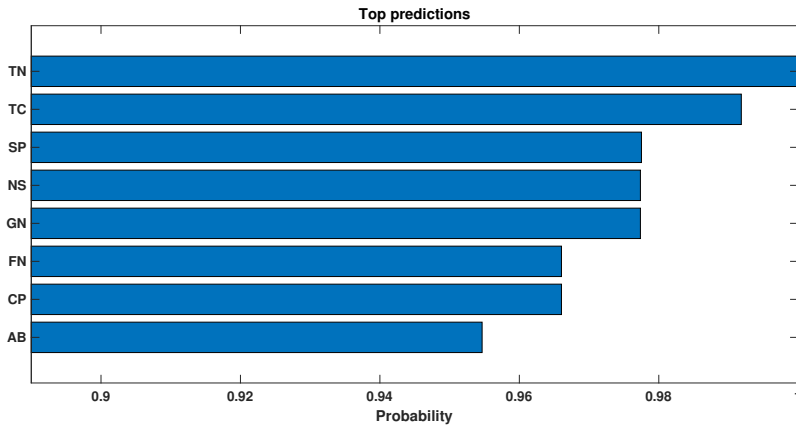


FIGURE 9.4: Seizure type predictions and their probabilities obtained using Googlenet. SP-Simple partial seizure, CP- Complex partial seizure, FN- Focal non-specific seizure, GN- Generalized non-specific seizure, AB- Absence seizure, TN- Tonic seizure, TC- Tonic-clonic seizure, and NS- Non-seizure.

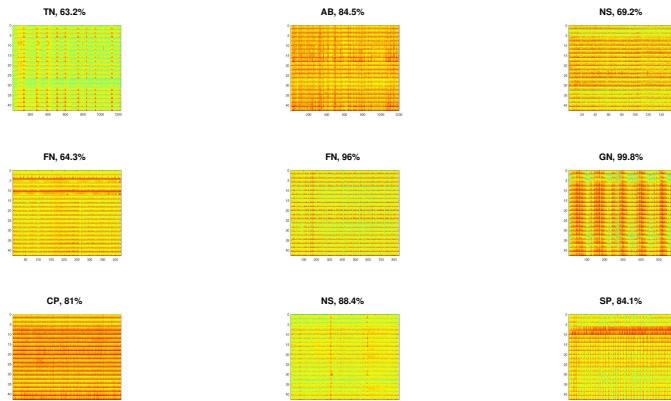


FIGURE 9.5: Validation images with predicted labels and predicted probabilities using Googlenet. The text written on top of the images are predicted labels and predicted probabilities. SP-Simple partial seizure, CP- Complex partial seizure, FN- Focal non-specific seizure, GN- Generalized non-specific seizure, AB- Absence seizure, TN- Tonic seizure, and NS- Non seizure.

from Alexnet (layers 13 to 16), Vgg16 (layers 32 and 34), Vgg19 (layer 39), Squeezenet (layer 59), Googlenet (layer 56), Inceptionv3 (layers 37, 41, and

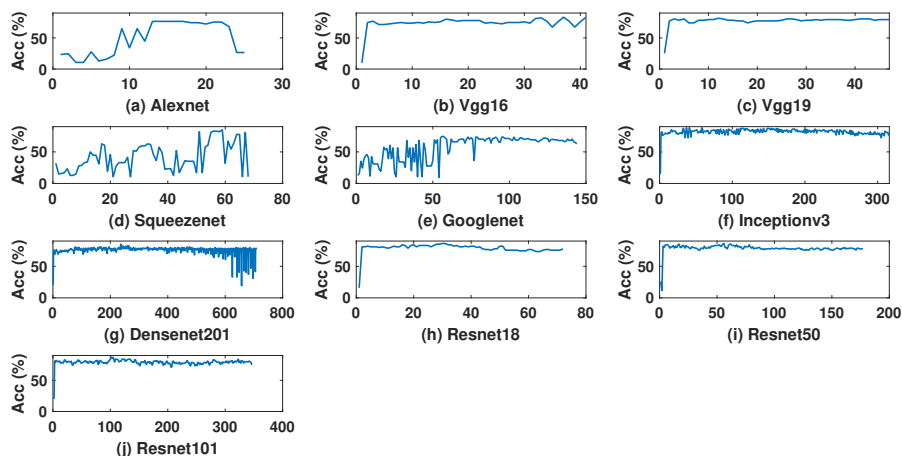


FIGURE 9.6: Classification accuracy obtained for extract image features approach. The accuracy was plotted for each layer (along x-axis) for each pretrained network.

58), Densenet201 (layer 236), Resnet18 (layers 30 and 31), Resnet50 (layer 56), and Resnet101 (layers 101, 102, 105) networks respectively. Table 9.3 shows the highest classification accuracy obtained using the extract image features approach. Overall, ReLU layer showed the highest accuracy in most of the pretrained networks as compared to other layers. Finally, the highest classification accuracy of 82.85% (Googlenet using LR of $1e-4$ and adam solver) and 88.30% (Inceptionv3 in layers 37, 41, and 58) was achieved using transfer learning and extract image features approach respectively.

9.4 Discussion

In this study, CNN was implemented successfully using scalp EEG for automated multi-class seizure type classification. The study was conducted using

TABLE 9.3: The highest classification accuracy obtained for extract image features using the pretrained network approach.

Pretrained network	Highest accuracy (%)	Layer number	Layer name
Alexnet	76.76	13 to 16	ReLU, Conv, ReLU, and Pool
Vgg16	83.33	32, 34	Pool and ReLU
Vgg19	81.82	39	fc
Squeezenet	85.11	59	ReLU
Googlenet	74.47	56	ReLU
Inceptionv3	88.30	37, 41, 58	Normalization, ReLU, and Normalization
Densenet201	85.11	236	ReLU
Resnet18	86.17	30, 31	Conv, and normalization
Resnet50	86.17	56	Conv
Resnet101	86.27	101, 102, 105	ReLU, Conv, and Conv

transfer learning and extract image features approach using ten pretrained networks. Both the approaches performed better for 8-class classification problem. We have performed a comparison between both the methods to identify the ideal model for seizure type classification. The best results from each pretrained network were taken into consideration for comparison. The best accuracy (using different solver and LR) of 77.66%, 69.15%, 65.96%, 69.15%, 82.85%, 71.28%, 75.53%, 77.66%, 72.34%, and 69.15% using Alexnet, Vgg16, Vgg19, Squeezenet, Googlenet, Inceptionv3, Densenet201, Resnet18, Resnet50, and Resnet101 pretrained networks respectively was taken into consideration for transfer learning approach. Similarly, the highest classification accuracy of 76.60%, 83.83%, 81.82%, 85.11%, 74.47%, 88.30%, 85.11%, 86.17%, 86.17%, and 87.23% using Alexnet, Vgg16, Vgg19, Squeezenet, Googlenet, Inceptionv3, Densenet201, Resnet18, Resnet50, and Resnet101 pretrained networks respectively were considered for extract image features approach. Fig. 9.7 shows the performance comparison between the results of transfer learning and extract image features using the pretrained network approach. Only for

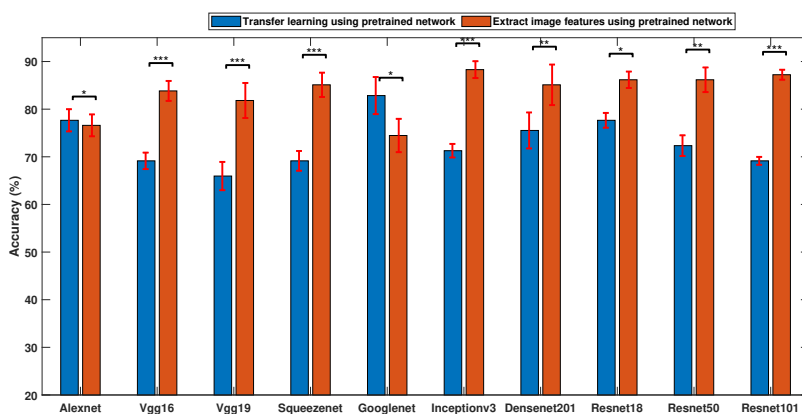


FIGURE 9.7: Performance comparison between Transfer learning and extract image features approach using pretrained network. The highest results obtained in each pretrained network was considered for comparison. $p < 0.05(*)$, $p < 0.01(**)$, $p < 0.001(***)$.

Alexnet and Googlenet, transfer learning approach outperformed image features approach. Further, an accuracy obtained using extract image features for Vgg16, Vgg19, Squeezenet, Inceptionv3, Densenet201, Resnet18, Resnet50, and Resnet101 pretrained models outperformed transfer learning approach.

Fig. 9.8 reports the comparison between different LR's in terms of number of epochs, numbers iterations, computation time and classification accuracy among all three solvers. We observe that the LR of 1e-3 exhibits less number of epochs and iterations with less computation time and contrary to the results obtained using LR of 1e-6. A similar observation was made for all the three solvers: sgd, rmsprop, and adam. Further, the highest classification accuracy was obtained for LR of 1e-4 using all the three solvers. We found that all ten pretrained networks showed similar observation.

Fig. 9.9 shows the comparison between the computation of taken for transfer learning and extract image features approach for each pretrained network

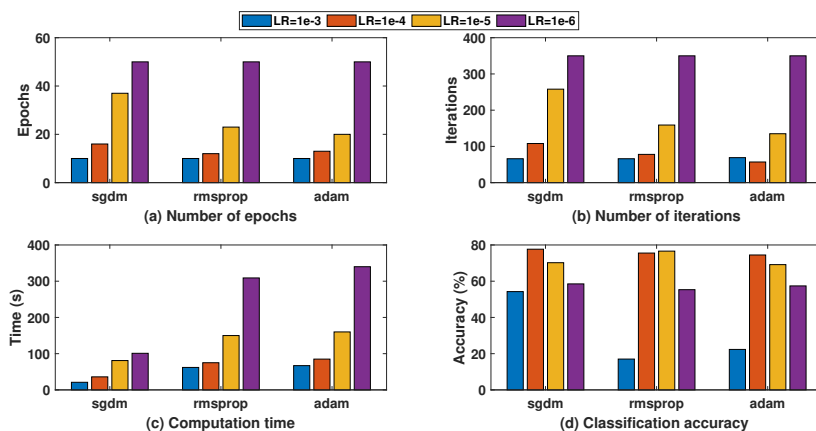


FIGURE 9.8: The comparison between different LR's in terms of number of epochs, numbers iterations, computation time and classification accuracy. The number of epochs, iterations and computation time increases as the LR becomes smaller.

in Matlab 2018a with a single GPU. Inceptionv3 has taken the highest computation time using both approaches. It is clear from Fig. 9.9 that the computation time required for extract image feature is high compared to the transfer learning method. This is because in extract image feature approach the SVM classification runs as many times of number of layers in the pretrained network. If we fix the best layer (refer to Table 9.3) with respect to the highest classification accuracy, the computation times gradually comes below the transfer learning approach. In case of inceptionv3 in layer 37, the computation time required was 3.6 minutes which is lesser to transfer leaning approach (52 minutes) of same the pretrained network.

In order to compare the CNN based approach, we have applied two more methods namely (1) Standard multilayer perceptron neural network (MLP-NN) approach and (2) Clustering approach. In the first method, we have applied discrete wavelet transform (DWT) using Haar wavelet on EEG signals

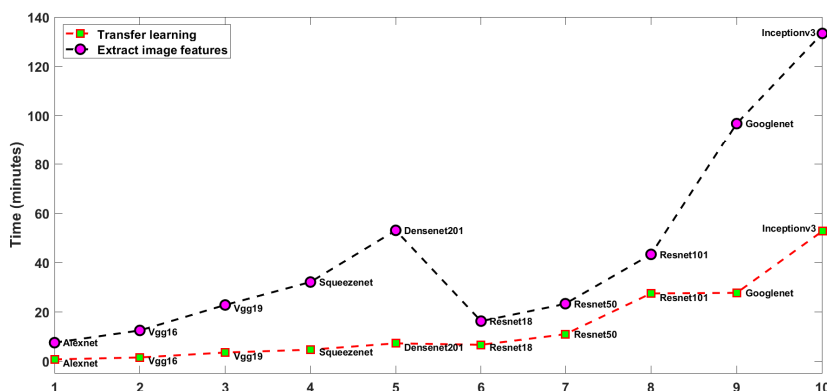


FIGURE 9.9: Comparison between the computation time taken for transfer learning and extract image features approach for each pretrained network. The computation time given for extract image features approach is the cumulative time for all the layers of pretrained network used for the SVM classification.

till 5th level and extracted various features as reported in [42, 128, 129, 132]. The extracted DWT based features were classified using optimal MLP-NN as reported in [66]. MLP-NN was trained with following configurations: 10 hidden neurons, two-layer feed-forward, tan-sigmoid at hidden layer, pure linear at output layer, Levenberg-Marquardt as training function, maximum epochs of 1000, learning rate of 0.01, and cross-entropy as cost function [66]. The highest classification accuracy of 58.60% was obtained using the features extracted from 4th level DWT coefficients. Further, the same features showed the highest classification accuracy of 60.63% using the SVM classifier using radial basis function (RBF) kernel. In SVM classifier, hyper-parameter of RBF kernel was selected from the best parameters of sigma and box using Bayesian optimization method. In the second method, we have applied k-means clustering using city block distance metric for the same DWT based

features as reported in [11, 78]. From the silhouette plot, we observed few silhouette values were between -0.4 and 0.2 indicating that those clusters are not well separated (those are belong to seizure types). The accuracy was evaluated using results of clustering method and results with an expert's label. The classification results showed the highest classification accuracy of 64.20% using k-means clustering method. Therefore, it shows that CNN based supervised learning approach is well suited than MLP-NN and clustering approach for the proposed 8-class classification problem.

Since this is the first of its kind study of automated classification of multi-class seizure type, exact comparison cannot be made. However, a recent study by [17] showed an F1 score of 0.907 using machine learning for 7-class seizure type classification. But, our study performed 8-class classification which is better than reported in [17]. Using the TUH database, a minimum variance modified fuzzy entropy obtained a sensitivity of 94.0% for classification of normal and epileptic seizures. Similarly, in our previous study [182], successive decomposition index using the SVM classifier showed a sensitivity of 95.80% using the same database. Further, many state-of-the-art methods have proposed a classification of normal vs seizures, non-seizure vs seizure, inter-ictal vs seizure, and pre-ictal vs ictal using various EEG databases but not provided the automated algorithm for classification of multi-class seizure type [9, 21, 27, 80, 84, 89, 136, 182].

The major contributions and significant findings of the proposed study are listed below:

1. Generating the spectrogram stack using multichannel EEG to feed as input for CNN.

2. In order to overcome the imbalance issue of CNN, we have generated balanced dataset using overlap technique.
3. Using a transfer learning approach, LR with $1e-4$ performed better in most of the solvers and pretrained networks.
4. The classification accuracy gets improved in deeper layers of the pre-trained networks due to higher-level features learned by CNN using extract image features approach. However, the performance of the Densenet201 started fluctuating in deeper layer features.
5. ReLU and Conv layers (refer to Table 9.3) showed the highest accuracy in most of the pretrained networks as compared to other layer using extract image feature approach.
6. ReLU layer does not saturate and gradient is always high due to its property. Conv layer have filters to extract edges, shapes, textures, and objects of an image (spectrogram). Therefore, these two layers have shown the highest classification accuracy using most of the pretrained networks.
7. Transfer learning approach using Alexnet and Googlenet outperformed extract image features approach.
8. Alexnet, Squeezenet and Googlenet did not show better performance in earlier layers using extract image features approach.
9. An accuracy obtained using extract image features for Vgg16, Vgg19, Squeezenet, Inceptionv3, Densenet201, Resnet18, Resnet50, and Resnet101 pretrained models outperformed transfer learning approach.

10. The highest classification accuracy of 82.85% (Googlenet using LR of $1e-4$ and adam solver) and 88.30% (Inceptionv3 in layers 37, 41, and 58) was achieved using transfer learning and extract image features approach respectively.
11. Extract image features approach outperformed transfer learning approach in terms of classification accuracy and computation time.

The proposed study was conducted on MATLAB 2018a with Intel core i7 CPU@2.20GHz and a single GPU. As a future scope, the obtained best model will be explored to enhance the classification results. Further, long short-term memory based deep learning approach will be introduced for classification of seizure types.

9.5 Conclusion

This study proposed an 8-class classification problem to classify seizure type using CNN. The EEG time series were converted into a spectrogram stack to feed as input for CNN. The algorithm was evaluated using transfer learning and extract image features using the ten pretrained networks. The proposed method showed the highest classification accuracy of 82.85% (Googlenet using LR of $1e-4$ and adam solver) and 88.30% (Inceptionv3 in layers 37, 41, and 58) using transfer learning and extract image features approach respectively. Comparison results showed that extract image features approach outperformed transfer learning approach in terms of classification accuracy and computation time.

Acknowledgment

The authors would like to thank the Temple University Hospital, Pennsylvania, USA, for permitting to use their database for research.

CHAPTER 10

Application of low-cost mobile health for remote monitoring of epilepsy patients

S Raghu, Natarajan Sriraam, Erik D Gommer, Danny M W Hilkmann, Yasin
Temel, Shyam Vasudeva Rao, Alangar Sathyaranjan Hegde, Pieter L Kubben

Under review

Year: 2020

Abstract

The objective of this study is to investigate the feasibility of smartphones for processing larger electroencephalography (EEG) recordings for the application towards remote monitoring of epilepsy patients. A mobile application was developed to automatically analyze and perform the classification of epileptic seizures. For this purpose, a previously described cross-database model was developed using successive decomposition index and matrix determinant as features, adaptive median feature baseline correction to overcome inter-database feature variation and post-processing based support vector machine for classification using five different EEG databases. The sezeet (seizure detect) Android application was built using Chaquopy software development kit which uses Python language in Android Studio. Different duration of EEG signals was tested on different versions of smartphones using sezeet app to check its feasibility. The computational time required to process the real-time EEG data on a smartphone and the resulting seizure classification suggest that mobile-health could be a great asset to monitor epilepsy patients. This study focused on utilizing the power of smartphones to implement the complete seizure detection model which eliminates the need for the cloud. More details on sezeet Android app can be found at <http://doi.org/10.5281/zenodo.3592415>.

10.1 Introduction

According to the International League Against Epilepsy (ILAE), epileptic seizures are characterized by an unpredictable occurrence pattern and transient dysfunctions of the central nervous system due to excessive and synchronous abnormal neuronal activity in the cortex [5]. Electroencephalography (EEG) can be used to determine the epileptogenic zone/to monitor ICU patients for seizures/monitor seizures for therapy adjustment. EEG signals are collected over a period of time and analyzed to detect seizure events. Today almost everyone uses smartphones and smartphone-based applications are being used for solving human real-life problems including health-related issues. Regarding epilepsy patients for remote monitoring, there is a need for developing an efficient smartphone application that processes the long-term EEG recordings for seizure detection. Therefore, the goal of this paper is to develop and evaluate the feasibility of a mobile app for remote monitoring of epilepsy patients.

In this context, an automatic mobile-based approach for epileptic seizure detection was proposed by Menshawy et al. [11] using time, frequency, entropy and discrete wavelet transform (DWT) based features with k-means clustering. EEG signals recorded from EEG headset were stored in smartphones and transmitted to the server. The pre-processing, feature extraction, feature normalization, feature selection, and classification model of EEG signals were performed at the cloud server. The results were sent to the smartphones of patients and physicians from the back end server. Based on the results of classification, caretakers will be notified to take the necessary action. The limitations of this study were in terms of memory as the complete EEG signal has

to be sent to the server and this approach was computationally expensive as a huge number of features were used. McKenzie et al. [224] assess the ability of Smartphone Brain Scanner-2 (SBS2) to detect epileptiform abnormalities using an Android tablet which was wirelessly connected to a 14-electrode EasyCap headset. An Android-based smartphone application for monitoring epilepsy patients was proposed using sub-band features and a support vector machine (SVM) classifier [225]. Mobile health was proposed to detect generalized tonic-clonic seizures which trigger an alarm for prompt timely interventions resulting in possibly reduce the risk of sudden unexpected death in epilepsy (SUDEP) [226].

Kornek et al. [227] have proposed a mobile system based epileptic seizure prediction using big data and deep learning in intracranial EEG signals. Typical stats like seizures per month, average sensitivity and average time in the warning were reported. Further, the cloud-based alert system using higher statistics [228], and seizure prediction using deep learning for big EEG data was proposed in [229, 230]. Other studies [11, 227, 228, 229, 230, 231, 232, 233, 234, 235] have utilized cloud computing for EEG analysis and seizure detection. Further, few mobile devices namely SmartWatch, Embrace Watch, Brain Sentinel, and EpiWatch App were developed for seizure detection to alert caretakers and to prevent SUDEP [236].

But the proposed study focuses on utilizing the power of smartphones to implement the complete seizure detection model which eliminates the need for the cloud. Our mobile-based seizure detection model provides information like the number of channels, sampling frequency, duration of EEG signal, frequency of seizure per channel, and seizure affected channels. Further, the app

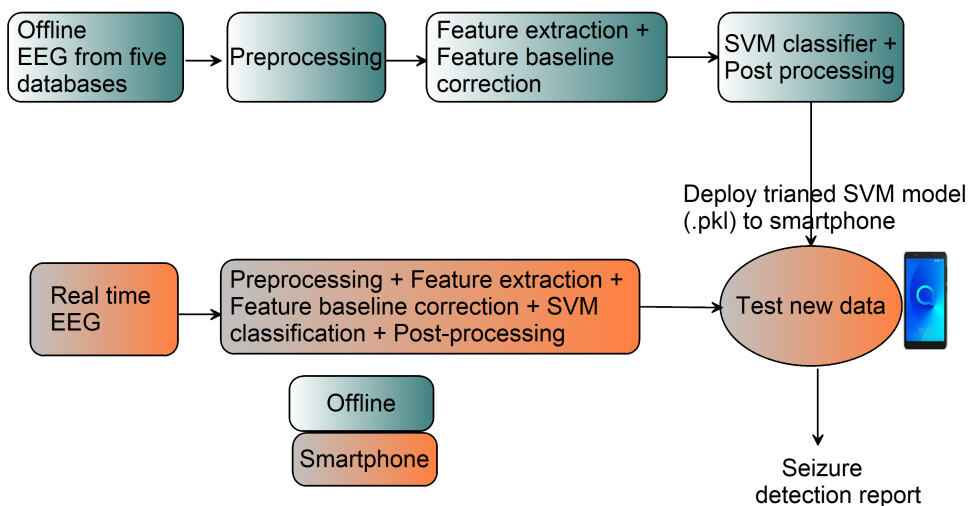


FIGURE 10.1: Block diagram of the proposed smartphone-based epilepsy patient monitoring approach.

was developed using open-source software which is open for researchers in public access and can be reproduced. Therefore, the proposed mobile-based approach would be a great tool for remote monitoring of epilepsy patients. Fig. 10.1 shows the block diagram of the proposed smartphone-based epilepsy patient monitoring approach.

10.2 Materials and methods

10.2.1 Clinical EEG recordings

In order to deploy the seizure detection model on the smartphone, the cross-database model in our previous study was developed using EEG recordings from Ramaiah Medical College and Hospitals (RMCH), Children's Hospital

Boston-Massachusetts Institute of Technology (CHB-MIT), Temple University Hospitals (TUH), Maastricht University Medical Centre (MUMC), and University of Bonn (UBonn) [237]. The same cross-database model was implemented on a smartphone and validated using 20 new epilepsy patient's EEG recordings collected from RMCH and MUMC databases. EEG recordings with a total duration of 13 hours was tested on the smartphone.

10.2.2 Chaquopy

Chaquopy is the Python software development kit (SDK) for Android [238] which allows reusing existing Python code on Android and takes advantage of PyPI packages including numpy, sci-kit learn, scipy and others. One can refer to the GitHub repository at <https://GitHub.com/chaquo/chaquopy> for more details on how to use Chaquopy. The Chaquopy-console template was used for running the seizure detection Python code on the Android app.

10.2.3 Seizure detection model

The optimized cross-database seizure detection model was built in a previous study [237]. Two features, successive decomposition index [182] and matrix determinant [89] were extracted from all five databases and features baseline were updated using adaptive median feature baseline correction [196]. The features were classified using the SVM classifier with the leave-one-database-out cross-validation method and a 10-tap moving average filter applied on classifier output as post-processing to reduce the false detections. This model was then written in Python language and exported into a pickle file for smartphones to test new EEG recordings.

10.2.4 Mobile-based seizure monitoring

As a proof of concept (POC) the Android app *sezeet* was tested for epileptic seizure detection in EEG signals. It is very important to investigate how different version or models of smartphones performs processing of EEG signals which will be useful to scalable the proposed method. Therefore, we have tested the proposed algorithm on Nokia, Moto X Play, and Redmi Note 4 mobiles. Overall, 20 new EEG recordings from epilepsy patients from both MUMC and RMCH centers were used to evaluate the efficiency of smartphones for seizure detection. Using *joblib* from *sklearn.externals*, the trained SVM model was dumped into *.pkl* file and loaded into *sezeet* app to test new EEG recordings.

10.3 Results

The goal of this paper is to validate the efficiency of smartphones for seizure detection which can be deployed for remote monitoring of epilepsy patients.

10.3.1 Smartphone results

The *sezeet* app was tested on three Android mobiles with the following configurations (1) Nokia 8.1 (Android 10) (2) Moto X Play (Android 8) and (3) Redmi Note 4 (Android 10). The screenshots of *sezeet* Android app results using Nokia are shown in Fig. 10.2 and the video of running app is available at <https://doi.org/10.5281/zenodo.3595429>. As can be seen from Fig. 10.2, the app pulls the information such as the number of channels, sampling frequency, and duration of the complete EEG data file. Further, it

displays the elapsed time required to process the complete EEG file, the number of seizure events detected per channel, and the total number of seizure epochs (each epoch length is 10s).

Fig. 10.3 shows the elapsed time taken by different smartphones for different duration of EEG recordings. The processing time of the sezeet app shows that a mobile platform is capable of handling huge EEG data and perform feature calculation and classification. Different mobile phones do not have much difference in processing time which indicates different versions of mobile phones can be used for implementation. For the new EEG recordings, we have observed the sensitivity of 93.5%, the specificity of 97.50%, and the false detection rate of 1.5/hr on the Android sezeet app. The results suggest that our proposed seizure detection algorithm could be a significant asset to monitor epilepsy patient's remotely using smartphones-based apps. The source code for sezeet Android app can be found at <http://doi.org/10.5281/zenodo.3592415>.

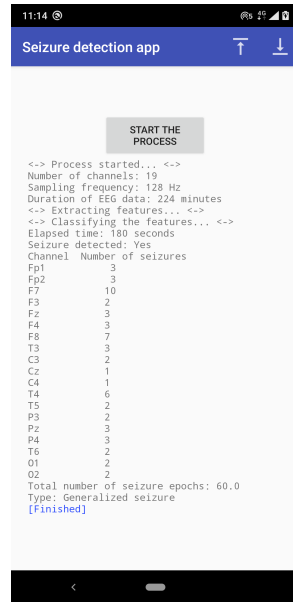
10.4 Discussion

10.4.1 Comparison with state-of-the-art studies

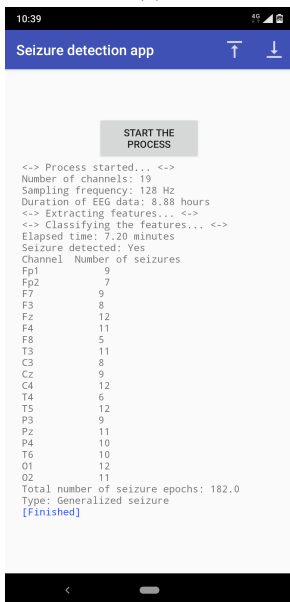
Few studies have attempted cloud, IoT and smartphones to analyze the EEG and detect seizure epochs. Menshawy et al. [11] have used the server to process the data in terms of preprocessing, feature engineering, and classification, send back the report to doctors and alarm the caretakers in case of seizure found. Cloud computing was effectively used in the studies [225, 231, 233, 235] to perform feature engineering and classification on the cloud. Further,



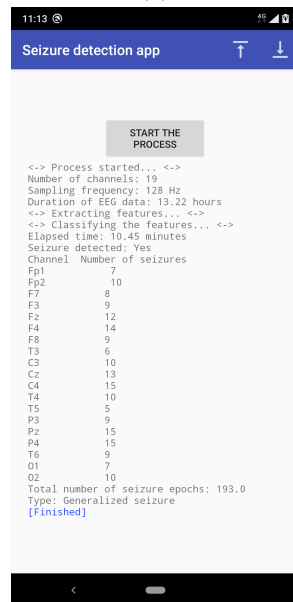
(a)



(b)



(c)



(d)

FIGURE 10.2: The screenshots of sezeet Android app results. (a) The MUMC database with 22 minutes of EEG data. The RMCH database with (b) 3.73 hours (c) 8.88 hours (d) 13.22 hours of EEG data.

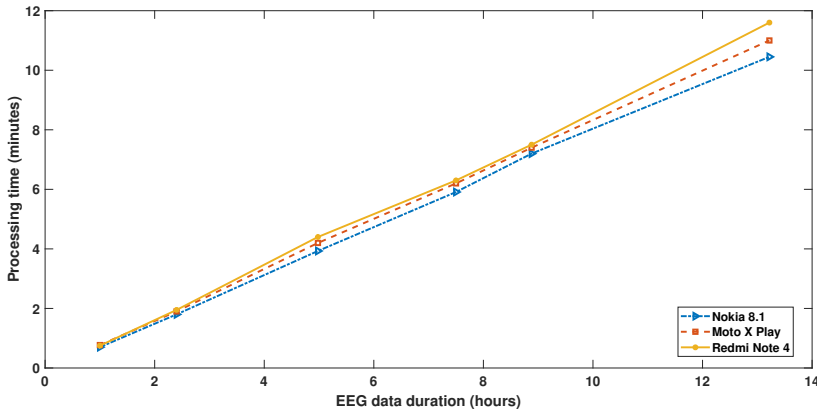


FIGURE 10.3: The processing time required to analyze and classify the different duration EEG signals on different smartphones.

mobile devices like SmartWatch, Embrace Watch, Brain Sentinel, EpiWatch App are in practice which detects only a particular type of seizures [236]. However, the proposed sezeet app is built using the cross-database model from five EEG databases and found to be effective in terms of computational time when tested on three different smartphones.

10.4.2 Contributions

The following is a summary of our contributions:

1. We developed the Android sezeet app using open source software for remote monitoring of epilepsy patients. The app is made available as open-source software to improve the reproducibility of our results.
2. The feasibility of smartphones for handling huge EEG recordings has been studied using the sezeet app. Further, we studied the time complexity in terms of the elapsed time of the mobile app using different

durations of EEG.

3. Running every task on cloud results in need of huge memory and can be cost expensive. The feasibility of automated seizure detection on a smartphone without the involvement of cloud infrastructure is the biggest contribution of this study.

10.4.3 Clinical significance

The idea of remote monitoring using smartphone apps will be useful to monitor epilepsy patients by analyzing EEG signals collected over a period of time. Smartphones can be used for multi-purpose uses in terms of health-care applications to improve the quality of patients lives. The advanced technology of smartphones can be applied to solve the workload burden of experts.

10.4.4 Future directions

In this study, a POC is provided for the low-cost mobile health for automated detection of epileptic seizures for remote monitoring. A future scope architecture of a remote monitoring system is shown in Fig. 10.4. A wireless EEG headset will be provided to epilepsy patient and continuous real-time EEG signals will be recorded and stored on smartphones. A cross-databases classification model present on the smartphone will classify the EEG signals and the report will be sent to the correspondent physician for further action.



FIGURE 10.4: A future scope architecture of the real-time mobile-based seizure detection and remote monitoring of epilepsy patients.

10.5 Conclusion

The feasibility of a mobile-based app for remote monitoring of epilepsy patients using the database-independent optimized algorithm was shown. The mobile app was made available as open-source software hence it can be reproducible by researchers according to their requirements. It was tested using three different versions of smartphones. The results suggest that smartphones are capable of handling huge EEG data for feature calculation and classification.

Acknowledgment

The authors are grateful to the Department of Clinical Neurophysiology, MUMC+, Maastricht, The Netherlands, and RMCH, Bengaluru, India for providing EEG recordings for research purpose. Authors also grateful to Dr. Ali Shoeb from CHB-MIT and Dr. R. G. Andrzejak from UBonn and team of TUH for permitting to use their database for research.

CHAPTER 11

General Discussion

Automated seizure detection is desirable in analyzing long-term EEG for remote monitoring to improve the quality of life for epilepsy patients. In this thesis, we have proposed a cross-database evaluation for the classification of epileptic seizures using five EEG databases collected from different centers. Such a cross-database approach also helps when insufficient EEG data containing epileptic seizures is available to build a new seizure detection model. The focus of this thesis is to build an algorithm using multiple databases and validate the algorithm on the left out database which can be implemented on mobile platforms for continuous remote monitoring of epilepsy patients. Further, this thesis focuses on an 8-class classification of seizure types using CNN's transfer-learning approach. In the subsequent sections, methodological aspects, FBC, classifier training, the effect of post-processing and comparison with other studies will be discussed. This chapter will be concluded with study limitations, future directions and important concluding remarks of the study.

11.1 Analysis of feature extraction methods

As the first step of our goal, we have proposed three novel features, namely MD, SDI, and sigmoid entropy. Eleven classification problems were considered using the UBonn database to ensure the suitability of the MD feature for the detection of epileptic seizures in Chapter 2. The classification was performed using both equal and unequal numbers of observations. Experimental results show the improvement in performance measures as the matrix order or a segmentation length increases. Finally, this method showed a classification accuracy of 97.56% using the RMCH database that is considered to be a

larger database than UBonn. The results were evident that the determinant of a square matrix can be a potential biomarker for EEG based seizure detection.

With the evidence of MD and wavelet transform, we have proposed a second novel feature called SDI in Chapter 3. This feature was tested on three databases namely RMCH, CHB-MIT, and TUH. As compared to the SDI method, the wavelet-based approach required the selection of mother wavelet and decomposition level for better results at the cost of computational time. SDI method outperformed other methods, namely spectral entropy, approximate entropy, sample entropy, and statistical features, log energy entropy derived from wavelet packet decomposition, and wavelet entropy in terms of computation time and classification results.

Chapter 4 proposed DWT based sigmoid entropy estimated using the wavelet coefficients in each sub-band. Five commonly used wavelets, namely Haar, Coif4, Dmey, Bior3.1, and RBio3.1, were examined and compared with different decomposition levels. Among five different wavelets, Bio3.1 in D4 sub-band, Rbio3.1, and Haar in A5 sub-band, Rbio3.1 in D3 sub-band was found to be the best choice for RMCH, UBonn, and CHB-MIT databases respectively. Further, Dmey wavelet showed the least performance for the UBonn database. The classification results obtained in D5 and A5 sub-bands using the CHB-MIT database was less as compared to other sub-bands. Sigmoid entropy measure for epileptic EEG was found to be lower than normal EEG, which is similar to the methods proposed in [19, 98]. Kappa coefficients obtained from all the databases belong to either a good or very good agreement category.

Complexity analysis and dynamic characteristics of EEG using MODWT

based entropies were studied in Chapter 5. We have investigated MODWT using four different wavelets, namely Haar, Coif4, Dmey, and Sym4 sub-bands until 7 levels. Further, we have explored the potentials of six entropies, namely sigmoid, Shannon, wavelet, Renyi, Tsallis, and SURE entropies in each sub-band.

11.2 Feature baseline correction

The biggest challenges were faced in this thesis while working with the MUMC (Chapter 6) and cross-database (Chapter 7) studies. In the MUMC database, we observed significant baseline feature value differences between the patients which are referred to as inter-patient variability in feature distributions. As a result, the performance of the classification model found to be poor due to the lack of clear separation between seizure and non-seizure features (SDI and MD). It was necessary to correct/update the feature baselines before training the SVM classifier. Previously, similar challenges were overcome by using MDM [20] and ANSFV [162] methods. In Chapter 6, we introduced a novel technique called AM-FBC using the median values of features SDI and MD. Classification results suggest that AM-FBC significantly improved seizure detection by overcoming the inter-subject variability in feature distribution. We observed a significant difference in terms of median values of SDI and MD features before and after AM-FBC.

We observe inter-database variability in feature distributions among five databases while working with cross-database evaluation (Chapter 7). In the RMCH database, SDI feature values for seizure are below the SDI values of

non-seizure from the other four databases. This is also the case for the MD feature values in the RMCH and MUMC databases. First, AM-FBC was applied to update the feature distribution among the patients (scenario was dominant in the MUMC database). Without AM-FBC in the inter-database level, the sensitivity was closed to zero for the RMCH database due to the reason that the seizure EEG feature values of the RMCH database were below the non-seizure EEG feature values in the training databases. Further, the sensitivity achieved for the MUMC database was very poor. Similarly, the specificity was 0 for the UBonn without applying AM-FBC because non-seizure EEG feature values of the UBonn database were above the seizure EEG feature values of the other four databases. Next, feature baseline correction was applied on five databases to correct the inter-database feature distribution variation. Wilcoxon rank-sum test showed significance difference ($p < 0.05$) for each database between seizure and non-seizures activities after applying AM-FBC. The influence of AM-FBC improved sensitivity (RMCH and MUMC) and specificity (UBonn). As a result, this study became the first study reporting cross-database evaluation for automated classification of epileptic seizures.

11.3 Effect of outliers removal

In Chapter 6, we have studied the effect of outliers removal on classification results and loss of diagnostic information. We observed that as the outlier removal factor k increases, the AUC and percentage of loss of feature samples decreases. In other words, the lower the k , the higher the classification results and loss of diagnostic information. As an optimal setting, $k = 1.5$ can be used

for real-time application as that has resulted in better AUC with just 1% of samples lost.

11.4 Effect of post-processing

As reported in [85, 181] post-processing was performed using a 5-tap MAF to the SVM classifier output in Chapters 6 and 7. The goal of post-processing is to reduce false alarms and improve classification results. As a result of post-processing, the false detections were reduced and the output was closely matched with ground truth labels. The length of the MAF for post-processing needs to be chosen properly. If the length of the filter is higher, it tends to a delay in seizure detection and short seizures will be missed out. The lower length of the filter will not improve the classification results but ideal for lower detection delay. In our study, it needs a delay of 10 s (5th order filter x segmentation length of 4 s = 20 s, due to 50% overlap it becomes 10 s data) to produce classification output of MAF. Finally, the classification results revealed that the FDR reduces when post-processing was applied.

11.5 Mobile based seizure monitoring

The proof of concept (POC) for epileptic seizure detection in EEG signals was tested on the Android app which was built using Chaquopy, a Python SDK for Android (Chapter 10). For the same purpose, the cross-database model was converted into Python language from Matlab code. Overall, 20 new epilepsy patients, EEG recording's from the MUMC and RMCH centers were used to evaluate the efficacy of smartphones for EEG signal analysis

and seizure detection. The mobile app was built in such a way to provide information such as the number of channels, sampling frequency, and duration of the complete EEG data file. Further, it estimates the elapsed time required to process the complete EEG file, the number of seizure events detected per channel, and the total number of seizure epochs. The processing capability in terms of the elapsed time of sezeet app shows that the mobile platform is capable of handling huge EEG data and perform feature engineering and machine learning. The computational time required to process the real-time EEG data on smartphone and classification results suggests that mobile-health could be a great asset to monitor epilepsy patients.

11.6 Classification of seizure types

The objective of Chapters 8 and 9 to perform a multi-class classification of epileptic seizure type, which includes simple partial, complex partial, focal non-specific, generalized non-specific, absence, tonic, and tonic-clonic, and non-seizures using CNN and transfer learning. It was implemented using the TUH EEG database using ten pretrained networks. In order to overcome the imbalance issue of CNN, we have generated a balanced dataset using the overlap technique. The transfer learning approach using Alexnet and Googlenet outperformed the extract image features approach. Similarly, classification accuracy gets improved in deeper layers of the pretrained networks due to higher-level features learned by CNN using extract image features approach. However, the performance of the Densenet201 started fluctuating in deeper layer features. ReLU and Conv layers showed the highest accuracy in most of the pretrained networks as compared to other layers using the extract image

feature approach. To the best of the author's knowledge, this is the first of its kind successful study using CNN for classification of seizure type into 8-class in the presence of non-seizure EEG.

11.7 Comparison with literature

Maximum of seven classification problems were considered using UBonn database in previous studies [41, 43, 48, 57, 198, 239]. In Chapter 2, eleven classification problems were considered to evaluate the MD feature. The studies proposed by [28, 38, 41, 42, 43, 45, 48, 49, 50, 52, 58, 59] have applied decomposition techniques to achieve 100% accuracy for the classification problem {A}-{E}, whereas the MD reached the accuracy of 99.45% without the help of any EEG signal decomposition method. For the first time histogram and Bivariate plots have been used to understand the discrimination between seizure and non-seizure EEG groups (refer to Chapter 2).

To the best of the author's knowledge, automated detection of epileptic seizures using SDI on RMCH, CHB-MIT, and TUH databases was the first study that was tested on three different EEG databases and showed consistent results (refer to Chapter 3). SDI feature proved to be superior in terms of classification results and computation time when compared against spectral [81], approximate [27], sample [8], log energy [21], and wavelet [36] entropy methods when implemented on all three databases and classified using the SVM classifier.

Only a few studies [84, 98, 137] have performed both segment and event-based seizure detection approaches and Chapter 4 is one of them. The seizure

detection algorithm using weighted permutation entropy proposed in [98] reports a lower measure for epileptic seizure EEG as compared to normal EEG signal. Further, similar results were obtained in [19] using minimum variance modified fuzzy entropy. In resemblance to [98] and [19], sigmoid entropy measure also exhibited lesser entropy for epileptic EEG than normal EEG in Chapter 4. Further, sigmoid entropy showed the highest classification results as compared to other entropy methods Shannon, Renyi, and Tsallis entropy. Very few studies [150, 151, 152, 153, 154, 155] have investigated MODWT on EEG signal. In Chapter 5, classification results showed that MODWT outperformed DWT using sigmoid entropy.

In terms of novel features proposed in this thesis, MD, SDI, and sigmoid entropies outperformed other feature extraction methods as reported in Chapters 2, 3, 4 and 5. To the best of the author's knowledge, the major highlight is that these proposed techniques were validated on three different databases (only two databases in Chapter 2) which was not reported in any of the previous studies.

Inter-subject variability in feature distribution is one of the biggest challenges in developing a patient-independent seizure detection algorithm. Previously in [178], five feature normalization techniques, namely MDM, mean memory, standard deviation memory, peak detector, and signal range was applied to a line length feature and MDM was outperformed. Further, same MDM technique was applied for seizure detection in [20, 162] and ANSFV technique in [179]. Similar to the above techniques, AM-FBC was proposed in Chapter 6 to overcome the inter-subject variability in feature distribution.

Bogaarts et al. [179] have proposed an algorithm to improve the AUC using ANSFV FBC and a Kalman filter to classifier output for post-processing. Further, Temko et al. [180] proposed post-processing of the SVM classifier output using a central linear MAF. Ahmed et al. [181] suggested a post-processing approach using the MAX operator and MAF that significantly improved the seizure detection results. In [180, 181], post-processing was applied using a 9-tap and 15-tap MAF respectively, which leads to a delay in the final decision of seizure detection. In total, 55 [180, 181], 65 [162] and 103 [20, 84, 179] features were used that leads to the computational expense of the overall algorithm during feature extraction and classification. The results presented in Chapter 6 show that our method with two features outperformed other state-of-the-art methods in terms of classification results. This study also provides the insights into the effect of outlier removal on classification results and loss of diagnostic information which was not reported in previous studies.

All the existing studies have validated their algorithms using cross-validation on the same database and no attempts have been made to extend their work on other databases to test the generalization capability. Even though multiple databases were used in [20, 42, 89, 122] for epileptic seizure classification, the cross-database framework was missing. The biggest contribution of this thesis is that we present the cross-database evaluation for the classification of epileptic seizures using five EEG databases collected from different centers (Chapter 7). To the best of the author's knowledge, this is the

first study reporting on the cross-database evaluation of the classification of epileptic seizures. In order to complete this task, we have framed the pipeline

using MD and SDI features, AM-FBC (in patient and database level), smoothing of the train and test data, and post-processing of the classifier output. The classification results showed that AM-FBC is essential to achieve the generalized results for all the databases by overcoming inter-database variability in feature distribution.

The ultimate goal of this thesis is to provide an optimized database-independent seizure detection model that can be implemented for remote monitoring of epilepsy patients. Few studies have attempted cloud, IoT and smartphones to analyze the EEG and detect seizure epochs. Menshawy et al. [11] have used the server to process the data in terms of preprocessing, feature engineering, and classification, send back the report to doctors and alarm the caretakers in case of seizure found. Cloud computing was effectively used in the studies [225, 231, 233, 235] to perform feature engineering and classification on the cloud. Further, mobile devices like SmartWatch, Embrace Watch, Brain Sentinel, EpiWatch App are in practice which detects only a particular type of seizures [236]. However, the proposed sezeet app is built using the cross-database model from five EEG databases and found to be effective in terms of computational time when tested on three different smartphones. Further, we have focused to utilize the power of the smartphone to implement a complete seizure detection model which eliminates the need for the cloud. Our mobile-based seizure detection model provides the information's like, seizure onset, seizure offset, frequency of seizures, and seizure affected channels. Therefore, our mobile-based approach would be a great tool to monitor epilepsy patients for remote monitoring applications.

11.8 Clinical significance

Remote monitoring of seizures in rural areas at scale requires a combination of automated seizure detection algorithms and affordable mobile health technologies (such as smartphones). We developed improved algorithms for automated seizure detection, validated them in a cross-database approach, and successfully evaluated the feasibility of a smartphone to run these algorithms on a dataset that we consider representative for one-day monitoring. Using our approach, the analysis could be done during nightly charging of the smartphone and results could be uploaded to a patient's personal health record or to a monitoring unit at the physician's site. The cross-database framework helps when sufficient epileptic seizures EEG data is not available to build a new seizure detection model. Further, the classification of seizure types will help to treat the patient either for medication, surgery, vagus nerve stimulation, and deep brain stimulation. We expect results obtained in our thesis will be helpful in the presurgery examination of epilepsy patients. The idea of remote monitoring using the smartphone app will be useful to keep monitor epilepsy patients by analyzing EEG signals collected over a period of time. Smartphones can be used for multi-purpose uses in terms of health-care applications to improve the quality of patients' lives. The advanced technology of smartphones can be applied to solve the workload burden of experts.

11.9 Study limitations

Due to the epileptiform discharges, some times chances of occurring false detections are high. Classification of epileptiform discharges as a third class



FIGURE 11.1: A future scope architecture of the real-time mobile-based seizure detection and remote monitoring of epilepsy patients.

other than seizure and non-seizure will be a great outcome in seizure detection. In terms of the classification of seizure types using CNN, the performance could be even improved for better clinical outcomes. Generating a balanced dataset using the overlap technique to overcome the imbalance issue of CNN might result in redundant data sometime.

11.10 Future directions

At the moment, a proof of concept (POC) is provided in this thesis for the automated detection of epileptic seizures for remote monitoring. A future scope architecture of a remote monitoring system is shown in Fig. 11.1. A wireless EEG headset will be provided to the patient and continuous real-time EEG signals will be recorded and stored on smartphones. A cross-databases classification model present on the smartphone will classify the EEG signals and the report will be sent to the correspondent physician for further action.

More precise classification can be done with a huge amount of seizure EEG data for classifier training. One can attempt to update the classifier model with

the expert review when the new EEG data classified as a seizure. In the case of false detection, the EEG epoch can be excluded from the training dataset. As a result, the optimized robust classification model can be obtained using an updated training dataset. The biggest challenge in seizure detection is artifacts and epileptiform discharges. An introduction of a classification model to classify seizure, non-seizure, artifacts and epileptiform discharges provided huge labeled data will help experts in reducing false detections. As we have used SDI and MD for cross-database evaluation, one can include sigmoid entropy to improve the performance. Further, hardware implementation or integrating classification model to the EEG system will be a great asset to improve the treatment procedure.

11.11 Conclusion

We would like to conclude the thesis with the following findings.

1. Epileptic seizure detection was significantly improved with novel features when validated on multiple EEG databases.
2. Wavelet-based studies showed the effect of decomposition level and mother wavelets. Further, complexity analysis and dynamic characteristics were explored in terms of energy and entropy in different levels of MODWT.
3. We observed that the lower the outlier removal factor improved the seizure detection performance at the cost of loss of feature samples.

4. For cross-database evaluation, AM-FBC plays a significant role in improving seizure detection results by overcoming inter-database variation of feature distribution.
5. Post-processing on classifier output showed improved classification results by reducing false detection.
6. Classification of seizure types using CNN based transfer learning and extract image feature approach with various pretrained models showed better classification accuracy.
7. Finally, mobile-based EEG analysis for seizure detection using a cross-database algorithm was successfully evaluated for remote monitoring of epilepsy patients. The app source code is made available as an open-source to improve the reproducibility of our results.

CHAPTER 12

Summary

In this thesis, we focused on database-independent, cross-database evaluation of classification of seizure for remote monitoring of epilepsy patients along with the multi-class classification of epileptic seizures. In this thesis, we contribute novel features and the FBC method to the scientific community.

Chapter 1 gives the general introduction about the thesis including problem statement, objective, and outline of the thesis. In Chapters 2 and 3, we showed that the MD and SDI features are computationally efficient against state-of-the-art methods and suitable for seizure detection. Wavelet-based entropies were studied and optimal sub-bands using different mother wavelets were identified for seizure detection in Chapters 4 and 5. Following the previous results of SDI and MD, in Chapter 6, we proposed AM-FBC to overcome the inter-subject variability in feature distribution. Finally, a cross-database evaluation was performed in Chapter 7 using five EEG databases collected from different centers. We used AM-FBC to overcome the inter-databases variability in feature distribution, smoothing of train and test data and post-processing to achieve significant results. The cross-database model was used to build a mobile-based EEG analysis for seizure monitoring. Chapter 9 describes transfer learning and CNN based multi-class classification of seizure types. Overall, extract the image features approach outperformed the transfer learning approach. Finally, this thesis is concluded with the feasibility of a mobile-based app for remote monitoring of epilepsy patients using the database-independent optimized algorithm in Chapter 10.

The results of this thesis contribute towards the clinical aspect in terms of reducing the neurologist burden in reviewing long-term EEG, speed up the treatment procedure and monitor epilepsy patients using a mobile app.

Samenvatting

In dit proefschrift hebben we ons gericht op database-onafhankelijke, databaseoverschrijdende evaluatie ten behoeve van classificatie van epileptische aanvallen voor remote monitoring bij epilepsiepatiënten.

Hoofdstuk 1 geeft de algemene inleiding over de scriptie inclusief probleemstelling, doelstelling en overzicht van de scriptie. In de Hoofdstukken 2 en 3 hebben we aangetoond dat de MD- en SDI-functies rekenkundig efficiënt zijn en geschikt voor automatische aanvals detectie. Op wavelet gebaseerde entropieën werden bestudeerd en geoptimaliseerde subbanden met behulp van verschillende moederwavelets werden geïdentificeerd voor aanvalssdetectie in Hoofdstukken 4 en 5. In navolging van de eerdere resultaten van SDI en MD, in Hoofdstuk 6, stelden we AM-FBC voor om de variabiliteit tussen de onderwerpen in de distributie van functies te ondervangen. Ten slotte werd een databaseoverschrijdende evaluatie uitgevoerd in Hoofdstuk 7 met behulp van vijf EEG-databases verzameld uit verschillende centra. We hebben AM-FBC gebruikt om de interdatabase-variabiliteit bij de distributie van functies, en het trainen en testen van gegevens en nabewerking te verbeteren om significante resultaten te bereiken. Het cross-database model werd gebruikt om een mobiele toepassing voor EEG-analyse te bouwen. Hoofdstuk 9 beschrijft transfer learning en CNN-gebaseerde multi-class classificatie of aanvals types. Ten slotte wordt dit proefschrift afgesloten met de haalbaarheid van een mobiele app voor monitoring op afstand in epilepsiepatiënten met behulp van het database-onafhankelijke geoptimaliseerde algoritme in Hoofdstuk 10.

Valorization

The existing EEG monitoring systems which include video EEG and ambulatory EEG is not affordable to an epilepsy patient due to its cost [240, 241]. When considering remote monitoring of epilepsy patients in rural places of India, the cost is always the biggest issue. The goal of this thesis is to develop cost-effective mobile-based remote monitoring of epilepsy patients using database-independent optimized algorithms and classification of seizure types. As we know that, manual inspection of long term EEG is time-consuming, tedious, prone to error and expert dependent. Therefore, automated detection of epileptic seizures has an impact on reducing the workload of a neurologist who reviews the long-term EEG during the evaluation of patients with epilepsy. Mobile-based system build using a cross-database algorithm will also help to keep monitor the epilepsy patients in terms of frequency of seizures, seizure onset and to warn the caretakers and doctors in case of emergency. The classification results achieved using cross-database evaluation were appreciable for clinical trials and it is the first of its kind study proposed using five EEG databases. The cross-database evaluation can also lead to cost reduction and time saving as developing a new algorithm is not required for new EEG databases. The classification of seizure types using EEG signals will be a great tool for doctors to take further clinical action on epilepsy patients.

The algorithms developed in this thesis can be made as software packages to run on hospitals. Further, it can also be associated with EEG recording systems as analysis software for real-time seizure detection. Such a compact

model can be installed at RMCH and MUMC hospitals for real-time monitoring.

As we have shown mobile-based seizure monitoring, in the future, EEG can be recorded using EEG headset and can be sent to mobile for analysis and reports can be shared with doctors for further clinical action. Such a system will be able to move epilepsy patients from hospital or ICU to the external environment and real-time monitoring can be done.

As we have proposed a model to overcome inter-database variability to work with multiple databases, AM-FBC can also be applied to other EEG or any physiological signals related to studies to build a robust and generalized algorithm. Such attempts will lead to having more training datasets for any classification model which is essential in machine learning.

Acknowledgments

First and foremost, I wish to place on records my heartfelt and sincere thanks to my supervisor Prof. N Sriraam for providing me an opportunity to do research under his guidance. I appreciate his contributions of time and ideas to make my work productive and stimulating. I would like to express my special appreciation and thanks to my advisor Dr. Pieter L Kubben, you have been a tremendous mentor for me. I would like to thank both Prof. N Sriraam and Dr. Pieter L Kubben for encouraging my research and for allowing me to grow as a research scientist. Your advice on both research as well as on my career have been priceless.

I am extremely grateful to Prof. dr. Yasin Temel for giving me an opportunity in his research team at MUMC. I am also very grateful to Dr. Erik D Gommer and Dr. Danny DW Hilkmann for being part of my thesis and for valuable guidance. I will forever be thankful to Dr. A S Hegde and Mr. Anjan Kumar for constant support in terms of patient data and clinical advice. Very special gratitude goes to Dr. Shyam Vasudeva Rao for trusting and giving an opportunity at MUMC.

I am also grateful to the following Maastricht University staff Dorine Collijn, Ankie Hochstenbach, Tom van den Crommenacker, Xavier Michael and department colleagues for constant support during my visit to Maastricht.

I thank the management of Ramaiah Institute of Technology, Department of Medical Electronics, colleagues and my friends at Institute. A heartfelt thanks to my supportive wonderful mentor and friend Prabhu Ravikla Vittal

for being my support in the moments of difficulties in this journey.

To my friends and colleagues, thank you for listening, offering me advice, and supporting me through this entire process. Special thanks to Rama Reddy, Prashant Pai, Priyanka Pai, Chandana S, Purnima, Tejaswini S and Uma Arun. There is no way to express how much it meant to me to have been a student of Pradeep Kumar G, you have been motivated me to become a researcher.

A special thanks to my family for their unconditional trust, timely encouragement, and endless patience. Words cannot express how grateful I am to my mother Lalithamma, father Shivarudhrappa, sister Sowmya, brother-in-law Manjunath, and niece Harshitha and Parinitha for the sacrifices that they have made on my behalf. A special thanks to Mrs. Geetha Rudrappa and his family members (Manjunath and Pavan) for constant support during my journey. I am also grateful to my other family members and friends who have supported me along the way.

Finally, I would like to thank, Google, Wikipedia, Mathworks Central, Stack Overflow, GitHub, Medium, Analytics Vidhya, Grammarly and Microsoft Word's spell checker.

Thanks for all your encouragement!

Curriculum Vitae



Raghu was born in 1988 in Bengaluru, India. He received his second master's (M.Tech.) in Communication System from Christ University Faculty of Engineering in 2016 and first master's (M.Sc.) degree from Bangalore University in 2011. He worked as a Research Associate at the Center for Medical Electronics and Computing, Ramaiah Institute of Technology, Bengaluru, India, from April 2016 to April 2017. During that time, he worked on the application of machine learning for a biomedical signal. He had received the best project award for his master's (M.Tech.) thesis. His research includes biomedical signal processing, machine learning, and epilepsy.

He continued his interest in research and enrolled in a Ph.D. at School for Mental Health and Neuroscience of the Faculty of Health, Medicine, and Life Sciences, Maastricht University, The Netherlands, through Ramaiah Institute of Technology.

He served as student Chair at 1st IEEE EMBS International Student Conference 2018 India which was held from 19th to 21st December 2018.

Raghu is currently working as Data Scientist at BuddhiMed Technologies, Bengaluru.

Publications

1. S Raghu, Natarajan Sriraam, Alangar Sathyaranjan Hegde, Pieter L Kubben, “A novel approach for classification of epileptic seizures using matrix determinant”, *Expert Systems with Applications*, Elsevier, 2019, vol. 127, pp. 323-341, 2019.
<https://doi.org/10.1016/j.eswa.2019.03.021>
2. S Raghu, Natarajan Sriraam, Shyam Vasudeva Rao, Alangar Satyaranjandas Hegde, Pieter L Kubben, “Automated detection of epileptic seizures using successive decomposition index and support vector machine classifier in long-term EEG”, *Neural Computing and Applications*, Springer, vol. 32, pp. 8965-8984, 2020.
<https://doi.org/10.1007/s00521-019-04389-1>
3. S Raghu, Natarajan Sriraam, Yasin Temel, Shyam Vasudeva Rao, Alangar Satyaranjandas Hegde, Pieter L Kubben, “Performance evaluation of DWT based sigmoid entropy in time and frequency domains for automated detection of epileptic seizures using SVM classifier”, *Computers in Biology and Medicine*, Elsevier, vol. 110, pp. 127-143, 2019.
<https://doi.org/10.1016/j.combiomed.2019.05.016>
4. S Raghu, Natarajan Sriraam, Yasin Temel, Shyam Vasudeva Rao, Alangar Satyaranjandas Hegde, Pieter L Kubben, “Complexity analysis and

dynamic characteristics of EEG using MODWT based entropies for identification of seizure onset”, *The Journal of Biomedical Research*, vol. 34, no. 3, pp. 211-225, 2019.

<http://www.jbr-pub.org.cn/article/doi/10.7555/JBR.33.20190021>

5. S Raghu, Natarajan Sriraam, Yasin Temel, Shyam Vasudeva Rao, Pieter L Kubben, “A convolutional neural network based framework for classification of seizure types”, 2019 41st Annual International Conference of the IEEE Engineering in Medicine and Biology Society (EMBC), Berlin, Germany, 2019, pp. 2547-2550.

<https://ieeexplore.ieee.org/abstract/document/8857359>

6. S Raghu, Natarajan Sriraam, Erik D Gommer, Danny M W Hilkmann, Yasin Temel, Shyam Vasudeva Rao, Pieter L Kubben, “Adaptive median feature baseline correction for improving recognition of epileptic seizures in ICU EEG”, *Neurocomputing*, Elsevier, vol. 407, pp. 385-398, 2020.

<https://doi.org/10.1016/j.neucom.2020.04.144>

7. S Raghu, Natarajan Sriraam, Erik D Gommer, Danny M W Hilkmann, Yasin Temel, Shyam Vasudeva Rao, Alangar Satyaranjandas Hegde, Pieter L Kubben, “Cross-database evaluation of EEG based epileptic seizures detection driven by adaptive median feature baseline correction”, *Clinical neurophysiology*, Elsevier, vol. 131, no. 7, pp. 1567-1578, 2020.

<https://doi.org/10.1016/j.clinph.2020.03.033>

8. S Raghu, Natarajan Sriraam, Yasin Temel, Shyam Vasudeva Rao, Pieter L Kubben, “EEG based multi-class seizure type classification using convolutional neural network and transfer learning”, *Neural Networks*, Elsevier, vol. 124, pp. 202-212, 2020.
<https://doi.org/10.1016/j.neunet.2020.01.017>
9. S Raghu, Natarajan Sriraam, Erik D Gommer, Danny M W Hilkman, Yasin Temel, Shyam Vasudeva Rao, Alangar Satyaranjandas Hegde, Pieter L Kubben, “Application of low-cost mobile health for remote monitoring of epilepsy patients”, Under review.
10. S Raghu, Natarajan Sriraam, Pieter L Kubben, Yasin Temel, Shyam Vasudeva Rao, Alangar Satyaranjandas Hegde, “A novel approach for automated classification of epileptic seizures using successive decomposition index in long-term EEG”, Poster presentation at EURON PhD days 2018, September 13-14 at the UCL in Brussels.
11. Natarajan Sriraam, S Raghu, Yasin Temel, Shyam Vasudeva Rao, Alangar Satyaranjandas Hegde, JV Mahendra, Pieter L Kubben, “Automated detection of epileptic seizures using DWT based features and SVM classifier,” 2019 2nd International Conference on Signal Processing and Communication (ICSPC), Coimbatore, India, 2019, pp. 263-266.
<https://ieeexplore.ieee.org/document/8976611>

Contact and Website



`raghu.sidida@gmail.com`

`r.raghu@maastrichtuniversity.nl`



`https://www.linkedin.com/in/raghu-s-21832436`



`https://github.com/Raghu17s`



`https://www.researchgate.net/profile/Raghu_Shivarudhrappa`



`https://scholar.google.co.in/citations?user=bEXEuwoAAAAJ`



<https://www.facebook.com/raghu.sidda>



https://www.instagram.com/im_raghul7s

Bibliography

- [1] J. I. Sirven. (2017). What is epilepsy? (Accessed: 01.02.2018), [Online]. Available: <https://www.epilepsy.com/learn/about-epilepsy-basics/what-epilepsy>.
- [2] J. Gotman, “Automatic recognition of epileptic seizures in the EEG”, *Electroencephalography and Clinical Neurophysiology*, vol. 54, pp. 530–540, 1982.
- [3] E. Niedermeyer and F. Silva, *Electroencephalography : basic principles, clinical applications, and related fields*, 5th ed. Philadelphia, London, Lippincott Williams and Wilkins, 2005, ISBN: 0781751268.
- [4] V. Salanova, T. Witt, R. Worth, T. R. Henry, R. E. Gross, J. M. Nazaro, and et al, “Long-term efficacy and safety of thalamic stimulation for drug-resistant partial epilepsy”, *Neurology*, vol. 84, pp. 1017–1025, 2015.
- [5] R. S. Fisher, J. H. Cross, J. A. French, N. Higurashi, E. Hirsch, F. E. Jansen, and et al, “Operational classification of seizure types by the international league against epilepsy: Position paper of the ilae commission for classification and terminology”, *Epilepsia*, vol. 58, no. 4, pp. 522–530, 2017. DOI: [10.1111/epi.13670](https://doi.org/10.1111/epi.13670).
- [6] W. T. Blume and M. Kaibara, *Atlas of pediatric electroencephalography*, 2nd ed. Philadelphia, Pa. : Lippincott-Raven, 1999, ISBN: 0781714346.

- [7] H. Blumenfeld, “Impaired consciousness in epilepsy”, *The Lancet Neurology*, vol. 11, no. 9, pp. 814–826, 2012.
- [8] C. P. Shen, S. T. Liu, W. Z. Zhou, F. S. Lin, A. Y. Y. Lam, H. Y. Sung, and et al, “A physiology-based seizure detection system for multichannel EEG”, *PLOS ONE*, vol. 8, pp. 1–9, Jun. 2013.
- [9] U. R. Acharya, S. V. Sree, A. P. C. Alvin, and J. S. Suri, “Use of principal component analysis for automatic classification of epileptic EEG activities in wavelet framework”, *Expert Systems with Applications*, vol. 39, no. 10, pp. 9072–9078, 2012.
- [10] B. Greene, S. Faul, W. Marnane, G. Lightbody, I. Korotchikova, and G. Boylan, “A comparison of quantitative EEG features for neonatal seizure detection”, *Journal of Clinical Neurophysiology*, vol. 119, no. 6, pp. 1248–61, 2008.
- [11] M. El-Menshawy, A. Benharref, and M. A. Serhani, “An automatic mobile-health based approach for EEG epileptic seizures detection”, *Expert Systems with Applications*, vol. 42, pp. 7157–7174, 2015.
- [12] A. Pietrangelo. (2017). Everything you need to know about epilepsy. (Accessed: 14.02.2018), [Online]. Available: <https://www.healthline.com/health/epilepsy>.
- [13] S. C. Schachter and J. I. Sirven. (2017). EEG. (Accessed: 01.02.2018), [Online]. Available: <https://www.epilepsy.com/learn/diagnosis/eeg>.

- [14] D. Y. Ko. (2017). Epileptiform discharges. (Accessed: 04.02.2018), [Online]. Available: <https://emedicine.medscape.com/article/1138880-overview>.
- [15] R. S. Fisher and et al., “Operational classification of seizure types by the international league against epilepsy: Position paper of the ilae commission for classification and terminology.”, *Epilepsia*, vol. 58 4, pp. 522–530, 2017.
- [16] I. E. Scheffer and et al., “ILAE classification of the epilepsies: Position paper of the ILAE commission for classification and terminology”, *Epilepsia*, vol. 58 4, pp. 512–521, 2017.
- [17] S. Roy, U. Asif, J. Tang, and S. Harrer, “Machine learning for seizure type classification: Setting the benchmark”, *ArXiv*, vol. abs/1902.01012, 2019.
- [18] U. R. Acharya, H. Fujita, V. K. Sudarshan, S. Bhat, and J. E. Koh, “Application of entropies for automated diagnosis of epilepsy using EEG signals: A review”, *Knowledge Based Systems*, vol. 88, pp. 85–96, 2015.
- [19] S. Raghu, N. Sriraam, G. P. Kumar, and A. S. Hegde, “A novel approach for real time recognition of epileptic seizures using minimum variance modified fuzzy entropy”, *IEEE Transactions on Biomedical Engineering*, vol. 65, pp. 2612–262, 2018.
- [20] J. G. Bogaarts, D. M. W. Hilkmann, E. D. Gommer, V. H. J. M. van Kranen-Mastenbroek, and J. P. H. Reulen, “Improved epileptic seizure

- detection combining dynamic feature normalization with EEG novelty detection”, *Medical and Biological Engineering and Computing*, vol. 54, no. 12, pp. 1883–1892, 2016.
- [21] S. Raghu, N. Sriraam, and G. P. Kumar, “Classification of epileptic seizures using wavelet packet log energy and norm entropies with recurrent Elman neural network classifier”, *Cognitive Neurodynamics*, vol. 11, pp. 51–66, 2016.
- [22] U. R. Acharya, S. V. Sree, G. Swapna, R. J. Martis, and J. S. Suri, “Automated EEG analysis of epilepsy: A review”, *Knowledge Based Systems*, vol. 45, pp. 147–165, 2013.
- [23] V. Kecman, *Learning and Soft Computing*. MIT Press, Cambridge, 2011, ISBN: 9780262527903.
- [24] H. Qu and J. Gotman, “A patient-specific algorithm for the detection of seizure onset in long-term EEG monitoring: Possible use as a warning device”, *IEEE Transactions on Biomedical Engineering*, vol. 44, pp. 115–122, 1997.
- [25] N. Sriraam and S. Raghu, “Classification of focal and non focal epileptic seizures using multi-features and SVM classifier”, *Journal of Medical Systems*, vol. 41, no. 10, p. 160, 2017.
- [26] A. M. Murro, D. W. King, J. R. Smith, B. B. Gallagher, H. F. Flanigin, and K. Meador, “Computerized seizure detection of complex partial seizures”, *Electroencephalography and Clinical Neurophysiology*, vol. 79, no. 4, pp. 330–333, 1991.

- [27] V. Srinivasan, C. Eswaran, and N. Sriraam, “Approximate entropy-based epileptic EEG detection using artificial neural networks”, *IEEE Transactions on Information Technology in Biomedicine*, vol. 11, pp. 288–295, 2007.
- [28] K. Samiee, S. Kiranyaz, M. Gabbouj, and T. Saramaki, “Long-term epileptic EEG classification via 2D mapping and textural features”, *Expert Systems with Applications*, vol. 42, no. 20, pp. 7175–7185, 2015.
- [29] S. V. Gigola, F. Ortiz, C. E. D’Attellis, W. Silva, and S. Kochen, “Prediction of epileptic seizures using accumulated energy in a multiresolution framework”, *Journal of Neuroscience Methods*, vol. 138, pp. 107–111, 2004.
- [30] M. Islam, A. Rastegarnia, and Z. Yang, “A wavelet-based artifact reduction from scalp EEG for epileptic seizure detection”, vol. 99, pp. 1–10, 2016.
- [31] W. Zhou, Y. Liu, Q. Yuan, and X. Li, “Epileptic seizure detection using lacunarity and Bayesian linear discriminant analysis in intracranial EEG”, *IEEE Transactions on Biomedical Engineering*, vol. 60, no. 12, pp. 3375–3381, 2013.
- [32] S. Raghunathan, A. Jaitli, and P. P. Irazoqui, “Multistage seizure detection techniques optimized for low-power hardware platforms”, *Epilepsy and behavior*, vol. 22, S61–S68, 2011.
- [33] R. G. Andrzejak, K. Lehnertz, F. Mormann, C. Rieke, P. David, and C. E. Elger, “Indications of nonlinear deterministic and finite-dimensional

structures in time series of brain electrical activity: Dependence on recording region and brain state”, *Physical Review Edition*, vol. 64, p. 061 907, 6 2001.

- [34] S. Bhattacharyya, A. Biswas, J. Mukherjee, A. K. Majumdar, B. Majumdar, S. Mukherjee, and A. K. Singh, “Feature selection for automatic burst detection in neonatal electroencephalogram”, *IEEE Journal on Emerging and Selected Topics in Circuits and Systems*, vol. 1, pp. 469–479, 2011.
- [35] K. Zeng, J. Yan, Y. Wang, A. Sik, G. Ouyang, and X. Li, “Automatic detection of absence seizures with compressive sensing EEG”, *Neurocomputing*, vol. 171, pp. 497–502, 2016.
- [36] S. Pravin Kumar, N. Sriraam, P. G. Benakop, and B. C. Jinaga, “Entropies based detection of epileptic seizures with artificial neural network classifiers”, *Expert Systems with Applications*, vol. 37, pp. 3284–3291, 2010.
- [37] S. Aydın, H. M. Saraoglu, and S. Kara, “Log energy entropy-based EEG classification with multilayer neural networks in seizure”, *Annals of Biomedical Engineering*, vol. 37, pp. 2626–2630, 2009.
- [38] A. T. Tzallas, M. G. Tsipouras, and D. I. Fotiadis, “Automatic seizure detection based on time-frequency analysis and artificial neural networks”, *Computational Intelligence and Neuroscience*, vol. 2007, pp. 313–333, 2007.

- [39] U. R. Acharya, S. L. Oh, Y. Hagiwara, J. H. Tan, and H. Adeli, “Deep convolutional neural network for the automated detection and diagnosis of seizure using EEG signals”, *Computers in Biology and Medicine*, vol. 100, pp. 270–278, 2018, ISSN: 0010-4825.
- [40] A. Zahra, N. Kanwal, N. ur Rehman, S. Ehsan, and K. D. McDonald-Maier, “Seizure detection from EEG signals using multivariate empirical mode decomposition”, *Computers in biology and medicine*, vol. 88, pp. 132–141, 2017.
- [41] A. Bhardwaj, A. Tiwari, M. R. Krishna, and M. V. Varma, “A novel genetic programming approach for epileptic seizure detection”, *Computer methods and programs in biomedicine*, vol. 124, pp. 2–18, 2016.
- [42] D. Chen, S. Wan, and F. S. Bao, “Epileptic focus localization using discrete wavelet transform based on interictal intracranial EEG”, *IEEE Transactions on Neural Systems and Rehabilitation Engineering*, vol. 25, pp. 413–425, 2017.
- [43] A. R. Hassan, S. Siuly, and Y. Zhang, “Epileptic seizure detection in EEG signals using tunable-q factor wavelet transform and bootstrap aggregating”, *Computer Methods and Programs in Biomedicine*, vol. 137, pp. 247–259, 2016.
- [44] M. Sharma, R. B. Pachori, and U. R. Acharya, “A new approach to characterize epileptic seizures using analytic time-frequency flexible wavelet transform and fractal dimension”, *Pattern Recognition Letters*, vol. 94, pp. 172–179, 2017.

- [45] A. B. Das, M. I. H. Bhuiyan, and S. M. S. Alam, “Classification of EEG signals using normal inverse Gaussian parameters in the dual-tree complex wavelet transform domain for seizure detection”, *Signal, Image and Video Processing*, vol. 10, no. 2, pp. 259–266, 2016.
- [46] M. Peker, B. Sen, and D. Delen, “A novel method for automated diagnosis of epilepsy using complex-valued classifiers”, *IEEE Journal of Biomedical and Health Informatics*, vol. 20, pp. 108–118, 2016.
- [47] Y. Kumar, M. Dewal, and R. Anand, “Epileptic seizures detection in EEG using DWT-based ApEn and artificial neural network”, *Signal, Image and Video Processing*, vol. 8, pp. 1323–1334, 2014.
- [48] C. Kamath, “Teager energy based filter-bank cepstra in EEG classification for seizure detection using radial basis function neural network”.
- [49] Z. R. Zamir, “Detection of epileptic seizure in EEG signals using linear least squares preprocessing”, *Computer Methods and Programs in Biomedicine*, vol. 133, pp. 95–109, 2016.
- [50] L. X. Guo, D. Rivero, and A. Pazos, “Epileptic seizure detection using multiwavelet transform based approximate entropy and artificial neural networks”, *Journal of Neuroscience Methods*, vol. 193, pp. 156–163, 2010.
- [51] H. Ocak, “Optimal classification of epileptic seizures in EEG using wavelet analysis and genetic algorithm”, *Signal Processing*, vol. 88, pp. 1858–1867, 2008.

- [52] F. Riaz, A. Hassan, S. Rehman, I. K. Niazi, and K. Dremstrup, “Emd-based temporal and spectral features for the classification of EEG signals using supervised learning”, *IEEE Transactions on Neural Systems and Rehabilitation Engineering*, vol. 24, pp. 28–35, 2016.
- [53] M. Diykh, Y. Li, and P. Wen, “Classify epileptic EEG signals using weighted complex networks based community structure detection”, *Expert Systems with Applications*, vol. 90, pp. 87–100, 2017.
- [54] A. A. Yusuff, A. A. Jimoh, and J. L. Munda, “Determinant-based feature extraction for fault detection and classification for power transmission lines”, *IET Generation*, vol. 5, pp. 1259–1267, 2011.
- [55] B. P. G. Salgado and V. I. Ponomaryov, “Feature extraction scheme for a textural hyperspectral image classification using gray-scaled HSV and NDVI image features vectors fusion”, *2016 International Conference on Electronics, Communications and Computers (CONIELECOMP)*, pp. 186–191, 2016.
- [56] M. Zhou and et al., “Epileptic seizure detection based on EEG signals and CNN”, *Front. Neuroinform.*, vol. 12, pp. 1–14, 2018.
- [57] I. Ullah, E. ul Haq Qazi, and H. A. Aboalsamh, “An automated system for epilepsy detection using EEG brain signals based on deep learning approach”, *Expert Systems with Applications*, vol. 107, pp. 61–71, 2018.

- [58] T. Zhang and W. Chen, “LMD based features for the automatic seizure detection of EEG signals using SVM”, *IEEE Transactions on Neural Systems and Rehabilitation Engineering*, vol. 25, pp. 1100–1108, 2017.
- [59] A. S. M. Murugavel and S. Ramakrishnan, “Hierarchical multi-class SVM with ELM kernel for epileptic EEG signal classification”, *Medical and Biological Engineering and Computing*, vol. 54, pp. 149–161, 2015.
- [60] L. Andrews, *Special functions of mathematics for engineers*. Oxford Science, Jul. 1997, ISBN: 9780819483713.
- [61] Online. (2017). Linear algebra. Accessed: 16.06.2017, [Online]. Available: <https://people.richland.edu/james/lecture/m116/matrices/determinant.html>.
- [62] X. Wang and E. Serpedin, “An overview on the applications of matrix theory in wireless communications and signal processing”, *Algorithms*, vol. 9, p. 68, 2016.
- [63] J. F. Grcar, “How ordinary elimination became gaussian elimination”, vol. 38, pp. 163–218, 2011.
- [64] D. Harville, *Matrix algebra from a statisticians perspective*. Springer, 2001, ISBN: 978-1-4613-0181-3.
- [65] S. Raghu and N. Sriraam, “Classification of focal and non-focal EEG signals using neighborhood component analysis and machine learning algorithms”, *Expert Systems with Applications*, vol. 113, pp. 18 –32, 2018, ISSN: 0957-4174.

- [66] S Raghu and N Sriraam, “Optimal configuration of multilayer perceptron neural network classifier for recognition of intracranial epileptic seizures”, *Expert Systems with Applications*, vol. 89, pp. 205–221, 2017.
- [67] N. Sriraam, K. Tamanna, L. Narayan, M. Khanum, S. Raghu, A. S. Hegde, and A. B. Kumar, “Multichannel EEG based inter-ictal seizures detection using Teager energy with backpropagation neural network classifier”, *Australasian Physical and Engineering Sciences in Medicine*, vol. 41, pp. 1047–1055, 2018.
- [68] N. Sriraam, S. Raghu, K. Tamanna, L. Narayan, M. Khanum, A. S. Hegde, and A. B. Kumar, “Automated epileptic seizures detection using multi-features and multilayer perceptron neural network”, 2018.
- [69] T. M. Mitchell, *Machine Learning*. McGraw-Hill, 1997.
- [70] Z. Tang and R. Li, “An improved neural network model and its applications”, *Journal of Information and Computing Science*, vol. 8, 1881–1888, 2011.
- [71] T. Fawcett, “An introduction to ROC analysis”, *Pattern Recognition Letters*, vol. 27, no. 8, pp. 861–874, 2006, ROC Analysis in Pattern Recognition.
- [72] A. Cichocki and S. Vorobyov, “Application of ICA for automatic noise and interference cancellation in multisensory biomedical signals.”, *Proceeding in Second International Workshop on ICA and BSS*, pp. 621–626, 2000.

- [73] T. K. Gandhi, B. K. Panigrahi, and S. Anand, “A comparative study of wavelet families for EEG signal classification”, *Neurocomputing*, vol. 74, pp. 3051–3057, 2011.
- [74] N. Nicolaou and J. Georgiou, “Detection of epileptic electroencephalogram based on permutation entropy and support vector machines”, *Expert Systems with Applications*, vol. 39, pp. 202–209, 2012.
- [75] M. Sharma, A. A. Bhurane, and U. R. Acharya, “MMSFL-OWFB: A novel class of orthogonal wavelet filters for epileptic seizure detection”, *Knowl.-Based Syst.*, vol. 160, pp. 265–277, 2018.
- [76] Y. Kaya, M. Uyar, R. Tekin, and S. Yildirim, “1D-local binary pattern based feature extraction for classification of epileptic EEG signals”, *Applied Mathematics and Computation*, vol. 243, pp. 209–219, 2014.
- [77] A. R. Hassan and A. Subasi, “Automatic identification of epileptic seizures from EEG signals using linear programming boosting”, *Computer Methods and Programs in Biomedicine*, vol. 136, pp. 65 –77, 2016.
- [78] U. Orhan, M. Hekim, and M. Ozer, “EEG signals classification using the k-means clustering and a multilayer perceptron neural network model”, *Expert Systems with Applications*, vol. 38, no. 10, pp. 13475–13481, 2011, ISSN: 0957-4174.
- [79] H. Adeli, Z. Zhou, and N. Dadmehr, “Analysis of EEG records in an epileptic patient using wavelet transform”, *Journal of Neuroscience Methods*, vol. 123, no. 1, pp. 69 –87, 2003.

- [80] U. R. Acharya, F. Molinari, S. V. Sree, S. Chattopadhyay, K.-H. Ng, and J. S. Suri, “Automated diagnosis of epileptic EEG using entropies”, *Biomedical Signal Processing and Control*, vol. 7, no. 4, pp. 401–408, 2012, ISSN: 1746-8094.
- [81] V. Srinivasan, C. Eswaran, and N. Sriraam, “Artificial neural network based epileptic detection using time-domain and frequency-domain features”, *Journal of Medical Systems*, vol. 29, pp. 647–660, 2005.
- [82] M. Sharma, A. Dhere, R. B. Pachori, and U. R. Acharya, “An automatic detection of focal EEG signals using new class of time–frequency localized orthogonal wavelet filter banks”, *Knowledge Based Systems*, vol. 118, pp. 217–227, 2017.
- [83] S. Raghu, N. Sriraam, Y. Temel, S. V. Rao, A. S. Hegde, and P. L. Kubben, “Performance evaluation of DWT based sigmoid entropy in time and frequency domains for automated detection of epileptic seizures using SVM classifier”, *Computers in Biology and Medicine*, vol. 110, pp. 127–143, 2019.
- [84] G. Bogaarts, E. D. Gommer, D. M. W. Hilkmann, V. van Kranen-Mastenbroek, and J. P. H. Reulen, “Optimal training dataset composition for SVM-based, age-independent, automated epileptic seizure detection”, *Medical and Biological Engineering and Computing*, vol. 54, pp. 1285–1293, 2016.
- [85] A. Temko, E. Thomas, W. Marnane, G. Lightbody, and G. Boylan, “EEG-based neonatal seizure detection with support vector machines”, *Clinical Neurophysiology*, vol. 122, pp. 464–473, 2011.

- [86] P. Mirowski, D. Madhavan, Y. LeCun, and R. Kuzniecky, “Classification of patterns of EEG synchronization for seizure prediction”, *Clinical Neurophysiology*, vol. 120, no. 11, pp. 1927–1940, 2009.
- [87] E. Pippa, E. I. Zacharaki, I. Mporas, V. Tsirka, M. P. Richardson, and Michael, “Improving classification of epileptic and non-epileptic EEG events by feature selection”, *Neurocomputing*, vol. 171, pp. 576–585, 2016.
- [88] A. Shoeb, H. Edwards, J. Connolly, B. Bourgeois, S. T. Treves, and J. Guttag, “Patient-specific seizure onset detection”, *Epilepsy and Behavior*, vol. 5, no. 4, pp. 483–498, 2004.
- [89] S Raghunath, N. Sriraam, A. S. Hegde, and P. L. Kubben, “A novel approach for classification of epileptic seizures using matrix determinant”, *Expert Systems with Applications*, vol. 127, no. 1, pp. 323–341, 2019, ISSN: 0957-4174.
- [90] P. Zhou and K. C. C. Chan, “Fuzzy feature extraction for multichannel EEG classification”, *IEEE Transactions on Cognitive and Developmental Systems*, vol. 10, no. 2, pp. 267–279, 2018.
- [91] M. BalaKrishnan, P. Colditz, and B. Boashash, “A multi-channel fusion based new-born seizure detection”, *J. Biomedical Science and Engineering*, vol. 7, pp. 533–545, 2014.
- [92] A. Subasi, J. Kevric, and M. Abdullah Canbaz, “Epileptic seizure detection using hybrid machine learning methods”, *Neural Computing and Applications*, pp. 1–9, 2017.

- [93] M. Li, W. Chen, and T. Zhang, “FuzzyEn-based features in FrFT-WPT domain for epileptic seizure detection”, *Neural Computing and Applications*, pp. 1–14, 2018. DOI: <https://doi.org/10.1007/s00521-018-3621-z>.
- [94] N. Mammone, G. Inuso, F. La Foresta, M. Versaci, and F. C. Morabito, “Clustering of entropy topography in epileptic electroencephalography”, *Neural Computing and Applications*, vol. 20, no. 6, pp. 825–833, 2011.
- [95] L. A. M. Pereira, J. P. Papa, A. V. Coelho, C. A. M. Lima, D. R. Pereira, and V. H. C. de Albuquerque, “Automatic identification of epileptic EEG signals through binary magnetic optimization algorithms”, *Neural Computing and Applications*, pp. 1–13, 2017.
- [96] M. K. Siddiqui, M. Z. Islam, and M. A. Kabir, “A novel quick seizure detection and localization through brain data mining on ECoG dataset”, *Neural Computing and Applications*, pp. 1–14, 2018. DOI: [10.1007/s00521-018-3381-9](https://doi.org/10.1007/s00521-018-3381-9).
- [97] A. Bhattacharyya, M. Sharma, R. B. Pachori, P. Sircar, and U. R. Acharya, “A novel approach for automated detection of focal EEG signals using empirical wavelet transform”, *Neural Computing and Applications*, vol. 29, no. 8, pp. 47–57, 2018.
- [98] N. S. Tawfik, S. M. Youssef, and M. Kholief, “A hybrid automated detection of epileptic seizures in EEG records”, *Computers & Electrical Engineering*, vol. 53, pp. 177–190, 2016.

- [99] R. Hopfengärtner, B. Kasper, W. Graf, S. Gollwitzer, G. Kreiselmeyer, and H. Stefan, “Automatic seizure detection in long-term scalp EEG using an adaptive thresholding technique: A validation study for clinical routine”, *Clinical Neurophysiology*, vol. 125, pp. 1289–1290, 2014.
- [100] A. Shoeb and J. Guttag, “Application of machine learning to epileptic seizure detection”, in *Proceedings of the 27th International Conference on International Conference on Machine Learning*, ser. ICML’10, 2010, pp. 975–982.
- [101] H. Shiao, V. Cherkassky, J. Lee, B. Veber, E. E. Patterson, B. H. Brinkmann, and G. A. Worrell, “SVM-based system for prediction of epileptic seizures from iEEG signal”, *IEEE Transactions on Biomedical Engineering*, vol. 64, no. 5, pp. 1011–1022, 2017.
- [102] A. S. Zandi, M. Javidan, G. A. Dumont, and R. Tafreshi, “Automated real-time epileptic seizure detection in scalp EEG recordings using an algorithm based on wavelet packet transform”, *IEEE Transactions on Biomedical Engineering*, vol. 57, no. 7, pp. 1639–1651, 2010.
- [103] G. Minasyan, J. Chatten, M. Chatten, and R. Harner, “Patient-specific early seizure detection from scalp electroencephalogram”, *Journal of Clinical Neurophysiology*, vol. 27, no. 3, pp. 163–78, 2010.
- [104] J. Sackellares, D. Shiau, J. Halford, S. LaRoche, and K. Kelly, “Quantitative EEG analysis for automated detection of nonconvulsive seizures in intensive care units”, *Epilepsy Behavior*, vol. 1, S69–S73, 2011.

- [105] D. Geng, W. Zhou, Y. Zhang, and S. Geng, “Epileptic seizure detection based on improved wavelet neural networks in long-term intracranial EEG”, *Biocybernetics and Biomedical Engineering*, vol. 36, no. 2, pp. 375–384, 2016.
- [106] K. Kelly, D. Shiau, and R. Kern, “Assessment of a scalp EEG-based automated seizure detection system”, *Journal of Clinical Neurophysiology*, vol. 121, no. 11, pp. 1832–1843, 2010.
- [107] A. Aarabi, R. Fazel-Rezai, and Y. Aghakhani, “A fuzzy rule-based system for epileptic seizure detection in intracranial EEG”, *Journal of Clinical Neurophysiology*, vol. 120, pp. 1648–1657, 2009.
- [108] M. J. van Putten, T. Kind, F. Visser, and V. Lagerburg, “Detecting temporal lobe seizures from scalp EEG recordings: A comparison of various features”, *Clinical Neurophysiology*, vol. 116, no. 10, pp. 2480–2489, 2005.
- [109] F. Pauri, F. Pierelli, G.-E. Chatrian, and W. W. Erdly, “Long-term EEG-video-audio monitoring: Computer detection of focal EEG seizure patterns”, *Electroencephalography and Clinical Neurophysiology*, vol. 82, no. 1, pp. 1–9, 1992.
- [110] D. Wang, D. Miao, and C. Xie, “Best basis-based wavelet packet entropy feature extraction and hierarchical EEG classification for epileptic detection”, *Expert System with Applications*, vol. 38, pp. 14 314–14 320, 2011.

- [111] A. V. Esbroeck, L. Smith, Z. Syed, S. P. Singh, and Z. N. Karam, “Multi-task seizure detection: Addressing intra-patient variation in seizure morphologies”, *Machine Learning*, vol. 102, pp. 309–321, 2015.
- [112] W. G. Besio, I. E. Martinez-Juarez, O. Makeyev, J. Gaitanis, A. S. Blum, R. S. Fisher, and A. V. Medvedev, “High-frequency oscillations recorded on the scalp of patients with epilepsy using tripolar concentric ring electrodes”, *IEEE Journal of Translational Engineering in Health and Medicine*, vol. 2, pp. 1–11, 2014.
- [113] I. Obeid and J. Picone, “The temple university hospital EEG data corpus”, *Frontiers in Neuroscience*, vol. 10, p. 196, 2016.
- [114] Database. (2016). Temple university EEG corpus. (Accessed: 04.02.2018), [Online]. Available: https://www.isip.piconepress.com/projects/tuh_eeg.
- [115] S. Raghu, N. Sriraam, and G. P. Kumar, “Effect of wavelet packet log energy entropy on electroencephalogram (EEG) signals”, *International Journal of Biomedical and Clinical Engineering*, vol. 4, no. 1, 32–43, 2015.
- [116] A. Delorme and S. Makeig, “EEGLAB: An open source toolbox for analysis of single-trial EEG dynamics including independent component analysis”, *Journal of Neuroscience Methods*, vol. 134, no. 1, pp. 9–21, 2004.

- [117] K. Fujiwara, M. Miyajima, T. Yamakawa, E. Abe, Y. Suzuki, Y. Sawada, M. Kano, T. Maehara, K. Ohta, T. Sasai-Sakuma, T. Sasano, M. Matsuura, and E. Matsushima, “Epileptic seizure prediction based on multivariate statistical process control of heart rate variability features”, *IEEE Transactions on Biomedical Engineering*, vol. 63, no. 6, pp. 1321–1332, 2016.
- [118] K. Samiee, P. Kovcs, and M. Gabbouj, “Epileptic seizure detection in long-term EEG records using sparse rational decomposition and local gabor binary patterns feature extraction”, *Knowledge Based Systems*, vol. 118, pp. 228–240, 2017.
- [119] C Nordqvist. (2017). Symptoms, causes, and treatment of epilepsy. Accessed: 01.02.2018, [Online]. Available: <https://www.medicalnewstoc.com/articles/8947.php>.
- [120] G. Henderson, E. C. Ifeachor, N. R. Hudson, C. Goh, N. J. Outram, S. Wimalaratna, C. D. Percio, and F. Vecchio, “Development and assessment of methods for detecting dementia using the human electroencephalogram”, *IEEE Transactions on Biomedical Engineering*, vol. 53, pp. 1557–1568, 2006.
- [121] P. Zhao, P. Van-Eetvelt, C. S. F. Goh, N. Hudson, S. Wimalaratna, and E. C. Ifeachor, “Characterization of EEGs in alzheimer’s disease using information theoretic methods”, *2007 29th Annual International Conference of the IEEE Engineering in Medicine and Biology Society*, pp. 5127–5131, 2007.

- [122] L. Vidyaratne and M. I Khan, “Real-time epileptic seizure detection using EEG”, *IEEE Transactions on Neural Systems and Rehabilitation Engineering*, vol. 25, pp. 2146–2156, 2017.
- [123] X. Li, G. Ouyang, and D. A. Richards, “Predictability analysis of absence seizures with permutation entropy.”, *Epilepsy research*, vol. 77, pp. 70–4, 2007.
- [124] Y. Song, J. A. Crowcroft, and J. Zhang, “Automatic epileptic seizure detection in EEGs based on optimized sample entropy and extreme learning machine.”, *Journal of Neuroscience Methods*, vol. 210 2, pp. 132–46, 2012.
- [125] J. Li, J. Yan, X. Liu, and G. Ouyang, “Using permutation entropy to measure the changes in EEG signals during absence seizures”, *Entropy*, vol. 16, pp. 3049–3061, 2014.
- [126] J. Xiang, C. Li, H. fang Li, R. Cao, B. Wang, X. Han, and J. Chen, “The detection of epileptic seizure signals based on fuzzy entropy.”, *Journal of Neuroscience Methods*, vol. 243, pp. 18–25, 2015.
- [127] L. Orosco, A. G. Correa, P. Diez, and E. Laciari, “Patient non-specific algorithm for seizures detection in scalp EEG”, *Computers in Biology and Medicine*, vol. 71, pp. 128 –134, 2016.
- [128] C. A. M. Lima, A. L. V. Coelho, and S. Chagas, “Automatic EEG signal classification for epilepsy diagnosis with relevance vector machines”, *Expert Systems with Applications*, vol. 36, pp. 10 054–10 059, 2009.

- [129] E. D. Ubeyli, “Combined neural network model employing wavelet coefficients for EEG signals classification”, *Digit. Signal Process.*, vol. 19, pp. 297–308, 2009.
- [130] O. Faust, U. R. Acharya, H. Adeli, and A. Adeli, “Wavelet-based EEG processing for computer-aided seizure detection and epilepsy diagnosis”, *Seizure*, vol. 26, pp. 56–64, 2015, ISSN: 1059-1311.
- [131] E. Magosso, M. Ursino, A. Zaniboni, and E. Gardella, “A wavelet-based energetic approach for the analysis of biomedical signals: Application to the electroencephalogram and electro-oculogram”, *Applied Mathematics and Computation*, vol. 207, pp. 42–62, 2009.
- [132] C. A. M. Lima and A. L. V. Coelho, “Kernel machines for epilepsy diagnosis via EEG signal classification: A comparative study”, *Artificial Intelligence in Medicine*, vol. 53, pp. 83–95, 2011.
- [133] Y. Jiang, D. Wu, Z. Deng, P. Qian, J. Wang, G. Wang, F. lai Chung, K.-S. Choi, and S. Wang, “Seizure classification from EEG signals using transfer learning, semi-supervised learning and TSK Fuzzy system”, *IEEE Transactions on Neural Systems and Rehabilitation Engineering*, vol. 25, pp. 2270–2284, 2017.
- [134] P. Thodoroff, J. Pineau, and A. Lim, “Learning robust features using deep learning for automatic seizure detection”, *CoRR*, vol. abs/1608.00220, 2016. arXiv: 1608.00220. [Online]. Available: <http://arxiv.org/abs/1608.00220>.
- [135] Y. Liu, W. Zhou, Q. Yuan, and S. Chen, “Automatic seizure detection using wavelet transform and SVM in long-term intracranial EEG”,

IEEE Transactions on Neural Systems and Rehabilitation Engineering, vol. 20, pp. 749–755, 2012.

- [136] D. Geng, W. Zhou, Y. Zhang, and S. Geng, “Epileptic seizure detection based on improved wavelet neural networks in long-term intracranial EEG”, *Biocybernetics and Biomedical Engineering*, vol. 36, no. 2, pp. 375–384, 2016, ISSN: 0208-5216.
- [137] A. S. Zandi, M. Javidan, G. A. Dumont, and R. Tafreshi, “Automated real-time epileptic seizure detection in scalp EEG recordings using an algorithm based on wavelet packet transform”, *IEEE Transactions on Biomedical Engineering*, vol. 57, pp. 1639–1651, 2010.
- [138] J. A. Uriguen and B. Garcia-Zapirain, “EEG artifact removal-state-of-the-art and guidelines.”, *Journal of Neural Engineering*, vol. 12 3, p. 031 001, 2015.
- [139] S. Mallat, “A theory for multi-resolution signal decomposition: The wavelet representation.”, *IEEE Trans. Pattern Anal*, vol. 11, pp. 674–693, 1989.
- [140] I. Daubechies, *10 lectures on wavelets*. Philadelphia: Capital City Press, 1992, ISBN: 978-0-898712-74-2.
- [141] J. Mateo and J. J. Rieta, “Application of artificial neural networks for versatile preprocessing of electrocardiogram recordings”, *Journal of Medical Engineering and Technology*, vol. 362, pp. 90–101, 2012.
- [142] C. E. Shannon, “A mathematical theory of communication”, *Mobile Computing and Communications Review*, vol. 5, pp. 3–55, 2001.

- [143] C. Tsallis, “Possible generalization of Boltzmann-Gibbs statistics”, *Journal of Statistical Physics*, vol. 52, no. 1, pp. 479–487, 1988.
- [144] J. Cohen, “A coefficient of agreement for nominal scales”, *Educational and Psychological Measurement*, vol. 20, no. 1, pp. 37–46, 1960.
- [145] A. Bezerianos, S. Tong, Y. Zhu, and N. Thakor, “Nonadditive information theory for the analysis of brain rhythms”, in *2001 Conference Proceedings of the 23rd Annual International Conference of the IEEE Engineering in Medicine and Biology Society*, vol. 2, 2001, pp. 1923–1925.
- [146] M. Saab and J. Gotman, “A system to detect the onset of epileptic seizures in scalp EEG”, *Clinical neurophysiology : official journal of the International Federation of Clinical Neurophysiology*, vol. 116 2, pp. 427–42, 2005.
- [147] L. Kuhlmann, A. N. Burkitt, M. J. Cook, K. L. Fuller, D. B. Grayden, L. Seiderer, and I. M. Y. Mareels, “Seizure detection using seizure probability estimation: Comparison of features used to detect seizures”, *Annals of Biomedical Engineering*, vol. 37, pp. 2129–2145, 2009.
- [148] A. S. Zandi, M. Javidan, G. A. Dumont, and R. Tafreshi, “Detection of epileptic seizures in scalp electroencephalogram: An automated real-time wavelet-based approach”, *Journal of Clinical Neurophysiology*, vol. 29, pp. 1–16, 2012.
- [149] P. O. Shafer, and J. I. Sirven. (). Epilepsy statistics. (Accessed on 18 January 2019), [Online]. Available: <https://www.epilepsy.com/learn/about-epilepsy-basics/epilepsy-statistics>.

- [150] Z. Zhang, Q. K. Telesford, C. Giusti, K. O. Lim, and D. S. Bassett, “Choosing wavelet methods, filters, and lengths for functional brain network construction”, *PloS one*, vol. 11, no. 6, e0157243, 2016.
- [151] J. M. Sorokin, J. T. Paz, and J. R. Huguenard, “Absence seizure susceptibility correlates with pre-ictal Beta oscillations.”, *Journal of physiology, Paris*, vol. 110 4 Pt A, pp. 372–381, 2016.
- [152] M. Li, W. Chen, and T. Zhang, “Application of MODWT and log-normal distribution model for automatic epilepsy identification”, *Bio-cybernetics and Biomedical Engineering*, vol. 37, no. 4, pp. 679–689, 2017.
- [153] G. Ouyang, X. Li, Y. Li, and X. Guan, “Application of wavelet-based similarity analysis to epileptic seizures prediction”, *Computers in Biology and Medicine*, vol. 37, no. 4, pp. 430–437, 2007.
- [154] L. Amini, C. Jutten, S. Achard, O. David, H. Soltanian-Zadeh, G. A. Hossein-Zadeh, P. Kahane, L. Minotti, and L. Vercueil, “Directed epileptic network from scalp and intracranial EEG of epileptic patients”, *2009 IEEE International Workshop on Machine Learning for Signal Processing*, pp. 1–6, 2009.
- [155] E. Juarez-Guerra, V. Alarcon-Aquino, and P. Gomez-Gil, “Epilepsy seizure detection in EEG signals using wavelet transforms and neural networks”, 2013, pp. 1–7.
- [156] D. B. Percival and H. O. Mofjeld, “Analysis of subtidal coastal sea level fluctuations using wavelets”, *Journal of the American Statistical Association*, vol. 92, 868–880, 1997.

- [157] D. B. Percival and A. T. Walden, *Wavelet Methods for Time Series Analysis*, ser. Cambridge Series in Statistical and Probabilistic Mathematics. Cambridge University Press, 2000. DOI: [10.1017/CBO9780511841044](https://doi.org/10.1017/CBO9780511841044)
- [158] R. R. Coifman and M. V. Wickerhauser, “Entropy-based algorithms for best basis selection”, *IEEE Trans. Information Theory*, vol. 38, pp. 713–718, 1992.
- [159] A. Renyi, “On measures of entropy and information”, pp. 547–561, 1961. [Online]. Available: <https://projecteuclid.org/euclid.bsm/1200512181>.
- [160] V. Gupta, T. Priya, A. K. Yadav, R. B. Pachori, and U. R. Acharya, “Automated detection of focal EEG signals using features extracted from flexible analytic wavelet transform”, *Pattern Recognition Letters*, vol. 94, pp. 180–188, 2017, ISSN: 0167-8655.
- [161] S. J. Kolb and B. Litt. (2019). Emergently admitted: Treating seizures. (Accessed: 26.04.2019), [Online]. Available: <https://www.epilepsy.com/learn/professionals/diagnosis-treatment/icu-care>.
- [162] L. Logesparan, A. J. Casson, and E. Rodriguez-Villegas, “Optimal features for online seizure detection”, *Medical and Biological Engineering and Computing*, vol. 50, no. 7, pp. 659–669, 2012.
- [163] A. Subasi and M. I. Gursoy, “EEG signal classification using PCA, ICA, LDA and support vector machines”, *Expert Systems with Applications*, vol. 37, no. 12, pp. 8659–8666, 2010.

- [164] M. Zhou, C. Tian, R. Cao, B. Wang, Y. Niu, T. Hu, H. Guo, and J. Xiang, “Epileptic seizure detection based on EEG signals and CNN”, *Frontiers in Neuroinformatics*, vol. 12, p. 95, 2018.
- [165] “Scalp EEG epileptogenic zone recognition and localization based on long-term recurrent convolutional network”, *Neurocomputing*, 2019. DOI: [doi:https://doi.org/10.1016/j.neucom.2018.10.108..](https://doi.org/10.1016/j.neucom.2018.10.108..)
- [166] Y. Yuan, G. Xun, Q. Suo, K. Jia, and A. Zhang, “Wave2Vec: Deep representation learning for clinical temporal data”, *Neurocomputing*, vol. 324, pp. 31 –42, 2019, Deep Learning for Biological/Clinical Data.
- [167] M. Z. Parvez and M. Paul, “Epileptic seizure detection by analyzing EEG signals using different transformation techniques”, *Neurocomputing*, vol. 145, pp. 190 –200, 2014.
- [168] M. Mursalin, Y. Zhang, Y. Chen, and N. V. Chawla, “Automated epileptic seizure detection using improved correlation-based feature selection with random forest classifier”, *Neurocomputing*, vol. 241, pp. 204 –214, 2017.
- [169] J.-L. Song, W. Hu, and R. Zhang, “Automated detection of epileptic EEGs using a novel fusion feature and extreme learning machine”, *Neurocomputing*, vol. 175, pp. 383 –391, 2016.
- [170] Y. Kumar, M. Dewal, and R. Anand, “Epileptic seizure detection using DWT based fuzzy approximate entropy and support vector machine”, *Neurocomputing*, vol. 133, pp. 271 –279, 2014.

- [171] K. Zeng, J. Yan, Y. Wang, A. Sik, G. Ouyang, and X. Li, “Automatic detection of absence seizures with compressive sensing EEG”, *Neurocomputing*, vol. 171, pp. 497–502, 2016.
- [172] R. R. Sharma, P. Varshney, R. B. Pachori, and S. K. Vishvakarma, “Automated system for epileptic EEG detection using iterative filtering”, *IEEE Sensors Letters*, vol. 2, no. 4, pp. 1–4, 2018.
- [173] A. Bhattacharyya, L. Singh, and R. B. Pachori, “Fourier–bessel series expansion based empirical wavelet transform for analysis of non-stationary signals”, *Digital Signal Processing*, vol. 78, pp. 185–196, 2018.
- [174] A. Bhattacharyya and R. B. Pachori, “A multivariate approach for patient-specific EEG seizure detection using empirical wavelet transform”, *IEEE Transactions on Biomedical Engineering*, vol. 64, no. 9, pp. 2003–2015, 2017.
- [175] R. Sharma and R. B. Pachori, “Classification of epileptic seizures in EEG signals based on phase space representation of intrinsic mode functions”, *Expert Systems with Applications*, vol. 42, no. 3, pp. 1106–1117, 2015.
- [176] D. Bhati, R. B. Pachori, and V. M. Gadre, “A novel approach for time–frequency localization of scaling functions and design of three-band biorthogonal linear phase wavelet filter banks”, *Digital Signal Processing*, vol. 69, pp. 309–322, 2017.

- [177] D. Bhati, M. Sharma, R. B. Pachori, and V. M. Gadre, “Time–frequency localized three-band biorthogonal wavelet filter bank using semidefinite relaxation and nonlinear least squares with epileptic seizure EEG signal classification”, *Digital Signal Processing*, vol. 62, pp. 259–273, 2017.
- [178] L. Logesparan, E. Rodriguez-Villegas, and A. J. Casson, “The impact of signal normalization on seizure detection using line length features”, *Medical and Biological Engineering and Computing*, vol. 53, no. 10, pp. 929–942, 2015.
- [179] J. G. Bogaarts, E. D. Gommer, D. M. W. Hilkmann, V. H. J. M. van Kranen-Mastenbroek, and J. P. H. Reulen, “EEG feature pre-processing for neonatal epileptic seizure detection”, *Annals of Biomedical Engineering*, vol. 42, no. 11, pp. 2360–2368, 2014.
- [180] A. Temko, E. Thomas, W. Marnane, G. Lightbody, and G. Boylan, “EEG-based neonatal seizure detection with support vector machines”, *Clinical Neurophysiology*, vol. 122, no. 3, pp. 464–473, 2011.
- [181] R. Ahmed, A. Temko, W. P. Marnane, G. B. Boylan, and G. Lightbody, “Exploring temporal information in neonatal seizures using a dynamic time warping based SVM kernel”, *Computers in biology and medicine*, vol. 82, pp. 100–110, 2017.
- [182] S Raghu, N. Sriraam, S. V. Rao, A. S. Hegde, and P. L. Kubben, “Automated detection of epileptic seizures using successive decomposition index and support vector machine classifier in long-term EEG”, *Neural Computing and Applications*, vol. 32, pp. 8965–8984, 2020. DOI: [10.1007/s00521-019-04389-1](https://doi.org/10.1007/s00521-019-04389-1).

- [183] A. D. Weerd, P. Despland, and P Plouin, “Neonatal EEG. the international federation of clinical neurophysiology”, *Electroencephalogr Clin Neurophysiol Suppl.*, vol. 52, pp. 149–57, 1999.
- [184] M. Krauledat, G. Dornhege, B. Blankertz, and K.-R. Müller, “Robustifying EEG data analysis by removing outliers”, vol. 2, pp. 259–274, 2009.
- [185] W. Li, W. Mo, X. Zhang, J. J. Squiers, Y. Lu, E. W. Sellke, W. Fan, J. M. DiMaio, and J. E. Thatcher, “Outlier detection and removal improves accuracy of machine learning approach to multispectral burn diagnostic imaging.”, *Journal of biomedical optics*, vol. 20 (12), p. 121 305, 2015.
- [186] I. Winkler, S. Haufe, and M. Tangermann, “Automatic classification of artifactual ICA-components for artifact removal in EEG signals”, *Behavioral and Brain Functions*, vol. 7, pp. 1–35, 2011.
- [187] Online. (2017). Detect and replace outliers in data. (Accessed: 05.04.2019), [Online]. Available: <https://www.mathworks.com/help/matlab/ref/filloutliers.html>.
- [188] R. Hopfengaertner, B. S. Kasper, W. Graf, S. Gollwitzer, and H. M. Hamer, “Automatic seizure detection in long-term scalp EEG using an adaptive thresholding technique: A validation study for clinical routine”, *Clinical Neurophysiology*, vol. 125, pp. 1346–1352, 2014.
- [189] R. Hussein, H. Palangi, R. K. Ward, and Z. J. Wang, “Optimized deep neural network architecture for robust detection of epileptic seizures

- using EEG signals”, *Clinical Neurophysiology*, vol. 130, pp. 25–37, 2019.
- [190] H. Khamis, A. Mohamed, and S. Simpson, “Frequency–moment signatures: A method for automated seizure detection from scalp EEG”, *Clinical Neurophysiology*, vol. 124, pp. 2317–2327, 2013.
- [191] A. M. Chan, F. T. Sun, E. H. Boto, and B. M. Wingeier, “Automated seizure onset detection for accurate onset time determination in intracranial EEG”, *Clinical Neurophysiology*, vol. 119, pp. 2687–2696, 2008.
- [192] Y. Zheng, G. Wang, K. Li, G. Bao, and J. Wang, “Epileptic seizure prediction using phase synchronization based on bivariate empirical mode decomposition”, *Clinical Neurophysiology*, vol. 125, pp. 1104–1111, 2014.
- [193] F. Fübass, P. Ossenblok, M. Hartmann, H. Perko, A. Skupch, G. Lindinger, L. Elezi, E. Pataraiia, A. Colon, C. Baumgartner, and T. Kluge, “Prospective multi-center study of an automatic online seizure detection system for epilepsy monitoring units”, *Clinical Neurophysiology*, vol. 126, no. 6, pp. 1124 –1131, 2015, ISSN: 1388-2457.
- [194] F. Fübass, S. Kampusch, E. Kaniusas, J. Koren, S. Pirker, R. Hopfengärtner, H. Stefan, T. Kluge, and C. Baumgartner, “Automatic multimodal detection for long-term seizure documentation in epilepsy”, *Clinical Neurophysiology*, vol. 128, no. 8, pp. 1466 –1472, 2017, ISSN: 1388-2457.

- [195] C. Baumgartner, J. Koren, M. Britto-Arias, S. Schmidt, and S. Pirker, “Epidemiology and pathophysiology of autonomic seizures: A systematic review”, *Clinical Autonomic Research*, vol. 29, pp. 137–150, 2019.
- [196] S. Raghu, N. Sriraam, E. D. Gommer, D. M. W. Hilkmann, Y. Temel, S. V. Rao, and P. L. Kubben, “Adaptive median feature baseline correction for improving recognition of epileptic seizures in ICU EEG”, *Neurocomputing*, vol. 407, pp. 385–398, 2020.
- [197] S. Raghu, N. Sriraam, Y. Temel, S. V. Rao, A. S. Hegde, and P. L. Kubben, “Complexity analysis and dynamic characteristics of EEG using MODWT based entropies for identification of seizure onset”, *Journal of Biomedical Research*, vol. 34 3, pp. 211–225, 2019.
- [198] M. Dilykh, Y. Li, and P. Wen, “Classify epileptic EEG signals using weighted complex networks based community structure detection”, *Expert Systems with Applications*, vol. 90, pp. 87–100, 2017.
- [199] N. D. Truong, A. D. Nguyen, L. Kuhlmann, M. R. Bonyadi, J. Yang, and O. Kavehei, “A generalised seizure prediction with convolutional neural networks for intracranial and scalp electroencephalogram data analysis”, *CoRR*, vol. abs/1707.01976, pp. 1–8, 2017.
- [200] I. Ullah, E. ul Haq Qazi, and H. A. Aboalsamh, “An automated system for epilepsy detection using EEG brain signals based on deep learning approach”, *Expert Systems with Applications*, vol. 107, pp. 61–71, 2018.

- [201] J. Birjandtalab, M. Heydarzadeh, and M. Nourani, “Automated EEG-based epileptic seizure detection using deep neural networks”, *2017 IEEE International Conference on Healthcare Informatics (ICHI)*, pp. 552–555, 2017.
- [202] F. Achilles, F. Tombari, V. Belagiannis, A. M. Loesch, S. Noachtar, and N. Navab, “Convolutional neural networks for real-time epileptic seizure detection”, *CMBBE Imaging and Visualization*, vol. 6, pp. 264–269, 2018.
- [203] U. R. Acharya, S. L. Oh, Y. Hagiwara, J.-H. Tan, and H. Adeli, “Deep convolutional neural network for the automated detection and diagnosis of seizure using EEG signals”, *Computers in biology and medicine*, vol. 100, pp. 270–278, 2018.
- [204] P. Thodoroff, J. Pineau, and A. Lim, “Learning robust features using deep learning for automatic seizure detection”, vol. abs/1608.00220, 2016. arXiv: 1608.00220. [Online]. Available: <http://arxiv.org/abs/1608.00220>.
- [205] M.-P. Hosseini, D. Pompili, K. V. Elisevich, and H. Soltanian-Zadeh, “Optimized deep learning for EEG big data and seizure prediction BCI via Internet of Things”, *IEEE Transactions on Big Data*, vol. 3, pp. 392–404, 2017.
- [206] M. Golmohammadi, S. Ziyabari, V. Shah, S. L. de Diego, I. Obeid, and J. Picone, “Deep architectures for automated seizure detection in scalpEEGs”, *CoRR*, vol. abs/1712.09776, 2017.

- [207] T. Uktveris and V. Jusas, “Application of convolutional neural networks to Four-class motor imagery classification problem”, *Information Technology and Control*, vol. 46, pp. 1–10, 2017.
- [208] Shelhamer. (2017). Bvlc_alexnet. github, Ed. <https://github.com/BVLC/caffe/tree/m>
- [209] K. Simonyan and A. Zisserman, “Very deep convolutional networks for large-scale image recognition”, *CoRR*, vol. abs/1409.1556, 2015, arXiv preprint arXiv:1409.1556.
- [210] C. Szegedy, W. Liu, Y. Jia, P. Sermanet, S. E. Reed, D. Anguelov, D. Erhan, V. Vanhoucke, and A. Rabinovich, “Going deeper with convolutions”, *2015 IEEE Conference on Computer Vision and Pattern Recognition (CVPR)*, pp. 1–9, 2015.
- [211] Matlab, *Pretrained VGG-19 CNN*, <https://www.mathworks.com/help/deeplearning> 2017.
- [212] A. Emami, N. Kunii, T. Matsuo, T. Shinozaki, K. Kawai, and H. Takahashi, “Seizure detection by convolutional neural network-based analysis of scalp electroencephalography plot images”, in *NeuroImage: Clinical*, vol. 22, 2019, p. 101 684.
- [213] N. D. Truong, A. D. Nguyen, L. Kuhlmann, M. R. Bonyadi, J. Yang, S. J. Ippolito, and O. Kavehei, “Convolutional neural networks for seizure prediction using intracranial and scalp electroencephalogram”, *Neural networks : the official journal of the International Neural Network Society*, vol. 105, pp. 104–111, 2018.

- [214] A. H. Ansari, P. J. Cherian, A. Caicedo, and G. Naulaers, “Neonatal seizure detection using deep convolutional neural networks.”, *International journal of neural systems*, p. 1 850 011, 2018.
- [215] R. San-Segundo, M. Gil-Martin, L. F. D’Haro-Enriquez, and J. M. Pardo, “Classification of epileptic EEG recordings using signal transforms and convolutional neural networks.”, *Computers in biology and medicine*, vol. 109, pp. 148–158, 2019.
- [216] W. Weng and K. Khorasani, “An adaptive structure neural networks with application to EEG automatic seizure detection”, *Neural networks : the official journal of the International Neural Network Society*, vol. 9 7, pp. 1223–1240, 1996.
- [217] A. Subasi, A. Alkan, E. Koklukaya, and M. K. Kiymik, “Wavelet neural network classification of EEG signals by using AR model with MLE preprocessing”, *Neural networks : the official journal of the International Neural Network Society*, vol. 18 7, pp. 985–97, 2005.
- [218] S. Ghosh-Dastidar and H. Adeli, “A new supervised learning algorithm for multiple spiking neural networks with application in epilepsy and seizure detection”, *Neural networks : the official journal of the International Neural Network Society*, vol. 22 10, pp. 1419–31, 2009.
- [219] M. Alfaro, A. J. Arguelles-Cruz, and I. C. Oria, “Pattern recognition for electroencephalographic signals based on continuous neural networks”, *Neural networks : the official journal of the International Neural Network Society*, vol. 79, pp. 88–96, 2016.

- [220] A. Tavanaei, M. Ghodrati, S. R. Kheradpisheh, T. Masquelier, and A. S. Maida, “Deep learning in spiking neural networks”, *Neural networks : the official journal of the International Neural Network Society*, vol. 111, pp. 47–63, 2018.
- [221] Deeplearning. (2019). Pretrained deep neural networks. (Accessed: 04.06.2019), [Online]. Available: <https://www.mathworks.com/help/deeplearning/ug/pretrained-convolutional-neural-networks.html>.
- [222] D. N. Networks. (2019). Extract image features using pretrained network. (Accessed: 04.06.2019), [Online]. Available: <https://www.mathworks.com/help/deeplearning/examples/extract-image-features-using-pretrained-network.html>.
- [223] M. D. Zeiler and R. Fergus, “Visualizing and understanding convolutional networks”, *ArXiv*, vol. abs/1311.2901, 2013.
- [224] E. D. McKenzie, A. S. P. Lim, E. C. W. Leung, A. J. Cole, A. D. Lam, A. Eloyan, and et al., “Validation of a smartphone-based EEG among people with epilepsy: A prospective study”, in *Scientific reports*, 2017.
- [225] Z. Lasefr, R. R. Reddy, and K. Elleithy, “Smart phone application development for monitoring epilepsy seizure detection based on EEG signal classification”, *2017 IEEE 8th Annual Ubiquitous Computing, Electronics and Mobile Communication Conference (UEMCON)*, pp. 83–87, 2017.

- [226] P. Ryvlin and S. Beniczky, “Seizure detection and mobile health devices in epilepsy: Update and future developments.”, *Epilepsia*, vol. 59 Suppl 1, pp. 7–8, 2018.
- [227] I. Kiral-Kornek, S. Roy, E. Nurse, B. Mashford, P. Karoly, T. Carroll, D. Payne, S. Saha, S. Baldassano, T. O’Brien, D. Grayden, M. Cook, D. Freestone, and S. Harrer, “Epileptic seizure prediction using big data and deep learning: Toward a mobile system”, *EBioMedicine*, vol. 27, pp. 103–111, 2018.
- [228] S. Baldassano, X. Zhao, B. H. Brinkmann, V. Kremen, J. M. Bernabei, M. D. Cook, T. Denison, G. Worrell, and B. Litt, “Cloud computing for seizure detection in implanted neural devices.”, *Journal of neural engineering*, vol. 16 2, p. 026 016, 2019.
- [229] M.-P. Hosseini, D. Pompili, K. V. Elisevich, and H. Soltanian-Zadeh, “Optimized deep learning for EEG big data and seizure prediction BCI via Internet of Things”, *IEEE Transactions on Big Data*, vol. 3, pp. 392–404, 2017.
- [230] M.-P. Hosseini, H. Soltanian-Zadeh, K. V. Elisevich, and D. Pompili, “Cloud-based deep learning of big EEG data for epileptic seizure prediction”, *2016 IEEE Global Conference on Signal and Information Processing (GlobalSIP)*, pp. 1151–1155, 2016.
- [231] S. Sareen, S. K. Sood, and S. K. Gupta, “An automatic prediction of epileptic seizures using cloud computing and wireless sensor networks”, *Journal of Medical Systems*, vol. 40, no. 11, p. 226, 2016.

- [232] P. M. Vergara, E. A. de la Cal, J. R. Villar, V. M. G. Suarez, and J. Sedano, “An IoT platform for epilepsy monitoring and supervising”, *J. Sensors*, vol. 2017, 6043069:1–6043069:18, 2017.
- [233] N. E. Cruz, J. Solarte, and A. Gonzalez-Vargas, “Automated epileptic seizure detection system based on a wearable prototype and cloud computing to assist people with epilepsy”, in *WEA*, 2018.
- [234] Z. Zhang, T. Wen, W. Huang, M. Wang, and C. Li, “Automatic epileptic seizure detection in EEGs using MF-DFA, SVM based on cloud computing.”, *Journal of X-ray science and technology*, vol. 25 2, pp. 261–272, 2017.
- [235] A. Marquez, M. Dunn, J. Ciriaco, and F. Farahmand, “ISeiz: A low-cost real-time seizure detection system utilizing cloud computing”, in *2017 IEEE Global Humanitarian Technology Conference (GHTC)*, 2017, pp. 1–7. DOI: [10.1109/GHTC.2017.8239249](https://doi.org/10.1109/GHTC.2017.8239249).
- [236] G. Krauss, “Mobile devices may provide accurate seizure detection and help prevent SUDEP”, *Neurology Reviews*, vol. 25 2, pp. 28–29, 2017.
- [237] S. Raghu, N. Sriraam, E. D. Gommer, D. M. W. Hilkman, Y. Temel, S. V. Rao, A. S. Hegde, and P. L. Kubben, “Cross-database evaluation of EEG based epileptic seizures detection driven by adaptive median feature baseline correction”, *Clinical Neurophysiology*, 2019.
- [238] M. H. Smith. (2016). Chaquopy python SDK for android. Accessed: 08.09.2019, [Online]. Available: <https://chaquo.com/chaquopy>.

- [239] L. Hussain, “Detecting epileptic seizure with different feature extracting strategies using robust machine learning classification techniques by applying advance parameter optimization approach”, *Cognitive Neurodynamics*, vol. 12, no. 3, 2018.
- [240] D. Dash, L. Hernandez-Ronquillo, F. Moien-Afshari, and J. F. Tellez-Zenteno, “Ambulatory EEG: A cost-effective alternative to inpatient video-EEG in adult patients”, *Epileptic Disorders*, vol. 14, pp. 290–297, 2012.
- [241] T. Chemmanam, A. Radhakrishnan, S. P. Sarma, and K. Radhakrishnan, “A prospective study on the cost-effective utilization of long-term inpatient video-EEG monitoring in a developing country”, *Journal of clinical neurophysiology : official publication of the American Electroencephalographic Society*, vol. 26 2, pp. 123–8, 2009.

Index

- Acknowledgment, 327
- Adaptive median feature baseline
correction, 192, 225
- Android, 296
- Bivariate plot, 38
- Chaquopy, 295
- Classification scenarios, 195, 229
- Conclusion, 317
- Contact, 335
- Convolutional neural network,
256, 271
- Cross-database, 215
- Curriculum vitae, 329
- Discrete wavelet transform, 109
- Event-based approach, 126
- Five databases, 221
- General discussion, 303
- General introduction, 3
- Graphical user interface, 84
- Histogram plot, 38
- Inter-database FBC, 227
- Inter-patient FBC, 226
- K-nearest neighbor, 33
- Kappa coefficient, 117, 130
- Maastricht University Medical
Centre, 187
- Matrix determinant, 28, 191
- Maximal overlap discrete wavelet
transform, 150
- Mobile health, 291
- Multi-layer perceptron, 33
- Outliers removal and correction,
192
- Outline of the thesis, 12
- Post-processing, 194, 197, 228
- Publications, 331
- Radar chart, 137
- Renyi entropy, 154

Segment-based approach, 122

Seizure types, 254, 269

Shannon entropy, 153

Sigmoid entropy, 110, 152

Smoothing train and test data, 227

Successive decomposition index,
75, 188

Summary, 319

Support vector machine, 33, 78

Sure entropy, 155

Topo plot, 82

Transfer learning, 272

Tsallis entropy, 154

Valorization, 325

Wavelet entropy, 154

